

# UNIVERSITÀ DEGLI STUDI DI MILANO

Facoltà di Medicina e Chirurgia

Dipartimento di Biotecnologie Mediche e Medicina Translazionale

Settore Scientifico Disciplinare BIO/10



Scuola di Dottorato in Scienze Biochimiche, Nutrizionali e Metaboliche

Corso di Dottorato di Ricerca in Biochimica

Ciclo XXVII

Using synthetic approaches to glycoconjugates to understand  
carbohydrate-mediated biochemical interactions

Dottoranda  
Maria Vetro  
R09702

Tutor: Prof. Diego Colombo

Coordinatore: Prof. Francesco Bonomi

A.A. 2013/2014



*A Federica,  
per non avermi mai abbandonata.*

*A mia sorella,  
per esserci sempre stata.*

# Index

Preface	7
Chapter 1	10
Protein Kinase B (Akt) as potential antitumoral target	10
1.1 Akt activation	11
1.2 Regulation of cellular processes by Akt	13
1.3 Main inhibitor categories	15
1.3.1 ATP-competitive protein kinase inhibitors	15
1.3.2 Allosteric inhibitors	15
1.3.3 Inhibitors of PIP <sub>3</sub> binding	17
Chapter 2	22
Synthetic analogues of natural compounds as potential inhibitors targeting Akt for anticancer drugs	22
2.1 Introduction	22
2.2 Aim of the work	27
2.3 Results and discussion	29
2.3.1 Synthesis of diesters <b>26a,b</b>	29
2.3.2 Attempt to reduce the synthetic steps to synthesize compounds <b>26a,b</b>	31
2.3.3 Synthesis of monoesters <b>27a,b</b>	32
2.3.4 Synthesis of glucuronides <b>28a,b</b>	35
2.4 Cell free evaluation of Akt inhibition	36
2.5 Cellular studies	38
2.6 Conclusions	40
2.7 Experimental section	41
2.7.1 General methods	41
2.7.2 Synthesis of diester derivatives <b>26a,b</b>	42
2.7.3 Synthesis of monoester derivatives <b>27a,b</b>	46

2.7.4 Synthesis of glucuronosyl derivatives <b>28a,b</b>	53
2.7.5 Akt Inhibition Assays	55
2.7.6 Cellular studies	55
Chapter 3	57
Fluorescent probes to study Akt inhibitor distribution	57
3.1 Introduction	57
3.2 Aim of the work	60
3.3 Results and discussion	61
3.3.1 Synthesis of fluorescent compounds <b>49a,b</b>	61
3.4 Conclusions	64
3.5 Experimental section	65
3.5.1 General methods	65
3.5.2 Synthesis of fluorescent compounds <b>49a,b</b>	66
Chapter 4	75
Gold nanoparticles as carriers for fully synthetic carbohydrate vaccine candidates against <i>Streptococcus pneumoniae</i>	75
4.1 Introduction	75
4.2 Aim of the work	83
4.3 Results and discussion	85
4.3.1 Synthesis of Thiol-Ending Ligands	86
4.3.2 Preparation of glyconanoparticles	91
4.3.3 Characterization of of glyconanoparticles	97
4.4 Immunological evaluation	104
4.5 Conclusions	108
4.6 Experimental section	109
4.6.1 General methods	109
4.6.2 Synthesis of thiol-ending trisaccharide related to serotype Pn19F.	111

4.6.3 Synthesis and characterization of the glyconanoparticles	116
4.6.4 Immunization studies	126
4.6.5 Enzyme-linked immunosorbent assay	126
4.6.6 GNP-ELISA	126
Bibliography	128

# Preface

This PhD Thesis deals with the synthesis of carbohydrates derivatives as analogues of natural compounds and their biological evaluation as tools for the study of biochemical regulatory pathways.

Carbohydrates, together with proteins, nucleic acids and lipids, are the building blocks on which complex living systems are based. This spectacular class of compounds acts as energetic sources, signaling regulators and components of cell surface. So, they are involved in many biological processes essential for the living cells, as immune response, inflammation, cell growth, cell-cell adhesion and so forth. The possibility to develop biochemical tools based on carbohydrates structures could be used to explain their functional role in many of these mechanisms and how to intervene to conceive new drugs systems for the treatment of several pathologies like cancers and bacterial infections, generally due to altered carbohydrate-mediated interactions.

The topic of this PhD thesis can be divided into two parts. The first one, composed by *Chapter 1, 2 and 3*, deals with the synthesis of glycosylglycerols ligands of Akt, a protein kinase overexpressed in many cancer cells, while the second part, resumed in *Chapter 4*, is oriented to the study of the opportunity to employ gold nanoparticles as alternative carriers for saccharide antigens in the vaccinology field.

*Chapter 1* is a general overview on protein kinase B, also known as Akt, which recently has attracted great attention because of its involvement in many crucial cellular process like proliferation, differentiation and apoptosis. Specifically, hyperactivated Akt is responsible of tumor formation, progression and invasion. So, the research of an effective method to prevent its activation could be a way to locate novel anticancer drugs.

*Chapter 2* describes the advancements leaded by our research group in the investigation on new Akt inhibitors based on  $\beta$ -glucosylglycerol. Starting from the synthetic analogues of a class of natural compounds, the sulfoquinovosyldiacylglycerols (SQDGs), which have showed good inhibiting properties with Akt, a novel category of potential Akt inhibitors has been developed. The synthesis of these novel compounds, related to the natural glucuronosyldiacylglycerols

(GlcADGs), is described in this chapter. Furthermore, the evaluation of their inhibitory activity on the isolated enzyme (Akt) and on cell systems, performed in collaboration with the Università di Milano Bicocca and the Istituto dei tumori di Milano, is also reported.

In *Chapter 3* the importance of fluorescent dye in biochemistry is reported. In particular, the most active compound reported in *Chapter 2* has been functionalized with a fluorescent probe in order to study its cell distribution and shed some light on its action mechanism. In this chapter the novel straightforward synthetic methodology to obtain fluorescent derivatives functionalized on the glycerol moiety is illustrated, while their biological evaluation is underway.

*Chapter 4* reports the potential application of gold nanoparticles as carriers for saccharide antigens related to *Streptococcus pneumoniae*, work achieved thanks to the collaboration with Prof. Soledad Penadés and Dr. Marco Marradi. In this chapter, the carbohydrate's world and that of nanotechnology combine together seeking to improve the development of fully synthetic carbohydrate vaccines. The trisaccharide repeating unit of *Streptococcus pneumoniae* serotype 19F, which I had previously synthesized in our laboratory, was properly functionalized during the six months spent in the Laboratory of GlycoNanotechnology of CIC biomaGUNE center (San Sebastián-Spain) as a Guest PhD student and conjugated to gold nanoparticles alone or together with the tetrasaccharide related to *S. pneumoniae* serotype 14 in order to develop multiantigenic systems. New different gold glyconanoparticles have been prepared and their immunological properties carried out by Dr. Dodi Safari at Eijkman Institute for Molecular Biology in Jakarta, are also reported in this chapter.



# **PART 1**

# Chapter 1

## Protein Kinase B (Akt) as potential antitumoral target

Among the most important proteins of the whole human genome, protein kinases are one of the largest families of genes in eukaryotes.<sup>1</sup> They are enzymes that catalyse the transfer of the terminal phosphate group from adenosine triphosphate ATP to protein substrates, specifically to the hydroxyl group of tyrosine (Tyr kinase) or the hydroxyl group of serine/threonine (Ser/Thr kinase). Since protein kinases represent key players in many crucial cellular processes like proliferation, differentiation and apoptosis,<sup>2,3</sup> the discovery of molecule kinase inhibitors has attracted growing interest for novel drug research and development as well as the identification of experimental tools for the understanding of the biological roles of this class of protein.

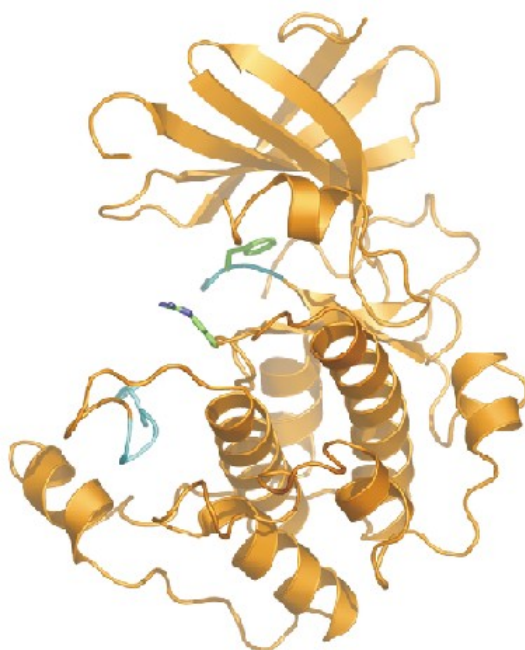


**Figure 1.1:** Structure of inactive PKB/Akt. Taken from Ref.<sup>4</sup>

The serine/threonine protein kinase B (PKB), also known as Akt (Figure 1.1), has recently garnered a great deal of attention as a promising molecular target for cancer therapy due to its critical role as a regulator of the cell's apoptotic machinery.<sup>5</sup> Akt is a 57-kDa soluble cytosolic protein with three structurally conserved domains namely an

N-terminal pleckstrin homology (PH) domain, a central kinase domain and a C-terminal regulatory domain, mainly consisting of hydrophobic aminoacids (HM).<sup>4</sup>

In the human genome have been identified genes coding for three highly homologous PKB isoforms, PKB $\alpha$ /Akt1, PKB $\beta$ /Akt2 and PKB $\gamma$ /Akt3 (Figure 1.2). Despite of the high structural homology, the physiological functions of the three isoforms are not superimposed.<sup>6</sup> In fact, PKB $\alpha$ /Akt1, ubiquitously expressed, is involved in cell survival pathways and growth control, PKB $\beta$ /Akt2, which is highly expressed in muscle and adipocytes, has been shown to be relevant for glucose metabolism, whereas the role of PKB $\gamma$ /Akt3, expressed predominantly in the brain, is unclear.

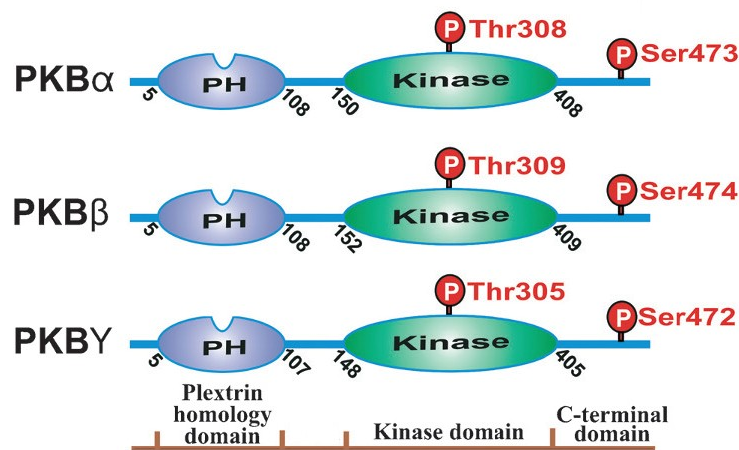
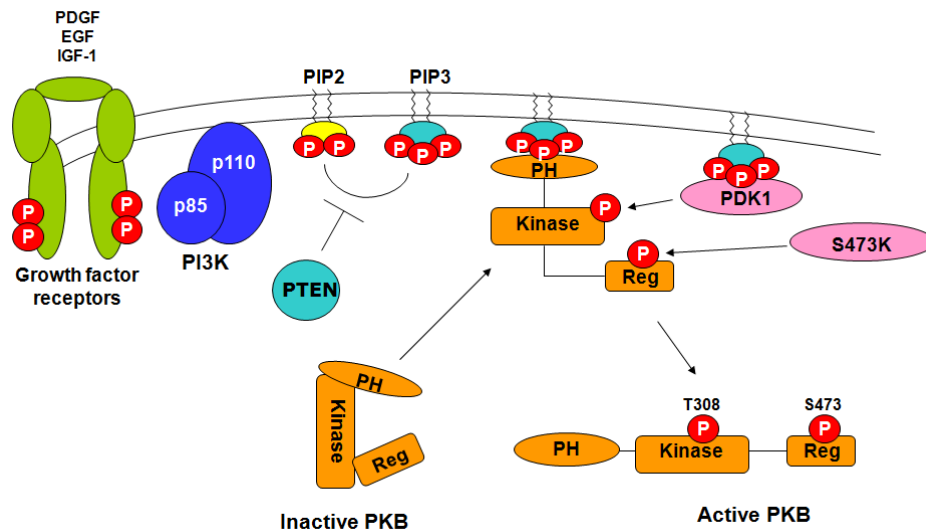


Figure 1.2: Three different PKB/Akt isoforms. Taken from Ref.<sup>7</sup>

## 1.1 Akt activation

The protein kinase B plays a key role as a component of the phosphoinositide 3-kinase (PI3K)-Akt-mTOR axis in tumor cell survival. In fact, hyperactivation of Akt is a common feature of tumor cells that has been linked to increased survival, invasion and drug resistance, and rapidly it became evident that this pathway could be an effective target for antineoplastic therapies. It has been shown that Akt is activated in a phosphatidylinositol-3-kinase (PI3K)-dependent manner (Figure 1.3). Akt is normally maintained in an inactive state through an intramolecular interaction between the PH domain and and kinase domain. The stimulation of PI3K by growth factors and cytokines generates, by means of the phosphorylation of position 3 of the phosphatidylinositol 4,5 diphosphate [PtdIn(4,5)P<sub>2</sub> or PIP<sub>2</sub>], the key second

phosphatidylinositol 3,4,5 triphosphate [PtdIn (3,4,5)P<sub>3</sub> or PIP<sub>3</sub>] in the plasma membrane, able to bind the PH domain of inactive Akt.<sup>8</sup> In consequence of the linkage between the phosphate in position 3 of the phosphoinositide and specific basic residues in the protein as salt bridges, a conformational change of protein kinase occurs, leading to the exposure of two phosphorylation sites that mediate activity.<sup>7</sup>



**Figure 1.3:** Activation and regulation of Akt. The phosphorylation of phosphatidylinositol 4,5 diphosphate PIP2 leads to the generation of phosphatidylinositol 3,4,5 triphosphate PIP3 able to bind the PH domain of an inactive Akt and to induce a conformational change resulting in the exposure of two phosphorylation sites. Their phosphorylation activates the Akt which dissociates from the plasma membrane and phosphorylates substrates in the cytoplasm and in the nucleus.

Specifically, threonine 308 in the catalytic site is phosphorylated by phosphoinositide-dependent kinase 1 (PDK-1) while serine 473 in the C-terminal hydrophobic motif is phosphorylated by an unidentified S473 kinase.<sup>9</sup> In particular, the phosphorylation of the serine is considered a crucial step in the Akt activation because it stabilizes the kinase domain in an active conformation state.<sup>10</sup> Once activated, Akt dissociates from the plasma membrane and can phosphorylate substrates in the cytoplasm and in the nucleus, as several signaling proteins. Another key regulator able to inhibit this activation cascade of the Akt is the phosphatase and tensin homologue PTEN, which possesses 3-phosphoinositide phosphatase activity. It is the second most frequently mutated tumor suppressor gene, again underscoring the medical relevance of the Akt pathway. When the function of PTEN is attenuated, PIP<sub>3</sub> levels increase and promote oncogenic processes.<sup>11</sup>

## 1.2 Regulation of cellular processes by Akt

Akt regulates many cellular processes including metabolism, proliferation, cell survival, growth and angiogenesis. For this reason, inappropriate activation of the PI3K/Akt pathway is cause of different human diseases.

One of the key roles of Akt is the regulation of glucose uptake into muscle and fat cells by the translocation of insulin regulated GLUT-4 (glucose transporter-4) from intracellular compartments to the plasma membrane, thus explaining as the Akt deregulation is implicated in diabetes.

It has been already largely proved the involvement of Akt in the cell-cycle regulation at different stage (Figure 1.4). Akt is able to promote G1/S transition through phosphorylation of several substrates, as inhibitors of cyclin-dependent kinase<sup>12,13</sup> (CDK) p21<sup>WAF1</sup> and p27<sup>kip1</sup>. Also, Akt promotes progression from S to G2 phase by phosphorylation of CDK2 leading to its cytoplasmatic localization, necessary for cell-cycle progression.<sup>14</sup> Kandel reported that constitutively activated Akt overcomes a G2/M cell-cycle checkpoint induced by DNA damage causing a continuous cellular division in the presence of mutagens. This could explain the frequent upregulation and overactivation of Akt in human cancer.<sup>15</sup>

Finally, Akt causes the cytoplasmatic accumulation of a dual-specific phosphatase, the cell division cell CDC25B, as a consequence of phosphorylative events, promoting mitotic entry.<sup>16</sup> Moreover, Akt is demonstrated to mediate cell survival inhibiting apoptosis process by the phosphorylation of downstream mediators, such as Bad, an associated death protein, GSK-3 (Glycogen Synthase Kinase 3), pro-caspase9, IκB kinase (IKK), Yes-associated protein (YAP)<sup>17,18</sup> and through the phosphorylation of different family members of forkhead transcription factors FOXO, which results in their exclusion from the nucleus and a lower transcriptional activity that is required to promote apoptosis. Increased Akt activity has been shown inducing cellular oncogenic transformation and tumor formation in breast, prostate, ovary and pancreas.<sup>19</sup> Akt hyperactivation is also considered a negative prognostic marker cancer<sup>20</sup> because it is more frequently found in poorly differentiated tumors, that generally are more invasive. For instance, several groups have proved Akt hyperactivation in human primary thyroid cancers,<sup>21,22</sup> which are generally employed for *in vivo* cellular studies. Also, the PI3K-Akt-mTor axis is strongly involved in many events that control the tumor progression and invasion, as cell mobility, metastasis and cell adhesion properties.<sup>23,24</sup>

The angiogenesis event, essential for tumor growth and metastasis,<sup>25</sup> is promoted by Akt modulating the activity of several downstream targets as FOXO, NOS (nitric oxide synthase) and GSK-3 $\beta$ .<sup>26</sup> These factors increase the hypoxia-inducible factor 1 alpha (HIF-1 $\alpha$ ) expression, an activator of the vascular endothelial growth factor (VEGF), demonstrating once again the involvement of Akt in tumor events.

Finally, many evidences support the role of Akt in the mechanisms of resistance to therapies based on cytotoxic agents, hormones, biological agents and radiation, making tumor cells resistant to antitumor agent.<sup>27</sup>

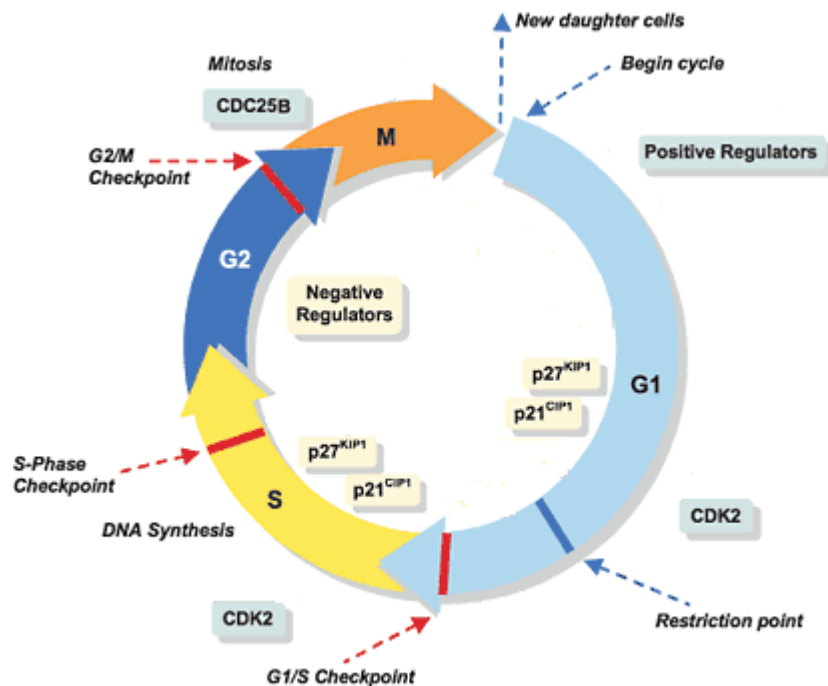


**Figure 1.4:** Akt and cell-cycle regulation with the main regulators involved.

### 1.3 Main inhibitor categories

In the last years, the search of potential inhibitors of the Akt has gained great attention. Among the strategies to inhibit this enzyme, compounds able to bind the ATP site, allosteric inhibitors binding a site adjacent to the ATP pocket and inhibitors of PIP<sub>3</sub> binding, have been developed over the years.

#### 1.3.1 ATP-competitive protein kinase inhibitors

A potential class of Akt inhibitors is focused on the ATP-binding site. Small molecules included isoquinolone-5-sulfonamides,<sup>28</sup> indazole,<sup>29</sup> aminofurazan analogues<sup>30</sup> and pyrazole<sup>31</sup> have been reported as ATP-binding site inhibitors. However, the highly conserved ATP-binding domain in kinases, makes difficult their application due to low selectivity. For instance, compound GSK690693 **1**,<sup>32</sup> a potent inhibitor of Akt1, 2 and 3 developed by GlaxoSmithKline, is able to inhibit the growth of ovarian, breast and prostate tumors in mice, but it inhibits also other kinases. Also an indazole-pyridine based compound A-443654 **2**,<sup>33</sup> identified by Abbott, is resulted active in blocking the growth of pancreatic and prostate tumors, but also in this case, without selectivity for Akt (Figure 1.5).

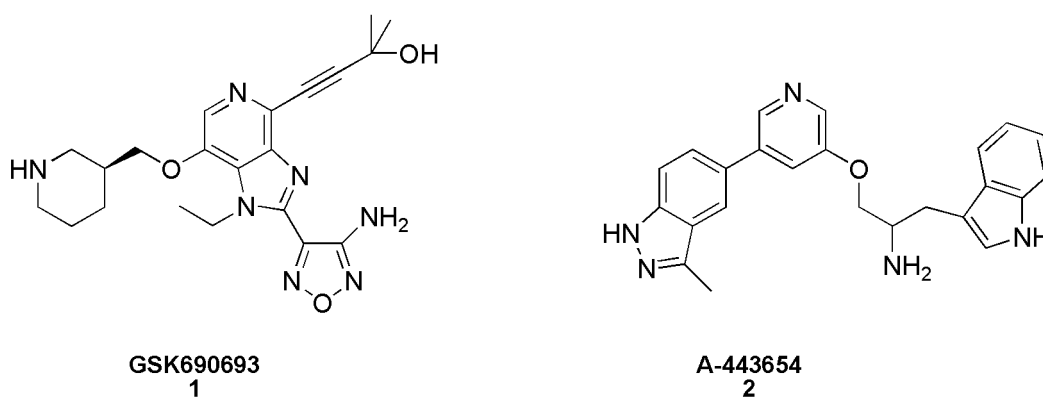


**Figure 1.5:** ATP-competitive inhibitors **1**, developed by GlaxoSmithKline, and **2**, identified by Abbott, both not having selectivity for Akt.

#### 1.3.2 Allosteric inhibitors

An allosteric inhibitor is a compound which binds the enzyme, in a site called allosteric, inducing a conformational change and reducing its affinity for the natural ligand. Using this effect, different allosteric inhibitors for Akt have been proposed, among that the fungal metabolite wortmannin **3**<sup>34</sup> and the flavonoid derivative LY294002 **4**<sup>35</sup> (Figure

1.6). Nevertheless, because of their toxicity and the low stability, together with the instability of **3** in water and the insolubility of **4**, their potential pharmaceutical applications are limited.

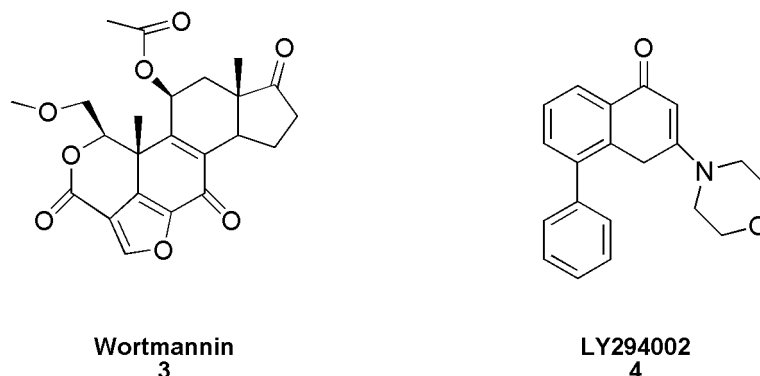


**Figure 1.6:** Allosteric inhibitors wortmannin **3** and flavonoid derivative LY294002 **4**.

A deep study devoted to seek better allosteric inhibitors was carried out by Lindsley and co-worker<sup>36</sup> which identified through a high throughput screening 2,3-diphenylquinoxaline **5** (Figure 1.7) as lead compound able of inhibiting specifically Akt. Particularly, in assays with Akt mutants lacking the PH domain, this compound displayed no inhibition; moreover, Akt inhibition was not competitive with ATP, suggesting an allosteric binding site. Based on this lead compound, these authors have developed a library of allosteric inhibitors by introducing structural chemical modification addressed to delete *gem*-dimethyl function and to replace the primary amine with several functionalized amines. Introducing these structural modifications, compound **6**, 10-fold more potent than **5**, was synthesized, even if it results poor soluble and lacking of cell activity. Proceeding toward the study of these lead compounds, these same authors have discovered a novel series of potent allosteric Akt kinase inhibitors based on a 2,3,5-trisubstituted pyridine core **7** with improved aqueous solubility, cell permeability and reduced molecular weight relative to the previously reported inhibitors<sup>37</sup> and, at a later stage, their further optimization to give **8a,b**.<sup>38</sup>



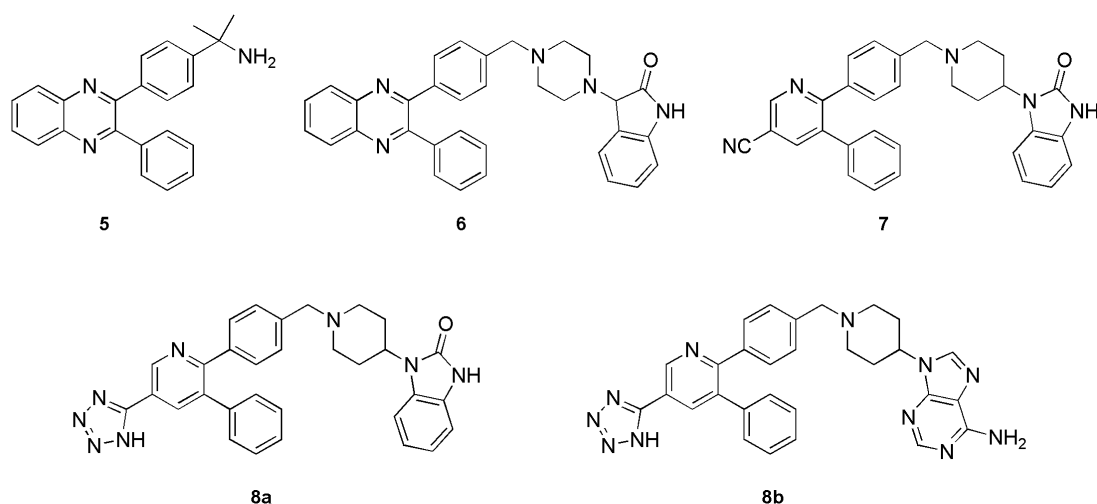
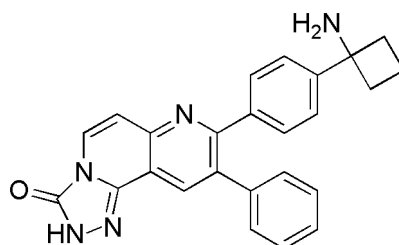


**Figure 1.7:** Allosteric inhibitors developed by Lindsley and co-workers.

Another 2,3-diphenylquinoxaline derivative, the MK-2206 **9**,<sup>39</sup> which inhibits the growth of several tumors, has been reported by Merck & Co. (Figure 1.8). This compound has recently entered a Phase I clinical trial in patients with solid tumors where it results tolerated. However, further developments of this promising compound are on hold. Thanks to their good selectivity for Akt, allosteric inhibitors have progressed quickly into clinical development.



**MK-2206**  
**9**

**Figure 1.8:** Compound MK-2206 **9** developed by Merc & Co. in phase I clinical trials.

### 1.3.3 Inhibitors of PIP<sub>3</sub> binding

An alternative to look for selective Akt inhibitor is targeting the pleckstrin homology PH domain. It is present in a relatively small number of kinases,<sup>40</sup> as phospholipase C- $\delta$  (PLC  $\delta$ ), Bruton's tyrosine kinase (BTK) and Akt. In particular, PH domain is answerable to bind phospholipids derivatives, playing a key role in the regulation of several

intracellular signalling, *i.e.* cell-cycle regulation, apoptosis and tumor progression in the case of Akt. Specifically, blocking the interaction between Akt PH domain and its natural phosphatidylinositol ligands, it is possible to interfere with the conformational change of the Akt preventing the exposure of the phosphorylation sites that mediate the activity. In this way, the kinase remains in the inactive state unable to phosphorylate signalling proteins in the cytoplasm and in the nucleus. This mechanism of inhibition can represent a promising approach in cancer drug discovery. So, new inhibitors targeting the PH domain have been designed and proposed as analogues of natural phosphatidylinositols. The structure of the phosphatidylinositol 3,4,5 triphosphate PIP<sub>3</sub> **10**, (Figure 1.9), is composed by an inositol ring with the phosphate group in position 3, accountable for the salt bridge with an arginine residue of the PH domain, and a 1,2-diacyl diacyl glycerol moiety with long lipophilic chains, necessary for the anchorage to the plasma membrane,<sup>40</sup> linked to the position 1 through a phosphate ester bridge.

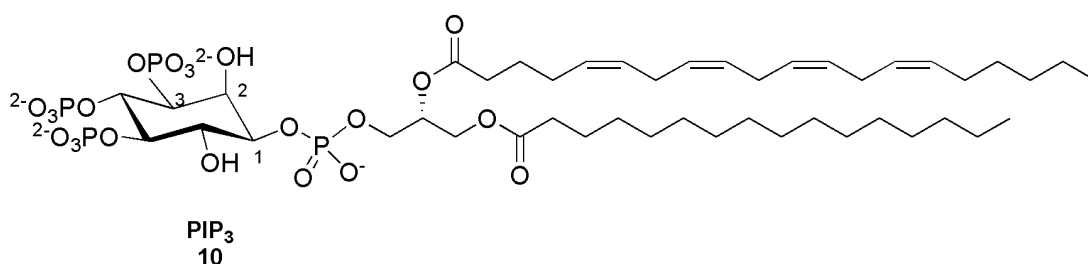


**Figure 1.9:** Chemical formula of phosphatidylinositol 3,4,5 triphosphate PIP<sub>3</sub> **10**, natural ligand of Akt PH domain, with palmitate (C16:0) on the *sn*-1 position and arachidonic acid (C20:4) on the *sn*-2 position of the glycerol moiety.

In order to obtain synthetic analogues of the natural PIP<sub>3</sub>, different chemical structural modifications have been taken into account.<sup>41</sup> To overcome drawbacks of stability, the labile phosphate ester linkage between the inositol ring and the diacylglycerol moiety has been substituted by carbonates or ether linkage instead of ester in the glycerol function was introduced and, finally, the same inositol ring has been replaced by similar scaffold. These new classes of inhibitors targeting the PH domain as analogues of natural phosphatidylinositols include phosphoinositide analogues, alkylphospholipids and inositol phosphates.

The first example of the use of phosphatidylinositol analogue as possible inhibitors was reported by Kozikowski.<sup>42,43</sup> The D-3-deoxy-phosphatidyl-*myo*-inositol **11** (DPI,

Figure 1.10) showed inhibition of Akt *in vitro* at low concentration, but resulted only a weak inhibitor *in vivo* in the different cellular system tested. The low inhibition of **11** could be explain by the hydrolysis of the ester lipids in the glycerol moiety by means of phospholipases. Hence the idea of introducing the more metabolically stable ether lipid chains. Also this new class of analogues, the D-3-deoxy-phosphatidyl-*myo*-inositol ether lipid **12** (DPIEL, Figure 1.10) was found to inhibit the Akt.<sup>44</sup> Nevertheless, its clinical use was severely limited because of its acid lability if orally administered, while the intravenously administration causes the induction of a massive hemolysis. Another structural modification focused to increase the stability of PIP<sub>3</sub> analogues, consists in the replacement of the phosphate bridge with a carbonate<sup>45</sup> (DCIEL, Figure 1.10). However, compound **13** does not result a good inhibitor of Akt/PI3K pathway in all cells lines tested. Molecular modeling and docking of these three classes, showed that DPIEL binds much more strongly to the Akt PH domain than DPI and DCIEL. Despite this, the inhibitory activity *in vivo* is hindered by physiological presence of natural substrates *myo*-inositol. Therefore, their toxicity and lower solubility have limited their development as potential drug candidates.

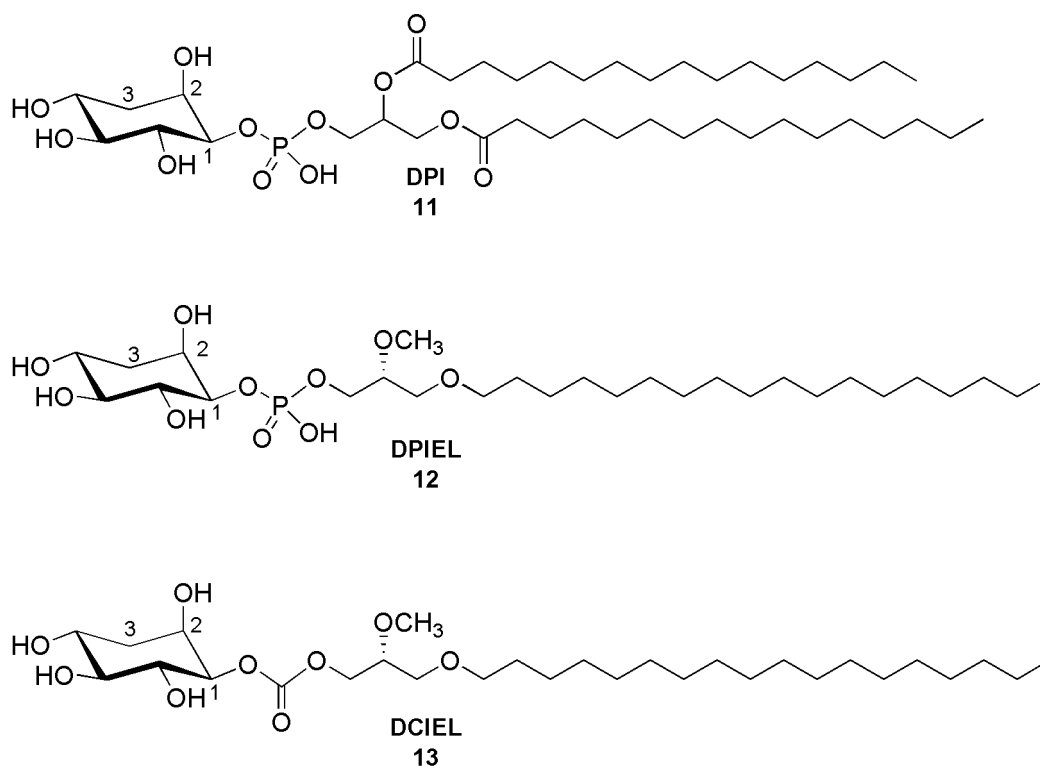
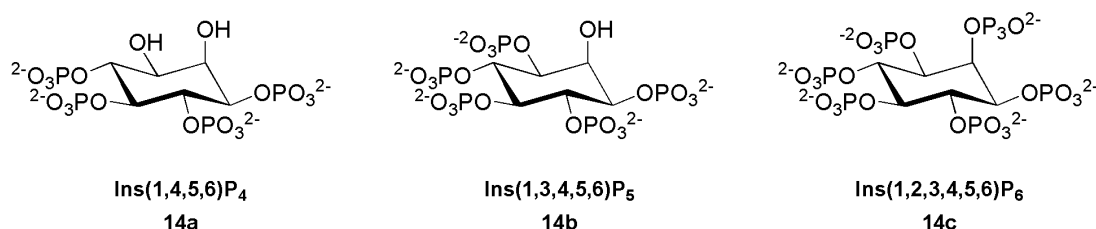


Figure 1.10: Phosphatidylinositol analogues.

Another class of compounds deeply studied are the inositolphosphate-based inhibitors (Figure 1.11). Besides their well-known role of second messengers, variously phosphorylated inositols **14a**, **14b** and **14c**, have attracted great attention as therapeutic molecules.



**Figure 1.11:** Inositolphosphate inhibitors.

Falasca<sup>46,47</sup> have proposed a competitive mechanism for these compounds against the natural ligand PIP<sub>3</sub> in the binding PH domain, probably preventing the translocation of Akt to the plasma membrane. Different inositol polyphosphates were evaluated and compound 1,3,4,5,6-pentakisphosphate **14b** [Ins(1,3,4,5,6)P<sub>5</sub>] resulted able to inhibit Akt activation *in vivo* at very low concentration.

In particular, compound **14b** promotes also apoptosis in human lung, ovarian and breast cancers characterized by an high Akt activity.

An innovative category of potential Akt kinase inhibitors are the more recent glucose-based inositol analogues<sup>48</sup> (Figure 1.12). In derivatives **15**, the inositol ring of the natural PIP<sub>3</sub> has been substituted by a glucose scaffold, in which the pyranosidic oxygen replaces the hydroxyl group in position 2 of the inositol, while the diacyl glycerol moiety is replaced by a more stable phosphoramidate group β-linked to the anomeric position of the sugar and carrying two acyl chains. Moreover, instead of the phosphate group in position 3 of the inositol ring, corresponding to the position 6 of the glucose, a carboxyl group was inserted in derivatives **16**. The long acyl chains have been also substituted by shorter ones, assuming that the long lipophilic chains are not needed for biological activity, but only for the anchorage to the membrane.<sup>40</sup>

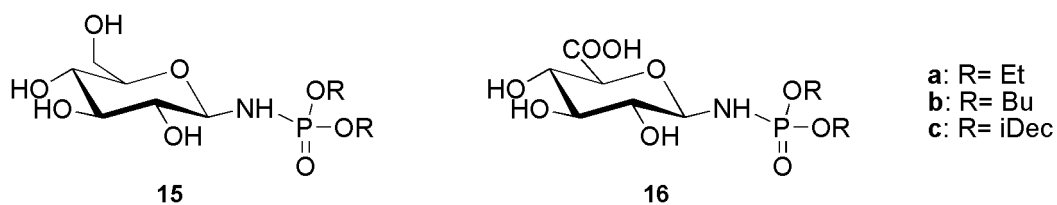


**Figure 1.12:** Glucose-based inositol analogues as inhibitors of Akt.

The inhibition power of these compounds against Akt activation, employing an *in vitro* Kinase Assay Kit, was evaluated. The results show that compounds **16** are more active than **15**, underlining the importance of a negative charge.

Research studies regarding these different classes of potential inhibitors developed over the years laid the foundation and, at the same time, paved the way towards the search for new classes of compounds to the aim of improving the knowledge about Akt/PI3K pathway and finding a new class of best inhibitors to use in cancer therapy.

## Chapter 2

### Synthetic analogues of natural compounds as potential inhibitors targeting Akt for anticancer drugs

#### 2.1 Introduction

The many biological processes in which Akt is involved, above all cell-cycle regulation and the various aspects of tumor cells like proliferation and differentiation, as well as the lacking of an adequate class of inhibitors already discussed in *Chapter 1*, make still now this protein kinase subject matter of research in order to find novel alternative inhibitors and promote the discovery of new anticancer drugs. In particular, compounds that interfere with the activation of Akt by preventing the binding of PH domain with the natural ligand phosphatidylinositol triphosphate PIP<sub>3</sub> could be desirable because of their potential higher selectivity.

Nature is often largely exploited as source of compounds characterized by potential therapeutic properties. For instance, the sulfoquinovosylacylglycerols **17** (SQDG) in which sulfoquinovose (6-deoxy-6-sulfo-glucose), with a negative charge in position 6 of the sugar, is  $\alpha$ -linked to the *sn*-3 position of an acylglycerol<sup>49</sup> are a class of natural glycoconjugates evaluated as promising compounds in different therapeutic areas including anti-cancer therapy. This class of compounds shows structural features common to PIP<sub>3</sub> **10**, the natural ligand of the PH domain highlighted in Figure 2.1, such as the glycerol motif bearing long acyl chains and a negative head.

Our research group headed by Professor Fiamma Ronchetti has developed over the years a synthetic procedure aimed to synthesize sulfoquinovosyldiacylglycerols analogues **18a-c** and the corresponding monoacylglycerol derivatives **19a-c** showed in Figure 2.2, based on the same 2-*O*- $\beta$ -D-glucosylglycerol scaffold.

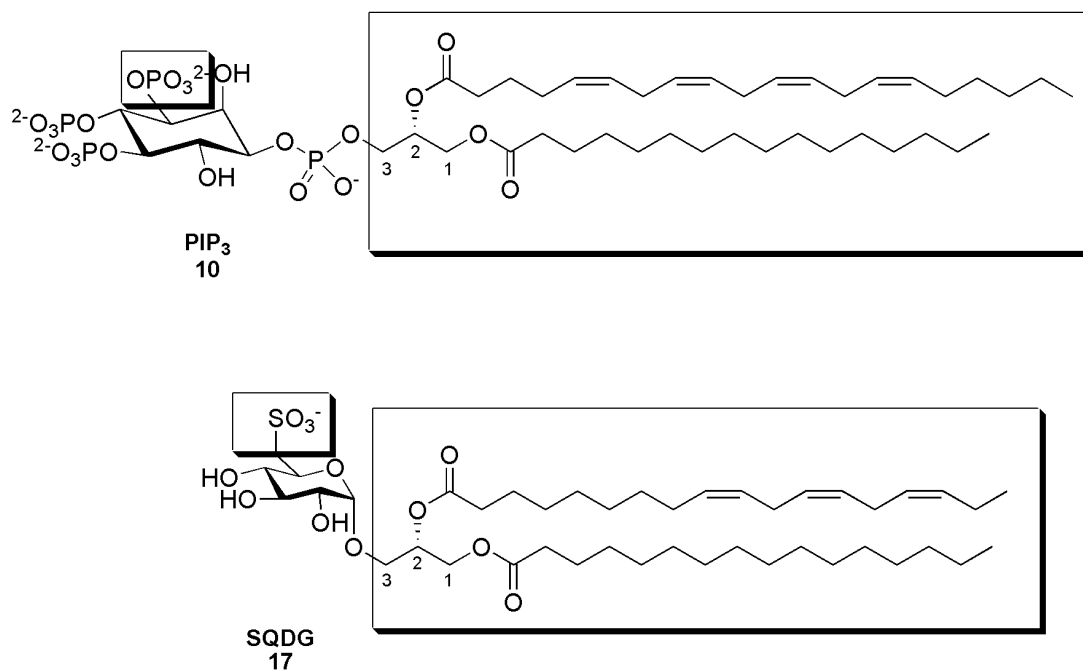


**Figure 2.1:** Natural sulfoquinovosylacylglycerols SQDG **17** and common features with the natural  $\text{PIP}_3$  **10**, natural ligand of Akt.

These compounds were synthesized and tested as anti-tumor promoters in cancer prevention studies.<sup>50</sup> As the natural SQDG, they possess the key features needed for interaction with the PH domain, as an acyl glycerol portion and a negative head. These likeness prompted us to evaluate the Akt inhibitory activity of our sulfolipids **18a-c** and **19a-c** together with others simplified compounds which were also synthesized. These last ones were the sulfoquinovosyl-2-*O*- $\beta$ -D-glycerol **20** which do not bear acyl chains on the glycerol moiety, the glucoglycerolipid **21**<sup>50</sup> lacking the characteristic sulfonate group to evaluate the influence of the negative charge, the methyl and octyl- $\beta$ -D-sulfoquinovosides **22** and **23**, in which the glycerol moiety is replaced by a lipophilic chain directly linked to the anomeric position and, finally, compound **24** where the anionic carboxyl group is replaced by the cationic amino group.

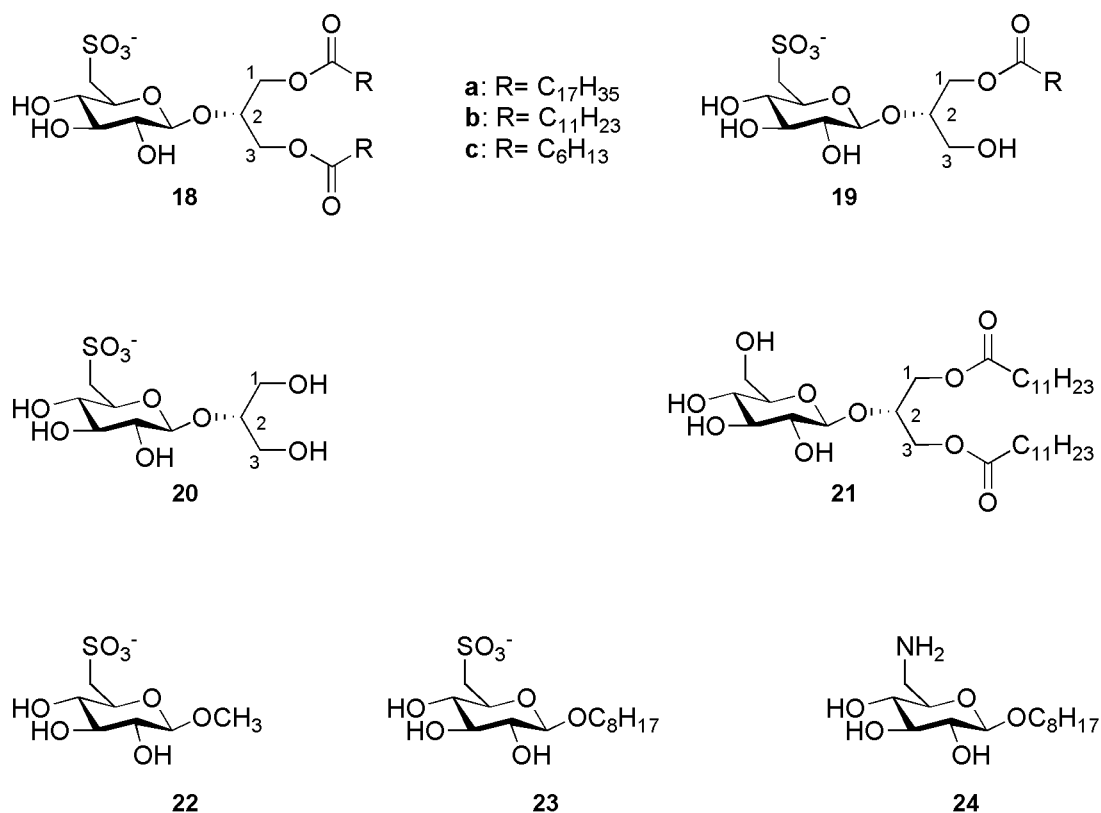


**Figure 2.2:** Sulfoquinovosyldiacylglycerols **18a-c**, the corresponding monoacylglycerol derivatives **19a-c** and simplified analogues **20-24**.

First of all, the synthesized compounds **18-24** were assayed *in vitro* using a cell-free assay, at fixed concentration of 100  $\mu\text{M}$ , employing a commercial Kinase Assay Kit.

The results of ELISA test, represented in Figure 2.3, show that compounds **18a** with sulfonate group and diacylglycerol with long chains, the corresponding monoacylglycerol **19a** and octyl sulfoquinovopyranoside **23** are the most active Akt inhibitors, which show as common features the longest alkyl chain and the anionic group in position 6 of the glucose scaffold. On the other hand, compound **20** missing of the acyl chains on the glycerol and the amino derivate **24**, with a positive charge, are the less active ones as further proof of the need of lipophilic moiety, which mimics the diacylglycerol group of  $\text{PIP}_3$ , and of a negative charge for the interaction with basic residues in the PH domain since a positive charge is not accepted by the enzymatic pocket for the presence of a repulsive cationic residues. Moreover, the length of the alkyl chain influences the potency of the sulfonate derivatives, indeed compounds with longer chains show higher activity, while the number of acyl chains seems to be not important (series **18** vs **19**).



The Akt1/2 kinase allosteric inhibitor (1,3-Dihydro-1-(1-((4-(6-phenyl-1H-imidazo[4,5-g]quinoxalin-7-yl)phenyl)methyl)-4-piperidinyl)-2H-benzimidazol-2-one trifluoroacetate salt hydrate, indicated as **A6730** from Sigma), included in ELISA studies as reference compound, showed 75% inhibition of Akt, demonstrating the strength of the test.

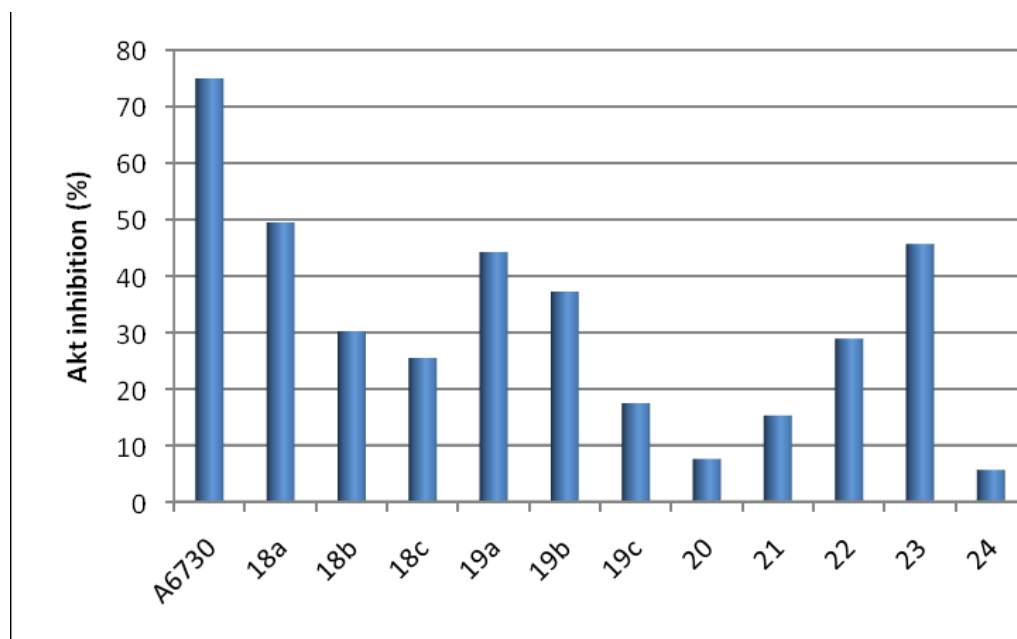


**Figure 2.3:** Inhibitory activity of compounds **18-24** against Akt. Akt activity was assayed through a specific ELISA test. Compounds were added at a concentration of 100 $\mu$ M and the data represent the mean of three independent experiments.

The most active *in vitro* compounds, with the exception of **18a**, which resulted insoluble in DMSO, together with compound **24** as negative control have been tested for their antiproliferative activity on three papillary thyroid carcinomas PTC cell lines characterized by constitutive activation of Akt pathway functionally related to RET/PTC-1 rearrangement (TPC-1 cells), to PI3KCA gene E542K mutation (K1 cells) and to decreased expression of the dual-specificity phosphatase PTEN (Nim-1 cells). Despite a comparable inhibitory efficacy of compounds **19a** and **23** in the Akt kinase assays only **19a** exhibited a biological effect being favored in the cellular tests (Figure 2.4a).

Next, the efficacy of the sulfoglycolipids compounds was assessed on the ovarian carcinoma cell line. To facilitate drug uptake and interaction with the target, cells were treated in the absence of serum. In this model, compound **19a** effectively reduced cell growth in a concentration-dependent manner, whereas compound **24** slightly affected

cell proliferation and compound **23** was substantially inactive up to 50  $\mu\text{M}$  (Figure 2.4). Again, despite a comparable inhibitory efficacy of compounds **19a** and **23** in the ELISA Akt kinase assay (Figure 2.3) only **19a** exhibited a biological effect being favored in the cellular tests.

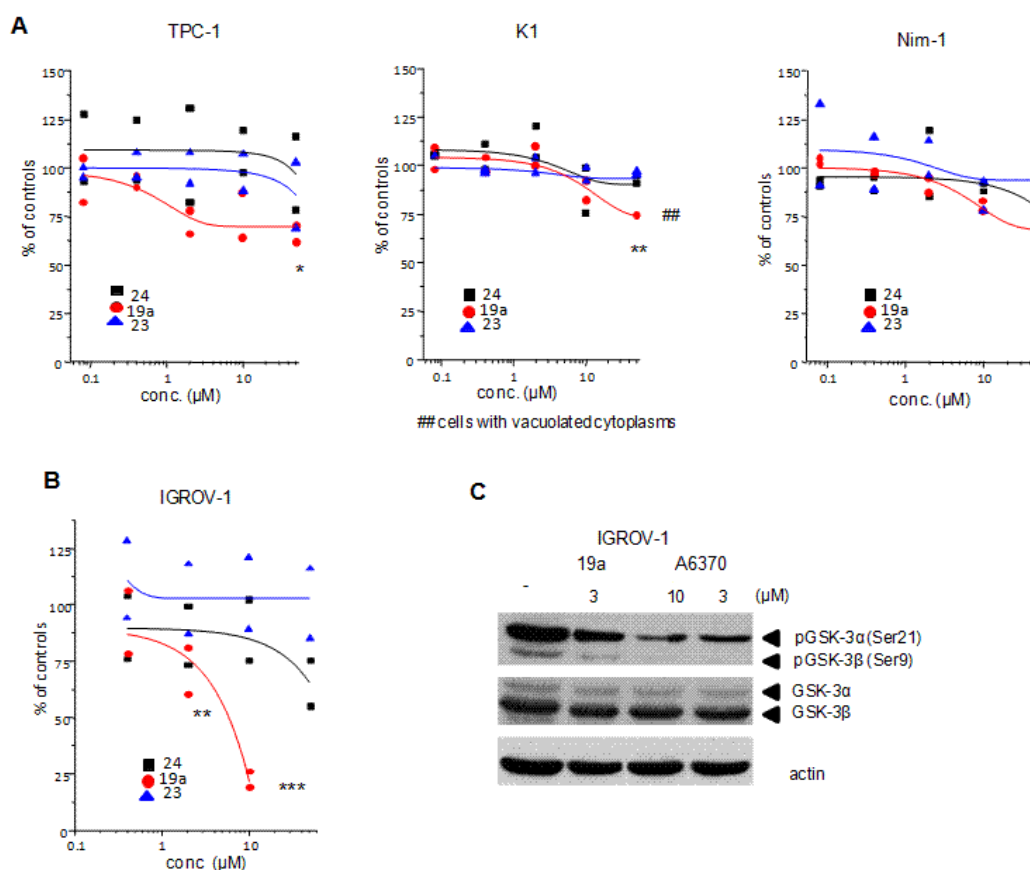


**Figure 2.4:** (A) Effect of selected sulfoglycolipids on papillary thyroid carcinoma and (B) ovarian carcinoma cell proliferation. Cells were exposed to vehicle or to different concentrations of the indicated compounds in complete medium for 72h (A) or for 24h (B). Cells were counted by a Coulter counter 72h after the beginning of the treatment. Mean dose-curves from data obtained in two independent experiments are reported. \*  $p < 0.05$ ; \*\*  $p < 0.001$ ; \*\*\*  $p < 0.0001$  versus vehicle-treated cells. (C) Inhibition of GSK-3 $\alpha$  and -3 $\beta$  phosphorylation in IGROV-1 cells exposed to compound **19a** and to known inhibitor (**A6730**) as reference compound. Cells were exposed to vehicle (-) or the indicated drug concentrations for 24h. Whole cell lysates were analyzed by Western blotting.

These preliminary results achieved with the synthetic analogues of SQDG prompted us towards the search of other potential inhibitors of Akt based on carbohydrate structure bearing a glycerol moiety properly functionalized and a different negative charge.

## 2.2 Aim of the work

Following our ongoing interest in the search of potential inhibitors binding the Akt PH domain and basing on the results previously obtained with the synthetic analogues of SQDG, we planned to prepare a new class of potential inhibitors, replacing the sulfonate group in position 6 of the glucose scaffold with a different negative charge, selecting the carboxylate group. This choice was motivated by a precedent investigation reported by Cipolla<sup>48</sup> in which synthetic compounds based on the glucose-scaffold and characterized by the presence of a carboxyl group in position 6 of the sugar, were evaluated as Akt inhibitors. The substitution of the sulfonate group in our synthetic SQDG with the carboxylate group led to the generation of new compounds that could be referred to another class on natural compounds, the glucuronosyldiacylglycerols **25** (GlcADG, Figure 2.5).

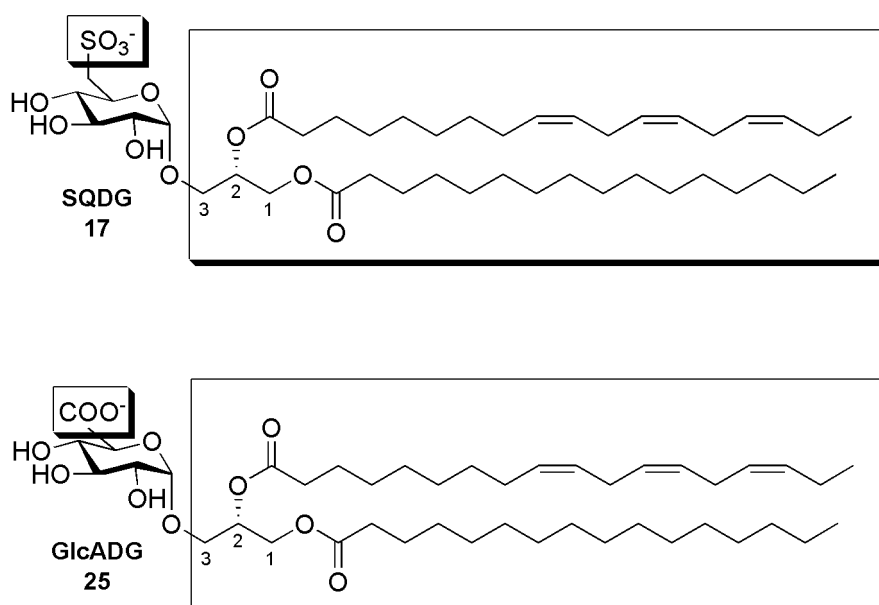


**Figure 2.5:** Natural sulfoquinovosyldiacylglycerol **17** (SQDG) and the corresponding natural glucuronosyldiacylglycerol **25** (GlcADG).

Natural GlcADGs have been found in bacteria,<sup>51</sup> fungi,<sup>52</sup> algae<sup>53</sup> and in some higher plants such as rice.<sup>54</sup> They share with the SQDG some biosynthetic pathways in chloroplasts. Indeed, in condition of phosphate deprivation, SQDG and GlcADG, produced by the same synthase (Figure 2.6), replace the phospholipids in the membrane lipid remodelling promoting the remobilization of the phosphorus.<sup>55,56,57</sup>

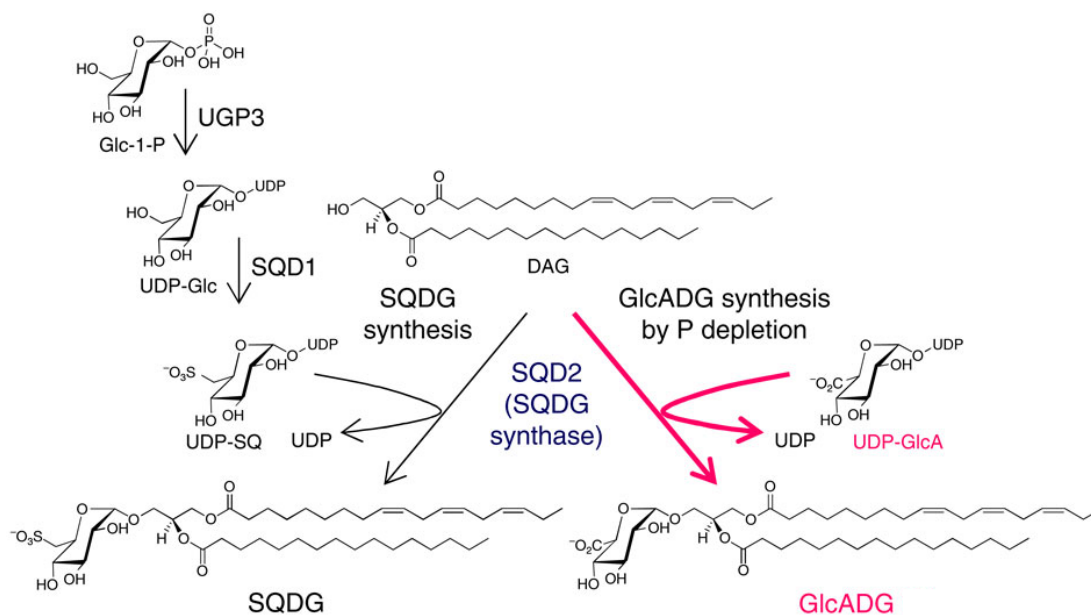


**Figure 2.6:** The biosynthesis of SQDG in chloroplast involves three different enzymes, the UGP-3, the SQD1 and the SQD2. The last one is also responsible of GlcADG in case of P-deficient conditions. Taken from Ref.<sup>54</sup>

Due to the strict structural resemblance of SQDG, GlcADG and PIP<sub>3</sub>, the natural activator of Akt, and relying to the results previously achieved for our synthetic sulfolipids, part of my PhD project was devoted to the preparation of a small library of synthetic analogues of GlcADG to test for Akt inhibition. Specifically, 2-*O*- $\beta$ -D-glucuronosyldiacylglycerols **26a** and **b** and the corresponding monoacyl **27a** and **b** in which the glucose is  $\beta$ -linked to the position 2 of the glycerol, as well as glucuronides **28a,b** as simplified anionic models, showed in Figure 2.7, have been synthesized.

The common scaffold for all of them remain a D-glucose  $\beta$ -linked to an acylglycerol with acyl chains of different length or directly connected to a lipophilic chain. The choice of the length of the chains was based on the results previously discussed that showed an higher activity for the longest chains.

All the compounds obtained (Figure 2.7) have been evaluated for their inhibitory activity on Akt, both in an isolated enzyme system and in an ovarian carcinoma cell line.

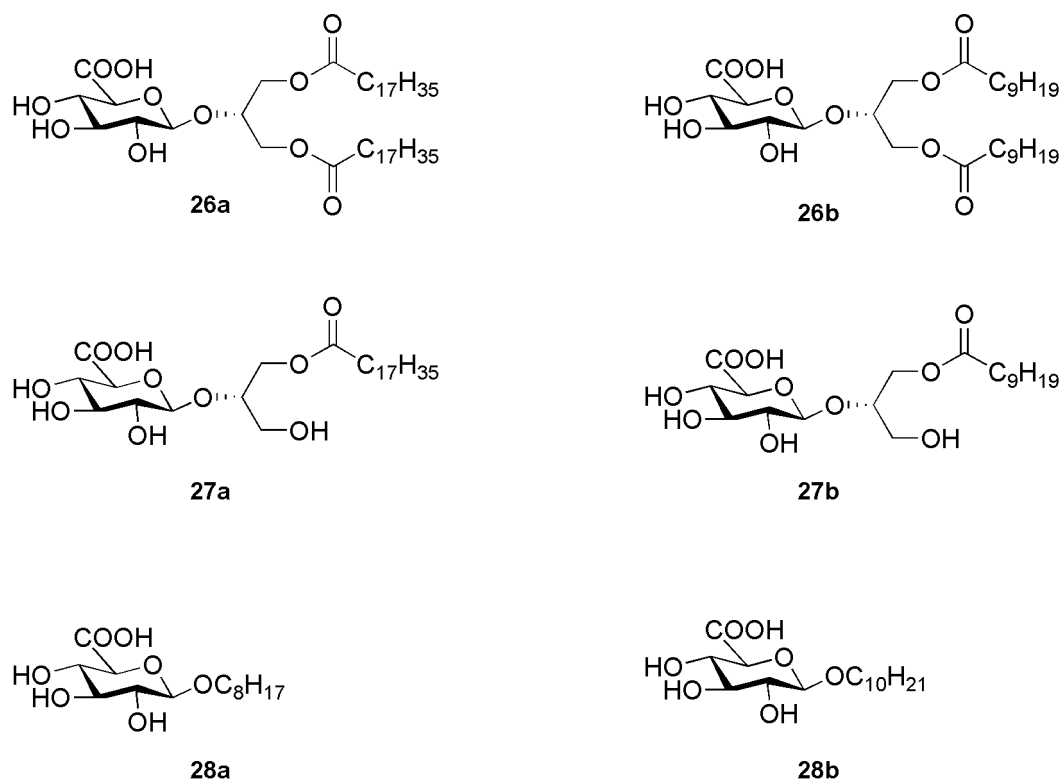


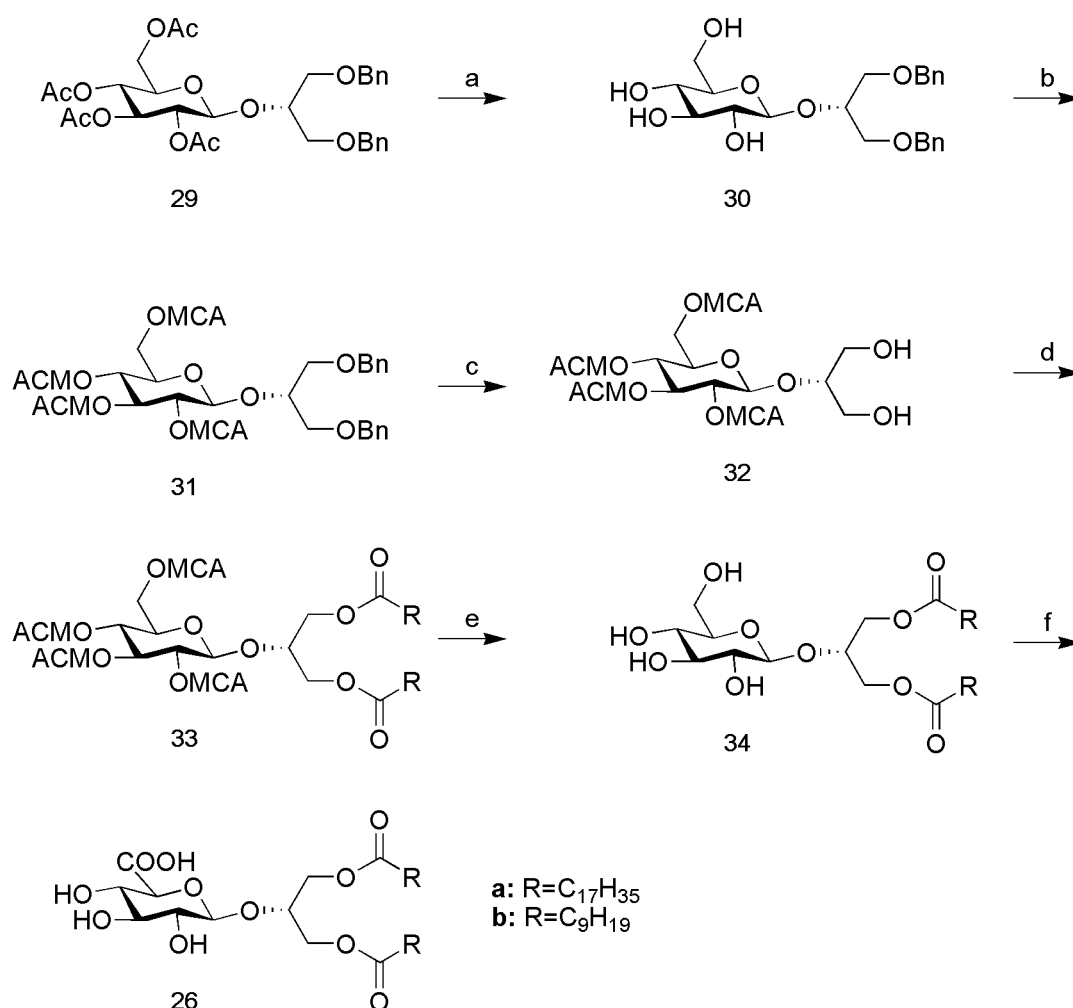
Figure 2.7: Structures of the GlcADGs analogues synthesized.

## 2.3 Results and discussion

### 2.3.1 Synthesis of diesters 26a,b

Compounds **26a,b** were prepared starting from the known 2-*O*-(2',3',4',6'-tetra-*O*-acetyl-β-*D*-glucopyranosyl)-*sn*-glycerol **29**, synthesized following a reported procedure developed by our research group<sup>58</sup> using glucose pentaacetate and 1,3-dibenzylglycerol, both commercially available. The following synthetic scheme was based on that already used for the synthesis of the sulfoquivonosil analogues **18a-c**<sup>50</sup> with the exception of the last oxidation step necessary to obtain the final compounds **26a,b**. Thus, the acetates on the sugar of compound **30** were removed with a Zemplén reaction and replaced with monochloroacetates as temporary protective groups by chloroacetic anhydride treatment in a dichloromethane/pyridine mixture at 0°C. The glycerol benzyl groups of compound **31** were removed by hydrogenolysis on 10% Pd/C in methanol to yield **32** that was functionalized on the free hydroxyl groups with the appropriate acid chloride achieving **33a** or **b**. The known 1,3-di-*O*-octadecanoyl-2-*O*-β-*D*-glucopyranosyl-*sn*-glycerol **34a**<sup>50</sup> and the corresponding didecanoyl **34b** were obtained *via* hydrazinolysis by means of hydrazine acetate treatment in a mixture of

methanol and ethyl acetate 1:1 at room temperature. A final oxidation step to obtain compounds **26a,b** was carried out by means of 2,2,6,6-tetramethyl-1-piperidinyl-oxy (TEMPO), a selective oxidant of primary alcohols, in the presence of NaClO 15% and NaClO<sub>2</sub> 20% aq solutions. A biphasic acetonitrile/sodium phosphate buffer pH 6.7 system was used and after stirring overnight at room temperature a water solution 0.5 M of sodium thiosulfate Na<sub>2</sub>S<sub>2</sub>O<sub>3</sub> and a few drops of acid chloride concentrated to set pH to 2 were added. Finally, the extraction with diethyl ether allows to achieve the products as acid (Scheme 2.1).

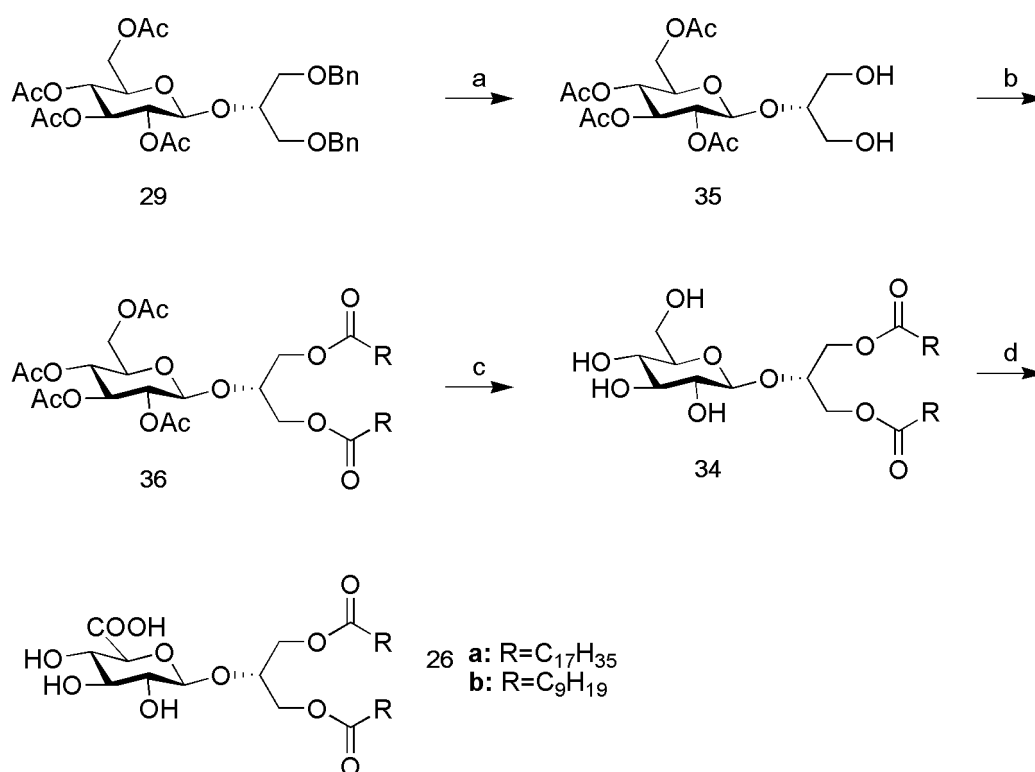


**Scheme 2.1:** a) CH<sub>3</sub>ONa, CH<sub>3</sub>OH, rt, 90%; b) Chloroacetic Anhydride, Py dry, CH<sub>2</sub>Cl<sub>2</sub> dry, 0°C, 93%; c) H<sub>2</sub> Pd/C (10%), CH<sub>3</sub>OH, 80%; d) Specific acid chloride, CH<sub>2</sub>Cl<sub>2</sub>/Py, -10°C, 60-70%; e) Hydrazine Acetate, AcOEt/CH<sub>3</sub>OH, rt, 42-43%; f) TEMPO, NaClO/NaClO<sub>2</sub>, CH<sub>3</sub>CN, 0.67M phosphate buffer (pH 6.7), rt, 43-80%.

### 2.3.2 Attempt to reduce the synthetic steps to synthesize compounds 26a,b

In order to reduce the synthetic steps to obtain compound **26a** or **b**, we have sketched the different synthetic scheme showed below (Scheme 2.2).

In this new strategy we performed the hydrogenolysis on the known **29** to give the tetraacetate **35** which was subsequently acylated the free hydroxyl groups of glycerol by acid chloride treatment achieving **36a** or **b**. At this point, following a recently reported procedure,<sup>59</sup> we used hydrazine hydrate in aqueous ethanol 85% at 45 °C to selectively remove the acetate groups from the sugar to obtain compound **34**.



**Scheme 2.2:** a) H<sub>2</sub>, Pd/C (10%), CH<sub>3</sub>OH, rt, 90%; b) Specific acid chloride, CH<sub>2</sub>Cl<sub>2</sub>/Py, -10°C, 35-40%; c) Hydrazine hydrate, EtOH aq. 85%, 45°C, 40%; d) TEMPO, NaClO/NaClO<sub>2</sub>, CH<sub>3</sub>CN, 0.67M phosphate buffer (pH 6.7), rt, 40-80%.

However, this reaction suffered from low reproducibility in our hands showing unexpected drawbacks. Very important seemed to be the reaction temperature. Working at room temperature, a white precipitate, probably due at the poor solubility of starting material, encumbered the advancement of the reaction, while at 30-35°C the reaction solution was clear, but checking through TLC none progress of reaction was evident. Also protracting the reaction time the result did not improve. On the other hand, raising the temperature at 55-60°C an high amount of by-products was

obtained in a short time. So, the best value of temperature of 45°C, adequate to take in solution the starting material and the reactive, was finally used to obtain compounds **34a** and **b**. Also, purification procedure was difficult. The removal of the solvent under vacuum in the presence of the unreacted hydrazine reactive due to high equivalents of reactive initially used (10 eq.) hampered the progress of the reaction causing the increase of the amount of by-products. To solve this drawback, the amount of reactive was reduced to 5 eq. and after 6h of magnetic stirring, the solvent was evaporated under stream of nitrogen. The crude thus recovered was subsequently purified by repeated flash chromatography with dichloromethane and methanol 9/1, giving as best result the 40% of yield.

Overcame this setback, the next step was based on the selective oxidation of the glucose primary hydroxyl group with TEMPO given **26a,b** with quantitative yield.

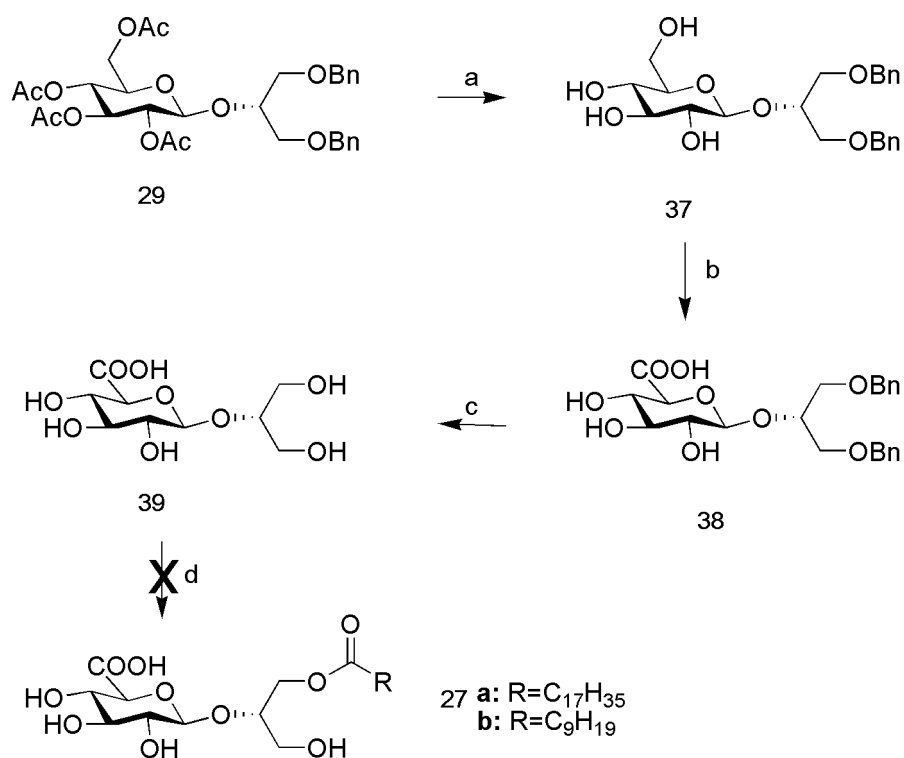
In conclusion, the reaction steps have been reduced to four against the seven steps required with the precedent strategy, but the inconvenients encountered in this new scheme have lengthened the time to achieve the same final product with an overall comparable yield.

### 2.3.3 Synthesis of monoesters **27a,b**

In an attempt to prepare the monoesters derivatives **27a** and **b** through a chemoenzymatic approach and avoiding the use of hydrazine because of low reproducibility, the fully protected compound **29** was converted with a classical Zemplén transesterification in the deacetylated **37**, which was efficiently oxidized by treatment with TEMPO in acetonitrile and buffer phosphate to yield compound **38**. The following hydrogenolysis provided compound **39** which could be selectively acylated at the *sn*-1 position of glycerol<sup>58</sup> by *Pseudomonas cepacia* lipase (LPS) catalized transesterification reaction in organic solvent, yielding in just four steps the desired products **27a** and **b** (Scheme 2.3).

However, when transesterification was carried out in the usual conditions, *i.e.* LPS in pyridine at 40°C employing 2,2,2-trifluoroethyl (TFE) esters as acyl carriers, the check of reaction progress by TLC showed a spot attributable to the product, but it was completely degraded after the work up.

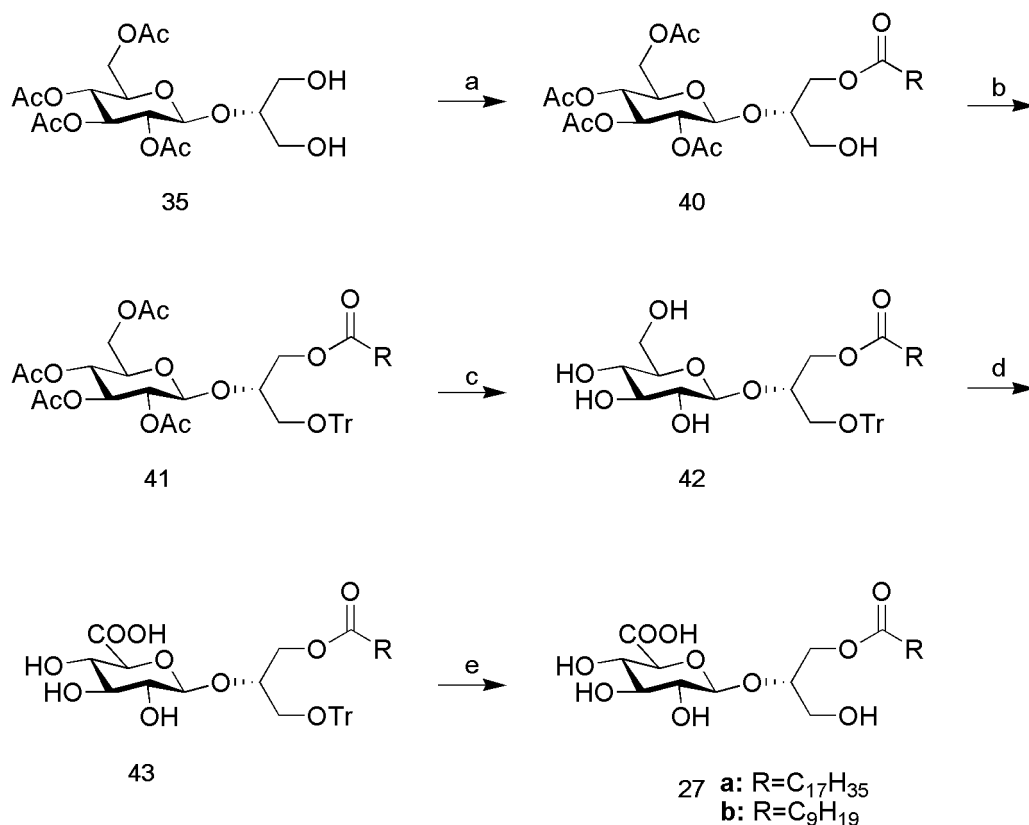




**Scheme 2.3:** a)  $CH_3ONa$ ,  $CH_3OH$ , rt, 90%; b) TEMPO,  $NaClO/NaClO_2$ ,  $CH_3CN$ , 0.67M phosphate buffer (pH 6.7), rt, 90%; c)  $H_2$  Pd/C (10%),  $CH_3OH$ , rt, 80%; d) *Pseudomonas cepacia* lipase (Amano PS), Py, TFE-octadecanoate or -decanoate, 45°C.

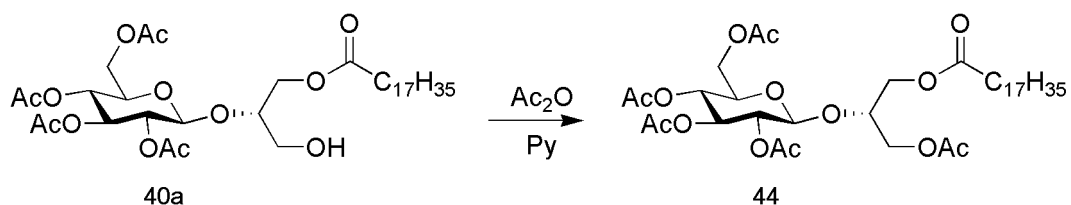
The inability to recover the product through this *via* compelled us to change strategy planning a different synthetic procedure (Scheme 2.4).

So, transesterification by means of LPS was performed on compound **35** and in this case the products **40a** or **b** were easily recovered by filtration on pad of celite, as already reported.<sup>60</sup> To protect the remaining primary free hydroxyl group of the glycerol moiety, from the following oxidation step, a conventional tritylation was performed using trityl chloride in pyridine at 100 °C. The obtained fully protected glucosylglycerols **41a,b** were converted into the deacetylated compound **42a,b** by hydrazine hydrate treatment in aqueous ethanol at 45°C for the selective removal of the sugar acetyls<sup>59</sup> using 10 eq. of hydrazine hydrate. Following TEMPO oxidation afforded the compound **43** while the removing of the trityl by giving the final compounds **27a,b** was carried out in dichloromethane exploiting the acidic resin MARATHON C, previously activated, which assured also the presence of the acid function in position 6 of the sugar.



**Scheme 2.4:** a) *Pseudomonas cepacia* lipase (Amano PS), Py, TFE-octadecanoate or -decanoate, 45°C, 74-82%; b) CPh<sub>3</sub>Cl, Py, 100°C, 96-70%; c) Hydrazine hydrate, EtOH aq., 45°C, 45-56%; d) TEMPO, NaClO/NaClO<sub>2</sub>, CH<sub>3</sub>CN, 0.67M phosphate buffer (pH 6.7), rt, 97-98%; e) DOWEX H<sup>+</sup>, CH<sub>2</sub>Cl<sub>2</sub>, rt, 76-81%.

Furthermore, to be sure about the formation of the correct stereoisomer, the derivative **40a** obtained from the enzymatic transesterification, was transformed into the 3-*O*-acetyl derivative **44** by acetic anhydride/pyridine treatment (Scheme 2.5). The <sup>1</sup>H NMR spectrum of the obtained compound **44** resulted identical to that of the known 1-*O*-octadecanoyl-3-*O*-acetyl-2-*O*-(2',3',4',6'-tetra-*O*-acetyl-β-D-glucopyranosyl)-*sn*-glycerol,<sup>58</sup> confirming the 2*S* configuration of compound **40a**.

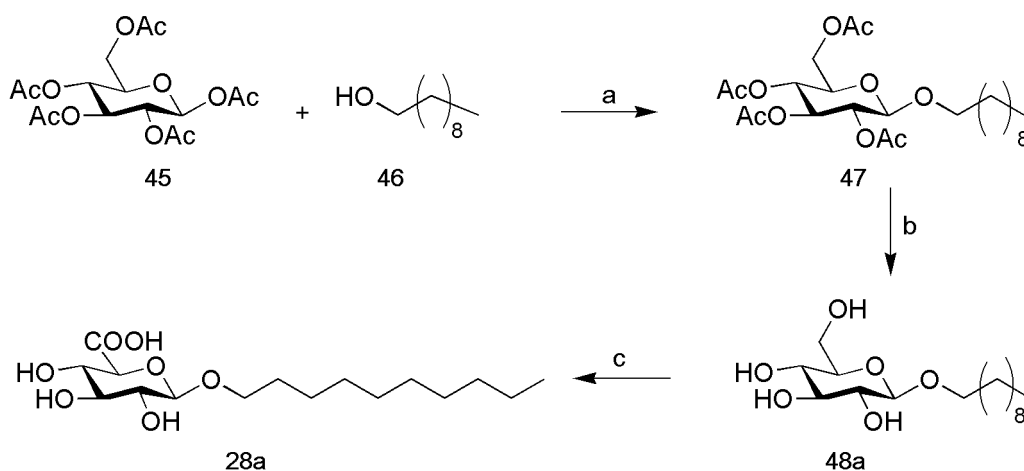


**Scheme 2.5:** acetylation of compound **40a**, by means of acetic anhydride in pyridine gives the known compound **44**.

As the enzymatic transesterifications employed to obtain the monoesters **40a** and **40b** differed just in the acyl carrier used, only the configuration of compound **40a** was assigned, assuming the same 2S configuration also for compound **40b**.

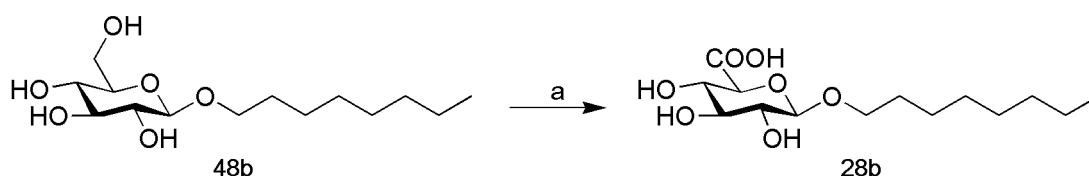
### 2.3.4 Synthesis of glucuronides **28a,b**

To synthesize the simplified glucuronides **28a**, commercial glucose pentaacetate **45** was used as starting material. The alkyl chain was introduced in Fisher conditions, using the corresponding alcohol **46** and boron trifluoride diethyl etherate  $\text{BF}_3 \cdot \text{Et}_2\text{O}$  as Lewis acid. The known decyl  $\beta$ -D-glucopyranoside **47**<sup>61</sup> was deacetylated with a classical Zemplén reaction and the free primary hydroxyl group of **48a** was converted in the carboxyl group of the product **28a**<sup>62</sup> in good yields by regioselective TEMPO oxidation (Scheme 2.6).



**Scheme 2.6:** a)  $\text{BF}_3 \cdot \text{Et}_2\text{O}$ , rt, 36%; b)  $\text{CH}_3\text{ONa}/\text{CH}_3\text{OH}$ , rt, 94%; c) TEMPO,  $\text{NaClO}/\text{NaClO}_2$ ,  $\text{CH}_3\text{CN}$ , 0.67M phosphate buffer (pH 6.7), rt, 53%.

Instead, the final compound **28b** was easily obtained in a single step by TEMPO oxidation of the commercial octyl  $\beta$ -D-glucopyranoside **48b** (Scheme 2.7).



**Scheme 2.7:** a) TEMPO,  $\text{NaClO}/\text{NaClO}_2$ ,  $\text{CH}_3\text{CN}$ , 0.67M phosphate buffer (pH 6.7), rt, 62%.

## 2.4 Cell free evaluation of Akt inhibition

Thanks to a collaboration with Dr. Barbara Costa of the University of Milano-Bicocca, the synthesized compounds, with the exception of compound **26a** that was not soluble in DMSO, were tested for their inhibitory activity against Akt (Akt1), using an *in vitro* ELISA kinase assay.

As shown in Figure 2.8, the effect of compounds **26b**, **27a-b** and **28a-b** tested at five different concentrations (1, 10, 50, 100 and 500  $\mu$ M) were compared to the alkylphospholipids (ALPs) miltefosine, a general inhibitor of the PI3K/Akt pathway, the perifosine, that is an Akt inhibitor targeting the PH domain,<sup>63</sup> and the surfactant sodium dodecyl sulfate (SDS). The results show that the Akt1 activity is poorly influenced by compound **28b**, while the other compounds showed a concentration-dependent inhibitory effect, **27a** and **26b** being the most potent inhibitors of Akt1 activity ( $IC_{50}$  19.71  $\mu$ M and 30.75  $\mu$ M respectively, Table 2.1).

Compound	$IC_{50}$ ( $\mu$ M)	95% Confidence Intervals
Compound <b>27a</b>	19.71	13.85-28.04
Compound <b>27b</b>	>100	
Compound <b>26b</b>	30.75	22.91-41.26
Compound <b>28a</b>	>100	
Compound <b>28b</b>	>100	
Miltefosine	>100	
Perifosine	43.35	22.65-83.17
SDS	>100	

**Table 2.1:** Compound concentration producing 50% inhibition of PKB1 activity.

Compounds **27b** and **28a** elicited a concentration-dependent inhibition of Akt1, however they displayed only slight efficacy, even at the maximum concentration: 24% and 39%, respectively. The  $IC_{50}$  values (Table 2.1) and the maximal efficacy indicated that the effect is higher for long than for short acyl chains (**27a** vs **27b** and **28a** vs **28b**, Table 2.1) and for the presence of a second acyl chain (**27b** vs **26b**, Table 2.1), in agreement with other data already reported.<sup>64</sup> The data obtained (Table 2.1 and Figure 2.8) for Miltefosine as well as SDS did not exhibit any significant inhibition of Akt in the ELISA test, but only a very weak inhibition was observed at very high concentrations, *i.e.* 500  $\mu$ M. On the contrary, Perifosine displayed a significant inhibition with an  $IC_{50}$

value of about 40  $\mu\text{M}$ , thus suggesting a specificity for the effect induced by glucuronides **27a** and **26b** and a potency that is comparable with that of Perifosine.

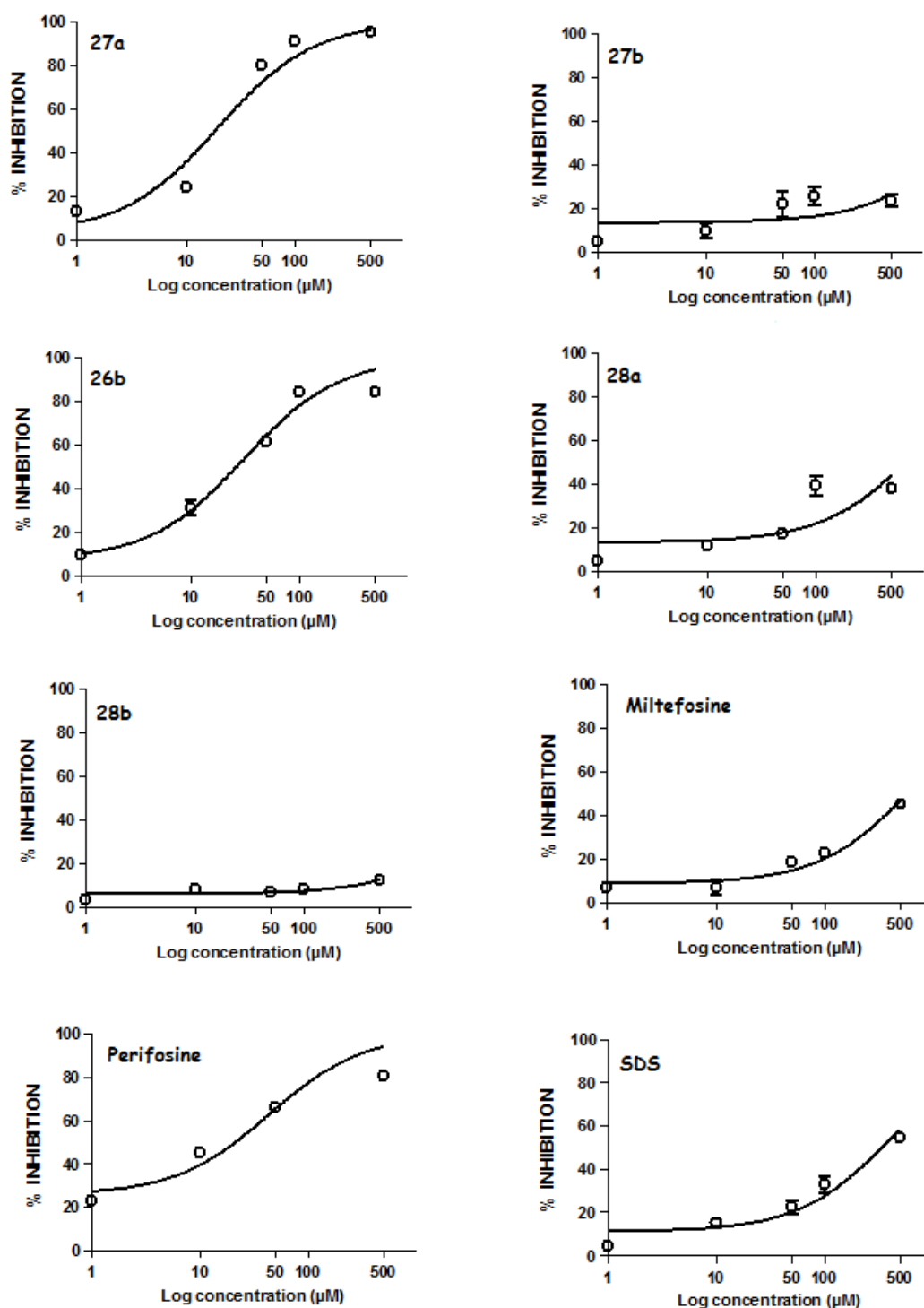


**Figure 2.8:** In vitro Akt1 Kinase Assay (ELISA) of compounds **26b**, **27a-b** and **28a-b**, Miltefosine, Perifosine and SDS at the indicated concentrations. Concentration-response (%inhibition) analysis.

## 2.5 Cellular studies

The same compounds assayed for Akt inhibition were also tested in cellular system by Dr. Paola Perego of the Istituto dei Tumori-Milano. Specifically, the antiproliferative activity was examined in the IGROV-1 ovarian carcinoma cell line which is characterized by heterozygous mutation (Hetc.955\_958delACTT) of the dual-specificity phosphatase PTEN, a negative regulator of Akt. A 72 h exposure to the compounds resulted in a concentration-dependent inhibition of IGROV-1 cell growth for three of the novel glucuronides, *i.e.* **26b** and **27a-b** (Figure 2.9). The inhibitory effect was evident for compound **26b** and **27a** with  $IC_{50}$  values ( $\pm$ SD) of  $156.7 \pm 23.0$  and  $49.0 \pm 7.6$  (SD)  $\mu$ M, respectively (Table 2.2). The **28a** and **28b** compounds induced a slight inhibition of IGROV-1 cell growth after 72 h exposure only when a concentration of 300  $\mu$ M was used. A modest inhibition of proliferation was also observed when cells were exposed to the **27b** compound, the  $IC_{50}$  value being around 300  $\mu$ M.

Since the **28a** and **28b** compounds do not contain glycerol in their structure, the present data suggest that the presence of glycerol might facilitate growth inhibition (**27b** vs **28a**). Moreover, long chains seem to enhance the activity because the **27a** compound carries a longer chain than **27b**.

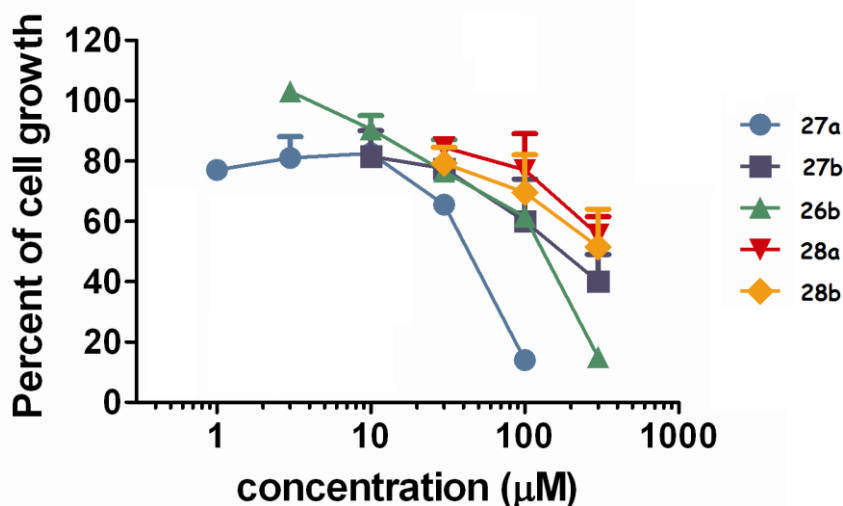


**Figure 2.9:** Cell sensitivity of human ovarian carcinoma cells (IGROV-1) as evaluated by growth inhibition assays. Cells were seeded and 24 h later they were exposed to the novel compounds for 72 h. At the end of incubation with the compounds, cells were counted with a cell counter. Results from a representative experiment are shown.

Further effort is required to optimize the growth inhibition properties of this class of compounds. Indeed, an analysis of inhibition of cell growth in cells exposed to 24 h to the studied compounds in serum-free medium indicated an increased potency for the two active compounds. Under these conditions, the IC<sub>50</sub> values ( $\pm$ SD) of compound **27a** and **26b** were  $3.35\pm 0.35$  and  $9.40\pm 5.0$   $\mu$ M, respectively (Table 2.2). This evidence raises the possibility that binding of the compounds to serum components can reduce their cellular uptake.

Compound	IC <sub>50</sub> ( $\mu$ M) $\pm$ SD
Compound <b>26b</b> with serum medium	156.7 $\pm$ 23.0
Compound <b>26b</b> serum free medium	9.40 $\pm$ 5.0
Compound <b>27a</b> with serum medium	49.0 $\pm$ 7.6
Compound <b>27a</b> serum free medium	3.35 $\pm$ 0.35

**Table 2.2:** Inhibition effect of compounds **27a** and **26b** towards IGROV-1 ovarian carcinoma cells in the presence of serum or in serum-free medium. When cells were exposed to 24 h to the tested compounds in serum-free medium an increased potency was showed.

To confirm the influence of serum presence in medium on cellular sensitivity to Akt inhibitors, we also tested the sensitivity of IGROV-1 cells to Perifosine in the presence or absence of serum in the medium (Table 2.3). Under our experimental conditions, we found that the growth inhibitory effect of the compound was favored in serum-free medium, thus implying that serum affects the stability of Perifosine. However, whereas for Perifosine a 2.8 fold increase in the anti-proliferative activity was observed upon incubation in serum-free medium, the fold-change for the novel compounds was higher, implying that they might be less stable or less prone to accumulate in the cells than Perifosine in the presence of serum.

FBS	IC <sub>50</sub> ( $\mu$ M) $\pm$ SD
+	2.21 $\pm$ 0.69
-	0.80 $\pm$ 0.29

**Table 2.3:** Sensitivity of IGROV-1 ovarian carcinoma cells to perifosine in the presence of serum or in serum-free medium. a Cell sensitivity was assessed by growth inhibition assays in which cells were exposed to perifosine for 72 h in serum (FBS)-containing medium or for 24 h in serum-free medium. Cells were counted 72 h after treatment start. IC<sub>50</sub> represents the perifosine concentration producing 50% inhibition of cell growth. The reported values are the mean  $\pm$  standard deviation of 3 independent experiments.

## 2.6 Conclusions

In conclusion, a synthetic procedure for the obtainment of new glucuronosylacylglycerols was presented in this chapter. Their inhibitory activity against Akt, both in an isolated enzyme system and in an ovarian carcinoma cell line, has been also reported. The two compounds exhibiting the best target inhibition activity in cell-free assay, *i.e.* compounds **26b** and **27a**, were found to be endowed with antiproliferative activity in ovarian carcinoma cells. Although inhibition of proliferation was observed, further efforts are needed to increase the potency of the compounds in *in vitro* cultured cells. Overall these data, by showing a clear modulation of Akt inhibition in relation to chain length and number, and also to the presence of glycerol in cell experiments, provide insights into the understanding of the structural features needed to achieve Akt inhibition.



## 2.7 Experimental section

### 2.7.1 General methods

**Chemical:** *Pseudomonas cepacia* lipase (LPS, lipase PS, specific activity 30.5 triacetin units/mg solid), from Amano Pharmaceutical Co. (Mitsubishi Italia), was supported on celite.<sup>60</sup> 2-*O*-(2',3',4',6'-Tetra-*O*-acetyl- $\beta$ -D-glucopyranosyl)-*sn*-glycerol **29**<sup>58,65</sup> 2-*O*-(2',3',4',6'-tetra-*O*-chloroacetyl- $\beta$ -D-glucopyranosyl)-*sn*-glycerol **32**<sup>66</sup> and the acyl carriers<sup>60</sup> trifluoroethyldecanoate and -octadecanoate were synthesized according to literature procedures.

All reagents and solvents used were purchased from Sigma-Aldrich as reagent grade and were purified before use by standard methods. Dry solvents and liquid reagents were distilled prior to use or dried on 4 Å molecular sieves. Air- and moisture sensitive liquids and solutions were transferred *via* oven-dried syringe through septa.

The acidic Dowex<sup>®</sup> Marathon<sup>™</sup> C sodium form resin was activated by washing it with 1M HCl and with distilled water prior to use. Column chromatography was carried out on flash silica gel (Aldrich 230–400 mesh) or by a Biotage Isolera<sup>™</sup> Prime flash purification system (Biotage-Uppsala, Sweden). Thin-layer chromatography (TLC) analysis was carried out on silica gel plate (Merck 60F<sub>254</sub>) with visualization under UV (254 nm) and/or developing with anisaldehyde based reagent [anisaldehyde (9.3 mL), H<sub>2</sub>SO<sub>4</sub> (12.5 mL), EtOH (340 mL), and CH<sub>3</sub>COOH (3.8 mL)]. Evaporation under reduced pressure was always effected with a bath temperature at 40°C.

The structures of all the new synthesized compounds were confirmed through full <sup>1</sup>H and <sup>13</sup>C NMR characterization and mass spectroscopy, which confirmed purity and identity of all synthesized compounds.

<sup>1</sup>H NMR analysis were performed at 500 MHz with a Bruker FT-NMR AVANCE<sup>™</sup> DRX500 spectrometer using a 5 mm z-PFG (pulsed field gradient) broadband reverse probe at 298 K unless otherwise stated, and <sup>13</sup>C NMR spectra at 125.76 MHz were done for all the new compounds. The signals were unambiguously assigned by 2D COSY and HSQC experiments (standard Bruker pulse program). Chemical shifts are reported as  $\delta$  (ppm) relative to residual CHCl<sub>3</sub>, CH<sub>3</sub>OD or pyridine fixed at 7.26, 3.30 ppm and 7.19 ppm (higher field signal), respectively, for <sup>1</sup>H NMR spectra and relative to CDCl<sub>3</sub> fixed at 77.0 ppm (central line), CD<sub>3</sub>OD at 49.0 ppm (central line) or pyridine at 123.0 ppm

(higher field signal, central line) for  $^{13}\text{C}$  NMR spectra. Scalar coupling constants (J) are reported in hertz (Hz). Splitting patterns are described by using the following abbreviations: *br*, broad; *s*, singlet; *d*, doublet; *t*, triplet; *m*, multiplet; *dd*, doublet of doublet; *ddd*, doublet of doublet of doublet.

Mass spectra were recorded in negative or positive-ion electrospray (ESI) mode on a Thermo Quest Finnigan LCQ DECA™ ion trap mass spectrometer. The mass spectrometer was equipped with a Finnigan ESI interface. Sample solutions were injected with a ionization spray voltage of 4.5 kV or 5.0 kV (positive and negative-ion mode, respectively), a capillary voltage of 32 V or -15 V (positive and negative-ion mode, respectively), and capillary temperature of 250 °C. Data were processed by Finnigan Xcalibur software system.

Optical rotations were determined on a Perkin–Elmer 241 polarimeter at 20 °C, in a 1 dm cell. Melting points were recorded on a Büchi 510 capillary melting point apparatus and were uncorrected.

**Biochemical:** Miltefosine, Perifosine and Sodium Dodecyl Sulfate (SDS) were purchased from Sigma. ELISA kit employed to screen inhibitors of Akt was the CycLex AKT/PKB kinase Assay/Inhibitor Screening Kit (CycLex, Eppendorf, Milano, Italy). Plates were pre-coated with “AKTide-2T”. Stausporine, used as “inhibitor control”, was purchase from Sigma-Aldric, Milano, Italy.

Human ovarian carcinoma IGROV-1 cell line, characterized by heterozygous mutation (Hetc. 995\_958delACTT), was used for *in vivo* assays. Cells were counted with Coulter Counter Z1, Beckman Coulter.

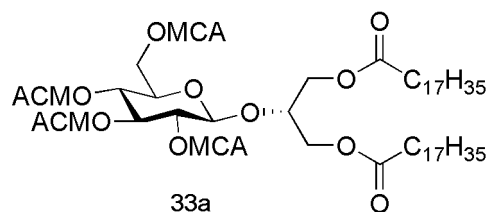
### 2.7.2 Synthesis of diester derivatives 26a,b

#### General procedure for the synthesis of monochloroacetyl protected 33a,b

2-*O*-(2',3',4',6'-Tetra-*O*-chloroacetyl- $\beta$ -D-glucopyranosyl)-*sn*-glycerol **32**<sup>66</sup> was dissolved in dry  $\text{CH}_2\text{Cl}_2$  (0.1M) and cooled at -10 °C. The proper acyl chloride (3 eq.) as a 15% (v/v)  $\text{CH}_2\text{Cl}_2$  solution and pyridine (6 eq.) as a 10% (v/v)  $\text{CH}_2\text{Cl}_2$  solution were added and the mixture stirred under Ar atmosphere. The reaction was monitored by TLC (Petroleum ether/AcOEt 7:3 and  $\text{CH}_2\text{Cl}_2/\text{CH}_3\text{OH}$  95:5) and stopped after 30 minutes diluting with  $\text{CH}_2\text{Cl}_2$  (15ml). The solution was washed with HCl 1M (10 ml), water (10

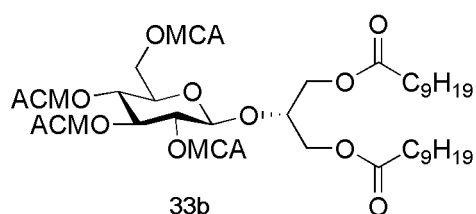
ml), NaHCO<sub>3</sub> saturated solution (10 ml) and finally water again (2×10ml). The collected aqueous phases were re-extracted with CH<sub>2</sub>Cl<sub>2</sub> (2×20ml), dried with anhydrous Na<sub>2</sub>SO<sub>4</sub>, filtered and evaporated. The crude obtained was purified by silica gel flash chromatography (petroleum ether/AcOEt 8:2) affording **33a** or **b**.

Application of the general procedure to compound **32** (212 mg, 0.378 mmol) with stearoyl chloride (343 mg, 1.134 mmol) afforded compound 1,3-di-*O*-octadecanoyl-2-*O*-(2',3',4',6'-tetra-*O*-acetyl-β-D-glucopyranosyl)-*sn*-glycerol **33a** as a white solid (249 mg, 0.228 mmol, 60% yield).



For characterization see Ref.<sup>50</sup>

Application of the general procedure to compound **32** (265 mg, 0.473 mmol) with decanoyl chloride (270 mg, 1.419 mmol) afforded compound 1,3-di-*O*-decanoyl-2-*O*-(2',3',4',6'-tetra-*O*-acetyl-β-D-glucopyranosyl)-*sn*-glycerol **33b** as an oil (294 mg, 0.338 mmol, 70% yield).



$[\alpha]_D^{20}$ : -3.3 (CHCl<sub>3</sub>, c 1.0);

<sup>1</sup>H-NMR (CDCl<sub>3</sub>): δ = 0.85-0.90 (m, 6H, 2 CH<sub>3</sub>), 1.20-1.34 (m, 24H, 12 CH<sub>2</sub>), 1.56-1.64 (m, 4H, 2 CH<sub>2</sub>), 2.27-2.33 (m, 4H, 2 CH<sub>2</sub>), 3.83 (ddd, 1H, J<sub>5',6'a</sub>=2.5 Hz, J<sub>5',6'b</sub>=5.1 Hz, J<sub>4',5'</sub>=10.0 Hz, H-5'), 3.98 (s, 2H, ClCH<sub>2</sub>), 4.01 (m, 2H, ClCH<sub>2</sub>), 4.04 (m, 2H, ClCH<sub>2</sub>), 4.05-4.27 (m, 5H, H-1a, H-1b, H-3a, H-3b and H-2), 4.14 (s, 2H, ClCH<sub>2</sub>), 4.29 (dd, 1H, J<sub>6'a,5'</sub>=2.5 Hz, J<sub>6'a,6'b</sub>=12.3 Hz, H-6'a), 4.36 (dd, 1H, J<sub>6'b,5'</sub>=5.1 Hz, H-6'b), 4.72 (d, 1H, J<sub>1',2'</sub>=7.9 Hz, H-1'), 5.05 (dd, 1H, J<sub>2',3'</sub>=9.6 Hz, H-2'), 5.14 (dd, 1H, J<sub>3',4'</sub>=9.6 Hz, H-4'), 4.32 (dd, 1H, H-3');

<sup>13</sup>C-NMR (CDCl<sub>3</sub>): δ= 14.1 (2 CH<sub>3</sub>), 22.6 (2 CH<sub>2</sub>), 24.8 (2 CH<sub>2</sub>), 29.1-29.4 (8 CH<sub>2</sub>), 31.8 (2 CH<sub>2</sub>), 34.0 (CH<sub>2</sub>), 34.1 (CH<sub>2</sub>), 40.1, 40.2, 40.3 and 40.5 (4 CH<sub>2</sub>Cl), 62.7 (C1 and C3), 63.1 (C6'), 69.6 (C4'), 71.3 (C5'), 72.2 (C2'), 73.7 (C3'), 75.9 (C2), 100.2 (C1'), 165.9, 166.2, 166.9, 167.0 (4 CO), 173.4 (2 CO);

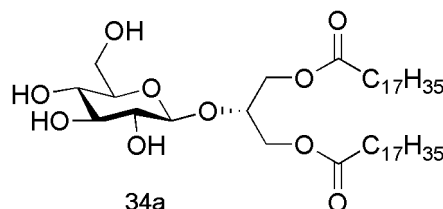
ESI-MS (CH<sub>3</sub>OH, negative-ion mode): m/z 867.1 [M-1]<sup>-</sup>, Calcd for C<sub>37</sub>H<sub>58</sub>Cl<sub>4</sub>O<sub>14</sub>, m/z 868.25 [M].

#### General procedure for the synthesis of compounds **34a,b**

The fully protected **33a**<sup>66</sup> or **b** was dissolved in a mixture of AcOEt/CH<sub>3</sub>OH 1:1 (~ 0.035 M) and hydrazine acetate (15 eq.) was added. The reaction was stirred under Ar

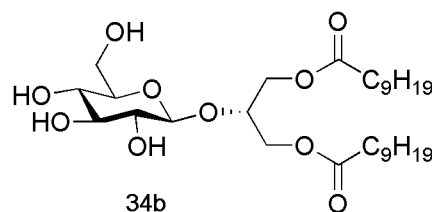
atmosphere at room temperature for 18h. Then, the solvent was evaporated under reduced pressure and the crude residue subjected to repeated flash column chromatography (CH<sub>2</sub>Cl<sub>2</sub>/CH<sub>3</sub>OH, from 95:5 to 90:10) yielding pure dyacylglucosylglycerols **34a,b**.

Application of the general procedure to compound **33a** (200 mg, 0.183 mmol) with hydrazine acetate (253 mg, 2.745 mmol) afforded compound 1,3-di-*O*-octadecanoyl-2-*O*-β-D-glucopyranosyl-*sn*-glycerol **34a** as a white solid (60 mg, 0.076 mmol, 42% yield).



For characterization see Ref.<sup>50</sup>

Application of the general procedure to compound **33b** (230 mg, 0.265 mmol) with hydrazine acetate (366 mg, 3.975 mmol) afforded compound 1,3-di-*O*-decanoyl-2-*O*-β-D-glucopyranosyl-*sn*-glycerol **34b** as a white solid (60 mg, 0.076 mmol, 43% yield).



Mp: 85.1-85.9°C;

$[\alpha]_D^{20}$ : -8.2 (CHCl<sub>3</sub>, *c* 1.0);

<sup>1</sup>H-NMR (CDCl<sub>3</sub>): δ = 0.86-0.91 (m, 6H, 2 CH<sub>3</sub>), 1.19-1.35 (m, 24H, 12 CH<sub>2</sub>), 1.56-1.65 (m, 4H, 2 CH<sub>2</sub>), 2.28-2.37 (m, 4H, 2 CH<sub>2</sub>), 3.32-3.44 (m, 2H, H-2' and H-5'), 3.51-3.58 (m, 2H, H-3' and H-4'), 3.78 (m, 1H, H-6'a), 3.89 (m, 1H, H-6'b), 4.04 (m, 1H, H-2), 4.14-4.22 (m, 2H, H-1a and H-3a), 4.27 (dd, 1H, J<sub>1b/3b,2</sub>=5.0 Hz, J<sub>1b/3b,1a/3a</sub>=11.5 Hz, H-1b or H-3b), 4.35 (dd, 1H, J<sub>1b/3b,2</sub>=3.8 Hz, J<sub>1b/3b,1a/3a</sub>=11.8 Hz, H-1b or H-3b), 4.41 (d, 1H, J<sub>1',2'</sub>=7.7 Hz, H-1');

<sup>13</sup>C-NMR (CDCl<sub>3</sub>): δ= 14.1 (2 CH<sub>3</sub>), 22.7 (2 CH<sub>2</sub>), 24.8 (2 CH<sub>2</sub>), 29.1-29.4 (8 CH<sub>2</sub>), 31.8 (2 CH<sub>2</sub>), 34.1 (CH<sub>2</sub>), 34.2 (CH<sub>2</sub>), 62.3 (C6'), 63.1 (C1 and C3), 70.1 (C3' or C4'), 73.5 (C2'), 75.8 (C5'), 76.0 (C2), 76.2 (C3' or C4'), 103.3 (C1'), 173.7 (CO), 174.1 (CO);

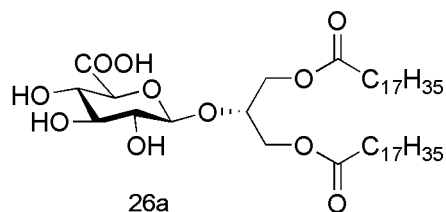
ESI-MS (CH<sub>3</sub>OH, positive-ion mode): *m/z* 585.4 [M+Na]<sup>+</sup>, calcd for C<sub>29</sub>H<sub>54</sub>O<sub>10</sub>, *m/z* 562.37 [M].

#### General procedure of oxidation to obtain the final products **26a,b**

Compound **34a**<sup>50</sup> or **34b** were suspended in a 55:45 mixture of CH<sub>3</sub>CN and 0.67M phosphate sodium buffer at pH 6.7 (0.1 M). TEMPO (0.21 eq.), NaClO<sub>2</sub> (20% aqueous solution, 3 eq.) and NaClO (15% aqueous solution, 0.15 eq.) were added. After stirring overnight at room temperature (TLC, CH<sub>2</sub>Cl<sub>2</sub>/CH<sub>3</sub>OH 90:10), Na<sub>2</sub>S<sub>2</sub>O<sub>3</sub> 0.5 M was added and the aqueous phase was acidified with a few drops of HCl 12 M and extracted with

Et<sub>2</sub>O. The organic layers were assembled, dried over anhydrous Na<sub>2</sub>SO<sub>4</sub>, filtered and evaporated under reduced pressure to give final products **26a** or **b**.

Application of the general procedure to compound **34a** (55 mg, 0.07 mmol) with TEMPO (2.5 mg, 0.015 mmol), NaClO<sub>2</sub> (100 μl of 20% aqueous solution, 0.21 mmol) and NaClO (5 μl of 15% aqueous solution, 0.011 mmol) afforded compound



1,3-di-*O*-octadecanoyl-2-*O*-β-D-glucuronopyranosyl-*sn*-glycerol **26a** as a white solid (24 mg, 0.03 mmol, 43% yield). The lower yield was due to the low solubility of the starting material in the reaction conditions.

Mp: 158-159°C;

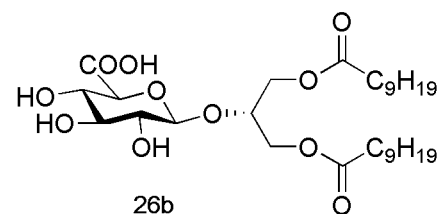
[α]<sub>D</sub><sup>20</sup>: the product **26a** was scarcely soluble making impossible the measurement of the optical rotation;

<sup>1</sup>H-NMR (CDCl<sub>3</sub>:CD<sub>3</sub>OD:D<sub>2</sub>O, 65:35:6, 315 K): δ= 0.82-0.87 (m, 6H, 2 CH<sub>3</sub>), 1.18-1.31 (m, 56H, 28 CH<sub>2</sub>), 1.53-1.61 (m, 4H, 2 CH<sub>2</sub>), 2.27-2.32 (m, 4H, 2 CH<sub>2</sub>), 3.24 (dd, 1H, J<sub>1',2'</sub>=7.8 Hz, J<sub>2',3'</sub>=9.1 Hz, H-2'), 3.42 (dd, 1H, J<sub>3',4'</sub>=9.0 Hz, H-3'), 3.45 (dd, 1H, J<sub>4',5'</sub>=9.5 Hz, H-4'), 3.56 (d, 1H, H-5'), 4.17-4.23 (m, 4H, H-2, H-1a, H-3a, and H-1b or H-3b), 4.30 (m, 1H, H-1b or H-3b), 4.41 (d, 1H, H-1');

<sup>13</sup>C-NMR (CDCl<sub>3</sub>:CD<sub>3</sub>OD:D<sub>2</sub>O, 65:35:6, 315 K): δ= 14.3 (2 CH<sub>3</sub>), 23.1 (2 CH<sub>2</sub>), 25.3 (2 CH<sub>2</sub>), 29.5-30.2 (24 CH<sub>2</sub>), 32.4 (2 CH<sub>2</sub>), 34.6 (2 CH<sub>2</sub>), 63.2 (C1 or C3), 64.0 (C1 or C3), 72.5 (C4'), 73.8 (C2'), 75.2 (C2), 75.6 (C5'), 76.6 (C3'), 103.2 (C1'), 174.8 (2 CO);

ESI-MS (CH<sub>3</sub>OH, negative-ion mode): m/z 799.7 [M-1]<sup>-</sup>, Calcd for C<sub>45</sub>H<sub>84</sub>O<sub>11</sub>, m/z 800.60 [M].

Application of the general procedure to compound **34b** (40 mg, 0.07 mmol) with TEMPO (2.5 mg, 0.015 mmol), NaClO<sub>2</sub> (100 μl of 20% aqueous solution, 0.21 mmol) and NaClO (5 μl of 15% aqueous solution, 0.011 mmol) afforded compound



1,3-di-*O*-decanoyl-2-*O*-β-D-glucuronopyranosyl-*sn*-glycerol **26b** as an oil (36 mg, 0.06 mmol, 88% yield).

[α]<sub>D</sub><sup>20</sup>: -18.9 (CH<sub>3</sub>OH, c 1.0);

<sup>1</sup>H-NMR (CD<sub>3</sub>OD): δ= 0.85-0.92 (m, 6H, 2 CH<sub>3</sub>), 1.22-1.36 (m, 24H, 12 CH<sub>2</sub>), 1.54-1.64 (m, 4H, 2 CH<sub>2</sub>), 2.29-2.37 (m, 4H, 2 CH<sub>2</sub>), 3.32 (dd, 1H, J<sub>1',2'</sub>=8.0 Hz, J<sub>2',3'</sub>=8.5 Hz, H-2'), 3.41 (dd, 1H, J<sub>3',4'</sub>=9.0 Hz, H-3'), 3.47 (dd, 1H, J<sub>4',5'</sub>=9.0 Hz, H-4'), 3.65 (*br* d, 1H, H-5'), 4.19-4.26 (m, 4H, H-2, H-1a, H-3a, and H-1b or H-3b), 4.31 (m, 1H, H-1b or H-3b), 4.46 (d, 1H, H-1');

$^{13}\text{C}$ -NMR ( $\text{CD}_3\text{OD}$ ):  $\delta$ = 14.5 (2  $\text{CH}_3$ ), 23.7 (2  $\text{CH}_2$ ), 26.0 (2  $\text{CH}_2$ ), 30.2-30.6 (8  $\text{CH}_2$ ), 33.1 (2  $\text{CH}_2$ ), 34.9 (2  $\text{CH}_2$ ), 63.9 (C1 or C3), 64.7 (C1 or C3), 73.5 (C4'), 74.8 (C2'), 75.9 (C2), 76.4 (C5'), 77.6 (C3'), 104.3 (C1'), 175.1 (CO), 175.2 (CO), 176.9 (br s, CO);

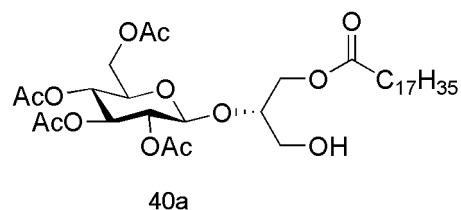
ESI-MS ( $\text{CH}_3\text{OH}$ , negative-ion mode):  $m/z$  575.3  $[\text{M}-1]^-$ , Calcd for  $\text{C}_{29}\text{H}_{52}\text{O}_{11}$ ,  $m/z$  576.35  $[\text{M}]^-$ .

### 2.7.3 Synthesis of monoester derivatives 27a,b

#### General procedure for the enzymatic synthesis of monoesters 40a or b

Compound 2-*O*-(2',3',4',6'-tetra-*O*-acetyl- $\beta$ -D-glucopyranosyl)-*sn*-glycerol **35**<sup>58,65</sup> was dissolved in dry pyridine (0.1 M) and the appropriate trifluoroethyl ester (6 eq.) and LPS (5 times the weight of starting material **35**) were added. The suspension was stirred at 45 °C and monitored by TLC ( $\text{CH}_2\text{Cl}_2/\text{CH}_3\text{OH}$  95:5). After 18 h the reaction was stopped and filtered to remove the enzyme which was washed with pyridine and methanol. The solvent was evaporated under vacuum and the crude purified by automated flash chromatography (Hexane/AcOEt) yielding **40a** or **b**.

Application of the general procedure to compound **35** (500 mg, 1.184 mmol) with trifluoroethyl octadecanoate (2.60 g, 7.10 mmol) and LPS (2.5 g) afforded compound 1-*O*-octadecanoyl-2-*O*-(2',3',4',6'-tetra-*O*-acetyl- $\beta$ -D-glucopyranosyl)-*sn*-glycerol **40a** as an amorphous solid (600 mg, 0.87 mmol, 74% yield) after purification by flash column chromatography (Hexane/AcOEt from 9:1 to 2:8).



Mp: 95.1-95.4 °C;

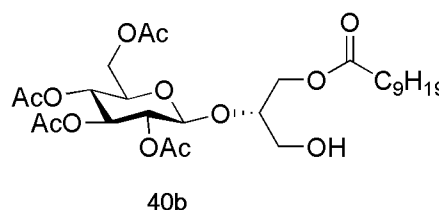
$[\alpha]_D^{20}$ : -4.7 ( $\text{CHCl}_3$ ,  $c$  0.5);

$^1\text{H}$  NMR ( $\text{CDCl}_3$ ):  $\delta$  = 0.87 (t, 3H,  $J$ =7.0 Hz,  $\text{CH}_3$ ), 1.19-1.34 (m, 28H, 14  $\text{CH}_2$ ), 1.61 (m, 2H,  $\text{CH}_2$ ), 2.00 (s, 3H,  $\text{COCH}_3$ ), 2.03 (s, 3H,  $\text{COCH}_3$ ), 2.05 (s, 3H,  $\text{COCH}_3$ ), 2.09 (s, 3H,  $\text{COCH}_3$ ), 2.30 (t, 2H,  $J$ =7.6 Hz,  $\text{CH}_2$ ), 3.58-3.69 (m, 2H, H-3a and H-3b), 3.76 (ddd, 1H,  $J_{5',6'a}=5.6$  Hz,  $J_{5',6'b}=2.6$  Hz,  $J_{4',5'}=9.7$  Hz, H-5'), 3.88 (m, 1H, H-2), 4.05-4.11 (m, 2H, H-1a and H-1b), 4.16 (dd, 1H,  $J_{6'a,6'b}=12.2$  Hz, H-6'a), 4.21 (dd, 1H, H-6'b), 4.61 (d, 1H,  $J_{1',2'}=8.0$  Hz, H-1'), 5.01 (dd, 1H,  $J_{2',3'}=9.7$  Hz, H-2'), 5.05 (dd, 1H,  $J_{3',4'}=9.7$  Hz, H-4'), 5.22 (dd, 1H, H-3');

$^{13}\text{C}$ -NMR ( $\text{CDCl}_3$ ):  $\delta$ = 14.1 ( $\text{CH}_3$ ), 20.5-20.07 (4  $\text{COCH}_3$ ), 22.7 ( $\text{CH}_2$ ), 24.9 ( $\text{CH}_2$ ), 28.9-30.0 (12  $\text{CH}_2$ ), 31.9 ( $\text{CH}_2$ ), 34.1 ( $\text{CH}_2$ ), 61.9 (C6'), 62.8 (C3), 63.1 (C1), 68.4 (C4'), 71.2 (C2'), 72.0 (C5'), 72.5 (C3'), 81.5 (C2), 101.2 (C1'), 169.2, 169.4, 170.2, 170.6 and 173.4 (5 CO);

ESI-MS ( $\text{CH}_3\text{OH}$ , positive-ion mode):  $m/z$  711.3  $[\text{M}+\text{Na}]^+$ , calcd for  $\text{C}_{35}\text{H}_{60}\text{O}_{13}$ ,  $m/z$  688.40  $[\text{M}]^+$ .

Application of the general procedure to compound **35** (500 mg, 1.184 mmol) with trifluoroethyl decanoate (1.8 g, 7.10 mmol) and LPS (2.5 g) afforded compound 1-*O*-decanoyl-2-*O*-(2',3',4',6'-tetra-*O*-acetyl- $\beta$ -D-glucopyranosyl)-*sn*-glycerol **40b** as an oil (560 mg, 0.97 mmol, 82% yield) after purification by flash column chromatography (Hexane/AcOEt from 7:3 to 3:7).



$[\alpha]_D^{20}$ : -1.0 (CHCl<sub>3</sub>, *c* 1.0);

<sup>1</sup>H-NMR (CDCl<sub>3</sub>):  $\delta$  = 0.87 (t, 3H, J=7.0 Hz, CH<sub>3</sub>), 1.20-1.35 (m, 12H, 6 CH<sub>2</sub>), 1.61 (m, 2H, CH<sub>2</sub>), 2.00 (s, 3H, COCH<sub>3</sub>), 2.03 (s, 3H, COCH<sub>3</sub>), 2.04 (s, 3H, COCH<sub>3</sub>), 2.09 (s, 3H, COCH<sub>3</sub>), 2.30 (t, 2H, J=7.6 Hz, CH<sub>2</sub>), 3.57-3.69 (m, 2H, H-3a and H-3b), 3.76 (ddd, 1H, J<sub>5',6'a</sub>=5.6 Hz, J<sub>5',6'b</sub>=2.3 Hz, J<sub>4',5'</sub>=9.8 Hz, H-5'), 3.88 (m, 1H, H-2), 4.05-4.12 (m, 2H, H-1a and H-1b), 4.16 (dd, 1H, J<sub>6'a,6'b</sub>=12.3 Hz, H-6'a), 4.20 (dd, 1H, H-6'b), 4.61 (d, 1H, J<sub>1',2'</sub>=8.0 Hz, H-1'), 5.00 (dd, 1H, J<sub>2',3'</sub>=9.8 Hz, H-2'), 5.04 (dd, 1H, J<sub>3',4'</sub>=9.8 Hz, H-4'), 5.21 (dd, 1H, H-3');

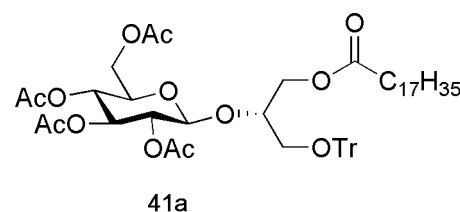
<sup>13</sup>C-NMR (CDCl<sub>3</sub>):  $\delta$  = 14.1 (CH<sub>3</sub>), 20.5-20.7 (4 COCH<sub>3</sub>), 22.7 (CH<sub>2</sub>), 24.9 (CH<sub>2</sub>), 29.0-29.5 (4 CH<sub>2</sub>), 31.8 (CH<sub>2</sub>), 34.1 (CH<sub>2</sub>), 61.9 (C6'), 62.8 (C3), 63.1 (C1), 68.4 (C4'), 71.2 (C2'), 72.0 (C5'), 72.5 (C3'), 81.5 (C2), 101.2 (C1'), 169.2, 169.4, 170.2, 170.6 and 173.4 (5 CO);

ESI-MS (CH<sub>3</sub>OH, positive-ion mode): *m/z* 599.3 [M+Na]<sup>+</sup>, calcd for C<sub>27</sub>H<sub>44</sub>O<sub>13</sub>, *m/z* 576.28 [M].

#### General procedure to prepare trityl derivatives **41a** or **b**

Compound **40** was dissolved in dry pyridine (0.1 M) and trityl chloride (2 eq.) was added. The reaction mixture was heated at 100 °C and stirred under argon for 3h (TLC, hexane: EtOAc 6:4). Then, the solvent was evaporated under reduced pressure and the obtained crude compound was submitted to flash chromatography (Hexane/AcOEt 75:25 + 1% TEA) to yield compound **41a** or **b**.

Application of the general procedure to compound **40a** (470 mg, 0.682 mmol) with trityl chloride (380 mg, 1.364 mmol) afforded compound 1-*O*-octadecanoyl-3-*O*-trityl-2-*O*-(2',3',4',6'-tetra-*O*-acetyl- $\beta$ -D-glucopyranosyl)-*sn*-glycerol **41a** as an oil (610 mg, 0.655 mmol, 96% yield).



$[\alpha]_D^{20}$ : -3.3 (CHCl<sub>3</sub>, *c* 1.0);

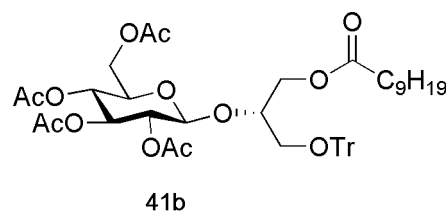
<sup>1</sup>H-NMR (Pyd<sub>5</sub>):  $\delta$  = 0.85 (t, 3H, J=6.5 Hz, CH<sub>3</sub>), 1.16-1.33 (m, 28H, 14 CH<sub>2</sub>), 1.64 (m, 2H, CH<sub>2</sub>), 1.96 (s, 3H, COCH<sub>3</sub>), 1.99 (s, 3H, COCH<sub>3</sub>), 2.01 (s, 3H, COCH<sub>3</sub>), 2.15 (s, 3H, COCH<sub>3</sub>),

2.35 (t, 2H,  $J=7.5$  Hz, CH<sub>2</sub>), 3.44 (dd, 1H,  $J_{3a,2}=6.0$  Hz,  $J_{3a,3b}=9.4$  Hz, H-3a), 3.57 (dd, 1H,  $J_{3b,2}=5.1$  Hz, H-3b), 4.13 (ddd, 1H,  $J_{5',6'a}=2.0$  Hz,  $J_{5',6'b}=4.3$  Hz,  $J_{4',5'}=9.6$  Hz, H-5'), 4.33 (dd, 1H,  $J_{6'a,6'b}=12.1$  Hz, H-6'a), 4.38 (m, 1H, H-2), 4.49 (dd, 1H,  $J_{1a,2}=5.8$  Hz,  $J_{1a,1b}=11.6$  Hz, H-1a), 4.56 (dd, 1H, H-6'a), 4.58 (dd, 1H,  $J_{1b,2}=3.5$  Hz, H-1b), 5.19 (d, 1H,  $J_{1',2'}=8.0$  Hz, H-1'), 5.48 (dd, 1H,  $J_{2',3'}=9.6$  Hz, H-2'), 5.50 (dd, 1H,  $J_{3',4'}=9.6$  Hz, H-4'), 5.77 (dd, 1H, H-3'), 7.26 (dd, 3H,  $J=7.3$  Hz, Ph), 7.35 (dd, 6H,  $J=7.4$  Hz, Ph), 7.65 (d, 6H,  $J=7.8$  Hz, Ph);

<sup>13</sup>C-NMR (Pyd<sub>5</sub>):  $\delta=13.8$  (CH<sub>3</sub>), 19.7-20.3 (4 COCH<sub>3</sub>), 22.4 (CH<sub>2</sub>), 24.7 (CH<sub>2</sub>), 28.6-28.8 (12 CH<sub>2</sub>), 31.6 (CH<sub>2</sub>), 33.8 (CH<sub>2</sub>), 62.1 (C6'), 63.4 (C3), 63.5 (C1), 68.7 (C4'), 71.6 (C2'), 71.7 (C5'), 72.9 (C3'), 77.0 (C2), 86.7 (OCPh<sub>3</sub>), 100.6 (C1'), 127.0 (3 CH, Ph), 127.8 (6 CH, Ph), 128.7 (6 CH, Ph), 144.0 (3 C, Ph), 169.1, 169.3, 169.8, 170.0 and 172.8 (5 CO);

ESI-MS (CH<sub>3</sub>OH, positive-ion mode):  $m/z$  953.5 [M+Na]<sup>+</sup>, calcd for C<sub>54</sub>H<sub>74</sub>O<sub>13</sub>,  $m/z$  930.51 [M].

Application of the general procedure to compound **40b** (508 mg, 0.881 mmol) with trityl chloride (491 mg, 1.762 mmol) afforded compound **1-O-decanoyl-3-O-trityl-2-O-(2',3',4',6'-tetra-O-acetyl- $\beta$ -D-glucopyranosyl)-sn-glycerol 41b** as an oil (510 mg, 0.623 mmol, 70% yield).



$[\alpha]_D^{20}:-3.4$  (CHCl<sub>3</sub>,  $c$  1.0);

<sup>1</sup>H-NMR (Pyd<sub>5</sub>):  $\delta=0.85$  (t, 3H,  $J=7.0$  Hz, CH<sub>3</sub>), 1.14-1.30 (m, 12H, 6 CH<sub>2</sub>), 1.63 (m, 2H, CH<sub>2</sub>), 1.96 (s, 3H, COCH<sub>3</sub>), 2.00 (s, 3H, COCH<sub>3</sub>), 2.01 (s, 3H, COCH<sub>3</sub>), 2.14 (s, 3H, COCH<sub>3</sub>), 2.34 (t, 2H,  $J=7.5$  Hz, CH<sub>2</sub>), 3.43 (dd, 1H,  $J_{3a,2}=6.0$  Hz,  $J_{3a,3b}=9.6$  Hz, H-3a), 3.57 (dd, 1H,  $J_{3b,2}=5.2$  Hz, H-3b), 4.13 (ddd, 1H,  $J_{5',6'a}=2.5$  Hz,  $J_{5',6'b}=4.4$  Hz,  $J_{4',5'}=9.5$  Hz, H-5'), 4.33 (dd, 1H,  $J_{6'a,6'b}=12.2$  Hz, H-6'a), 4.38 (m, 1H, H-2), 4.49 (dd, 1H,  $J_{1a,2}=6.0$  Hz,  $J_{1a,1b}=11.6$  Hz, H-1a), 4.55 (dd, 1H, H-6'a), 4.58 (dd, 1H,  $J_{1b,2}=3.6$  Hz, H-1b), 5.19 (d, 1H,  $J_{1',2'}=8.0$  Hz, H-1'), 5.48 (dd, 1H,  $J_{2',3'}=9.5$  Hz, H-2'), 5.51 (dd, 1H,  $J_{3',4'}=9.5$  Hz, H-4'), 5.77 (dd, 1H, H-3'), 7.26 (dd, 3H,  $J=7.3$  Hz, Ph), 7.35 (dd, 6H,  $J=7.4$  Hz, Ph), 7.64 (d, 6H,  $J=7.8$  Hz, Ph);

<sup>13</sup>C-NMR (Pyd<sub>5</sub>):  $\delta=13.8$  (CH<sub>3</sub>), 19.6-20.4 (4 COCH<sub>3</sub>), 22.4 (CH<sub>2</sub>), 24.7 (CH<sub>2</sub>), 28.4-29.6 (4 CH<sub>2</sub>), 31.6 (CH<sub>2</sub>), 33.8 (CH<sub>2</sub>), 62.0 (C6'), 63.4 (C3), 63.5 (C1), 68.7 (C4'), 71.6 (C2'), 71.7 (C5'), 72.9 (C3'), 77.0 (C2), 86.6 (OCPh<sub>3</sub>), 100.6 (C1'), 127.0 (3 CH, Ph), 127.8 (6 CH, Ph), 128.7 (6 CH, Ph), 144.0 (3 C, Ph), 169.1, 169.3, 169.8, 170.0 and 172.8 (5 CO);

ESI-MS (CH<sub>3</sub>OH, positive-ion mode):  $m/z$  841.3 [M+Na]<sup>+</sup>, calcd for C<sub>46</sub>H<sub>58</sub>O<sub>13</sub>,  $m/z$  818.39 [M].

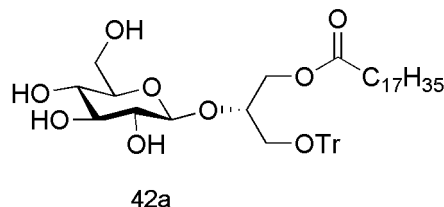
#### General procedure of hydrazinolysis to give compounds **42a** or **b**

Compound **41** was dissolved in EtOH 85% (0.1 M) and hydrazine hydrate (10 eq.) was added drop by drop. The reaction mixture was left stirring overnight at 45 °C. The



solvent was evaporated under pressure and the crude was purified by flash chromatography (CH<sub>2</sub>Cl<sub>2</sub>/CH<sub>3</sub>OH 95:5) to yield title compounds.

Application of the general procedure to compound **41a** (596 mg, 0.640 mmol) with hydrazine hydrate (300  $\mu$ L, 6.40 mmol) afforded compound 1-*O*-octadecanoyl-3-*O*-trityl-2-*O*- $\beta$ -D-glucopyranosyl-*sn*-glycerol **42a** as an oil (223 mg, 292  $\mu$ mol, 45% yield).



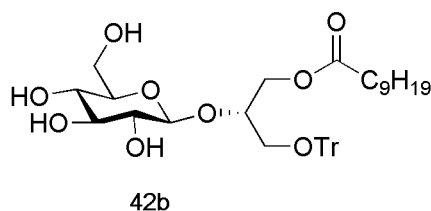
$[\alpha]_D^{20}$ : +6.3 (CHCl<sub>3</sub>, *c* 1.0);

<sup>1</sup>H-NMR (Pyd<sub>5</sub>):  $\delta$  = 0.85 (t, 3H, *J*=7.0 Hz, CH<sub>3</sub>), 1.15-1.31 (m, 28H, 14 CH<sub>2</sub>), 1.61 (m, 2H, CH<sub>2</sub>), 2.32 (m, 2H, CH<sub>2</sub>), 3.54 (dd, 1H, *J*<sub>3a,2</sub>=6.6 Hz, *J*<sub>3a,3b</sub>=9.4 Hz, H-3a), 3.66 (dd, 1H, *J*<sub>3b,2</sub>=4.7 Hz, H-3b), 3.92 (m, 1H, H-5'), 3.99 (m, 1H, H-2'), 4.19-4.27 (m, 2H, H-3' and H-4'), 4.34 (m, 1H, H-6'a), 4.46 (m, 1H, H-6'b), 4.49 (m, 1H, H-2), 4.66-4.72 (m, 2H, H-1a and H-1b), 5.04 (d, 1H, *J*<sub>1',2'</sub>=7.7 Hz, H-1'), 7.23 (dd, 3H, *J*=7.3 Hz, Ph), 7.32 (dd, 6H, *J*=7.4 Hz, Ph), 7.64 (d, 6H, *J*=7.8 Hz, Ph);

<sup>13</sup>C-NMR (Pyd<sub>5</sub>):  $\delta$  = 13.8 (CH<sub>3</sub>), 22.4 (CH<sub>2</sub>), 24.7 (CH<sub>2</sub>), 28.8-29.7 (12 CH<sub>2</sub>), 31.6 (CH<sub>2</sub>), 33.9 (CH<sub>2</sub>), 62.4 (C6'), 63.7 (C3), 63.8 (C1), 71.2 (C3' or C4'), 74.7 (C2'), 76.0 (C2), 77.9 (C3' or C4' and C5'), 86.6 (OCPh<sub>3</sub>), 104.3 (C1'), 126.9 (3 CH, Ph), 127.8 (6 CH, Ph), 128.7 (6 CH, Ph), 144.2 (3 C, Ph), 173.0 (CO);

ESI-MS (CH<sub>3</sub>OH, positive-ion mode): *m/z* 785.3 [M+Na]<sup>+</sup>, calcd for C<sub>46</sub>H<sub>66</sub>O<sub>9</sub>, *m/z* 762.47 [M].

Application of the general procedure to compound **41b** (475 mg, 0.580 mmol) with hydrazine hydrate (270  $\mu$ L, 5.80 mmol) afforded compound 1-*O*-decanoyl-3-*O*-trityl-2-*O*- $\beta$ -D-glucopyranosyl-*sn*-glycerol **42b** as an oil (210 mg, 322  $\mu$ mol, 56% yield).



$[\alpha]_D^{20}$ : +7.8 (CHCl<sub>3</sub>, *c* 1.0);

<sup>1</sup>H-NMR (Pyd<sub>5</sub>):  $\delta$  = 0.83 (t, 3H, *J*=7.0 Hz, CH<sub>3</sub>), 1.07-1.28 (m, 12H, 6 CH<sub>2</sub>), 1.60 (m, 2H, CH<sub>2</sub>), 2.31 (m, 2H, CH<sub>2</sub>), 3.54 (dd, 1H, *J*<sub>3a,2</sub>=6.5 Hz, *J*<sub>3a,3b</sub>=9.4 Hz, H-3a), 3.66 (dd, 1H, *J*<sub>3b,2</sub>=4.7 Hz, H-3b), 3.92 (m, 1H, H-5'), 3.98 (m, 1H, H-2'), 4.18-4.26 (m, 2H, H-3' and H-4'), 4.33 (dd, 1H, *J*<sub>5',6'a</sub>=4.9 Hz, *J*<sub>6'a,6'b</sub>=11.5 Hz, H-6'a), 4.45 (dd, 1H, *J*<sub>5',6'ab</sub>=2.2 Hz, H-6'b), 4.49 (m, 1H, H-2), 4.65-4.71 (m, 2H, H-1a and H-1b), 5.03 (d, 1H, *J*<sub>1',2'</sub>=7.7 Hz, H-1'), 7.23 (dd, 3H, *J*=7.3 Hz, Ph), 7.32 (dd, 6H, *J*=7.4 Hz, Ph), 7.63 (d, 6H, *J*=7.8 Hz, Ph);

<sup>13</sup>C-NMR (Pyd<sub>5</sub>):  $\delta$  = 13.8 (CH<sub>3</sub>), 22.4 (CH<sub>2</sub>), 24.7 (CH<sub>2</sub>), 28.7-29.3 (4 CH<sub>2</sub>), 31.5 (CH<sub>2</sub>), 33.8 (CH<sub>2</sub>), 62.4 (C6'), 63.7 (C3), 63.8 (C1), 71.2 (C3' or C4'), 74.7 (C2'), 76.0 (C2), 77.9

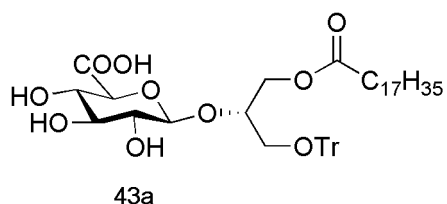
(C3' or C4' and C5'), 86.6 (OCPh<sub>3</sub>), 104.3 (C1'), 126.9 (3 CH, Ph), 127.8 (6 CH, Ph), 128.7 (6 CH, Ph), 144.2 (3 C, Ph), 173.0 (CO);

ESI-MS (CH<sub>3</sub>OH, positive-ion mode): m/z 673.2 [M+Na]<sup>+</sup>, calcd for C<sub>38</sub>H<sub>50</sub>O<sub>9</sub>, m/z 650.35 [M].

#### General procedure of oxidation to obtain products **43a,b**

Compound **42a** or **42b** was suspended in a 55:45 mixture of CH<sub>3</sub>CN and 0.67M phosphate sodium buffer at pH 6.7 (0.1 M). TEMPO (0.21 eq.), NaClO<sub>2</sub> (20% aqueous solution, 3 eq.) and NaClO (15% aqueous solution, 0.15 eq.) were added. After stirring for 3 hours at room temperature (TLC, CH<sub>2</sub>Cl<sub>2</sub>/CH<sub>3</sub>OH 9:1), acetonitrile was removed under reduced pressure and the aqueous phase was extracted with Et<sub>2</sub>O. The organic layers were assembled, dried over anhydrous Na<sub>2</sub>SO<sub>4</sub>, filtered and evaporated to give the compound **43a** or **b** as an amorphous solid, which were used without further purification in the next step.

Application of the general procedure to compound **42a** (223 mg, 0.292 mmol) with TEMPO (10 mg, 0.061 mmol), NaClO<sub>2</sub> (400 μl of 20% aqueous solution, 0.876 mmol) and NaClO (25 μl of 15% aqueous solution, 0.044 mmol) afforded 1-*O*-octadecanoyl-3-*O*-trityl-2-*O*-β-D-glucuronopyranosyl-*sn*-glycerol **43a** (220 mg, 0.283 mmol, 97% yield) as an amorphous solid.



Mp: 98-99 °C;

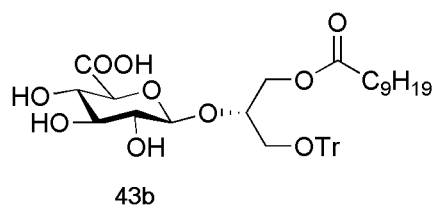
[α]<sub>D</sub><sup>20</sup>: -11.1 (CHCl<sub>3</sub>:CH<sub>3</sub>OH 65:35, c 1.0);

<sup>1</sup>H-NMR (Pyd<sub>5</sub>): δ= 0.85 (t, 3H, J=7.0 Hz, CH<sub>3</sub>), 1.13-1.35 (m, 28H, 14 CH<sub>2</sub>), 1.59 (m, 2H, CH<sub>2</sub>), 2.28 (m, 2H, CH<sub>2</sub>), 3.56 (dd, 1H, J<sub>3a,2</sub>=6.6 Hz, J<sub>3a,3b</sub>=9.2 Hz, H-3a), 3.68 (dd, 1H, J<sub>3b,2</sub>=4.4 Hz, H-3b), 4.03 (dd, J<sub>1',2'</sub>=7.6 Hz, J<sub>2',3'</sub>=8.0 Hz, 1H, H-2'), 4.25 (m, 1H, H-3'), 4.32-4.42 (m, 2H, H-4' and H-5'), 4.54 (m, 1H, H-2), 4.60-4.71 (m, 2H, H-1a and H-1b), 5.06 (d, 1H, H-1'), 7.19 (dd, 3H, J=7.4 Hz, Ph), 7.31 (dd, 6H, J=7.4 Hz, Ph), 7.63 (d, 6H, J=7.8 Hz, Ph);

<sup>13</sup>C-NMR (Pyd<sub>5</sub>): δ= 13.8 (CH<sub>3</sub>), 22.4 (CH<sub>2</sub>), 24.7 (CH<sub>2</sub>), 28.8-29.7 (12 CH<sub>2</sub>), 31.6 (CH<sub>2</sub>), 33.8 (CH<sub>2</sub>), 63.5 (C1 and C3), 73.1 (C4' or C5'), 74.4 (C2'), 75.5 (C2), 76.5 (C4' or C5'), 77.6 (C3'), 86.6 (OCPh<sub>3</sub>), 103.7 (C1'), 126.8 (3 CH, Ph), 127.8 (6 CH, Ph), 128.7 (6 CH, Ph), 144.1 (3 C, Ph), 173.0 (CO), 174.3 (CO);

ESI-MS (CH<sub>3</sub>OH, negative-ion mode): m/z 775.5 [M-1], calcd for C<sub>46</sub>H<sub>64</sub>O<sub>10</sub>, m/z 776.45 [M].

Application of the general procedure to compound **42b** (210 mg, 0.323 mmol) with TEMPO (10 mg, 0.061 mmol), NaClO<sub>2</sub> (440 μl of 20% aqueous solution, 0.969 mmol) and NaClO (25 μl of 15% aqueous solution, 0.048 mmol) afforded 1-*O*-decanoyl-3-*O*-trityl-2-*O*-β-*D*-glucuronopyranosyl-*sn*-glycerol **43b** (211 mg, 0.317 mmol, 98% yield) as an amorphous solid.



Mp: 154-155 °C;

$[\alpha]_D^{20}$ : -11.3 (CHCl<sub>3</sub>:CH<sub>3</sub>OH 65:35, *c* 1.0);

<sup>1</sup>H-NMR (Pyd<sub>5</sub>): δ = 0.84 (t, 3H, *J* = 7.0 Hz, CH<sub>3</sub>), 1.07-1.28 (m, 12H, 6 CH<sub>2</sub>), 1.57 (m, 2H, CH<sub>2</sub>), 2.26 (m, 2H, CH<sub>2</sub>), 3.56 (dd, 1H, *J*<sub>3a,2</sub> = 6.6 Hz, *J*<sub>3a,3b</sub> = 9.0 Hz, H-3a), 3.64 (dd, 1H, *J*<sub>3b,2</sub> = 4.2 Hz, H-3b), 3.99 (dd, *J*<sub>1',2'</sub> = 7.8 Hz, *J*<sub>2',3'</sub> = 8.5 Hz, 1H, H-2'), 4.16-4.27 (m, 3H, H-3', H-4' and H-5'), 4.57 (m, 1H, H-2), 4.65 (dd, 2H, *J*<sub>1'a,2</sub> = 4.8 Hz, *J*<sub>1'a,1'b</sub> = 11.5 Hz, H-1a), 4.70 (dd, 2H, *J*<sub>1'b,2</sub> = 4.0 Hz, H-1b), 5.00 (d, 1H, H-1'), 7.20 (dd, 3H, *J* = 7.4 Hz, Ph), 7.31 (dd, 6H, *J* = 7.4 Hz, Ph), 7.62 (d, 6H, *J* = 7.8 Hz, Ph);

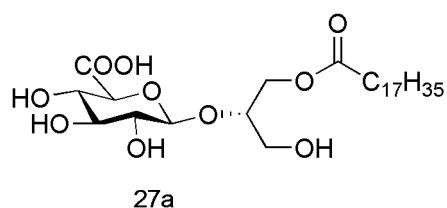
<sup>13</sup>C-NMR (Pyd<sub>5</sub>): δ = 13.8 (CH<sub>3</sub>), 22.4 (CH<sub>2</sub>), 24.6 (CH<sub>2</sub>), 28.7-29.3 (4 CH<sub>2</sub>), 31.5 (CH<sub>2</sub>), 33.8 (CH<sub>2</sub>), 63.2 (C1), 63.4 (C3), 73.2 (C4' or C5'), 74.3 (C2'), 74.9 (C2), 76.0 (C4' or C5'), 77.7 (C3'), 86.6 (OCPh<sub>3</sub>), 103.1 (C1'), 126.8 (3 CH, Ph), 127.8 (6 CH, Ph), 128.7 (6 CH, Ph), 144.1 (3 C, Ph), 173.0 (CO), 175.6 (CO);

ESI-MS (CH<sub>3</sub>OH, negative-ion mode): *m/z* = 663.2 [M-1]<sup>-</sup>, calcd for C<sub>38</sub>H<sub>48</sub>O<sub>10</sub>, *m/z* 664.32 [M].

#### General procedure to obtain final products **27a,b**

Compound **43** was dissolved in CH<sub>2</sub>Cl<sub>2</sub> (0.1 M) and the same amount on weight of starting material of Dowex® Marathon™ C, H<sup>+</sup> form was added. The reaction was stirred at room temperature under nitrogen atmosphere until TLC analysis (CH<sub>2</sub>Cl<sub>2</sub>:CH<sub>3</sub>OH 9:1) showed disappearance of the starting material and formation of a new product. The white suspension obtained was filtered and the residue washed with CH<sub>2</sub>Cl<sub>2</sub> was eliminated, while the remaining solid was then washed with AcOEt and *i*PrOH and evaporated under reduced pressure yielding the desired pure product.

Application of the general procedure to compound **43a** (50 mg, 0.064 mmol) with Dowex® Marathon™ C, H<sup>+</sup> form (50 mg) afforded 1-*O*-octadecanoyl-2-*O*-β-*D*-glucuronopyranosyl-*sn*-glycerol **27a** (60 mg, 0.112 mmol, 76% yield) as a white solid.



Mp: 127-128 °C;

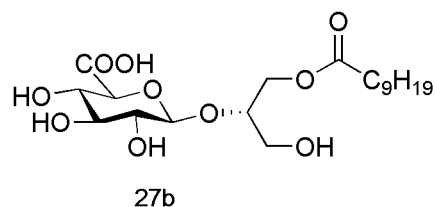
$[\alpha]_D^{20}$ : -29.3 (CHCl<sub>3</sub>:CH<sub>3</sub>OH 65:35, c 0.5);

<sup>1</sup>H-NMR (Pyd<sub>5</sub>): δ= 0.85 (t, 3H, J=7.0 Hz, CH<sub>3</sub>), 1.13-1.31 (m, 28H, 14 CH<sub>2</sub>), 1.64 (m, 2H, CH<sub>2</sub>), 2.37 (m, 2H, CH<sub>2</sub>), 4.10 (dd, J<sub>1',2'</sub>=7.8 Hz, J<sub>2',3'</sub>=8.9 Hz, 1H, H-2'), 4.16 (dd, 1H, J<sub>3a,2</sub>=5.5 Hz, J<sub>3a,3b</sub>=11.5 Hz, H-3a), 4.23 (dd, 1H, J<sub>3b,2</sub>=4.9 Hz, H-3b), 4.33 (dd, 1H, J<sub>3',4'</sub>=8.9 Hz, H-3'), 4.52 (m, 1H, H-2), 4.60 (dd, 1H, J<sub>4',5'</sub>=8.9 Hz, H-4'), 4.66 (d, 1H, H-5'), 4.69-4.77 (m, 2H, H-1a and H-1b), 5.22 (d, 1H, H-1');

<sup>13</sup>C-NMR (Pyd<sub>5</sub>): δ= 13.8 (CH<sub>3</sub>), 22.4 (CH<sub>2</sub>), 24.7 (CH<sub>2</sub>), 28.8-29.5 (12 CH<sub>2</sub>), 31.6 (CH<sub>2</sub>), 33.9 (CH<sub>2</sub>), 62.2 (C3), 63.9 (C1), 72.9 (C4'), 74.3 (C2'), 77.3 (C3' and C5'), 78.7 (C2), 104.5 (C1'), 172.1 (CO), 173.1 (CO);

ESI-MS (CH<sub>3</sub>OH, negative-ion mode): m/z 533.3 [M-1]<sup>-</sup>, calcd for C<sub>27</sub>H<sub>50</sub>O<sub>10</sub>, m/z 534.34 [M].

Application of the general procedure to compound **43b** (140 mg, 0.210 mmol) with Dowex® Marathon™ C, H<sup>+</sup> form (140 mg) afforded 1-O-decanoyl-2-O-β-D-glucuronopyranosyl-*sn*-glycerol **27a** (72 mg, 0.170 mmol, 81% yield) as a white sticky solid.



$[\alpha]_D^{20}$ : -31.6 (CHCl<sub>3</sub>:CH<sub>3</sub>OH 65:35, c 1.0);

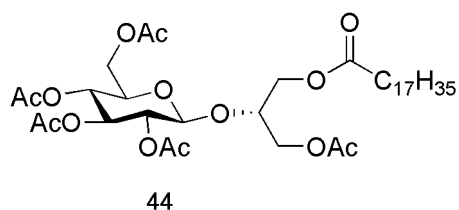
<sup>1</sup>H-NMR (Pyd<sub>5</sub>): δ= 0.82 (t, 3H, J=7.0 Hz, CH<sub>3</sub>), 1.09-1.27 (m, 12H, 6 CH<sub>2</sub>), 1.62 (m, 2H, CH<sub>2</sub>), 2.36 (m, 2H, CH<sub>2</sub>), 4.09 (dd, J<sub>1',2'</sub>=7.8 Hz, J<sub>2',3'</sub>=8.4 Hz, 1H, H-2'), 4.15 (dd, 1H, J<sub>3a,2</sub>=5.5 Hz, J<sub>3a,3b</sub>=11.4 Hz, H-3a), 4.21 (dd, 1H, J<sub>3b,2</sub>=4.8 Hz, H-3b), 4.32 (dd, 1H, J<sub>3',4'</sub>=8.9 Hz, H-3'), 4.51 (m, 1H, H-2), 4.58 (dd, 1H, J<sub>4',5'</sub>=8.9 Hz, H-4'), 4.64 (d, 1H, H-5'), 4.68-4.76 (m, 2H, H-1a and H-1b), 5.20 (d, 1H, H-1');

<sup>13</sup>C-NMR (Pyd<sub>5</sub>): δ= 13.7 (CH<sub>3</sub>), 22.4 (CH<sub>2</sub>), 24.7 (CH<sub>2</sub>), 28.7-29.2 (4 CH<sub>2</sub>), 31.5 (CH<sub>2</sub>), 33.8 (CH<sub>2</sub>), 62.2 (C3), 63.8 (C1), 72.8 (C4'), 74.3 (C2'), 77.2 (C5'), 77.3 (C3'), 78.7 (C2), 104.5 (C1'), 172.1 (CO), 173.1 (CO);

ESI-MS (CH<sub>3</sub>OH, negative-ion mode): m/z 421.5 [M-1]<sup>-</sup>, Calcd for C<sub>19</sub>H<sub>34</sub>O<sub>10</sub>, m/z 422.22 [M].

#### Configuration assignment of compound 40a

Compound **40a** (27 mg, 0.038 mmol) was dissolved in dry pyridine (1 mL) and acetic anhydride (500 μL, Py/Ac<sub>2</sub>O 2:1 v/v) was added. The reaction was stirred at room temperature and stopped after 3 hours (TLC, hexane/AcOEt 6:4). Then the solvent was evaporated under reduced pressure and the crude purified by flash chromatography (hexane/AcOEt 7:3) and the obtained pure compound (oil, 24



mg, 0.033 mmol, 82% yield) resulted identical to the known 1-*O*-octadecanoyl-3-*O*-acetyl-2-*O*-(2',3',4',6'-tetra-*O*-acetyl- $\beta$ -D-glucopyranosyl)-*sn*-glycerol **44**.<sup>60</sup>

$[\alpha]_D^{20}$ : -8.7 (CHCl<sub>3</sub>, c 1);

<sup>1</sup>H NMR (CDCl<sub>3</sub>):  $\delta$  = 0.86 (t, 3H, J=7.0 Hz, CH<sub>3</sub>), 1.19-1.33 (m, 28H, 14 CH<sub>2</sub>), 1.59 (m, 2H, CH<sub>2</sub>), 1.98 (s, 3H, COCH<sub>3</sub>), 2.00 (s, 3H, COCH<sub>3</sub>), 2.01 (s, 3H, COCH<sub>3</sub>), 2.04 (s, 3H, COCH<sub>3</sub>), 2.06 (s, 3H, COCH<sub>3</sub>), 2.29 (t, 2H, J=7.6 Hz, CH<sub>2</sub>), 3.67 (ddd, 1H, J<sub>5',6'a</sub>=2.4 Hz, J<sub>5',6'b</sub>=5.1 Hz, J<sub>4',5'</sub>=10.0 Hz, H-5'), 4.04 (m, 1H, H-2), 4.06-4.20 (m, 5H, H-1a, H-1b, H-3a, H-3b and H-6'a), 4.22 (dd, 1H, J<sub>6'a,6'b</sub>=12.3 Hz, H-6'b), 4.61 (d, 1H, J<sub>1',2'</sub>=7.9 Hz, H-1'), 4.96 (dd, 1H, J<sub>2',3'</sub>=9.6 Hz, H-2'), 5.04 (dd, 1H, J<sub>3',4'</sub>=9.6 Hz, H-4'), 5.17 (dd, 1H, H-3');

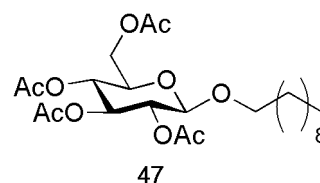
<sup>13</sup>C-NMR (CDCl<sub>3</sub>):  $\delta$ =14.1 (CH<sub>3</sub>), 20.4-20.08 (5 COCH<sub>3</sub>), 22.7 (CH<sub>2</sub>), 24.8 (CH<sub>2</sub>), 28.9-29.9 (12 CH<sub>2</sub>), 31.9 (CH<sub>2</sub>), 34.1 (CH<sub>2</sub>), 62.0 (C6'), 63.1 (C1), 63.3 (C3), 68.4 (C4'), 71.3 (C2'), 71.9 (C5'), 72.7 (C3'), 75.6 (C2), 100.8 (C1'), 169.1, 169.3, 170.2, 170.5, 170.6 and 173.3 (6 CO);

ESI-MS (CH<sub>3</sub>OH, positive-ion mode): m/z 753.5 [M+Na]<sup>+</sup>, calcd for C<sub>37</sub>H<sub>62</sub>O<sub>14</sub>, m/z 730.41 [M].

#### 2.7.4 Synthesis of glucuronosyl derivatives 28a,b

##### Synthesis of 2',3',4',6'-tetra-*O*-acetyl-*n*-decyl- $\beta$ -D-glucopyranosyl **47**

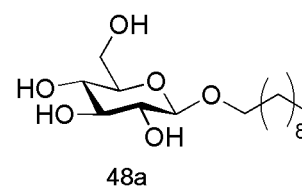
To a solution of glucose pentaacetate **45** in dry CH<sub>2</sub>Cl<sub>2</sub> (0.1 M) in Ar atmosphere, decanoyl alcohol (3 eq., 4.5 ml) was added and after cooling to -10 °C also BF<sub>3</sub>·Et<sub>2</sub>O (3.25 eq., 3.0 ml) was added dropwise. The reaction mixture was left stirring at room for 4 hours, then diluted with 50 ml of CH<sub>2</sub>Cl<sub>2</sub> and washed with saturated aqueous NaHCO<sub>3</sub> (50 ml), H<sub>2</sub>O (50 ml) and brine (50 ml). The organic layers were dried (Na<sub>2</sub>SO<sub>4</sub>), filtered and concentrated under vacuum. <sup>1</sup>H NMR analysis of the crude mixture showed the formation of two diastereoisomers. Purification of the crude product using silica gel gradient flash chromatography (hexane/AcOEt from 8:2 to 1:1) afforded 1.34 g (2.74 mmol, 36%) of the major  $\beta$  diastereoisomer **47**, as a white solid.



For characterization see Ref.<sup>67</sup>

##### Synthesis of *n*-decyl- $\beta$ -D-glucopyranosyl **48a**

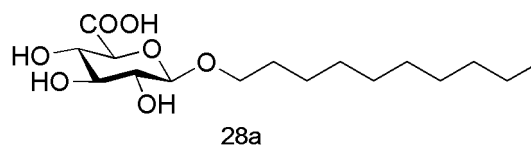
To a solution of **47** (1.30 g, 2.66 mmol) in CH<sub>3</sub>OH (5 mL) CH<sub>3</sub>ONa 0.7 M in CH<sub>3</sub>OH (3 eq., 11.5 ml) was added. The reaction was stirred for 5 hours at room temperature and quenched with Dowex H<sup>+</sup> washing with CH<sub>3</sub>OH. After removal of the solvent under vacuum, the resulting white solid product **48a** (802 mg, 2.503 mmol, 94%) was used without further purification in the next step.



For characterization see Ref.<sup>67</sup>

### Synthesis of *n*-decyl-β-D-glucopyranosiduronic acid **28a**

Compound **48a** (100 mg, 0.312 mmol) was suspended in a 55:45 mixture of CH<sub>3</sub>CN and 0.67M phosphate sodium buffer at pH 6.7 (0.1 M, 3 ml). TEMPO (0.21 eq., 10 mg, 0.065 mmol), NaClO<sub>2</sub>

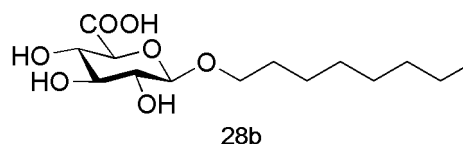


(20% aqueous solution, 3 eq., 0.936 mmol, 430 μl) and NaClO (15% aqueous solution, 0.15 eq., 0.047 mmol, 25 μl) were added. After stirring 4 hours at room temperature (TLC, CH<sub>2</sub>Cl<sub>2</sub>/CH<sub>3</sub>OH 85:15), 10 ml of Na<sub>2</sub>S<sub>2</sub>O<sub>3</sub> 0.5 M and a few drops of HCl 12 M were added. The aqueous phase was extracted with Et<sub>2</sub>O (3×10 ml) and the organic layers were assembled, dried over anhydrous Na<sub>2</sub>SO<sub>4</sub>, filtered and evaporated under reduced pressure. The crude was purified by silica gel flash chromatography (CH<sub>2</sub>Cl<sub>2</sub>/CH<sub>3</sub>OH from 8:2 to 7:3) to give **28a** (55 mg, 0.164 mmol, 53%) as a white solid.

For characterization see Ref.<sup>62</sup>

### Synthesis of *n*-octyl-β-D-glucopyranosiduronic acid **28b**

The commercial octyl-β-D-glucopyranosyl (100 mg, 0.342 mmol) was suspended in a 55:45 mixture of CH<sub>3</sub>CN and 0.67M phosphate sodium buffer at pH 6.7 (0.1 M, 3.5 ml). TEMPO (0.21 eq., 11 mg, 0.072 mmol), NaClO<sub>2</sub>



(20% aqueous solution, 3 eq., 1.026 mmol, 460 μl) and NaClO (15% aqueous solution, 0.15 eq., 0.051 mmol, 25 μl) were added. After stirring 4 hours at room temperature (TLC, CH<sub>2</sub>Cl<sub>2</sub>/CH<sub>3</sub>OH 85:15), 10 ml of Na<sub>2</sub>S<sub>2</sub>O<sub>3</sub> 0.5 M and a few drops of HCl 12 M were added. The aqueous phase was extracted with Et<sub>2</sub>O (10 ml ×3) and the organic layers were assembled, dried over anhydrous Na<sub>2</sub>SO<sub>4</sub>, filtered and evaporated under reduced pressure. The crude was purified by silica gel flash chromatography (CH<sub>2</sub>Cl<sub>2</sub>/CH<sub>3</sub>OH from 8:2) to give **28b** (65 mg, 0.212 mmol, 62%) as a white solid.

For characterization see Ref.<sup>62</sup>

### 2.7.5 Akt Inhibition Assays

*Akt1 ELISA activity assay.* The inhibitory activity of compounds **26a,b**, **27a,b** and **28a,b** Miltefosine, Perifosine and Sodium Dodecyl Sulfate SDS was tested employing the CycLex AKT/PKB kinase Assay/Inhibitor Screening Kit. Plates were pre-coated with “AKTide-2T” which can be efficiently phosphorylated by Akt1. The detector antibody specifically detects the phosphorylated “AKTide-2T”. Particularly, to perform the test, the samples **26b**, **27a,b**, **28a,b** and SDS were dissolved in DMSO (note that **26a** was insoluble in this solvent), and Miltefosine and Perifosine in water. The prepared solutions were diluted in Kinase Buffer to a final concentration of 500, 100, 50, 10 and 1  $\mu$ M. Compounds were added together with constitutive active form of human Akt1 (25 m units/well), and allowed to phosphorylate the bound substrate following the addition of  $Mg^{2+}$  and ATP. The amount of phosphorylated substrate was measured by binding it with horseradish peroxidase conjugate of an anti-phospho-AKTide-2T monoclonal antibody, which then catalyzes the conversion of the chromogenic substrate tetra-methylbenzidine from the colourless reduced form to the yellow oxidized product, after the addition of the stopping reagent. The absorbance of the resulting solution is determined spectrophotometrically at  $\lambda = 450$  nm, and it is related to Akt1 activity in the tested solution. Staurosporine at the final concentration of 1  $\mu$ M was employed as “inhibitor control” as indicated in the assay protocol.

Each experiment was performed in triplicate.

### 2.7.6 Cellular studies

*Compounds preparation.* All tested compounds were easily dissolved in 100% DMSO at 50 mM, while Perifosine was dissolved in H<sub>2</sub>O at 20 mM.

*Cell culture and cell growth assay.* The human ovarian carcinoma IGROV-1 cell line<sup>68</sup> was grown in RPMI-1640 medium supplemented with 10% fetal bovine serum at 37°C in 5% CO<sub>2</sub> atmosphere. For cell growth inhibition assays, cells were plated in 12 well-plates at 10000 cells/cm<sup>2</sup> in complete medium. The day after seeding, cells were exposed to solvent (DMSO) or to different concentration of the novel compounds for 72 h. For tests in serum-free medium, the day after seeding complete medium was substituted with serum-free medium and the cells were exposed to the compounds. Twenty four hours later drug-containing medium was replaced with complete medium.

Cells were harvested using trypsin and counted 96 h after seeding by a Coulter Counter.

Each experiment was performed three times. The percentages of inhibition in drug-treated *versus* untreated samples are reported in dose-response curves.  $IC_{50}$  represents the drug concentration inhibiting growth by 50%.



## Chapter 3

### Fluorescent probes to study Akt inhibitor distribution

#### 3.1 Introduction

The application of fluorescent probes in biochemistry is of considerable interest because it can enable the study of several biological pathways and explain cascades of activation/inhibition. With their use, advantages in understanding the protein activity in their natural environment, in real-time and in non-invasive fashion, can also be reached. This gives insight into the protein physiological behavior allowing to gain information about their alterations in pathological contexts, which can be exploited to develop therapeutic strategies.

The phenomenon of fluorescence, first described by Herschel in 1845 for the quinine,<sup>69</sup> starts when a molecule in a singlet electronic ground state ( $S_0$ ) absorbs energy which promotes the transition of an electron to an higher energy state ( $S_1$ ). This excited electron quickly returns to the previous level through more excited state with intermediate energy, as illustrated in the Jabłoński diagram (Figure 3.1).

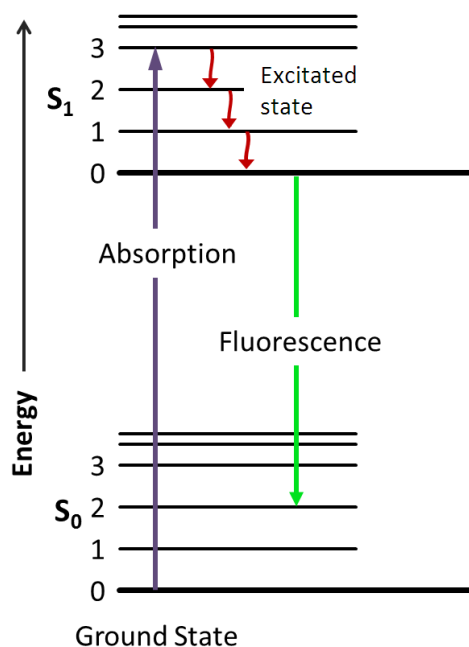
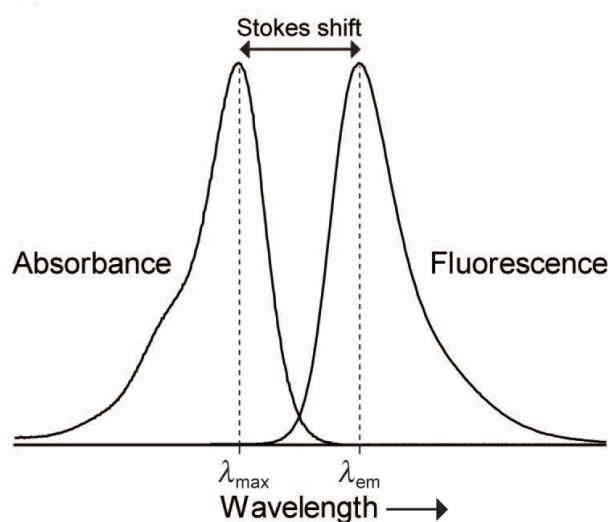


Figure 3.1: Jabłoński diagram.

If the decay takes place with photon emission produces the fluorescent effect which manifests itself with the emission of light having a longer wavelength and lower energy than the absorbed radiation. The most striking examples of fluorescence occur when the absorbed radiation is in the ultraviolet region of the spectrum, invisible to the human eye, and the emitted light is in the visible region.

In Figure 3.2 a generic absorption/emission spectrum is reported. The maximal absorption ( $\lambda_{\max}$ ) is related to the energy between the ground state  $S_0$  and the higher energy level reached by the electron  $S_1$ . The maximal emission wavelength ( $\lambda_{\text{em}}$ ) is longer than  $\lambda_{\max}$ , and their difference, demonstrated by Stokes,<sup>70</sup> is therefore called “Stokes shift”. This parameter is an index of the applicability of the fluorophores. Small Stokes shifts reveal susceptibility to self-quenching *via* energy transfer, limiting their use.<sup>71</sup> Other characteristics of the fluorophores are the lifetime of the excited state ( $\tau$ ), that generally have a range from 0.1 to 100 ns and influence the time-resolved measurement<sup>72</sup> and fluorescence polarization applications,<sup>73</sup> the quantum efficiency ( $\Phi$ ), which is the ratio of photons fluoresced and absorbed, and the extinction coefficient ( $\epsilon$ ).

Fluorophores can be used in many ways, including as labels for biomolecules, enzyme substrates or environmental indicators. The choice between a fluorophore or another is based on their specific chemical properties, such as reactivity, stability or lipophilicity, and photophysical properties, *e.g.*  $\lambda_{\max}$ ,  $\lambda_{\text{em}}$ ,  $\tau$ ,  $\epsilon$  and  $\Phi$ .



**Figure 3.2:** Generic absorption and emission spectra.  $\lambda_{\max}$ ,  $\lambda_{\text{em}}$  and Stokes shift are shown.

As touched on before, Herschel found that the quinine, a natural compound relevant for both medicinal and organic chemistry, had fluorescent properties. To date, more classes of fluorescent dyes<sup>74</sup> have been developed and gathered on the basis of their origins and chemical characteristics. The main fluorophores, reported in function of their brightness vs the wavelength, are shown in Figure 3.3.

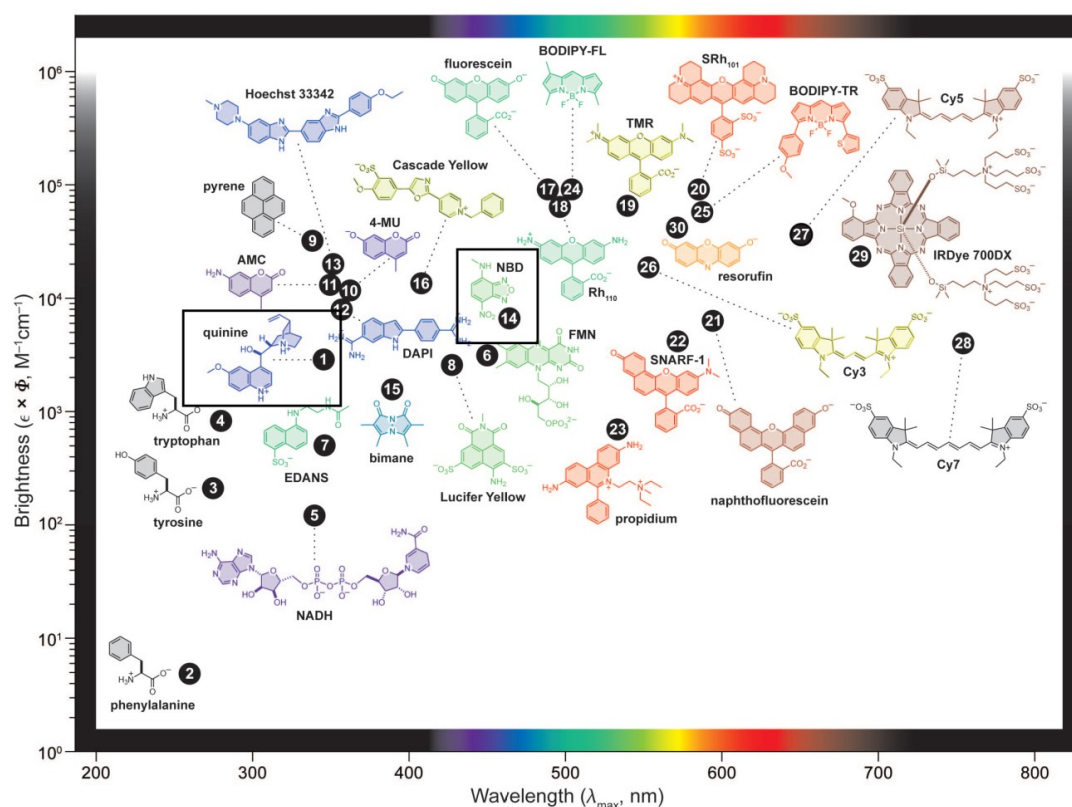


**Figure 3.3:** Plot of fluorophore brightness ( $\epsilon \times \Phi$ ) vs the wavelength of maximum absorption ( $\lambda_{max}$ ) for the major classes of fluorophores. The color of the structure indicates its wavelength of maximum emission ( $\lambda_{em}$ ). For clarity, only the fluorophoric moiety of some molecules is shown. In evidence quinine and NBD, used as fluorophore in this PhD thesis (see below). Taken from Ref.<sup>74</sup>

Apart from the quinine, the Nature offers a lot of others fluorophores. Among these, aromatic amino acids as phenylalanine, tyrosine and tryptophan have fluorescence properties, first described by Weber.<sup>75</sup> The latter is the most fluorescent amino acid used as index for a variety of processes like protein folding and ligand binding.<sup>76</sup> Also polycyclic aromatics compounds are largely used as fluorescent dyes, as naphthalene and pyrene derivatives. In particular, pyrene exhibits a long-lived excited state with  $\tau > 100$  ns which allows to study protein conformation.<sup>77</sup> A small heterocyclic fluorophore is the 4-chloro-7-nitro-1,2,3-benzoxadiazole (NBD-Cl).<sup>78</sup> When it binds to a

primary amine its fluorescent properties are disclosed. This fluorophore can be easily conjugated to small molecules, such as sugars<sup>79</sup> and exploited in the preparation of lipid probes<sup>80</sup> and novel kinase substrates.<sup>81</sup>

These are just some examples of the main fluorophores known, but there are many others. Therefore, elaboration of these core structures could provide numerous others probes for assaying biological systems since biochemical and biological pathways require ever more sophisticated and tailored probes.

### 3.2 Aim of the work

The possibility of studying with fluorescent probes the intracellular distribution of our synthetic inhibitors of the Akt is at the basis of this PhD chapter. This would allow us to better understand if the glucuronosyl derivatives enter the cells and, eventually, inhibitory properties are applied on the Akt in the cytosol or in the nucleus. Fluorescent compounds constitute interesting and powerful tools for drug discovery programs and also, as in our case, could be used to explain the action mechanism.

To this end, the 1-*O*-octadecanoyl-2-*O*- $\beta$ -D-glucuronopyranosyl-*sn*-glycerol **27a**, which resulted the most active Akt inhibitor among the synthesized analogues reported in *Chapter 2*, was selected and functionalized with a fluorescent dye to the free hydroxyl group on the glycerol moiety. We decided to use the 7-nitro-1,2,3-benzoxadiazole (NBD) fluorescent group since in literature a similar example is reported. Indeed Sakaguchi<sup>82</sup> used the NBD probe to demonstrate the localization of sulfoquinovosylmonoacylglycerols SQMG.

So, the purpose of this part of PhD project was to synthesize two compounds, **49a** and **49b** showed in Figure 3.4, carrying the same fluorophore but attached to the hydroxyl group of the glycerol moiety with chains of different length. In this way, we obtained two compounds with different polarity related to the compound of interest **27a** to study its localization.

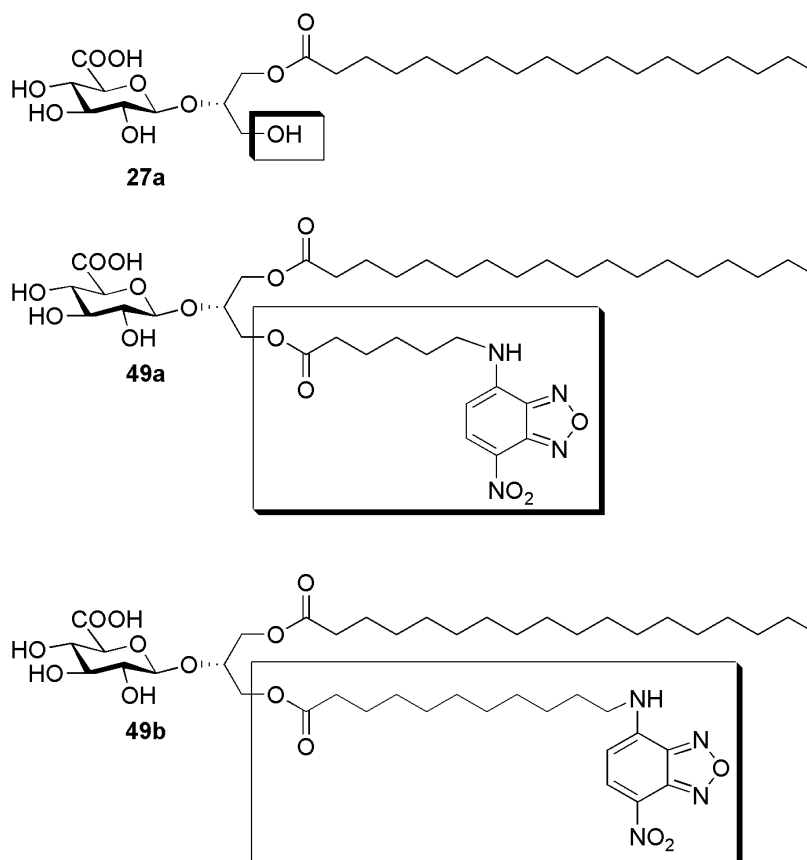
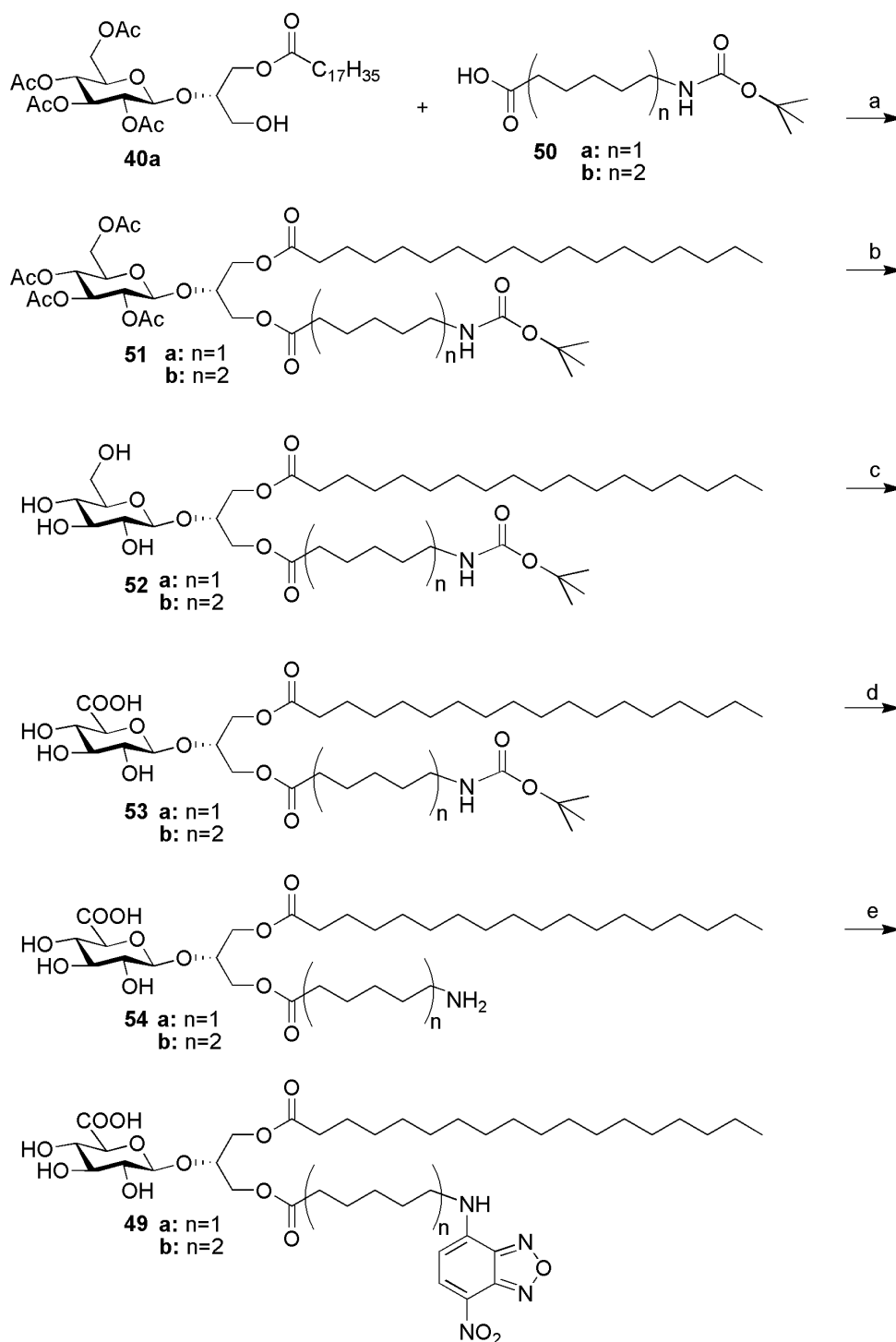


**Figure 3.4:** Compound **27a**, which resulted the most active Akt inhibitor among the synthesized analogues reported in *Chapter 2*, and derivatives **49a** and **b** with fluorescent probe.

### 3.3 Results and discussion

#### 3.3.1 Synthesis of fluorescent compounds **49a,b**

To prepare the desired products **49a** and **49b**, the same synthetic scheme was planned, which foresees to start from 1-*O*-octadecanoyl-2-*O*-(2',3',4',6'-tetra-*O*-acetyl- $\beta$ -D-glucopyranosyl)-*sn*-glycerol **40a** (Scheme 3.1). To introduce the spacer with the amino group, necessary for the following reaction with the NBD-Cl, Boc-amino-aliphatic acid with two different length were chosen. Specifically, the 6-(Boc-amino)hexanoic acid **50a** or the 11-(Boc-amino)undecanoic acid **50b**, were inserted on the glycerol moiety of the compound **40a** by means of a condensation reaction with 2 equivalents of *N*-(3-dimethylaminopropyl)-*N'*-ethylcarbonimide hydrochloride EDCI and 4 eq. of 4-(dimethylamino)pyridine DMAP in dichloromethane 0.1M. Under this condition, the reaction proceeded to completion in an hour at room temperature under magnetic stirring, affording compound **51a** or **b** with high yield.



**Scheme 3.1:** a) EDCI, DMAP,  $\text{CH}_2\text{Cl}_2$  dry, rt, 97-85%; b) Hydrazine hydrate, EtOH aq. 85%, 45°C, 40-46%; c) TEMPO, NaClO/NaClO<sub>2</sub>,  $\text{CH}_3\text{CN}$ , 0.67M phosphate buffer (pH 6.7), rt, quantit.; d) TFA,  $\text{CH}_2\text{Cl}_2$ , rt, quantit.; e) NBD-Cl, NaHCO<sub>3</sub>,  $\text{CH}_3\text{CN}$ , H<sub>2</sub>O, 55°C, 35-43%.

The following reaction was the hydrazinolysis performed using 5 eq. of hydrazine hydrate, which proved to be the best amount of reagent to use obtained from several previous attempts, as already discussed in *Chapter 2* section 2.3.2, in aqueous ethanol

at 45°C, to give **52**. The switch from primary hydroxyl group in position 6 of the sugar to carboxyl group was accomplished by oxidation performed with TEMPO in acetonitrile and buffer sodium phosphate mixture and NaClO/NaClO<sub>2</sub> system. The product **53** was recovered as pure compound with Et<sub>2</sub>O extraction and subsequently the Boc protection on the nitrogen was easily removed after 30 minutes under magnetic stirring with trifluoroacetic acid (10 eq.) in dichloromethane. Finally, the free amine **54** was reacted with the NBD chloride reagent to achieve the two fluorescent compounds **49a** or **b**. This last reaction was carried out in acetonitrile 0.1M with the adding dropwise of the reactive dissolved in acetonitrile (1 eq., 18 mL/mmol) and an aqueous NaHCO<sub>3</sub> solution (3 eq., 6 mL/mmol), since basic condition is necessary for the formation of the product. The reaction mixture was stirring for 1 hour and half at 55°C. Afterwards TLC analysis (CH<sub>2</sub>Cl<sub>2</sub>/MeOH 85:15) showed the formation of a fluorescent spot corresponding to the desired product.

The fluorescent properties of the two synthesized compounds **49a** and **b** were also estimated. The spectra reported in Figure 3.5 show for both the compounds a maximum peak of emission at 520 nm with excitation at 432 nm, as expected from the literature.<sup>74</sup>

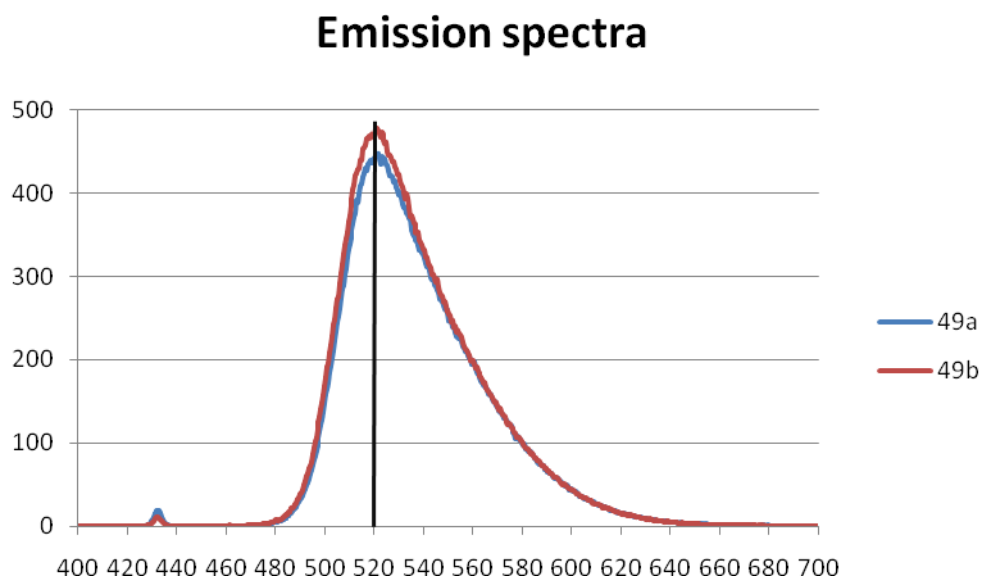


**Figure 3.5:** Spectra of emission of compounds **49a** and **b**. With excitation at 432 nm a maximum peak at 520 nm for both compounds is evident.

### 3.4 Conclusions

A straightforward synthetic strategy for the achievement of functionalized compounds **49a** and **b** as derivatives of the glucuronosylacylglycerol inhibitor **27a** is presented in this chapter. The applied procedure employs the insertion of an amino spacer on the glycerol moiety and the following attachment of a fluorescent group.

The biological evaluation of these two compounds aimed to study their cell localization is now underway. The knowledge gained from this work might shed light on their action mechanism and eventually suggest some modifications to their structural features in order to obtain more active compounds.



## 3.5 Experimental section

### 3.5.1 General methods

**Chemical:** All chemicals and solvents were purchased as reagent grade from Sigma–Aldrich and were used as received, except for  $\text{CH}_2\text{Cl}_2$  which was distilled from calcium hydride prior to use. Air- and moisture sensitive liquids and solutions were transferred *via* oven-dried syringe.

All reactions were monitored by TLC analysis carried out on silica gel plate (Merck 60F<sub>254</sub>). Flash column chromatography (FCC) was performed on silica gel high-purity grade, pore size 60Å, 230-400 mesh particle size (Sigma-Aldrich) or by a Biotage Isolera™ Prime flash purification system (Biotage-Uppsala, Sweden). Evaporation under reduced pressure was effected with a bath temperature at 40°C or under stream of nitrogen.

The structures of all the new synthesized compounds were confirmed through full  $^1\text{H}$  and  $^{13}\text{C}$  NMR characterization and mass spectroscopy, which confirmed purity and identity of all synthesized compounds.

$^1\text{H}$  NMR analysis were performed at 500 MHz with a Bruker FT-NMR AVANCE™ DRX500 spectrometer using a 5 mm z-PFG (pulsed field gradient) broadband reverse probe at 298 K unless otherwise stated, and  $^{13}\text{C}$  NMR spectra at 125.76 MHz were done for all the new compounds. Chemical shifts are reported as  $\delta$  (ppm) relative to residual  $\text{CHCl}_3$  or  $\text{CH}_3\text{OD}$  fixed respectively at 7.26 and 3.30 ppm (higher field signal) for  $^1\text{H}$  NMR spectra and relative to  $\text{CDCl}_3$  fixed at 77.0 ppm (central line) and  $\text{CD}_3\text{OD}$  at 49.0 ppm (central line) for  $^{13}\text{C}$  NMR spectra. Integrals are in accordance with assignments and coupling constants (J) are given in hertz (Hz). For detailed peak assignments 2D spectra were measured (COSY and HSQC). Splitting patterns are described by using the following abbreviations: *br*, broad; *s*, singlet; *d*, doublet; *t*, triplet; *m*, multiplet; *dd*, doublet of doublet; *ddd*, doublet of doublet of doublet; *td*, triplet of doublet; *dt*, doublet of triplet.

Mass spectra were recorded in negative or positive-ion electrospray (ESI) mode on a Thermo Quest Finnigan LCQ DECA™ ion trap mass spectrometer. The mass spectrometer was equipped with a Finnigan ESI interface. Sample solutions were injected with a ionization spray voltage of 4.5 kV or 5.0 kV (positive and negative-ion

mode, respectively), a capillary voltage of 32 V or -15 V (positive and negative-ion mode, respectively), and capillary temperature of 250 °C. Data were processed by Finnigan Xcalibur software system.

Optical rotations were determined on a Perkin–Elmer 241 polarimeter at 20°C, in a 1 dm or 1 cm cell. Melting points were recorded on a Büchi 510 capillary melting point apparatus and were uncorrected.

Fluorimeter of final compounds was measured with Luminiscence Spectrometer LS 50B (Perkin-Elmer).

### 3.5.2 Synthesis of fluorescent compounds 49a,b

#### General procedure of the condensation reaction with Boc-amino-aliphatic acid

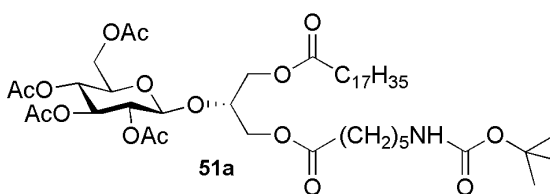
1-*O*-octadecanoyl-2-*O*-(2',3',4',6'-tetra-*O*-acetyl-β-*D*-glucopyranosyl)-*sn*-glycerol **40** was dissolved in dry CH<sub>2</sub>Cl<sub>2</sub> (0.1M). The proper Boc-amino-aliphatic acid (2 eq.), EDCI (4 eq.) and DMAP (2 eq.) were added and the mixture stirred under Ar atmosphere for 1 hour (TLC check Hexane/AcOEt 6:4). The reaction was poured into brine solution (30ml) and extracted with CH<sub>2</sub>Cl<sub>2</sub> (3×30ml). The organic phase was dried over anhydrous Na<sub>2</sub>SO<sub>4</sub>, filtered and the solvent was removed in vacuum to afford the crude product which was purified by automatic flash chromatography (Hexane/AcOEt 65:35 to 30:70) giving **51a** or **b**.

Application of the general procedure to **40a** (787 mg, 1.14 mmol) with 6-(Boc-amino)hexanoic acid (576 mg, 2.28 mmol), EDCI (874 mg, 4.56 mmol) and DMAP (278 mg, 2.28 mmol) afforded compound 1-*O*-octadecanoyl-3-*O*-(6-terbutoxycarbonylamino-hexanoyl)-2-*O*-(2',3',4',6'-tetra-*O*-acetyl-β-*D*-glucopyranosyl)-*sn*-glycerol **51a** as a white solid (997 mg, 1.105 mmol, 97% yield).

Mp: 59.4-61.8°C;

[α]<sub>D</sub><sup>20</sup>: -8.2 (CHCl<sub>3</sub>, *c* 1.0);

<sup>1</sup>H-NMR (CDCl<sub>3</sub>): δ = 0.87 (t, 3H, J=7.0 Hz, CH<sub>3</sub>), 1.22-1.37 (m, 30H, 15 CH<sub>2</sub>), 1.46 (s, 9H, 3 CH<sub>3</sub>), 1.48 (m, 2H, CH<sub>2</sub>), 1.58-1.67 (m, 4H, 2 CH<sub>2</sub>), 2.00 (s, 3H, COCH<sub>3</sub>), 2.02 (s, 3H, COCH<sub>3</sub>), 2.03 (s, 3H, COCH<sub>3</sub>), 2.08 (s, 3H, COCH<sub>3</sub>), 2.28-2.35 (m, 4H, 2 CH<sub>2</sub>), 3.10 (*br t*, 2H, CH<sub>2</sub>N), 3.69 (ddd, 1H, J<sub>5',6'a</sub>=2.5 Hz, J<sub>5',6'b</sub>=5.0 Hz, J<sub>4',5'</sub>=10.0 Hz, H-5'), 4.05 (m, 1H, H-2), 4.05-4.27 (m, 6H, H-1a, H-1b, H-3a, H-3b, H-6'a and H-6'b), 4.59 (*br s*, 1H, NH), 4.63

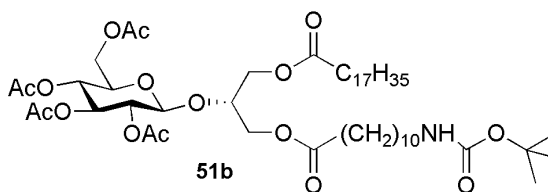


(d, 1H,  $J_{1',2'}=8.0$  Hz, H-1'), 4.98 (dd, 1H,  $J_{2',3'}=9.6$  Hz, H-2'), 5.06 (dd, 1H,  $J_{3',4'}=9.6$  Hz, H-4'), 5.19 (dd, 1H, H-3');

$^{13}\text{C}$ -NMR ( $\text{CDCl}_3$ ):  $\delta= 14.1$  ( $\text{CH}_3$ ), 20.4-21.0 (4  $\text{COCH}_3$ ), 22.7 ( $\text{CH}_2$ ), 24.4 ( $\text{CH}_2$ ), 24.8 ( $\text{CH}_2$ ), 26.3 ( $\text{CH}_2$ ), 28.4 (3  $\text{CH}_3$ ), 29.2-29.7 (13  $\text{CH}_2$ ), 31.9 ( $\text{CH}_2$ ), 33.8 ( $\text{CH}_2$ ), 34.1 ( $\text{CH}_2$ ), 40.0 ( $\text{CH}_2\text{N}$ ), 60.4 ( $\text{C6}'$ ), 61.9 ( $\text{C1}$ ), 63.1 ( $\text{C3}$ ), 68.3 ( $\text{C4}'$ ), 71.2 ( $\text{C2}'$ ), 71.9 ( $\text{C5}'$ ), 72.7 ( $\text{C3}'$ ), 75.6 ( $\text{C2}$ ), 79.0 ( $\text{C}(\text{CH}_3)_3$ ), 100.8 ( $\text{C1}'$ ), 156.0 ( $\text{COBoc}$ ), 169.2, 169.4, 170.2 and 170.6, (4  $\text{COCH}_3$ ), 173.1 and 173.4 (2 CO);

ESI-MS ( $\text{CH}_3\text{OH}$ , positive-ion mode):  $m/z$  924.5  $[\text{M}+\text{Na}]^+$ , calcd for  $\text{C}_{46}\text{H}_{79}\text{NO}_{16}$ ,  $m/z$  901,54  $[\text{M}]$ .

Application of the general procedure to **40a** (805 mg, 1.168 mmol) with 11-(Boc-amino)undecanoic acid (704 mg, 2.336 mmol), EDCI (895 mg, 4.672 mmol) and DMAP (285 mg, 2.336 mmol) afforded compound 1-*O*-



octadecanoyl-3-*O*-(11-terbutoxycarbonylamino-undecanoyl)-2-*O*-(2',3',4',6'-tetra-*O*-acetyl- $\beta$ -*D*-glucopyranosyl)-*sn*-glycerol **51b** as a white solid (1090 mg, 1.121 mmol, 96% yield).

Mp: 83.6-84.2°C;

$[\alpha]_D^{20}$ : -5.8 ( $\text{CHCl}_3$ ,  $c$  0.6);

$^1\text{H}$ -NMR ( $\text{CDCl}_3$ ):  $\delta = 0.88$  (t, 3H,  $J=7.0$  Hz,  $\text{CH}_3$ ), 1.25 (*br s*, 40H, 20  $\text{CH}_2$ ), 1.44 (s, 9H, 3  $\text{CH}_3$ ), 1.48 (m, 2H,  $\text{CH}_2$ ), 1.54-1.65 (m, 4H, 2  $\text{CH}_2$ ), 2.00 (s, 3H,  $\text{COCH}_3$ ), 2.02 (s, 3H,  $\text{COCH}_3$ ), 2.03 (s, 3H,  $\text{COCH}_3$ ), 2.08 (s, 3H,  $\text{COCH}_3$ ), 2.31 (td, 4H,  $J=2.6$  Hz,  $J=7.6$ , 2  $\text{CH}_2$ ), 3.09 (*br t*, 2H,  $\text{CH}_2\text{N}$ ), 3.69 (ddd, 1H,  $J_{5',6'a}=2.5$  Hz,  $J_{5',6'b}=5.0$  Hz,  $J_{4',5'}=10.0$  Hz, H-5'), 4.05 (m, 1H, H-2), 4.05-4.27 (m, 6H, H-1a, H-1b, H-3a, H-3b, H-6'a and H-6'b), 4.50 (*br s*, 1H, NH), 4.63 (d, 1H,  $J_{1',2'}=8.0$  Hz, H-1'), 4.98 (dd, 1H,  $J_{2',3'}=9.6$  Hz, H-2'), 5.06 (dd, 1H,  $J_{3',4'}=9.6$  Hz, H-4'), 5.19 (dd, 1H, H-3');

$^{13}\text{C}$ -NMR ( $\text{CDCl}_3$ ):  $\delta= 14.1$  ( $\text{CH}_3$ ), 20.6-20.9 (4  $\text{COCH}_3$ ), 22.7 ( $\text{CH}_2$ ), 24.7 ( $\text{CH}_2$ ), 24.8 ( $\text{CH}_2$ ), 26.8 ( $\text{CH}_2$ ), 28.4 (3  $\text{CH}_3$ ), 29.1-30.0 (18  $\text{CH}_2$ ), 31.9 ( $\text{CH}_2$ ), 34.0 ( $\text{CH}_2$ ), 34.1 ( $\text{CH}_2$ ), 40.6 ( $\text{CH}_2\text{N}$ ), 61.9 ( $\text{C1}$ ), 63.0 ( $\text{C3}$ ), 63.1 ( $\text{C6}'$ ), 68.3 ( $\text{C4}'$ ), 71.2 ( $\text{C2}'$ ), 71.9 ( $\text{C5}'$ ), 72.7 ( $\text{C3}'$ ), 75.7 ( $\text{C2}$ ), 79.0 ( $\text{C}(\text{CH}_3)_3$ ), 100.8 ( $\text{C1}'$ ), 156.0 ( $\text{COBoc}$ ), 169.1 169.4, 170.2 and 170.6, (4  $\text{COCH}_3$ ), 173.3 (2 CO);

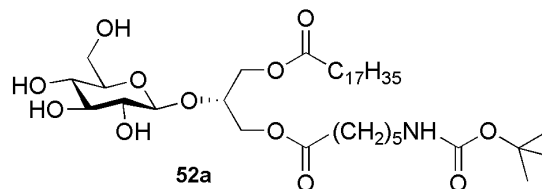
ESI-MS ( $\text{CH}_3\text{OH}$ , positive-ion mode):  $m/z$  999.4  $[\text{M}+\text{Na}]^+$ , calcd for  $\text{C}_{51}\text{H}_{89}\text{NO}_{16}$ ,  $m/z$  971,62  $[\text{M}]$ .

#### General procedure of hydrazinolysis to give compounds **52a** or **b**

Compound **51** was dissolved in EtOH 85% (0.1 M) and hydrazine hydrate (5 eq.) was added drop by drop. The reaction mixture was left stirring 6 hours at 45°C. Then, the

solvent was evaporated under stream of nitrogen and the crude was purified by flash chromatography (CH<sub>2</sub>Cl<sub>2</sub>/CH<sub>3</sub>OH 95:5) to yield title compounds.

Application of the general procedure to **51a** (458 mg, 0.507 mmol) with hydrazine hydrate (123  $\mu$ l, 2.53 mmol) afforded compound 1-*O*-octadecanoyl-3-*O*-(6-terbutoxycarbonylamino-hexanoyl)-2-*O*- $\beta$ -D-glucopyranosyl-*sn*-glycerol **52a** as an oil (171 mg, 0.233 mmol, 46% yield).



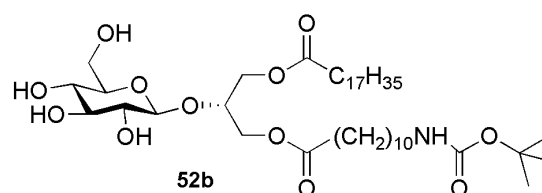
$[\alpha]_D^{20}$ : -5.9 (CH<sub>3</sub>OH, *c* 1.0);

<sup>1</sup>H-NMR (CD<sub>3</sub>OD):  $\delta$  = 0.89 (t, 3H, *J*=7.0 Hz, CH<sub>3</sub>), 1.23-1.36 (m, 30H, 15 CH<sub>2</sub>), 1.42 (s, 9H, 3 CH<sub>3</sub>), 1.47 (m, 2H, CH<sub>2</sub>), 1.57-1.65 (m, 4H, 2 CH<sub>2</sub>), 2.35 (td, 4H, *J*=2.8 Hz, *J*=7.5 Hz, 2 CH<sub>2</sub>), 3.02 (dd, 2H, *J*=6.9 Hz, *J*=12.8 Hz, CH<sub>2</sub>N), 3.16 (dd, 1H, *J*<sub>1',2'</sub>=8.0 Hz, *J*<sub>2',3'</sub>=9.0 Hz, H-2'), 3.26-3.36 (m, 3H, H-3', H-4' and H-5'), 3.65 (dd, 1H, *J*<sub>5',6'a</sub>=5.2 Hz, *J*<sub>6'a,6'b</sub>=12.0 Hz, H-6'a), 3.85 (d, 1H, *J*<sub>6'a,6'b</sub>=12.0 Hz, H-6'b), 4.17 (dd, 1H, *J*<sub>1b/3b,2</sub>=5.0 Hz, *J*=10.0 Hz, H-2), 4.23 (d, 3H, *J*<sub>1b/3b,2</sub>=5.0 Hz, H-1a, H-1b, H-3a or H-3b), 4.28 (dd, 1H, *J*<sub>3a/3b,2</sub>=5.0 Hz, *J*<sub>3a/3b,1a/1b</sub>=11.4 Hz, H-3a or H-3b), 4.41 (d, 1H, *J*<sub>1',2'</sub>=8.0 Hz, H-1');

<sup>13</sup>C-NMR (CD<sub>3</sub>OD):  $\delta$ = 14.4 (CH<sub>3</sub>), 23.7 (CH<sub>2</sub>), 25.9 (CH<sub>2</sub>), 26.0 (CH<sub>2</sub>), 27.3 (CH<sub>2</sub>), 28.8 (3 CH<sub>3</sub>), 30.2-30.8 (13 CH<sub>2</sub>), 33.1 (CH<sub>2</sub>), 34.8 (CH<sub>2</sub>), 34.9 (CH<sub>2</sub>), 41.2 (CH<sub>2</sub>N), 62.9 (C6'), 64.3 (C1), 64.8 (C3), 71.4 (C4'), 75.6 (C2'), 76.1 (C2), 77.5 (C5'), 78.0 (C3'), 79.8 (C(CH<sub>3</sub>)<sub>3</sub>), 104.4 (C1'), 158.5 (COBoc), 175.1 and 175.4 (2 CO);

ESI-MS (CH<sub>3</sub>OH, positive-ion mode): *m/z* 756.4 [M+Na]<sup>+</sup>, calcd for C<sub>38</sub>H<sub>71</sub>NO<sub>12</sub>, *m/z* 733.49 [M].

Application of the general procedure to **51b** (558 mg, 0.576 mmol) with hydrazine hydrate (140  $\mu$ l, 2.88 mmol) afforded compound 1-*O*-octadecanoyl-3-*O*-(11-terbutoxycarbonylamino-undecanoyl)-2-*O*- $\beta$ -D-glucopyranosyl-*sn*-glycerol **52b** as an oil (185 mg, 0.230 mmol, 40% yield).



$[\alpha]_D^{20}$ : -8.0 (CH<sub>3</sub>OH, *c* 1.0);

<sup>1</sup>H-NMR (CD<sub>3</sub>OD):  $\delta$ =0.89 (t, 3H, *J*=7.0 Hz, CH<sub>3</sub>), 1.22-1.36 (m, 40H, 20 CH<sub>2</sub>), 1.42 (s, 9H, 3 CH<sub>3</sub>), 1.47 (m, 2H, CH<sub>2</sub>), 1.56-1.65 (m, 4H, 2 CH<sub>2</sub>), 2.34 (td, 4H, *J*=4.4 Hz, *J*=7.4 Hz, 2 CH<sub>2</sub>), 3.01 (t, 2H, *J*=7.0 Hz, CH<sub>2</sub>N), 3.17 (dd, 1H, *J*<sub>1',2'</sub>=8.0 Hz, *J*<sub>2',3'</sub>=9.1 Hz, H-2'), 3.25-3.36 (m, 3H, H-3', H-4' and H-5'), 3.65 (dd, 1H, *J*<sub>5',6'a</sub>=4.7 Hz, *J*<sub>6'a,6'b</sub>=12.5 Hz, H-6'a), 3.85 (d, 1H, *J*<sub>6'a,6'b</sub>=12.5 Hz, H-6'b), 4.15-4.26 (m, 4H, H-2, H-1a, H-1b, H-3a or H-3b), 4.29 (dd, 1H, *J*<sub>3a/3b,2</sub>=4.6 Hz, *J*<sub>3a/3b,1a/1b</sub>=11.3 Hz, H-3a or H-3b), 4.42 (d, 1H, *J*<sub>1',2'</sub>=8.0 Hz, H-1');

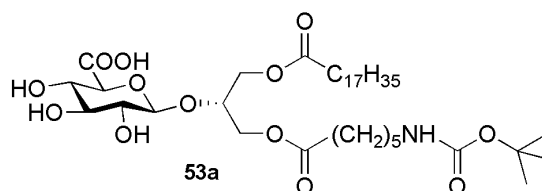
$^{13}\text{C}$ -NMR ( $\text{CD}_3\text{OD}$ ):  $\delta$ = 14.4 ( $\text{CH}_3$ ), 23.7 ( $\text{CH}_2$ ), 26.0 ( $\text{CH}_2$ ), 27.9 ( $\text{CH}_2$ ), 28.8 (3  $\text{CH}_3$ ), 30.2-30.8 (13  $\text{CH}_2$ ), 33.1 ( $\text{CH}_2$ ), 34.9 ( $\text{CH}_2$ ), 41.4 ( $\text{CH}_2\text{N}$ ), 62.9 ( $\text{C6}'$ ), 64.1 ( $\text{C1}$ ), 64.7 ( $\text{C3}$ ), 71.6 ( $\text{C4}'$ ), 75.0 ( $\text{C2}'$ ), 76.0 ( $\text{C2}$ ), 78.0 ( $\text{C5}'$ ), 78.1 ( $\text{C3}'$ ), 79.7 ( $\text{C}(\text{CH}_3)_3$ ), 104.4 ( $\text{C1}'$ ), 158.5 ( $\text{COBoc}$ ), 175.2 and 175.3 (2  $\text{CO}$ );

ESI-MS ( $\text{CH}_3\text{OH}$ , positive-ion mode):  $m/z$  826.47 [ $\text{M}+\text{Na}$ ] $^+$ , calcd for  $\text{C}_{43}\text{H}_{81}\text{NO}_{12}$ ,  $m/z$  803.57 [ $\text{M}$ ].

#### General procedure of oxidation to obtain compounds 53a,b

Compound **52a** or **b** was suspended in a 55:45 mixture of  $\text{CH}_3\text{CN}$  and 0.67M phosphate sodium buffer at pH 6.7 (0.1 M). TEMPO (0.21 eq.),  $\text{NaClO}_2$  (20% aqueous solution, 3 eq.) and  $\text{NaClO}$  (15% aqueous solution, 0.15 eq.) were added. After stirring overnight at room temperature (TLC,  $\text{CH}_2\text{Cl}_2/\text{CH}_3\text{OH}$  9:1), the reaction mixture was diluted with diethyl ether (10 mL). The organic layer was separated and the aqueous layer was extracted again with diethyl ether (2x10 mL). The combined organic extracts were dried over  $\text{Na}_2\text{SO}_4$ , filtered, and the solvent was eliminated under reduced pressure to afford the crude product **53a** or **b** with quantitative yield, which were employed in the following step without further purification.

Application of the general procedure to **52a** (155 mg, 0.211 mmol) with TEMPO (7 mg, 0.044 mmol),  $\text{NaClO}_2$  (290  $\mu\text{l}$  of 20% aqueous solution, 0.633 mmol) and  $\text{NaClO}$  (16  $\mu\text{l}$  of 15% aqueous solution, 0.032 mmol) afforded compound 1-*O*-octadecanoyl-3-*O*-(6-terbutoxycarbonylamino-hexanoyl)-2-*O*- $\beta$ -D-glucuronopyranosyl-*sn*-glycerol **53a** as a glass (158 mg, 0.211 mmol, quantitative yield).



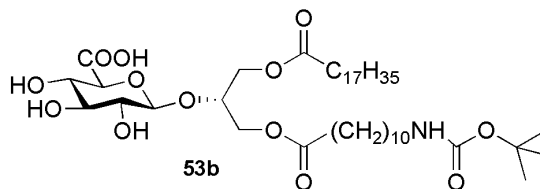
$[\alpha]_D^{20}$ : -8.9 ( $\text{CHCl}_3$ ,  $c$  1.2);

$^1\text{H}$ -NMR ( $\text{CDCl}_3:\text{CD}_3\text{OD}$  9:1):  $\delta$ = 0.79 (t, 3H,  $J=7.0$  Hz,  $\text{CH}_3$ ), 1.13-1.29 (m, 30H, 15  $\text{CH}_2$ ), 1.35 (s, 9H, 3  $\text{CH}_3$ ), 1.38-1.41 (m, 2H,  $\text{CH}_2$ ), 1.49-1.57 (m, 4H, 2  $\text{CH}_2$ ), 2.26 (m, 4H, 2  $\text{CH}_2$ ), 2.98 (t, 2H,  $J=6.9$  Hz,  $\text{CH}_2\text{N}$ ), 3.26 (dd, 1H,  $J_{1',2'}=7.9$  Hz,  $J_{2',3'}=9.0$  Hz, H-2'), 3.40 (dd, 1H,  $J_{3',4'}=9.0$  Hz, H-3'), 3.56 (dd, 1H,  $J_{4',5'}=9.7$  Hz, H-4'), 3.71 (1H, d, H-5'), 4.04 (dd, 1H,  $J_{1b/3b,2}=5.0$  Hz,  $J=10.0$  Hz, H-2), 4.11 (dd, 1H,  $J_{3a/3b,2}=5.0$  Hz,  $J_{3a/3b,1a/1b}=11.8$  Hz, H-3a or H-3b), 4.13-4.18 (m, 2H, H-1a, H1b), 4.19 (dd, 1H,  $J_{3a/3b,2}=5.0$  Hz,  $J_{3a/3b,1a/1b}=11.8$  Hz, H-3a or H-3b), 4.34 (d, 1H, H-1');

$^{13}\text{C}$ -NMR ( $\text{CD}_3\text{OD}$ ):  $\delta$ = 13.9 ( $\text{CH}_3$ ), 20.1 ( $\text{CH}_2$ ), 22.5 ( $\text{CH}_2$ ), 24.2 ( $\text{CH}_2$ ), 24.6 ( $\text{CH}_2$ ), 26.0 ( $\text{CH}_2$ ), 28.2 (3  $\text{CH}_3$ ), 29.0-30.1 (12  $\text{CH}_2$ ), 31.7 ( $\text{CH}_2$ ), 33.7 ( $\text{CH}_2$ ), 33.9 ( $\text{CH}_2$ ), 40.1 ( $\text{CH}_2\text{N}$ ), 62.8 ( $\text{C1}$ ), 63.4 ( $\text{C3}$ ), 71.1 ( $\text{C4}'$ ), 72.7 ( $\text{C2}'$ ), 74.3 ( $\text{C2}$ ), 77.5 ( $\text{C5}'$ ), 75.7 ( $\text{C3}'$ ), 79.3 ( $\text{C}(\text{CH}_3)_3$ ), 103.0 ( $\text{C1}'$ ), 156.5 ( $\text{COBoc}$ ), 170.8 ( $\text{COOH}$ ), 173.7 and 174.0 (2  $\text{CO}$ );

ESI-MS (CH<sub>3</sub>OH, negative-ion mode): m/z 746.4 [M-1]<sup>-</sup>, calcd for C<sub>38</sub>H<sub>69</sub>NO<sub>13</sub>, m/z 747.47 [M].

Application of the general procedure to **52b** (75 mg, 0.093 mmol) with TEMPO (3 mg, 0.019 mmol), NaClO<sub>2</sub> (126 μl of 20% aqueous solution, 0.279 mmol) and NaClO (7 μl of 15% aqueous solution, 0.014 mmol) afforded compound 1-*O*-



octadecanoyl-3-*O*-(11-terbutoxycarbonylamino-undecanoyl)-2-*O*-β-D-glucuronopyranosyl-*sn*-glycerol **53b** as a glass (76 mg, 0.093 mmol, quantitative yield).

$[\alpha]_D^{20}$ : -8.2 (CHCl<sub>3</sub>, c 1.8);

<sup>1</sup>H-NMR (CD<sub>3</sub>OD: CDCl<sub>3</sub>: 6:3): δ= 0.85 (t, 3H, J=7.0 Hz, CH<sub>3</sub>), 1.20-1.32 (m, 40H, 20 CH<sub>2</sub>), 1.40 (s, 9H, 3 CH<sub>3</sub>), 1.43-1.48 (m, 2H, CH<sub>2</sub>), 1.53-1.62 (m, 4H, 2 CH<sub>2</sub>), 2.31 (m, 4H, 2 CH<sub>2</sub>), 3.00 (t, 2H, J=7.0 Hz, CH<sub>2</sub>N), 3.23 (t, 1H, J<sub>1',2'</sub>=7.9 Hz, H-2'), 3.40 (t, 1H, J<sub>3',4'</sub>=9.0 Hz, H-3'), 3.44 (t, 1H, J<sub>4',5'</sub>=9.0 Hz, H-4'), 3.55 (1H, d, H-5'), 4.19-4.27 (m, 4H, H-2, H1a, H1b, H-3a or H-3b), 4.32 (m, 1H, H-3a or H-3b), 4.42 (d, 1H, H-1');

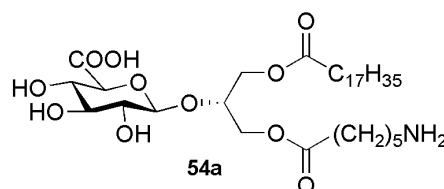
<sup>13</sup>C-NMR (CD<sub>3</sub>OD): δ= 14.3 (CH<sub>3</sub>), 23.3 (CH<sub>2</sub>), 25.5 (CH<sub>2</sub>), 27.5 (CH<sub>2</sub>), 28.7 (3 CH<sub>3</sub>), 29.8-30.6 (20 CH<sub>2</sub>), 32.6 (CH<sub>2</sub>), 34.7 (CH<sub>2</sub>), 41.1 (CH<sub>2</sub>N), 63.6 (C1), 64.3 (C3), 72.9 (C4'), 74.4 (C2'), 74.6 (C2), 77.1 (C3'), 77.5 (C5'), 79.6 (C(CH<sub>3</sub>)<sub>3</sub>), 103.6 (C1'), 157.9 (CONBoc), 174.9 and 175.0 (2 CO), 175.9 (COOH);

ESI-MS (CH<sub>3</sub>OH, negative ion mode): m/z 816.8 [M-1]<sup>-</sup>, calcd for C<sub>43</sub>H<sub>79</sub>NO<sub>13</sub>, m/z 817.55 [M].

#### General procedure of Boc deprotection

To a solution of compound **53a** or **b** in CH<sub>2</sub>Cl<sub>2</sub> (0.1 M) TFA (10 eq.) was added drop by drop. The reaction mixture turn yellow and after 30 minutes the TLC check (CH<sub>2</sub>Cl<sub>2</sub>/CH<sub>3</sub>OH 8:2) showed disappearance of the starting material and formation of the product. The solvent was evaporated and the crude product **54a** or **b**, which did not need further purification, was recovered with quantitative yield.

Application of the general procedure to **53a** (150 mg, 0.200 mmol) with TFA (154 μL, 2.00 mmol) afforded compound 1-*O*-octadecanoyl-3-*O*-(6-amino-hexanoyl)-2-*O*-β-D-glucuronopyranosyl-*sn*-glycerol **54a** as a white vax (129 mg, 0.200 mmol, quantitative yield).



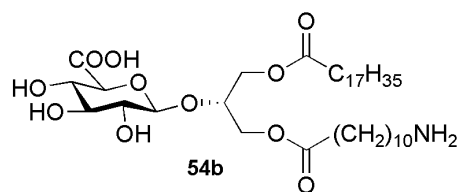
$[\alpha]_D^{20}$ : -1.20 (CH<sub>3</sub>OH, c 2.8);

$^1\text{H-NMR}$  ( $\text{CD}_3\text{OD}$ ):  $\delta=0.88$  (t, 3H,  $J=6.7$  Hz,  $\text{CH}_3$ ), 1.27 (s, 30H, 15  $\text{CH}_2$ ), 1.37-1.44 (m, 2H,  $\text{CH}_2$ ), 1.54-1.70 (m, 4H, 2  $\text{CH}_2$ ), 2.36 (dt, 4H,  $J=7.3$  Hz,  $J=14.7$  Hz, 2  $\text{CH}_2$ ), 2.93 (t, 2H,  $J=7.4$  Hz,  $\text{CH}_2\text{N}$ ), 3.22 (t, 1H,  $J_{1',2'}=8\text{Hz}$ , H-2'), 3.40 (t, 1H,  $J_{3',4'}=9.0$  Hz, H-3'), 3.52 (t, 1H,  $J_{4',5'}=9.0$  Hz, H-4'), 3.81 (1H, d, H-5'), 4.15 (dd, 1H,  $J=4.8$  Hz,  $J=9.7$  Hz, H-2), 4.18-4.26 (m, 4H, H-1a, H1b, H-3a and H-3b), 4.50 (d, 1H, H-1');

$^{13}\text{C-NMR}$  ( $\text{CD}_3\text{OD}$ ):  $\delta= 14.4$  ( $\text{CH}_3$ ), 17.8 ( $\text{CH}_2$ ), 21.0 ( $\text{CH}_2$ ), 23.7 ( $\text{CH}_2$ ), 25.2 ( $\text{CH}_2$ ), 26.8 ( $\text{CH}_2$ ), 28.1 ( $\text{CH}_2$ ), 30.2-30.7 (10  $\text{CH}_2$ ), 33.0 ( $\text{CH}_2$ ), 34.5 ( $\text{CH}_2$ ), 34.9 ( $\text{CH}_2$ ), 40.5 ( $\text{CH}_2\text{N}$ ), 64.1 (C1), 63.8 (C3), 64.8 (C2), 73.0 (C4'), 74.6 (C2'), 76.7 (C3'), 77.3 (C5'), 104.5 (C1'), 172.4 (COOH), 174.9 and 175.3 (2 CO);

ESI-MS ( $\text{CH}_3\text{OH}$ , positive-ion mode):  $m/z$  665.5  $[\text{M}+18]^+$ , calcd for  $\text{C}_{33}\text{H}_{61}\text{NO}_{11}$ ,  $m/z$  647.42  $[\text{M}]$ .

Application of the general procedure to **53b** (70 mg, 0.085 mmol) with TFA (65  $\mu\text{L}$ , 0.85 mmol) afforded compound 1-*O*-octadecanoyl-3-*O*-(11-amino-undecanoyl)-2-*O*- $\beta$ -D-glucuronopyranosyl-*sn*-glycerol **54b** as an oil (61 mg, 0.085 mmol, quantitative yield).



$[\alpha]_D^{20}$ : -1.1 ( $\text{CH}_3\text{OH}$ ,  $c$  2.0);

$^1\text{H-NMR}$  ( $\text{CD}_3\text{OD}$ ):  $\delta=0.89$  (t, 3H,  $J=6.9$  Hz,  $\text{CH}_3$ ), 1.24-1.35 (m, 40H, 20  $\text{CH}_2$ ), 1.54-1.69 (m, 6H, 3  $\text{CH}_2$ ), 2.34 (q, 4H,  $J=7.4$  Hz, 2  $\text{CH}_2$ ), 2.91 (t, 2H,  $J=7.6$  Hz,  $\text{CH}_2\text{N}$ ), 3.22 (dd, 1H,  $J_{1',2'}=7.9$  Hz,  $J_{2',3'}=9.0$  Hz, H-2'), 3.39 (t, 1H,  $J_{3',4'}=9.0$  Hz, H-3'), 3.50 (t, 1H,  $J_{4',5'}=9.0$  Hz, H-4'), 3.73 (1H, d, H-5'), 4.17-4.28 (m, 5H, H-1a, H1b, H-3a, H-3b and H-2), 4.47 (d, 1H, H-1');

$^{13}\text{C-NMR}$  ( $\text{CD}_3\text{OD}$ ):  $\delta= 14.4$  ( $\text{CH}_3$ ), 23.7 ( $\text{CH}_2$ ), 25.9 ( $\text{CH}_2$ ), 26.0 ( $\text{CH}_2$ ), 27.4 ( $\text{CH}_2$ ), 28.5 ( $\text{CH}_2$ ), 30.1-30.7 (17  $\text{CH}_2$ ), 33.0 ( $\text{CH}_2$ ), 34.9 (2 $\text{CH}_2$ ), 40.8 ( $\text{CH}_2\text{N}$ ), 64.1 (C1), 64.7 (C3), 73.2 (C4'), 74.7 (C2'), 76.4(C2), 76.7(C5'), 77.5 (C3'), 104.4 (C1'), 173.6 (COOH), 175.2 and 175.3 (2 CO);

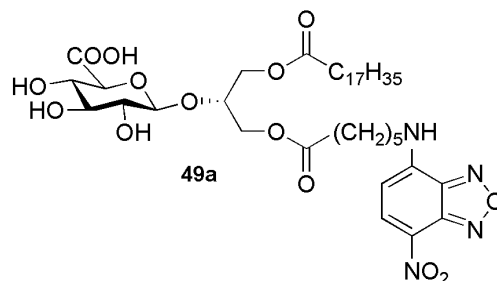
ESI-MS ( $\text{CH}_3\text{OH}$ , positive-ion mode):  $m/z$  740.50  $[\text{M}+23]^+$ , calcd for  $\text{C}_{38}\text{H}_{71}\text{NO}_{11}$ ,  $m/z$  717.50  $[\text{M}]$ .

### Synthesis of final compounds 49a and b

Compound **54a** or **b** was dissolved in acetonitrile (0.1 M) and a solution of NBD-Cl (1.0 eq.) in acetonitrile (18 mL/mmol) and sodium bicarbonate (3.0 equiv) in water (6 mL/mmol), were added dropwise. The reaction mixture was stirred at 55  $^\circ\text{C}$  for 1 hour away from the light. Then acetonitrile was concentrated under reduced pressure, the pH was adjusted to  $\sim 2.0$  with 10 ml of HCl 0.1 N and the mixture was extracted with  $\text{CH}_2\text{Cl}_2$  (3x15 mL) The combined organic layers were washed with  $\text{H}_2\text{O}$ , dried over  $\text{Na}_2\text{SO}_4$  and the solvent was evaporated under vacuum. The crude obtained was

purified by flash column chromatography (CH<sub>2</sub>Cl<sub>2</sub>/CH<sub>3</sub>OH 85:15) to afford the final compound **49a** or **b**.

Application of the general procedure to **54a** (120 mg, 0.185 mmol) with NBD-Cl (37 mg, 0.185 mmol) and NaHCO<sub>3</sub> (47 mg, 0.565 mmol) afforded compound 1-*O*-octadecanoyl-3-*O*-(6-[(7-nitro-2,1,3-benzoxadiol-4-yl)amino]-hexanoyl)-2-*O*-β-*D*-glucuronopyranosyl-*sn*-glycerol **49a** as a brown solid (52 mg, 0.065 mmol, 35% yield).



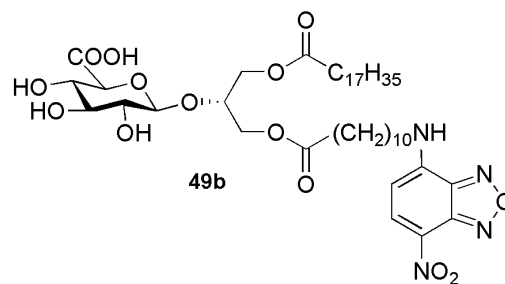
$[\alpha]_D^{20}$ : not measurable;

<sup>1</sup>H-NMR (CD<sub>3</sub>OD): δ=0.88 (t, 3H, J=7.0 Hz, CH<sub>3</sub>), 1.23-1.34 (m, 30H, 15 CH<sub>2</sub>), 1.45-1.53 (m, 2H, CH<sub>2</sub>), 1.54-1.64 (m, 2H, CH<sub>2</sub>), 1.66-1.72 (m, 2H, CH<sub>2</sub>), 1.76-1.82 (m, 2H, CH<sub>2</sub>), 2.33 (t, 2H, J=7.3 Hz, CH<sub>2</sub>), 2.39 (t, 2H, J=7.3 Hz, CH<sub>2</sub>N), 3.21 (dd, 1H, J<sub>1',2'</sub>=7.8 Hz, J<sub>2',3'</sub>=9.0 Hz, H-2'), 3.39 (t, 1H, J<sub>3',4'</sub>=9.0 Hz, H-3'), 3.45 (t, 1H, J<sub>4',5'</sub>=9.0 Hz, H-4'), 3.58 (d, 1H, H-5'), 4.20-4.26 (m, 4H, H-1a, H1b, H-3a and H-3b), 4.28-4.37 (m, 1H, H-2), 4.45 (d, 1H, H-1'), 6.33 (*br d*, 1H, Ar), 8.53 (*br d*, 1H, Ar);

<sup>13</sup>C-NMR (CD<sub>3</sub>OD): δ= 14.4 (CH<sub>3</sub>), 23.7 (CH<sub>2</sub>), 25.6 (CH<sub>2</sub>), 25.9 (CH<sub>2</sub>), 27.5 (CH<sub>2</sub>), 30.2-30.8 (10 CH<sub>2</sub>), 33.1 (CH<sub>2</sub>), 34.7 (CH<sub>2</sub>), 34.9 (CH<sub>2</sub>), 40.6 (CH<sub>2</sub>N), 64.0 (C1), 64.8 (C3), 73.6 (C4'), 74.9 (C2'), 75.8 (C2), 76.4 (C5'), 77.7 (C3'), 104.2 (C1'), 174.9 and 175.3 (2 CO);

ESI-MS (CH<sub>3</sub>OH, negative-ion mode): *m/z* 809.6 [M-1]<sup>-</sup>, calcd for C<sub>39</sub>H<sub>62</sub>N<sub>4</sub>O<sub>14</sub>, *m/z* 810.42 [M].

Application of the general procedure to **54b** (50 mg, 0.069 mmol) with NBD-Cl (14 mg, 0.069 mmol) and NaHCO<sub>3</sub> (18 mg, 0.207 mmol) afforded compound 1-*O*-octadecanoyl-3-*O*-(11-[(7-nitro-2,1,3-benzoxadiol-4-yl)amino]-undecanoyl)-2-*O*-β-*D*-glucuronopyranosyl-*sn*-glycerol **49b** as a brown solid (43 mg, 0.049 mmol, 43% yield).



$[\alpha]_D^{20}$ : not measurable;

<sup>1</sup>H-NMR (CD<sub>3</sub>OD+20% CDCl<sub>3</sub>): δ=0.89 (t, 3H, J=7.0 Hz, CH<sub>3</sub>), 1.24-1.37 (m, 40H, 20 CH<sub>2</sub>), 1.57-1.65 (m, 6H, 3 CH<sub>2</sub>), 1.79 (dt, 2H, J=7.5 Hz, J=14.9 Hz, CH<sub>2</sub>), 1.95-2.11 (m, 2H, CH<sub>2</sub>), 2.35 (dt, 2H, J=4.7 Hz, J=7.5 Hz, CH<sub>2</sub>N), 3.26 (t, 1H, J<sub>1',2'</sub>=8.0 Hz, H-2'), 3.44 (t, 1H, J<sub>3',4'</sub>=9.0 Hz, H-3'), 3.48-3.55 (m, 1H, H-4'), 3.63 (t, 1H, J<sub>4',5'</sub>=9.0 Hz, H-5'), 4.21-4.29 (m, 4H, H-1a, H1b, H-3a and H-3b), 4.31-4.38 (m, 1H, H-2), 4.47 (d, 1H, H-1'), 6.32 (d, 1H, J=8.8 Hz, Ar), 8.53 (d, 1H, J=8.8 Hz, Ar);



$^{13}\text{C}$ -NMR ( $\text{CD}_3\text{OD}+20\% \text{CDCl}_3$ ):  $\delta= 14.4$  ( $\text{CH}_3$ ),  $23.5$  ( $\text{CH}_2$ ),  $25.7$  ( $2 \text{CH}_2$ ),  $27.9$  ( $\text{CH}_2$ ),  $28.8$  ( $\text{CH}_2$ ),  $29.9$ - $30.5$  ( $17 \text{CH}_2$ ),  $32.8$  ( $\text{CH}_2$ ),  $34.8$  ( $2 \text{CH}_2$ ),  $40.6$  ( $\text{CH}_2\text{N}$ ),  $63.7$  ( $\text{C1}$ ),  $64.5$  ( $\text{C3}$ ),  $73.2$  ( $\text{C4}'$ ),  $74.4$  ( $\text{C2}'$ ),  $75.5$  ( $\text{C2}$ ),  $75.8$  ( $\text{C5}'$ ),  $77.3$  ( $\text{C3}'$ ),  $103.9$  ( $\text{C1}'$ ),  $174.9$  and  $175.1$  ( $2 \text{CO}$ );

ESI-MS ( $\text{CH}_3\text{OH}$ , negative-ion mode):  $m/z$  879.5 [ $\text{M}-1$ ] $^-$ , calcd for  $\text{C}_{44}\text{H}_{72}\text{N}_4\text{O}_{14}$ ,  $m/z$  880.50 [ $\text{M}$ ].

## **PART 2**

## Chapter 4

### Gold nanoparticles as carriers for fully synthetic carbohydrate vaccine candidates against *Streptococcus pneumoniae*

#### 4.1 Introduction

Vaccination is a key strategy for the control of many infectious diseases. Although the introduction of antibiotics in therapy 50 years ago has slowed down the research in this field, today multidrug-resistance and adverse effects have pushed towards new strategies to improve the vaccines in use.

Carbohydrates expressed at pathogen surface, such as capsular polysaccharides of many bacteria or the dense array of oligosaccharides of HIV virus, are involved in interactions with host cells and play a pivotal role in the immune response, usually masking the highly immunogenic protein material and avoiding an effective production of specific and functional antibodies. Because polysaccharides are typical T-independent antigens,<sup>83</sup> they are poor immunogens and unable to establish long-term immunological memory. In 1931, Avery and Goedel<sup>84</sup> have demonstrated that the conjugation of the polysaccharide of *Streptococcus pneumoniae* serotype 3 bacteria to an immunogenic protein carrier enhances the immunogenicity of the carbohydrate by inducing a T-dependent switch, with the formation of a long-lasting memory response. This evidence has opened the way to the concept of conjugate vaccines, which have been highly successful in preventing infectious diseases.<sup>85,86</sup>

However, many others features need to be improved. One bottleneck is the natural source of the carbohydrate antigens currently used in vaccine preparations. Not all bacterial strains can be cultured on sufficient scale and the process of isolation and purification from bacterial cultures can be complicated, besides the fact that these processes require many checks at different stages raising the cost of the vaccine.<sup>87</sup> In the last years, much effort has been devoted to the individuation of the smallest saccharide structures able to evoke an immunological response. In this way, thank also to the improvements in the synthetic carbohydrate chemistry field, the possibility to use synthetic carbohydrate fragments of the corresponding natural antigens have been

exploited and well-defined chemical structures lacking of impurities and with less or no batch-to-batch variability can be produced.<sup>88</sup> Another upside to take into account about the use of synthetic oligosaccharides is also the possibility to functionalize their reducing end, during the synthesis, with a spacer amenable for the following chemoselective conjugation. Consequently, synthetic oligosaccharide-protein conjugates vaccines have emerged as an attractive option. In 2004, the first large-scale synthesis of the polysaccharide capsular antigen of *Haemophilus influenzae* type b (Hib) was reported by Bencomo *et al.*<sup>89</sup> and the first semi-synthetic carbohydrate conjugate vaccine was introduced in Cuba's national vaccination program. The minimum portion of antigen necessary to evoke an immunological response has been also found for glycosylphosphatidylinositol (GPI), an important toxin in malaria disease. Seeberger<sup>90</sup> has proposed the synthesis of GPI glycan fractions, and in particular, suggested that a pentasaccharide residue likely represents the minimal epitope for naturally elicited anti-GPI antibodies. The synthesis of the minimum fraction with immunological activity was reported also for many other human pathogens, such as *Shigella flexeri* 2a,<sup>91</sup> *Neisseria meningitides A*,<sup>92,93</sup> *Streptococcus pneumoniae* 6C<sup>94</sup> and 14.<sup>95</sup>

Many of these natural saccharide antigens are characterized by the presence of labile portions in the original structure that can be easily subjected to hydrolysis, *e.g.* phosphate bridges. These capsular polysaccharide require transporting and storing in cold conditions due to their limited shelf-life at room temperature. This inconvenient has addressed the research toward the generation of new molecular entities related to natural structures to be used in the development of glycoconjugates vaccines. Examples of synthetic analogues of natural antigen, in which chemical modifications improve the chemical stability maintaining the immunological properties unaltered or close to corresponding original structure, are reported in the literature for many pathogen bacteria, such as *Streptococcus pneumoniae* 19F<sup>96</sup> and *Neisseria meningitides A*.<sup>97,98</sup>

Although the use of synthetic glycan antigens may improve many of the discussed aspects, no-specific methods are used for the conjugation of the antigens to the protein carrier introducing heterogeneity in the resulting glycoconjugates, which can show diverse pharmacokinetic and immunological properties due to different glycan/protein ratios and glycosylation sites.<sup>85</sup> Another main concern to solve about

glycoconjugate vaccines is the risk of carrier-induced epitope suppression. For this reason, the search for new carriers that may overcome the hurdles encountered with the use of proteins is object of intense research.

Among the different strategies, nanoparticulate systems have attracted very interest because they could offer advantages over proteins as vaccine carriers.<sup>99</sup> One of the most important aspects is their small size, which allows administration through several routes and influences the uptake by antigen presenting cells (APCs), but above all what is important is the possibility to insert, in the same nanostructure, different antigenic components which may increase the efficacy of the vaccine candidate. Thus, nanostructures can be used to more effectively manipulate or deliver immunologically active components and successful applications of nanotechnology in the field of immunology could enable the generations of new vaccines.<sup>100</sup> In addition, the assembly of more units of carbohydrate antigens in the same scaffold leads to the generation of glycoclusters with high-avidity interactions for the receptor involved in the immunological response.<sup>101</sup> In fact, it is well-known that carbohydrate-carbohydrate<sup>102</sup> and carbohydrate-protein interactions,<sup>103,104</sup> are weakly and of low affinity. To overcome these drawbacks, carbohydrates are generally aggregated in nature into higher-order oligomeric structures. This so-called "cluster glycoside effect" noted by Lee and co-workers in 1995,<sup>103</sup> has inspired the design of different multivalent systems, in which, as effect of the phenomenon of multivalency, the overall binding can be much stronger than the combination of the individual binding events.<sup>105</sup>

In the last years, various strategies have been used to translate this knowledge to the preparation and design of synthetic multivalent systems that could be used as delivery systems in the vaccinology field. This is reflected in the development of different structures, such as glycoliposomes,<sup>106</sup> glycopolymers,<sup>107</sup> glycopeptides and glycoproteins,<sup>108</sup> glyocalixarene,<sup>109</sup> glycodentrimers,<sup>110</sup> glycocyclodextrines,<sup>111</sup> glycofullerenes<sup>112</sup> and glyconanoparticles.<sup>113</sup> These multivalent model systems, thanks to their ability to mimic the natural presentation of biomolecules, are starting to emerge as potential vaccines able to evoke an immune response higher than the one of the polysaccharide antigens used in classical vaccination. Also, it has been observed that the degree of carbohydrates loading influence the immunogenicity of the vaccine.<sup>114</sup>

Several examples of conjugation of synthetic repeating units of natural polysaccharide antigens to nanoplateforms have been developed with the aim to conceive fully synthetic carbohydrate vaccines. For instance, a liposome-based vaccine exposing carbohydrate epitopes has been developed against *Shigella flexneri* serotype 2a (SF2a).<sup>115</sup> In particular, glycoliposomes carrying at their surface a T cell epitope peptide and synthetic repeating units of *O*-specific polysaccharide moiety of *Shigella flexneri* have been prepared, and the synthetic system has induced a specific, long lasting and protective immune response against SF2a in mice. Recently, a liposome-based oligosaccharide system has been developed as vaccine against *Streptococcus pneumoniae* serotype 14.<sup>116</sup> Liposomes carrying a single repeating unit of the antigen and a glycosylceramide as a stimulator of Natural Killer T cells (NKT), essential for class switching and affinity maturation, have shown ability to generate high titers of IgG antibodies and memory responses against *S. pneumoniae*.

Many studies are underway to develop anti-cancer vaccine using Tumor-Associate Carbohydrate Antigens (TACAs), expressed in abnormal amounts and with unique structural modifications on the surface of cancer cells. TACAs have been extensively used as markers for cancer detection and disease progression. Boons<sup>117</sup> has developed a three components vaccine, able to elicit in mice high titers of IgG antibody in which Tn antigen (Gal-NAc $\alpha$ -O-Ser/Thr, TACAs) is carried by liposomes together with a TLR2 agonist and a T-helper epitope. Another system used as carrier for synthetic carbohydrate anti-cancer antigens is based on bacteriophage Q $\beta$ .<sup>118</sup> Also in this case the high local density of the Tn antigen on the carrier was found to be crucial for induction of Tn-specific IgG titers.

Also the envelope glycoprotein gp120 of HIV virus was targeted in a study on the research of a vaccine against the virus. The high mannose-type oligosaccharides have been individuated as a target to develop carbohydrate-based vaccines against the HIV virus due to their ability to bind the broadly neutralizing 2G12 antibody. Synthetic analogues of the natural undecasaccharide were synthesized and conjugated to different carriers in order to explore the possibility to prepare synthetic multivalent HIV vaccines that may elicit a 2G12-like antibody response. The group of Wang assembled oligomannose clusters on a cholic acid<sup>119</sup> and on a D-galactose<sup>120</sup> scaffold, whereas Danishefsky's group constructed oligomannose motifs on cyclic peptide scaffolds.<sup>121</sup> Others nanostructures as a dendrons<sup>122</sup> or icosahedral virus capsides<sup>123</sup>

were evaluated as potential carriers for a fully synthetic vaccine anti-HIV. However, although these systems were able to induce a carbohydrate-specific immune response in animals, the IgG antibodies were unable to bind to gp120 or to neutralize the virus. All these examples are a clear demonstration of how nanotechnology-based approaches can be used as an alternative to conventional protein carrier vaccine. In the context of nanotechnology, gold nanoparticles represent a useful carrier for synthetic vaccines. Gold nanoparticles coated with carbohydrate molecules have been extensively evaluated as potential multivalent systems for carbohydrate antigens.<sup>113</sup> The first synthesis of gold nanoparticles coated with suitably functionalized carbohydrates, named *glyconanoparticles* (GNPs), was developed in 2001 by Penadés and co-workers<sup>124</sup> to study carbohydrate-mediated interactions (Figure 4.1).

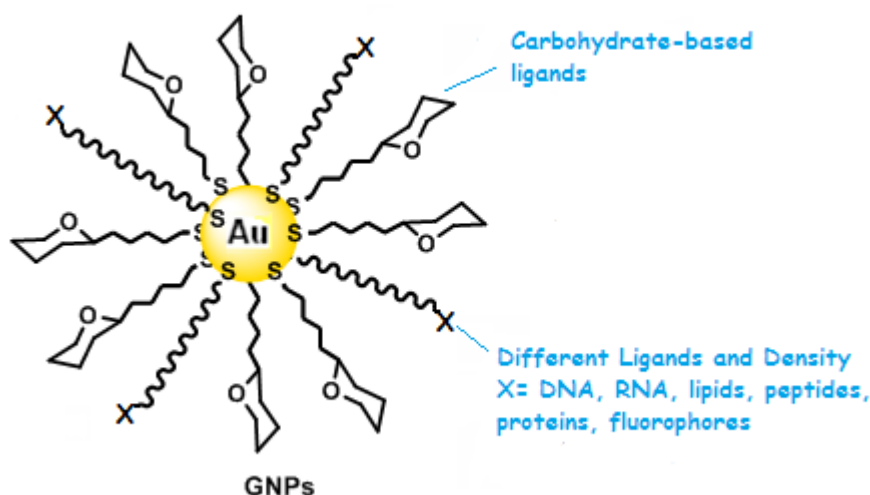


**Figure 4.1:** General scheme of gold glyconanoparticles (GNPs). GNPs consist of an inorganic core of nanometric size which is functionalized with suitably-derivatized carbohydrates together with other different ligands.

The *in situ* reduction of chloroauric acid ( $\text{HAuCl}_4$ ) in the presence of carbohydrate ligands bearing a thiol-ending group allows the formation of stable and water soluble gold GNPs. An advantage of this synthetic procedure is that the organic materials/Au(III) ratio allows to control the growth of the gold nanoclusters to give an average gold diameter ranging from 1 to 10 nm. In comparison with other multivalent systems above cited, gold glyconanoparticles offer some benefits. Chemically defined composition and globular shape with an exceptionally small core size are their main

characteristics.<sup>124, 125</sup> They are known for their inertness and for their ease preparation and purification. The carbohydrate coating provides stability and dispersibility in biological media, biocompatibility and non-cytotoxicity.<sup>113</sup> As multivalent systems, they can display large number of molecules on a reduced surface. Furthermore the insertion on the gold surface of several ligands in a controlled way,<sup>126, 127</sup> and their presentation can be modulated by the proper choice of linkers with a different degree of rigidity and flexibility.<sup>128</sup>

Thus, gold glyconanoparticles have been designed and evaluated as carriers to improve classical vaccination, with the attempt to develop fully synthetic carbohydrate-based vaccine. The first example of GNPs used as carriers for tumoral antigens (Tumor Associate Carbohydrate Antigens, TACA) was reported by Penadés.<sup>126</sup> Gold nanoparticles bearing various proportions of the mucine-associated sTn antigen (Neu5Ac $\alpha$ 2-6GalNAc $\alpha$ -O-Ser/Thr) expressed on a variety of epithelial cancer cells, the Lewis<sup>y</sup> antigen, able to elicit antibodies against some types of carcinomas, a peptide from tetanus toxoid as T cell helper, and glucose as inert component to control the density of the other components were designed and prepared as a platform for potential anticancer vaccines.

Another potential anticancer vaccine based on glyconanotechnology, containing a TACA supported on Au-NPs, has been designed by Barchi and co-workers.<sup>129,130</sup> They have reported the preparation of a three-component vaccine related to Thomsen Friedenreich disaccharide TF (Gal $\beta$ 1-3GalNAc $\alpha$ -O-Ser/Thr) as potential antigen, that is present in about 90% of carcinomas but is rarely expressed in normal tissue. A 28-residue peptide from the complement derived protein C3d as molecular adjuvant to induce B-cells activation and a thiol-ending spacer to modulate the ratio of the ligands to the gold surface were also attached on the nanoparticles. Biological tests have shown that these GNPs have been able to induce an immunological response in mice.

Gold nanoparticles coated with analogues of the capsular polysaccharide of *Neisseria meningitidis* type A (MenA) were proposed by Scrimin<sup>131</sup> ELISA test of these nanoparticles showed a very strong binding to polyclonal human antibodies against MenA. Factors that affect the T cell response, such as the numbers of repeating units of antigen arranged on the gold surface or the size of glyconanoparticles, are also reported.<sup>132</sup>



Recently, the group of Penadés developed gold nanoparticles bearing selected fragments of capsular polysaccharide antigens which have been evaluated as potential carriers for fully synthetic carbohydrate-based vaccines against *S. pneumoniae* serotype 14 (Figure 4.2).<sup>133</sup>

Specifically, GNPs carrying the synthetic branched tetrasaccharide repeating unit of serotype 14, [Pn14,  $\beta$ -D-galactopyranosyl-(1 $\rightarrow$ 4)- $\beta$ -D-glucopyranosyl-(1 $\rightarrow$ 6)-[ $\beta$ -D-glucopyranosyl-(1 $\rightarrow$ 4)]-2-acetamido-2-deoxy-D-glucopyranoside, Figure 4.2b], identified as the smallest structure necessary to evoke an immunological response,<sup>95</sup> were studied. Gold glyconanoparticles with tetrasaccharide Pn14 together with D-glucose, used to aid water solubility and to modify the antigen density and the T-helper ovalbumin 323-339 peptide (OVA<sub>323-339</sub>), prerequisite for the induction of IgG against the tetrasaccharide, in a 45:50:5 molar ratio were prepared. They resulted able to induce specific IgG antibodies against native capsular polysaccharide Pn14 and sera obtained from mice immunized with this GNP were able to opsonize *S. pneumoniae* type 14 bacteria in an opsonophagocytosis assay.

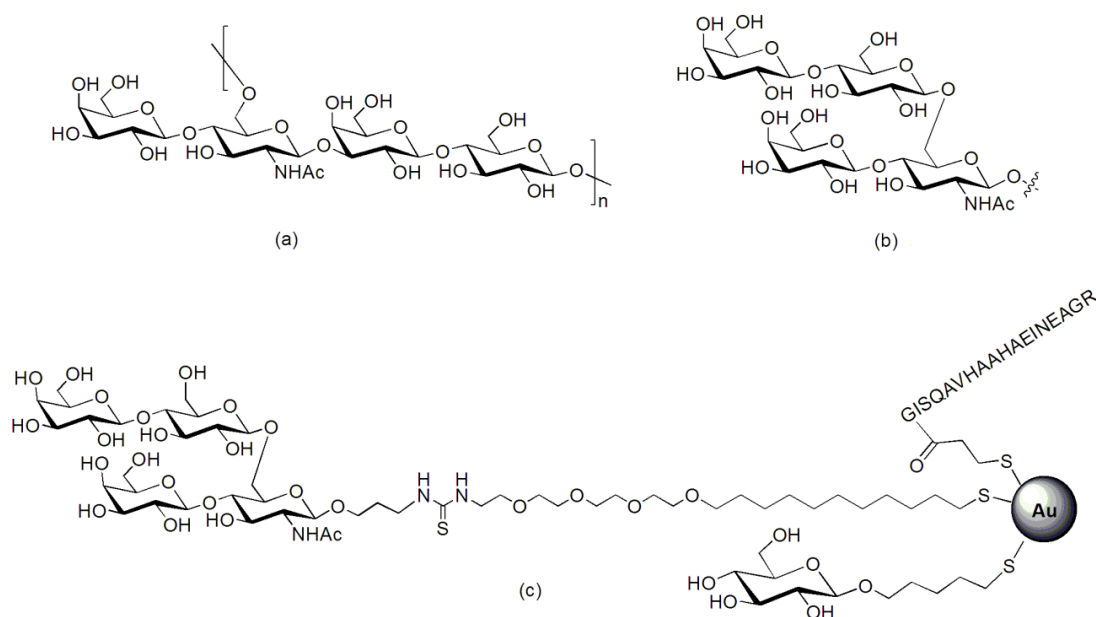


**Figure 4.2:** (a) *Streptococcus pneumoniae* capsular polysaccharide serotype 14  $\beta$ -D-galactopyranosyl-(1 $\rightarrow$ 4)- $\beta$ -D-glucopyranosyl-(1 $\rightarrow$ 6)-[ $\beta$ -D-glucopyranosyl-(1 $\rightarrow$ 4)]-2-acetamido-2-deoxy-D-glucopyranoside; (b) synthetic branched tetrasaccharide repeating unit resulted able to elicit IgG *in vivo*; (c) glyconanoparticle bearing the *Streptococcus pneumoniae* serotype 14, glucose and OVA peptide in a 45:50:5 molar ratio able to invoke an immunological response.<sup>133</sup>

Infections from *Streptococcus pneumoniae* are still a global health concern, and for this reason they are target of many studies. Even though there are vaccines against this bacterium, it is estimated that 1.6 million people die from this infection every year, of whom one million are children.<sup>134,135</sup> So, nowadays the research towards a better vaccine is still open.

*S. pneumoniae* belongs to the class of encapsulated bacteria that present coats of saccharides involved in the interaction with cell and protein, including antibodies. It is the causative agent of a variety of diseases, as bacterial sepsis, pneumonia, meningitis and otitis particularly affecting the elderly and the children. To date, 93 capsular serotypes have been identified, with different structures and immunogenicity,<sup>136</sup> whereof 23 are components of the first polysaccharide vaccine against *S. pneumoniae* currently available, the PneumoVax, launched in 1983. Unfortunately, PneumoVax resulted poorly immunogenic in children, elderly and immunocompromised people and in adults gives only a partial protection without the generation of immunological memory. This clinical limitation is attributed to the nature of carbohydrates, typically known as T-independent antigens. Following the introduction of the concept of “glycoconjugate vaccine”, Prevnar, a new vaccine containing seven of the most virulence polysaccharides capsular antigens, conjugated to the non-toxic cross reactive material from diphtheria toxic CRM<sub>197</sub> protein, has been licensed in 2000. Today, Prevnar 13, with more antigens, is in use against this bacterium, and other formulations are in development.

However, Prevnar 13 is expensive,<sup>137</sup> poorly thermostable,<sup>138</sup> with limited immunogenicity and it shows a variable level of protection in different individuals and ethnic groups. These limitations and the promising results reported by the group of Penadés on the use of gold nanoparticles as carrier for saccharide antigens related to *Streptococcus pneumoniae* serotype 14, prompted us to further explore this construction also with other serotype of saccharide antigens of the bacterium, in order to verify if this strategy could protect against a wider range of *S. pneumoniae* serotypes.

## 4.2 Aim of the work

This part of PhD project was directed to the preparation of a new type of gold nanoparticles covered with the antigenic determinant of *Streptococcus pneumoniae* serotype 19F, which is another among the most virulence factor of the bacterium, alone or together with the one of serotype 14. This strategy will allow an additional validation of gold nanoparticles as carriers for saccharide antigens and the development of new multiantigenic system, mimicking the commercial multiantigenic conjugate vaccines.

Thus, inspired by the results reported in a previous investigation of Penadés group, new gold nanoparticles have been prepared (Figure 4.3). Firstly, GNPs carrying the trisaccharide repeating unit of the *Streptococcus pneumoniae* serotype 19F antigen [Pn19F PS, 2-acetamido-2-deoxy  $\beta$ -D-mannopyranosyl-(1 $\rightarrow$ 4)- $\alpha$ -D-glucopyranosyl-(1 $\rightarrow$ 2)- $\alpha$ -L-rhamnopyranoside] were prepared in order to demonstrate that the activity of this kind of constructions can be generalized and it is not limited to serotype 14.

Beyond this first aim, we also investigated on the necessity of the presence of glucose on the glyconanoparticles, generally used to aid water solubility and modify antigen density. In other words, if the absence of this sugar does not modify the stability and dispersibility of the system, it would be possible to remove glucose and increase the amount of antigen carried by the gold nanoparticles for achieving a better immune response together with the possibility of administrating a lower amount of vaccine. To test this, we prepared GNPs coated only with trisaccharide Pn19F and OVA peptide.

Finally, we prepared a third type of GNPs coated with both saccharide antigen serotypes 19F and 14 to develop new “multiantigenic” gold nanoparticles displaying different carbohydrate antigens on a single nanoparticle. In this way, we can investigate if gold nanoparticles with capsular polysaccharide antigen fragments of different serotypes of a single bacterium have the potential to mimick the effect of commercial multiantigenic conjugate vaccines.

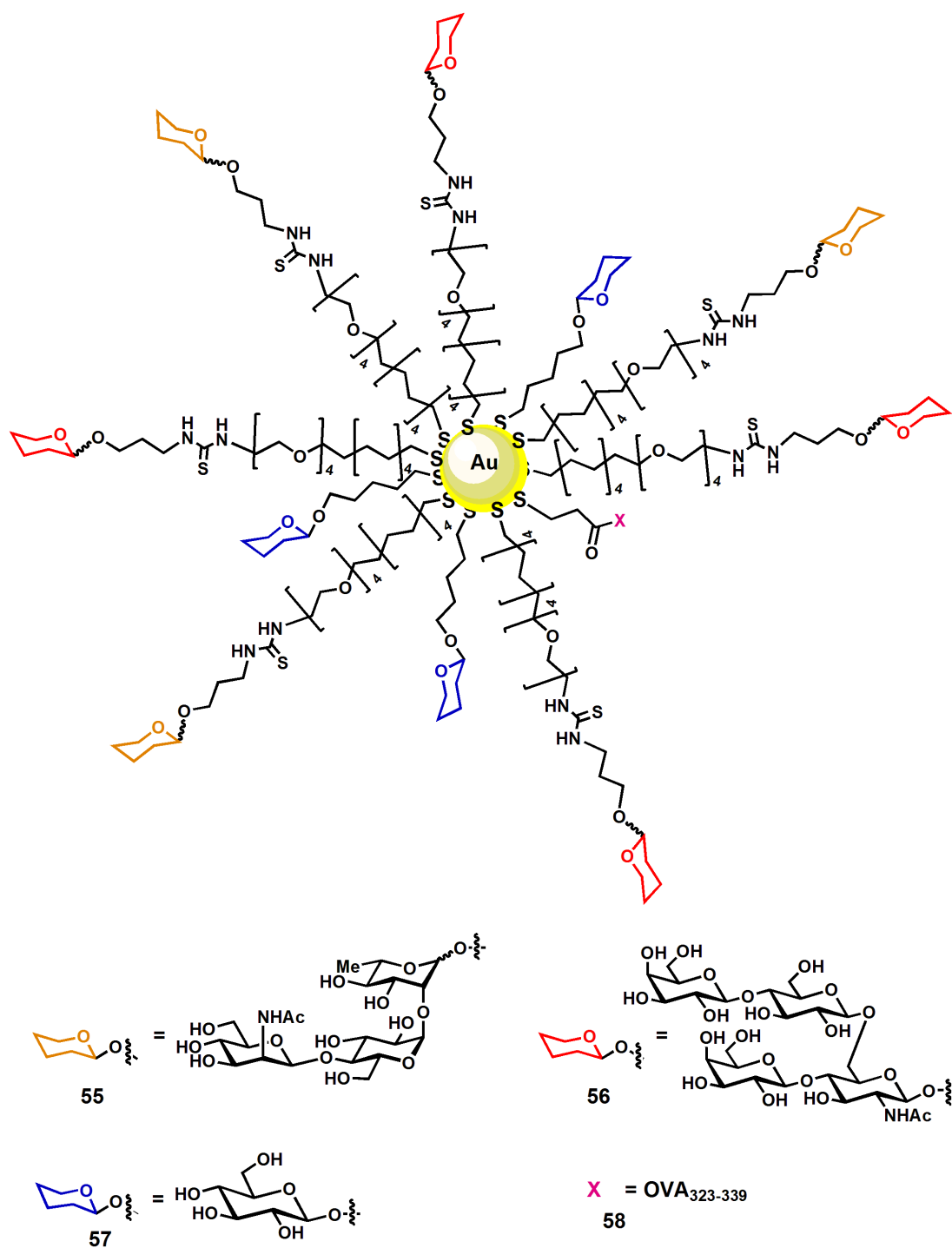


**Figure 4.3:** Schematic representation of gold glyconanoparticles (GNPs) carrying saccharide antigens related to *Streptococcus pneumoniae* proposed in this thesis. The trisaccharide related to serotype 19F **55** alone or together with tetrasaccharide related to serotype 14 **56**, functionalized with long thiol linker, as *active component* in combination with glucose **57**, functionalized with a short thiol linker used as *inner component*, and OVA peptide **58** used as T-helper, in various molar ratio, were linked on the gold surface.

### 4.3 Results and discussion

During the six months period of my PhD spent in the Laboratory of GlycoNanotechnology of Prof. Penadés, I have prepared different gold glyconanoparticles with the aim to develop fully synthetic carbohydrate-based vaccine against *Streptococcus pneumoniae*. In particular, the objective has been to assess the possibility to employ GNPs as carriers of multivalent antigenic systems able to evoke an immune response.

To prepare the GNPs, the first step has been the synthesis of the thiol ending ligands that have to be linked on the gold nanocluster surface, exploiting the well-known affinity of sulfur for gold,<sup>139</sup> *i.e.* the saccharide antigen, glucose and OVA peptide.

The choice of the linker used to attach the neoglycoconjugates to the gold nanoparticles is very important. In fact, the nature, the length and the flexibility of the spacers are key factors in controlling the presentation of ligands and their behavior in the molecular recognition process.<sup>113,128</sup> As for the tetrasaccharide related to Pn14, the trisaccharide repeating unit of serotype 19F antigen was conveniently functionalized with a long thiol linker, the 23-mercapto-3,6,9,12-tetraoxatricosyl isothiocyanate, characterized by an aliphatic portion of eleven carbon atoms, that confers rigidity to the inner organic shell to protect the gold core, and a hydrophilic portion of tetraethylenglycol, which provides flexibility to the glycans on the GNPs.

On the other hand,  $\beta$ -D-glucose, used to confer solubility to the gold nanoparticles and to modify the concentration of the active components, was functionalized with a short linker of five carbon atoms. This allows the saccharide antigens, the Pn19F and Pn14, to protrude above the gold surface with respect to the glucose.

Finally, the T-helper ovalbumin 323-339 peptide (OVA<sub>323-339</sub>), was inserted on the GNPs, since it was already demonstrated that its presence, in the minimum quantity of 5%, is essential to induce the generation of IgG against the native polysaccharide of *S. pneumoniae*.<sup>133</sup> To allow the binding of OVA peptide to the gold surface of the glyconanoparticles, an additional glycine and mercapto-propionic acid linker at the *N*-terminus were added.

### 4.3.1 Synthesis of Thiol-Ending Ligands

#### Thiol-ending Pn19F Trisaccharide:

Regarding the *Streptococcus pneumoniae* 19F antigen used in the preparation on the GNPs, we have decided to use the trisaccharide repeating unit **59** with an aminopropyl linker at the reducing end necessary for the functionalization with the long thiol-ending linker (Figure 4.4). Indeed, it was demonstrated that the single trisaccharide **59** and the natural repeating unit **60** have comparable inhibitory activity in a classical competitive ELISA assay in the binding between the 19F polysaccharide and the anti-19F human polyclonal antibody (Ref.<sup>96</sup> and unpublished data).

These data justify our idea to use the single repeating unit **59**, synthesized starting from the protected repeating unit **61** which was obtained following a well-established and reproducible synthetic route developed in our research group (Scheme 4.1).<sup>140</sup>

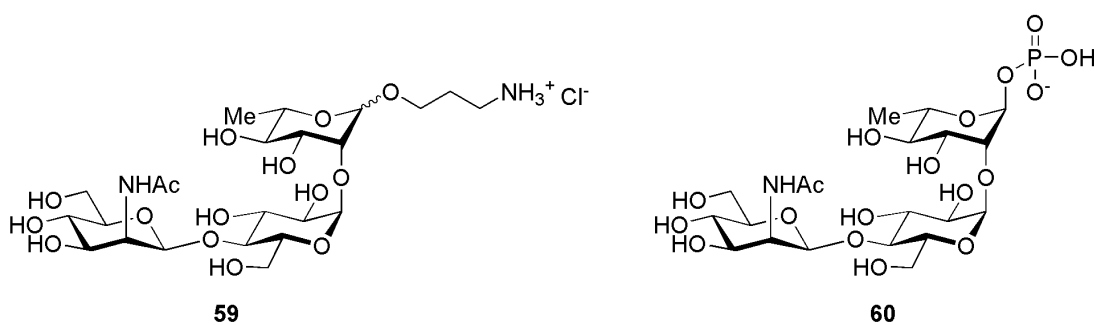
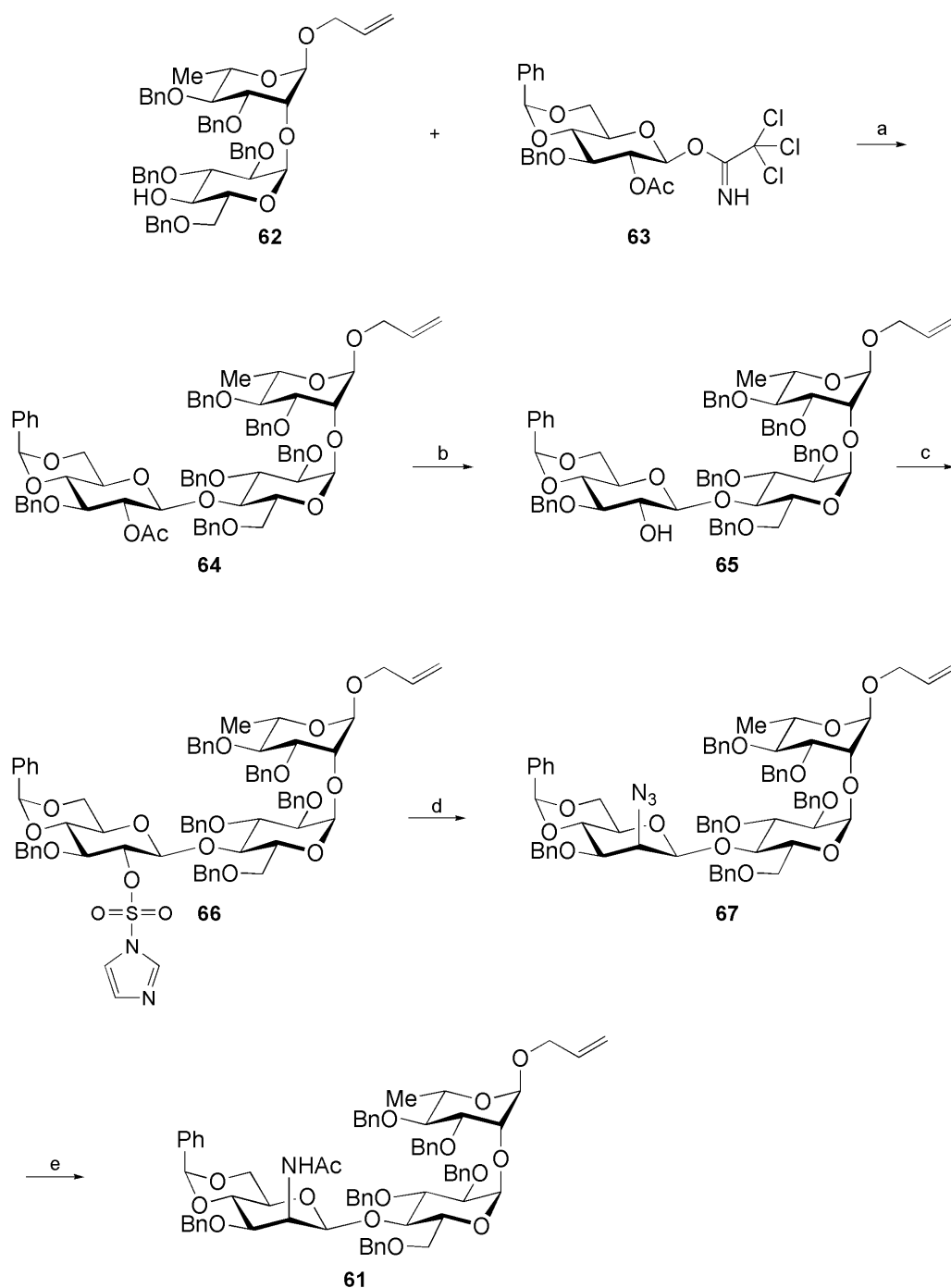


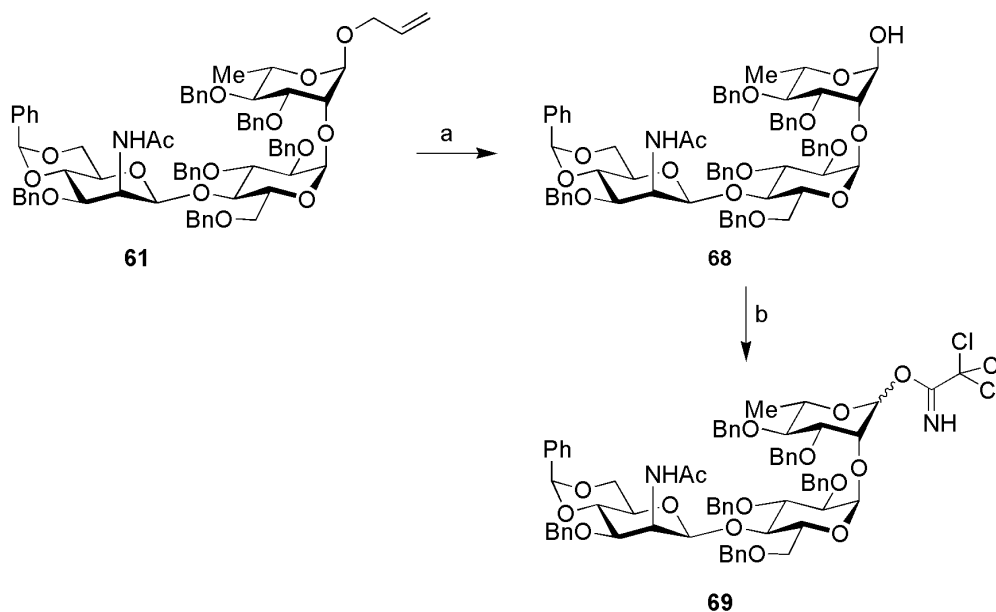
**Figure 4.4:** Trisaccharide related to Pn19F PS with amino-linker **59** and natural trisaccharide related to Pn19F PS, 2-acetamido-2-deoxy  $\beta$ -D-mannopyranosyl-(1 $\rightarrow$ 4)- $\alpha$ -D-glucopyranosyl-(1 $\rightarrow$ 2)- $\alpha$ -L-rhamnopyranoside-(1-OPO<sub>4</sub>H<sup>-</sup>) **60**.

Briefly, a glycosylation reaction was performed between the acceptor disaccharide **62** and the glucose donor **63**, with the neighbouring group participation of the acetate in position 2 chosen to obtain only the beta anomer of the trisaccharide **64**. With a Zemlén reaction, the acetate protecting group was easily removed and replaced with the imidazolyl sulfate to give **66**. The following substitution with an azido nucleophile invert the configuration from glucose to mannose and the reduction and *in situ* acetylation of compound **67** gave the desired fully protected repeating unit of *S. pneumoniae* serotype 19F **61**.



**Scheme 4.1:** a) TESOTf, CH<sub>2</sub>Cl<sub>2</sub> dry, -20°C, 75%; b) CH<sub>3</sub>ONa, CH<sub>3</sub>OH, rt, 95%; c) NaH, sulfonyldiimidazole, DMF, -40°C, 85%; d) NaN<sub>3</sub>, DMF, 80°C, 70%; e) Zn, THF/Ac<sub>2</sub>O/AcOH, rt, 70%.

Then, the protected repeating unit **61** was submitted to further derivatization and specifically allyl protective group was removed to obtain **68**, while the following functionalization of the free hydroxyl group with the trichloroacetimidate, an excellent leaving group, gave donor **69** for the next step (Scheme 4.2).



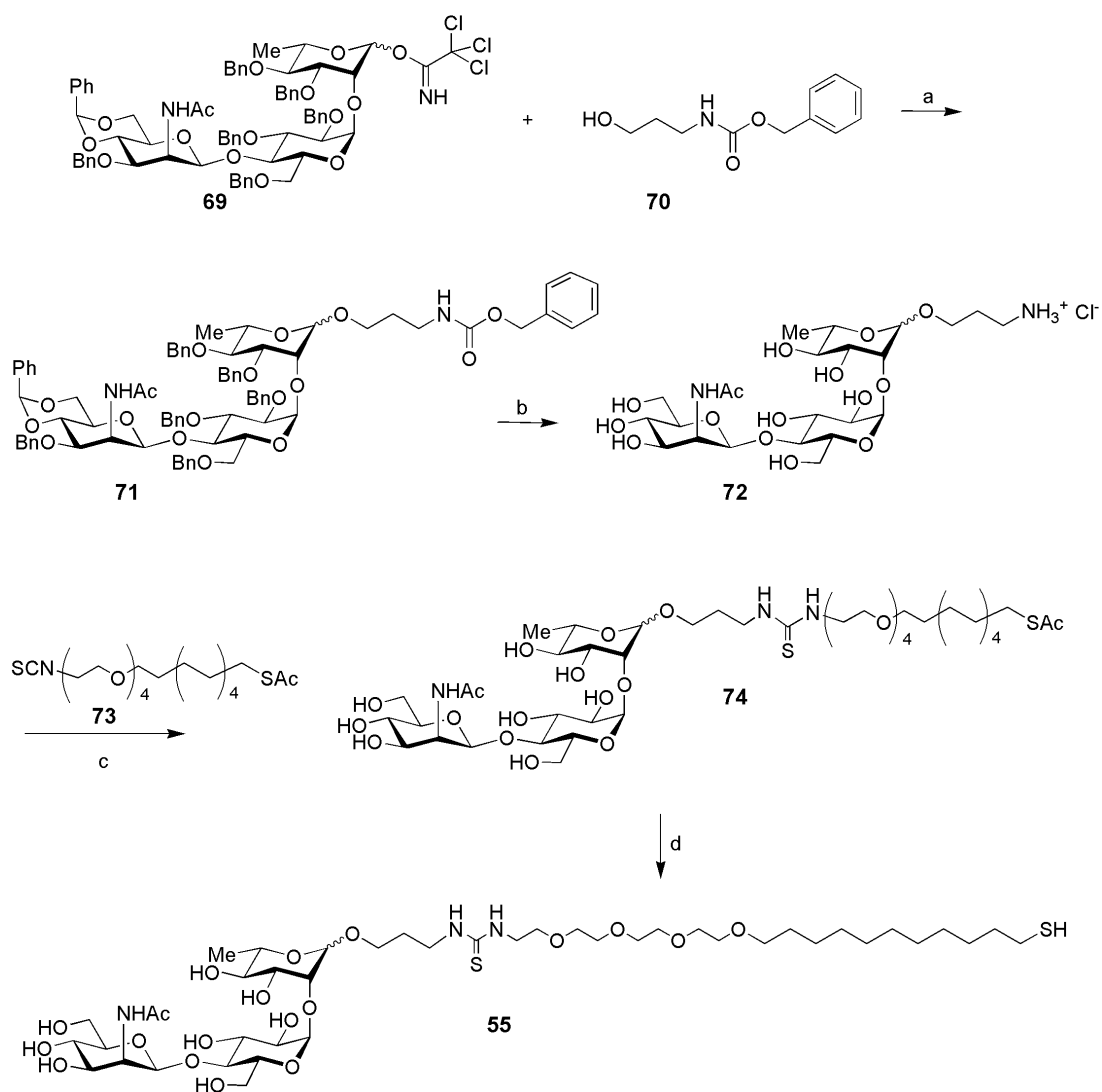
**Scheme 4.2:** a) *I* step Ir catalyst, THF dry; *II* step I<sub>2</sub>, THF/H<sub>2</sub>O 4:1, rt, 90%; b) Cl<sub>3</sub>CCN, CH<sub>2</sub>Cl<sub>2</sub> dry, rt, 90%.

The repeating unit of Pn19F was then coupled with *N*-(benzyloxycarbonyl)-3-aminopropyl-carbamate as the acceptor *N*-protected spacer **70** (Scheme 4.3). Starting from donor **69** the glycosidation reaction was carried out in dry dichloromethane at 0°C using trimethylsilyl triflate (TMSOTf) as acid promoter and molecular sieves. The reaction was not selective and the glycosidation product **71** was obtained as a alpha/beta mixture. Initially, we decided to go on in the work using the alpha/beta mixture, because previous investigations (unpublished data), showed that the two diastereoisomers have a comparable activity in an ELISA test. Later, we decided to separate the mixture to prepare also GNPs coated only with the natural alpha anomer. The separation of the anomeric mixture was performed at this stage through a preparative TLC using the system hexane/ethyl acetate 1:1 as eluent. Then, the following reactions have been carried out both on the alpha/beta mixture and only on the alpha anomer.

Compound **71** was submitted to hydrogenolysis with palladium hydroxide on activated charcoal using as solvent a mixture of ethyl acetate/methanol/water with an additional amount (1 eq.) of HCl 0,1M in water. All the benzyl groups were removed and product **72**, isolated as the chloride salt, was used to perform the coupling reaction with 23-mercapto-3,6,9,12-tetraoxatricosyl isothiocyanate **73**. Also in this case a mixture of solvents, in particular water/isopropanol/acetonitrile 1:1:1, was



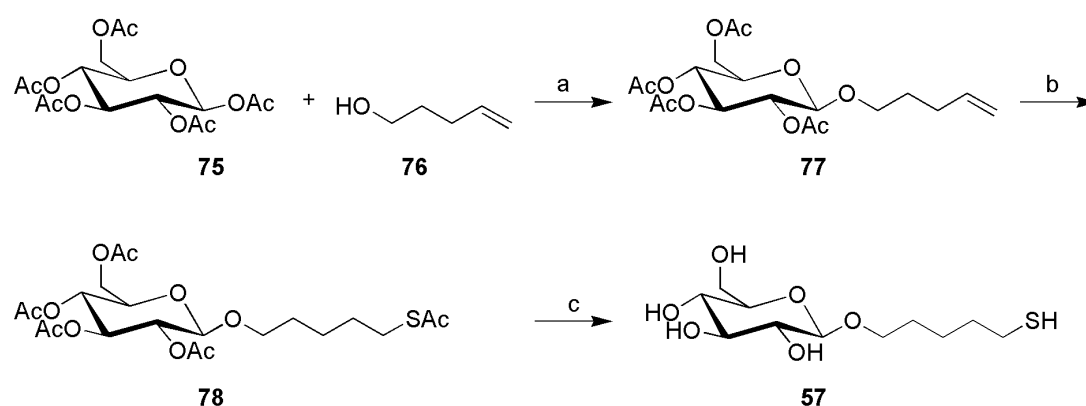
necessary to dissolve both the saccharide and the linker, and the pH was set to basic by addition of triethylamine. Evaporation of the solvents and trituration of the crude product with diethyl ether until complete removal of the unreacted linker gave the pure thioacetyl derivatives **74**. Finally, Zémpfen transesterification, with sodium methoxide in methanol and purification on Sephadex LH-20 provided the suitably functionalized trisaccharide conjugate **55** (Scheme 4.3).



**Scheme 4.3:** a) TMSOTf, m.s. 4Å, CH<sub>2</sub>Cl<sub>2</sub> dry, 0°C, 90%; b) Pd(OH)<sub>2</sub>, H<sub>2</sub>, AcOEt/CH<sub>3</sub>OH/H<sub>2</sub>O 1:1:1. HCl 0.1M, rt, quant.; c) H<sub>2</sub>O/iPrOH/CH<sub>3</sub>CN 1:1:1, TEA 0.05M, rt, 75%; d) CH<sub>3</sub>ONa, CH<sub>3</sub>OH, rt, 90%.

### Glucose thiol-ending

The 5-(Thio)pentyl  $\beta$ -D-glucopyranoside, chosen to assist the water dispersibility and biocompatibility of the GNPs, was synthesized following a reported procedure.<sup>127</sup> Briefly, the commercially available glucose pentacetate **75**, was glycosidated with 4-penten-1-ol **76** under Fisher conditions to give **77**, followed by free radical mediated thioacetylation with thioacetic acid. Compound **78** was finally converted with a Zémlen reaction in the desired derivative **57** in good overall yields (Scheme 4.4).



**Scheme 4.4:** a)  $\text{BF}_3 \cdot \text{Et}_2\text{O}$ ,  $\text{CH}_2\text{Cl}_2$  dry, rt; b)  $\text{CH}_3\text{COSH}$ , AIBN, THF, reflux, c)  $\text{CH}_3\text{ONa}$ ,  $\text{CH}_3\text{OH}$ , Ar, rt.

### OVA<sub>323-339</sub> peptide T-helper

The presence of the OVA<sub>323-339</sub> peptide, as a T-helper, has been shown to be essential for the induction of an antibody response to the antigen. So, it has been used in the minimal amount required (5%) also in the preparation of GNPs with the Pn19F as antigen. The OVA<sub>323-339</sub> peptide **58** (Figure 4.5) with an additional glycine and mercapto-propionic acid linker at the *N*-terminus HS(CH<sub>2</sub>)<sub>2</sub>C(O)GISQAVHAAHAEINEAGR was obtained from GenScript Corp (Piscataway, NJ, USA).

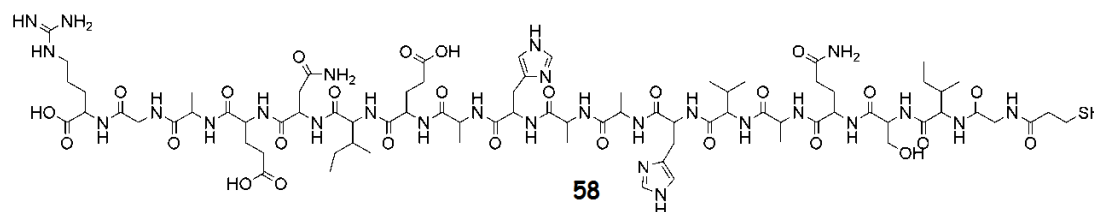


**Figure 4.5:** T-helper OVA<sub>323-339</sub> peptide structure with an additional glycine and mercapto-propionic acid linker at the *N*-terminus **58**.

### 4.3.2 Preparation of glyconanoparticles

Having in hand all the components with the thiol-ending function, the next step has been the GNPs preparation. In this PhD thesis, the so-called direct *in situ* formation of glyconanoparticles based on a modification of Brust's method<sup>141</sup> and developed by the group of Penadés<sup>127</sup> was used (Figure 4.6). The protocol consists in treating a water solution of a Au(III) salt with sodium borohydride as reductive agent in the presence of an excess of the thiol-ending glycoconjugates in order to assure full coverage of the GNP surface. The reducing agent was used with the double role to reduce the gold to Au(0) and keep the thiols in their reduced state for binding to the gold. Moreover, the use of direct method allows to obtain nanoparticles incorporating different ligands in various proportions on the gold surface.

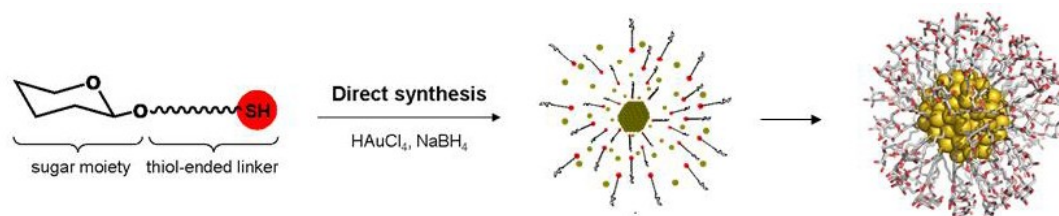


**Figure 4.6:** Schematic representation of the GNPs formation with the direct method.

In detail, the first step required for the preparation of the GNPs is to make a mixture of the thiol-ending compounds that have to be linked on the gold surface of the nascent GNP in the desired proportion. To confirm the ligands ratio, <sup>1</sup>H NMR spectrum was registered before performing the reaction. Then, to a methanolic solution of the mixture of thiol-ending conjugates (5 equiv.), was added an aqueous solution of tetrachloroauric acid (HAuCl<sub>4</sub>, 1 equiv.). The resulting mixture was reduced with sodium borohydride (NaBH<sub>4</sub>, 27 equiv.) and the suspension was vigorously shaken for 2 hours. GNPs achieved in this way were purified for centrifugal filtering using a mixture of water/methanol and then by dialysis. Freeze-drying gave GNPs as a dark solid which can be stored at 4°C for months and redissolved in water prior to use. By this methodology, GNPs bearing different amounts of the trisaccharide repeating unit related to 19F *Streptococcus pneumoniae*, alone or together with the tetrasaccharide of the serotype 14, were prepared and described in detail below.

The starting aim of this work has been to prepare and test new GNPs, analogue to the ones with 45:50:5 molar ratio of Pn14, glucose and OVAp, which gave the best immunogenic response in a previous work,<sup>133</sup> but bearing a different saccharide antigen, *i.e.* the trisaccharide repeating thiol ending unit **55** related to 19F *Streptococcus pneumoniae*. In this way, we could compare the two systems and extend the knowledge on the properties of GNPs as potential carriers of different antigens. So, GNPs **79**, showed in Figure 4.7, were prepared by mixing trisaccharide **55**, glucose **57** and OVAp **58** in presence of  $\text{HAuCl}_4$  and  $\text{NaBH}_4$  following the classical procedure before described.

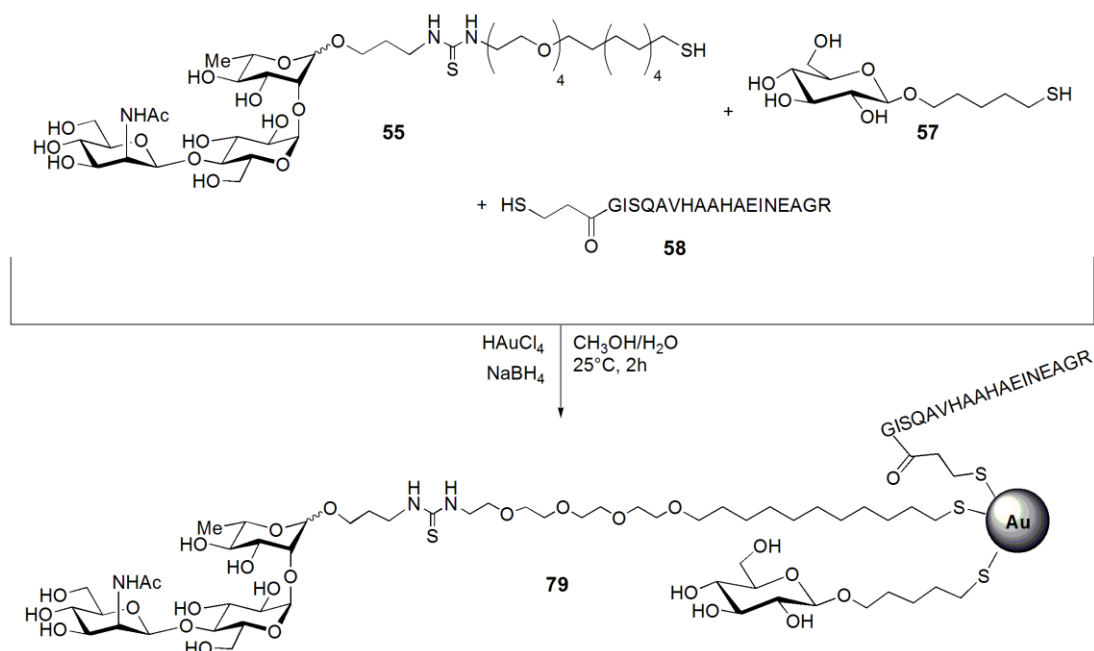


**Figure 4.7:** Preparation of GNPs **79** composed of Pn19F **55**, glucose **57** and OVAp **58** in 45:50:5 molar ratio. The percentage is referred to the ligand ratio in the starting mixture, which is maintained in the mixture after the nanoparticle formation.

The second purpose of this work has been to investigate the role of glucose in the behavior of gold nanoparticles. If the absence of this sugar does not modify the stability and dispersibility of the resulting system, the glucose can be removed and this can allow to increase the amount of the *active component*, the trisaccharide, carried by the GNPs. So, this prompted the preparation of glyconanoparticle **80** coated only by the repeating unit related to Pn19F **55** and OVA peptide **58** T-helper in 95:5 molar ratio (Figure 4.8).

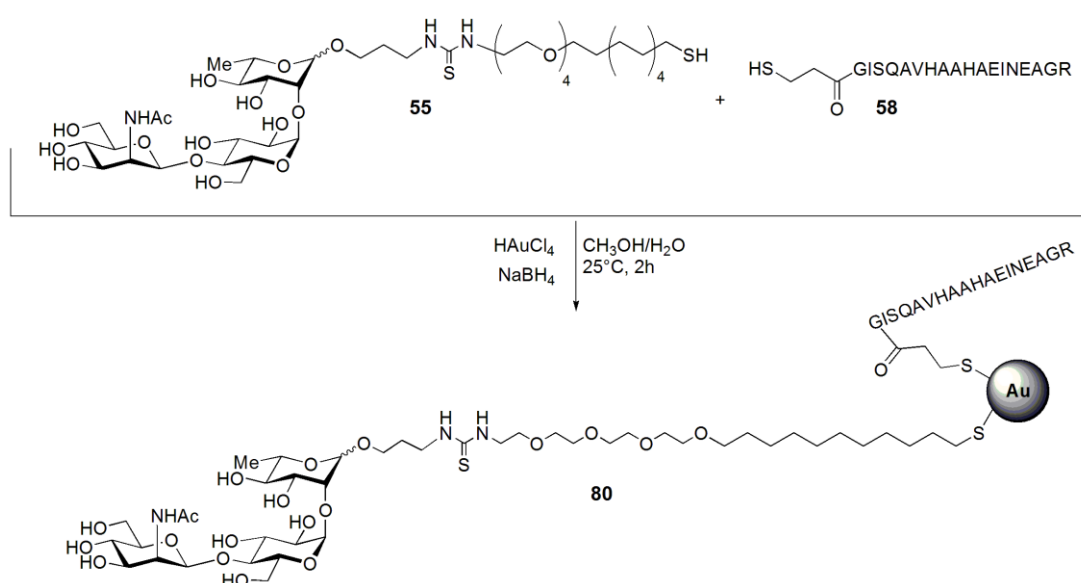


**Figure 4.8:** Preparation of GNPs **80** composed of Pn19F **55** and OVAp **58** in 95:5 molar ratio. The percentage is referred to the ligand ratio in the starting mixture, which is maintained in the mixture after the nanoparticle formation.

Another idea in the last part of this work was to develop new "multiantigenic GNPs", coated with serotype 14 and serotype 19F of *S. pneumoniae* antigens both arranged in the same Au-nanoparticles. The GNPs **81** with a 40:40:15:5 molar ratio of the thiol-ending trisaccharide 19F **55**, the thiol-ending tetrasaccharide 14 **56**, the  $\beta$ -D-glucose **57** and OVA peptide **58** were prepared according to the standard methodology (Figure 4.9). This molar ratio maintains the percentage of each *active component*, e.g. the two carbohydrate antigens Pn14 and Pn19F, close to the one used in the GNP loaded with only one antigen. To do this, the quantity of D-glucose has been reduced from 50% to 15%, approximately. Indeed, an advantage of the direct method used to prepare all the GNPs of this work, is the possibility to modify the density of derivatives attached on the gold surface in a controlled way. To decrease the percentage of one component, in this case glucose, another component can be introduced, the tetrasaccharide.<sup>125</sup>

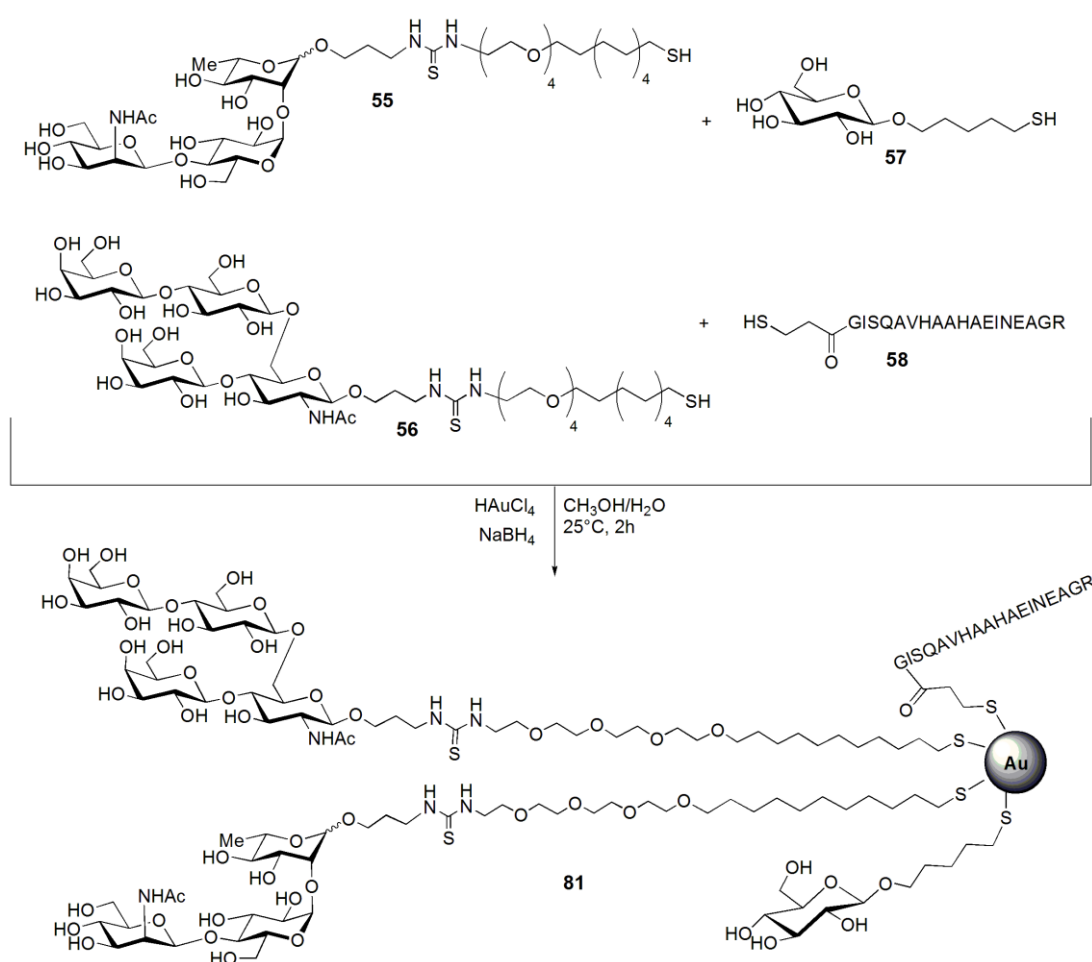


**Figure 4.9:** Preparation of GNPs **81** composed of Pn19F **55**, Pn14 **56**, glucose **57** and OVAp **58** with the molar ratio of 40:40:15:5. The percentage is referred to the ligand ratio in the starting mixture, which is maintained in the mixture after the nanoparticle formation.

Finally, glyconanoparticle **82** with a molar ratio of ligands of 45:50:5 were also prepared using only the alpha anomer of the trisaccharide repeating unit **55** of Pn19F, glucose **57** and OVAp **58** (Figure 4.10).

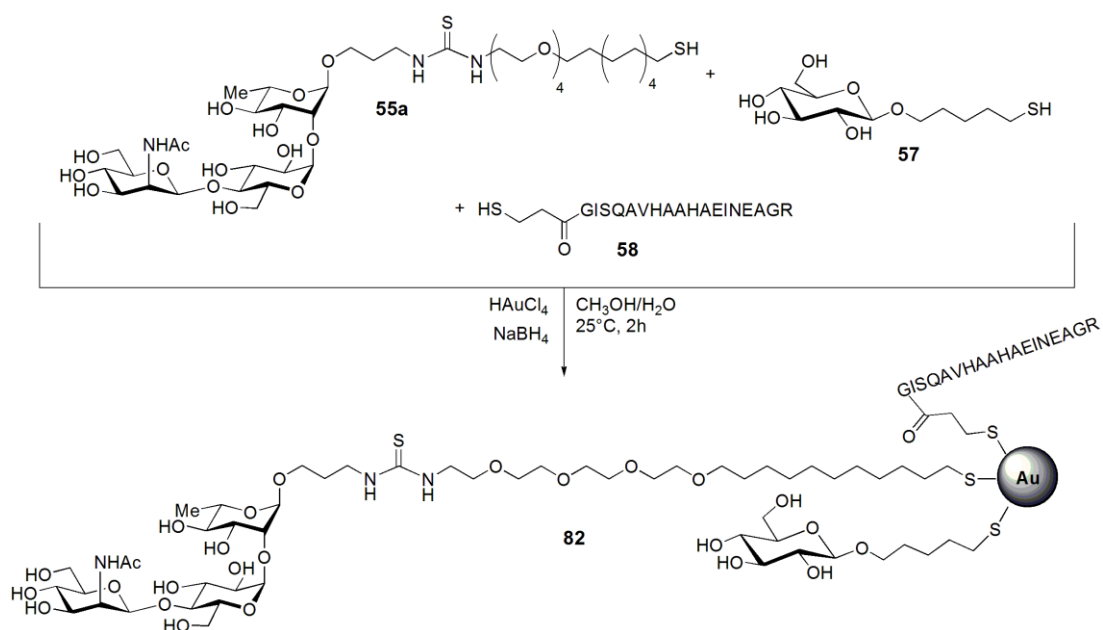


**Figure 4.10:** Preparation of GNPs **82** composed of alpha anomer Pn19F **55a**, glucose **57** and OVAp **58** in 45:50:5 molar ratio. The percentage is referred to the ligand ratio in the starting mixture, which is maintained in the mixture after the nanoparticle formation.

The amount, the molar ratio of ligands and the structure of the GNPs prepared are summarised in Table 4.1.

GNPs	Total amount produced ( $\mu\text{g}$ )	Thiol-ending ligands	Structure
79	992	Pn19F/Glc/OVAp 45:50:5	
80	808	Pn19F/OVAp 95:5	
81	1130	Pn19F/Pn14/Glc/OVAp 40:40:15:5	
82	504	Pn19F $\alpha$ /Glc/OVAp 45:50:5	

**Table 4.1:** Gold GNPs prepared in this PhD project functionalized with thiol-ending repeating units of *Streptococcus pneumoniae* Pn19F **55** and Pn14 **56**,  $\beta$ -D-glucose **57** and OVA peptide T helper **58**.

\*The total amount of GNP produced and summarized in this table, has been achieved repeating more times the reaction procedure reported in the experimental.



### 4.3.3 Characterization of glyconanoparticles

In order to characterize the prepared glyconanoparticles different techniques were used, such as Transmission Electron Microscopy (TEM), Ultraviolet-Visible (UV/Vis), Circular Dichroism (CD), and Nuclear Magnetic Resonance (NMR).

All GNPs were found to be water-soluble and stable under physiological conditions without flocculation. They showed an exceptionally small core with an average diameter of 1.2 nm, as demonstrated by Transmission Electron Microscopy (TEM) examination. In addition, TEM micrographs showed uniform dispersion of the GNPs and no aggregation was evident. Based on the gold core size (determined by TEM analysis) and Murray's table,<sup>142</sup> an average molecular formula and the corresponding molecular weights were estimated.

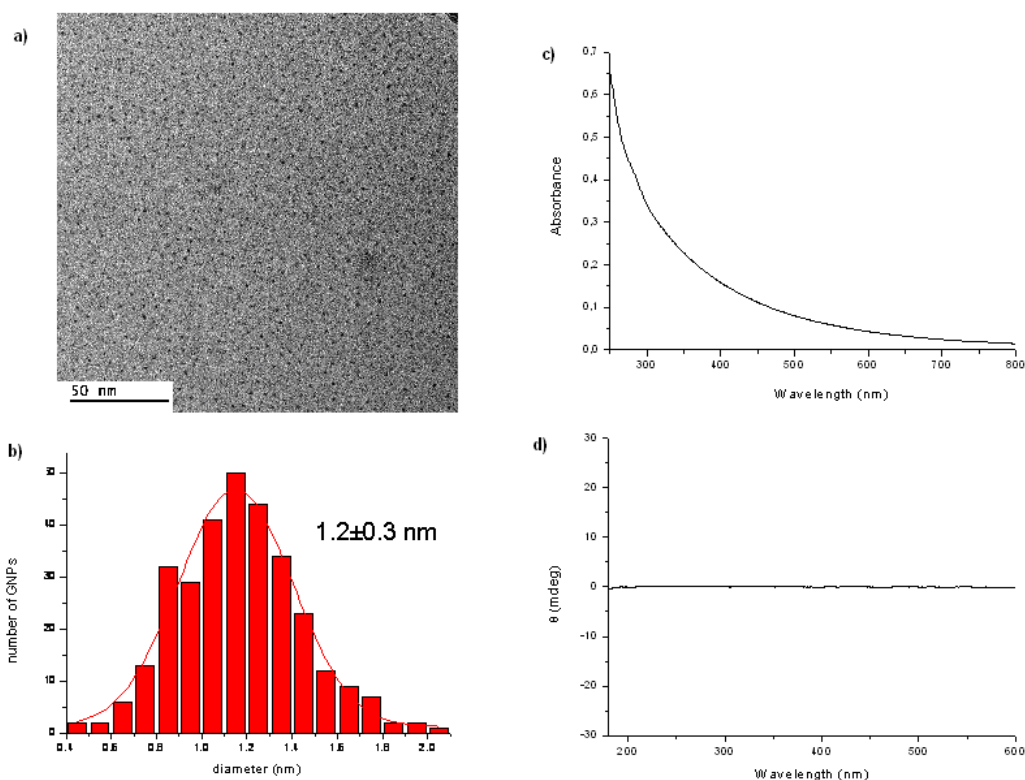


**Figure 4.11:** As example, the characterization of glyconanoparticles **79** (Pn19F/Glc/OVAp 45:50:5) was herein reported. a) TEM micrograph in H<sub>2</sub>O; b) size-distribution histogram obtained by measuring around 400 nanoparticles; c) UV/Vis spectrum obtained with concentration 0.10 mg/ml in H<sub>2</sub>O; d) CD spectrum obtained with concentration 0.25 mg/ml in H<sub>2</sub>O.

For the characterization of the others GNPs see experimental section.

Also the Ultraviolet-visible (UV/Vis) spectra can give an indication of the GNPs dimensions. Small GNPs with a diameter below 2 nm do not show the plasmon absorption band around at 520 nm.<sup>143</sup> In our case, the registered UV/Vis spectra never showed a surface plasmon band, which is a further confirmation of the small size of the GNPs.

The Circular Dichroism (CD) spectroscopy measures differences in the absorption of the polarized light and it is routinely used to study chiral molecules. Generally, metallic nanoparticles are achiral, but the conjugation with biomolecules can impart chirality and create a plasmon-induced CD signal in the visible spectral region.<sup>144</sup> The absence of regular structure results in zero CD intensity, while an ordered structure gives a spectrum which could contain both positive and negative signals. All the GNPs prepared were analyzed by CD but none of them showed a signal in the spectrum despite the presence of the sugar on the gold surface (Figure 4.11).

The <sup>1</sup>H NMR spectra of GNPs generally features broader peaks compared to those of the corresponding free ligands. Furthermore, the comparison of the <sup>1</sup>H NMR spectrum of the starting mixture with the unreacted collected fractions after cluster formation can give a good qualitative indication about the ratio of the different ligands attached on the GNPs. This is useful to confirm that the ratio of the ligands covering nanoparticles is the same as in the initial mixture used to prepare GNPs. All the prepared GNPs were controlled with NMR analyses, which confirmed the expected molar ratio of the ligands (Figure 4.12).

Additionally, the *active component* loaded on GNPs was also evaluated by quantitative NMR (<sup>1</sup>H qNMR): 20  $\mu$ L of D<sub>2</sub>O containing 0.05 wt. % of 3-(trimethylsilyl) propionic-2,2,3,3-*d*4 acid, sodium salt (TSP-*d*4) as an internal standard was added to a known quantity of GNPs dissolved in 180  $\mu$ L of D<sub>2</sub>O. The amount of saccharide attached to nanoparticles was determined by comparison of the integral of the broad signal of selected regions of the spectrum with the singlet of the internal standard.<sup>145</sup> After the analysis, the TSP can be removed by dialysis, so this non-destructive approach can be easily used to know the moles of ligands per mg of GNP.

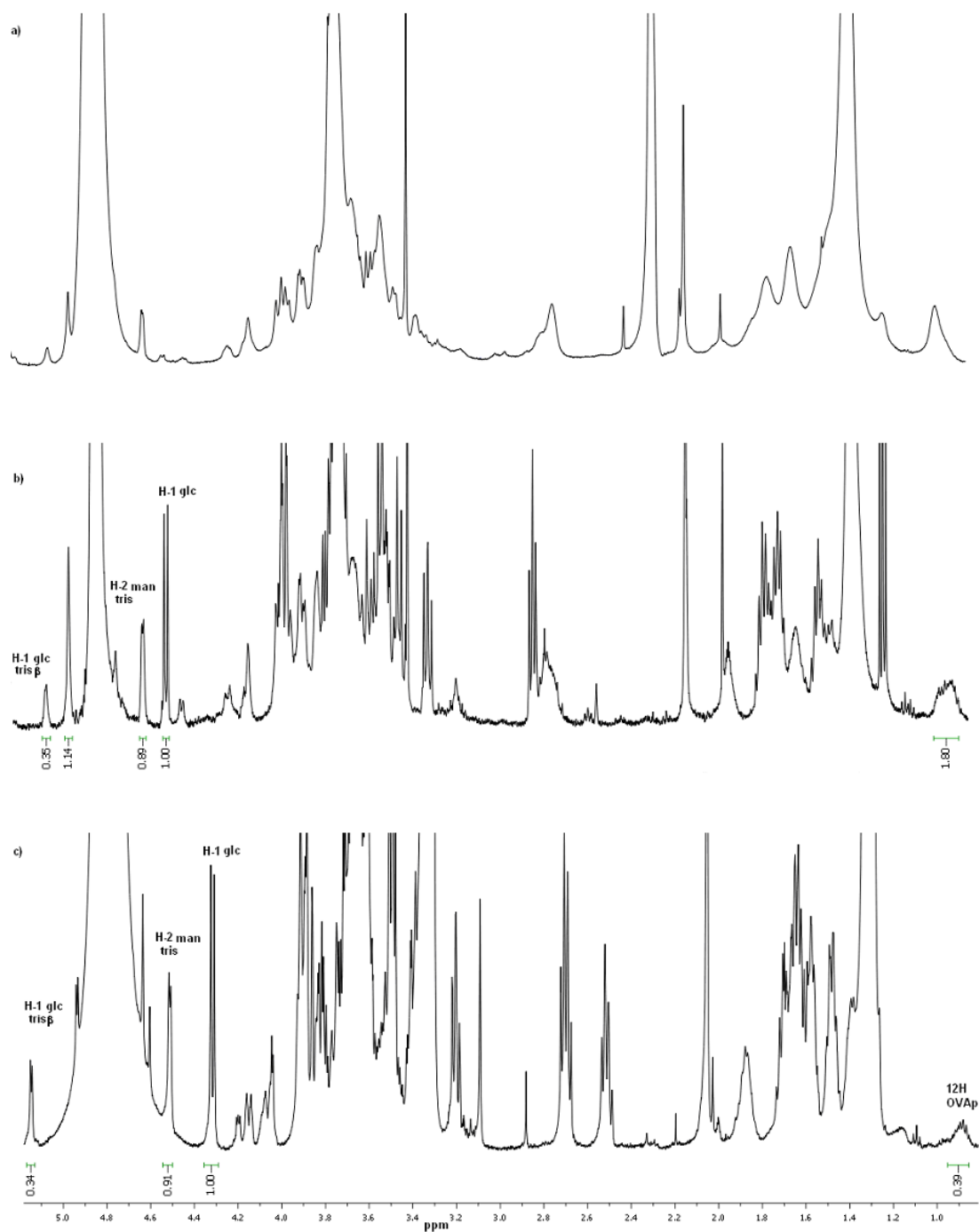


**Figure 4.12:** a)  $^1\text{H}$  NMR (500 MHz,  $\text{D}_2\text{O}$ ) of GNP **79** (c)  $^1\text{H}$  NMR (500 MHz,  $\text{CD}_3\text{OD}:\text{D}_2\text{O}$  5:1) of the mixture used to prepare GNP **79** and (b)  $^1\text{H}$  NMR of the mixture after the preparation of the GNP. Integration of selected signals shows that the ratio between trisaccharide **55**, glucose conjugate **57**, and OVA peptide **58** is about 45:50:5. Furthermore, comparison of the integration of selected signals in the  $^1\text{H}$  NMR spectrum of the mixture before (c) and after (b) the preparation of the GNP, with the exception of the OVAp signal which is overestimated, confirms the correct molar ratio of ligands attached on the Au nanoparticles.

For the spectra related to the others GNPs see experimental section.

### Calculation of the amount of antigen loaded on the GNPs

The amount of antigen related to *S. pneumoniae* arranged on the GNPs prepared in this thesis was determined in two different ways:

- 1) By calculation of the GNP molecular formula through TEM measurements of the gold core and estimation of the number of attached ligand using the statistic calculation of the Murray's table
- 2) By qNMR of the GNPs with TSP as internal standard, as described before (section 4.3.3)

For example, the calculation of the amount of trisaccharide ligand arranged on the GNP **79** with Pn19F/Glc/OVA 45:50:5 molar ratio is hereafter reported.

By TEM micrographs, the average diameter found is  $1.2 \pm 0.3$  nm which corresponds to nanoparticles of 79 gold atoms with 60 surface atoms and 38 minimal ligands, according to Murray's table<sup>142</sup> (Figure 4.13).

22 *Langmuir*, Vol. 14, No. 1, 1998

Hostetler et al.

Table 2. Results from Modeling of Gold Core Sizes, Shapes, and Alkanethiolate Coverages, and of Size-Dependent  $T_2$  Broadening of Proton NMR of  $\text{CH}_3$  Resonances

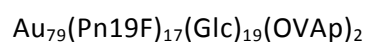
#atoms (shape) <sup>a</sup>	$R_{\text{CORE}}$ , nm	#surface atoms/ %defect/area nm <sup>2</sup>	calc TGA %organic/ %coverage/#chains	calc $R_{\text{TOTAL}}$ , nm	calc NMR $\nu_{\text{FWHM}}$ , Hz
79 (TO <sup>+</sup> )	0.65	60/60%/8.30	33.0/63%/38	2.6	15
116 (TO <sup>-</sup> )	0.71	78/61%/11.36	31.8/68%/53	2.6	16
140 (TO <sup>+</sup> )	0.81	96/50%/11.43	27.9/55%/53	2.7	17
201 (TO)	0.87	128/47%/15.22	26.5/55%/71	2.8	18
225 (TO <sup>+</sup> )	0.98	140/43%/15.19	24.4/51%/71	2.9	19
309 (CO)	1.1	162/52%/19.64	23.3/57%/92	3.0	22
314 (TO <sup>+</sup> )	1.0	174/41%/19.46	22.9/52%/91	3.0	20
459 (TO <sup>+</sup> )	1.2	234/36%/24.34	20.2/49%/114	3.1	23
586 (TO)	1.2	272/35%/28.94	19.1/50%/135	3.2	24
807 (TO <sup>+</sup> )	1.4	348/31%/34.86	17.1/47%/163	3.3	27
976 (TO <sup>-</sup> )	1.5	390/31%/40.02	16.4/48%/187	3.4	28
1289 (TO)	1.6	482/27%/47.22	14.9/46%/221	3.5	32
2406 (TO)	2.0	752/22%/69.86	12.2/43%/326	3.9	42
2951 (TO <sup>+</sup> )	2.2	876/21%/79.44	11.4/42%/371	4.1	47; 94 <sup>b</sup>
4033 (TO)	2.4	1082/19%/97.00	10.3/42%/453	4.3	55; 110 <sup>b</sup>
4794 (TO <sup>+</sup> )	2.6	1230/18%/108.28	9.7/41%/506	4.4	61; 122 <sup>b</sup>
6266 (TO)	2.8	1472/16%/128.66	8.9/41%/601	4.7	70; 140 <sup>b</sup>

<sup>a</sup> CO = cuboctahedron; TO = ideal truncoctahedron (all sides equal); TO<sup>+</sup> = truncoctahedron in which  $(0 < n - m \leq 4)$ , where  $n$  is the number of atoms between (111) facets and  $m$  is the number of atoms between (111) and (100) facets; TO<sup>-</sup> = truncoctahedron in which  $(-4 \leq n - m < 0, m > 1)$ . <sup>b</sup> The second value is the calculated linewidth for the methylene peak.

**Figure 4.13:** Murray's table shows for gold nanoparticles having a diameter of 1.2 nm ( $R_{\text{CORE}} \sim 0.65$  nm) 79 atoms of Au with 60 surface atoms and 38 chains.

The <sup>1</sup>H NMR analysis of the mixture of the three components before and after the **79** GNP formation confirmed a ratio of 45:50:5 (Figure 4.12).

By the combination of these results, the average molecular formula estimated was:



that gave an average molecular weight of 41.8 KDa

In this way, 160  $\mu\text{g}$  of GNP **79**, which was the amount of gold nanoparticles exactly weighted, correspond to 3.8 nmol of GNPs, that multiplied for the number of ligands of the trisaccharide conjugate **55** (*i.e.* seventeen) give 64.6 nmol and, consequently, 65.1  $\mu\text{g}$  of trisaccharide arranged on the gold surface.

On the other hand, qNMR analysis (Figure 4.14) performed on the same amount of GNPs gave 13.6 nmol of trisaccharide which corresponding only to 13.7  $\mu\text{g}$  of trisaccharide **55**.

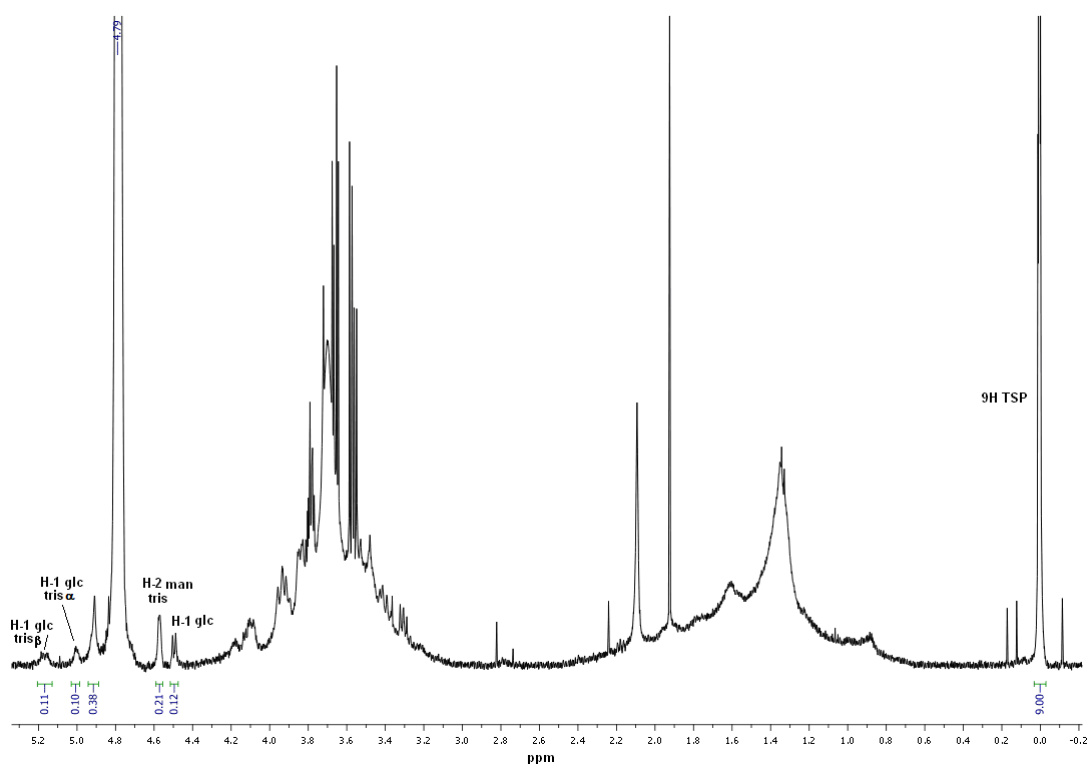


**Figure 4.14:**  $^1\text{H}$  qNMR (500MHz,  $\text{D}_2\text{O}$ ): 160  $\mu\text{g}$  of GNP **79** were dissolved in 180  $\mu\text{L}$  of  $\text{D}_2\text{O}$  and 20  $\mu\text{L}$  of  $\text{D}_2\text{O}$  containing 0.05 wt.% TPS were added; 13.65 nmol of trisaccharide **55** were found which corresponding to 13.7  $\mu\text{g}$  of trisaccharide conjugate antigen.

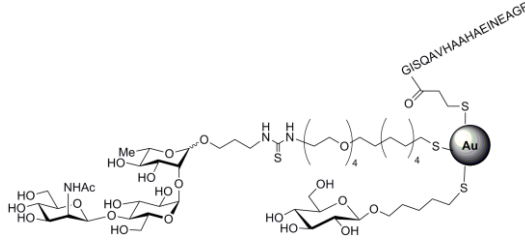
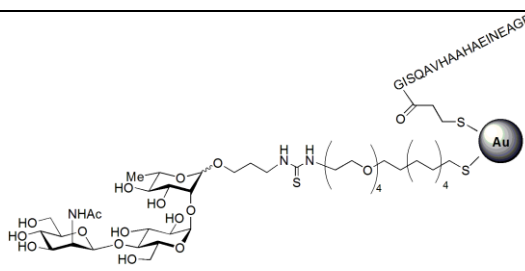
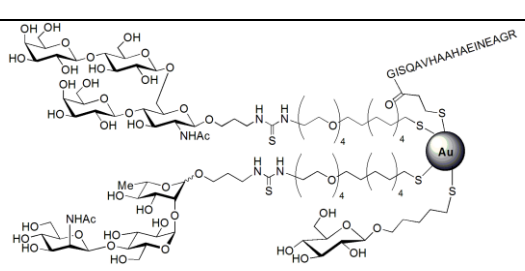
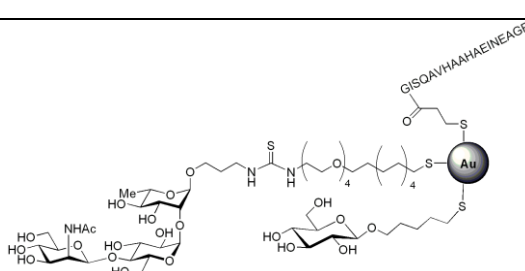
In Table 4.2, the quantity of the trisaccharide Pn19F and tetrasaccharide Pn14, which cover the gold surface of the GNPs prepared, calculated with the two methods are resumed.

As demonstrated, the amount of *active component* arranged on the GNP calculated with these two ways is very different. Apparently, the qNMR is not the most appropriate method to estimate the amount of organic compounds bound on the gold surface most probably because of the greater difficulty of integration in the GNP

spectra and to the different proton relaxation times of organic compound coupled to gold atoms. Moreover, the valuation based on the TEM analysis and Murray's table could not be enough precise due to the manual measurement of the diameter of gold core. However, we decided to use this last application to determinate the antigen carried by the GNPs for the immunization assays in order to avoid differences with previous investigation and to have comparable values.<sup>133</sup>

To verify our hypothesis on the limitation of qNMR analysis, the same experiment was performed using free glucose. A quantity of glucose, equal to the quantity attached to the GNP **79** calculated by TEM analysis, was dissolved in D<sub>2</sub>O and the same volume of TSP used in GNP **79** analysis was added. In this case, the amount of glucose obtained by qNMR was the one expected, but in this experiment glucose was not attached on the gold surface and consequently the signal of the anomeric proton of glucose and the singlet of the TSP were easily integrated. This experiment can confirm that the presence of the inorganic portion, *i.e.* the Au, influences the proton relaxation time, with effects on the signal integration ratio.

In the literature is also reported a similar problem when the amount of compound loaded on the gold surface was calculated with quantitative NMR and thermogravimetric analysis. Also in this case, the comparison of the data indicated reproducibility within 15%.<sup>131</sup>

GNPs	Weighed GNP ( $\mu\text{g}$ )	Antigen loaded ( $\mu\text{g}$ )		Structure
		TEM analysis <sup>(a)</sup>	qNMR <sup>(b)</sup>	
79	160	65.5	13.7	 <p>Pn19F/Glc/OVAp 45:50:5</p>
80	160	104.3	10.5	 <p>Pn19F/OVAp 95:5</p>
81	372	Pn19F		
		104.2	38.0	
		Pn14		
		122.6	48.5	Pn19F/Pn14/Glc/OVAp 40:40:15:5
82	504	154	Not performed	 <p>Pn19F<math>\alpha</math>/Glc/OVAp 45:50:5</p>

**Table 4.2:** Amount of antigen carried by the different the GNPs sent for the immunization assays.

(a) Value obtained by average molecular formula based on the average size of GNPs after TEM analysis;

(b) Value obtained by quantitative NMR using TSP as internal standard.

#### 4.4 Immunological evaluation

All the gold glyconanoparticles described in this PhD thesis have been tested *in vivo* in mice, after ethical approval. Inbred 6-week-old female BALB/c mice have been immunized intracutaneously with GNPs in mixture with Quillaja purified saponin (Quil-A) as adjuvant.

As a first step, an ELISA assay was performed on sera to measure the antibodies against native polysaccharide related to serotype 14 and 19F of *Streptococcus pneumoniae*. When polysaccharide serotype 14 was used as coating material in the ELISA plate, specific anti-type 14 polysaccharide IgG antibodies (anti-Pn14 PS IgG) were found in the sera of mice immunized with GNP **81**, carrying both serotype 14 and 19F, and **83** with only Pn14. On the contrary, in the ELISA with polysaccharide serotype 19F (Pn19F PS) as coating material, IgG antibodies were not detected in the sera of mice immunized with the GNPs. In this case, antibodies were only found in the sera of mice immunized with vaccine PVC13, the 13-valent pneumococcal conjugate vaccine, used as positive control, even if with a lower amount with respect to the Pn14PS ELISA, but in according with the literature<sup>146</sup> (Figure 4.15).

The inactivity of sera collected from mice immunized with GNPs **79**, **80** and **82** towards the native 19F polysaccharide could be due to the inability of the single trisaccharide repeating unit on the GNPs to function as epitope *in vivo*, although our previous data demonstrated *in vitro* inhibitory activity in a classical competitive ELISA assay. This would suggest that a longer saccharide fragment (more than one repeating unit) is necessary to induce the activation of the immune system. Another explanation of the inability to elicit antibody could be ascribed to the absence of the phosphate group. The aminopropyl linker is in fact directly attached to the sugar instead of having a phosphate bridge at the reducing end.

On the other hand, the high activity showed by GNP **81** even higher than the activity of **83**, could be explained by an adjuvant effect of the trisaccharide antigen Pn19F, which is charged on the GNPs together with tetrasaccharide antigen Pn14. Several carbohydrate-based compounds, as polysaccharides derived from bacteria,<sup>147</sup> are known to have immunostimulating properties, acting as adjuvants, which enhance the immune response increasing also the production of antibodies.<sup>148</sup> For instance, galactosylceramide has been largely evaluated as immunostimulant over the years, as well as mannosamine. It may be possible that the mannosaminic portion of the



trisaccharide repeating unit related to Pn19F used in the preparation of the GNPs, exhibits its immunostimulant properties enhancing the activity of the tetrasaccharide repeating unit related to Pn14 since the immune response of GNP **81** is higher than the one of GNPs **83** carrying only the tetrasaccharide related to Pn 14.

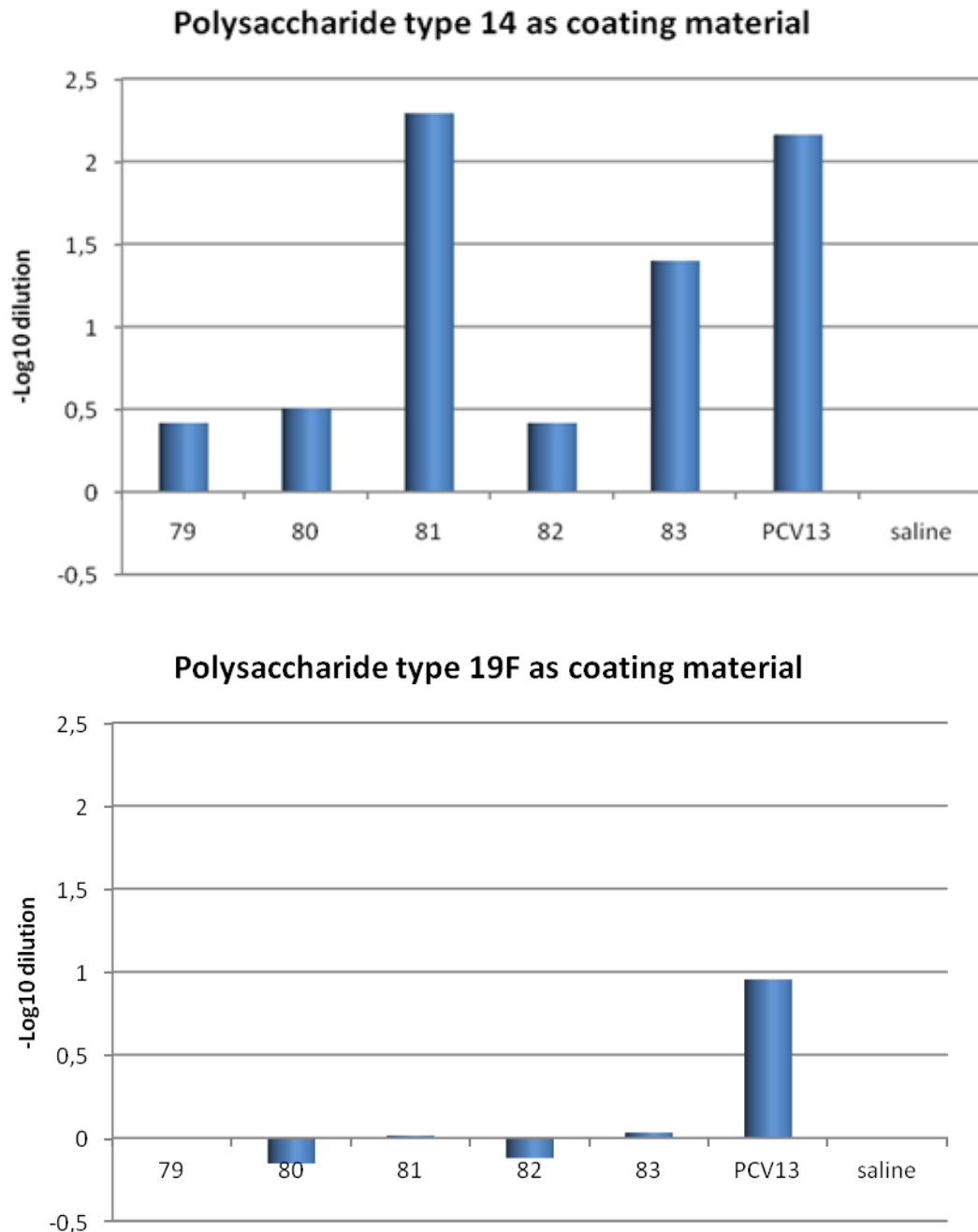


**Figure 4.15:** Specific anti-*S. pneumoniae* type 14 polysaccharide (Pn14 PS) and anti-*S. pneumoniae* type 19F polysaccharide (Pn19F PS) IgG antibodies determined by ELISA. ELISA were performed using Pn14 PS and Pn19F PS as coating material. The level of antibodies is expressed as the log<sub>10</sub> of the dilution giving twice the OD obtained for control mice. PVC13 and saline buffer immunization served as positive and negative control respectively.

Further investigation to clarify this preliminary result obtained with Pn19F and Pn14 polysaccharide as coating materials was carried out using the gold nanoparticles to cover the ELISA plate (Figure 4.16), following a procedure already reported.<sup>149</sup>

With this assay, we could verify if the GNPs, used as coating material, are recognized by the sera of immunized mice. When GNP **83** carrying the branched tetrasaccharide antigen related to Pn14 of *S. pneumoniae* was used as coating material in the ELISA plate, we found high level of IgG antibodies in sera of mice immunized with GNPs covered with the saccharide Pn14, *i.e.* **83** and **81** and PVC13 positive control. Also, lower IgG binding in mice sera from **79**, **80**, **82** immunization was observed, but this can be due to interaction from other part of GNPs such as peptide and linker, as previously reported.<sup>133</sup>

The same ELISA was performed with GNP **79** carrying the trisaccharide repeating unit of serotype 19F as coating material. In this case, IgG antibodies against **79** were found in sera of mice immunized with **81**, carrying both Pn19F and Pn14, **79**, **80** and **82**, even if in a lower titer with respect to ELISA with GNP **83** as coating material.

It is worth noting that there is no difference in the activity of GNPs **79** carrying trisaccharide Pn19F in alpha/beta mixture together with glucose and OVAp 45:50:5 molar ratio and **82** with the same molar ratio of the three components, but with only alpha anomer of trisaccharide Pn19F, confirming our previous results (unpublished data). Furthermore, the higher amount of trisaccharide Pn19F carried by GNP **80** respect with **79** does not reflect a greater activity.

These last results are very interesting because they indicate that the trisaccharide repeating unit is antigenic, despite it is not able to induce the production of antibodies IgG that recognize the native polysaccharide 19F. However, other experiments are currently underway to find the correct epitope fragment and to get more information on the applicability of these GNPs as carrier for saccharide antigens of *S. pneumoniae*.

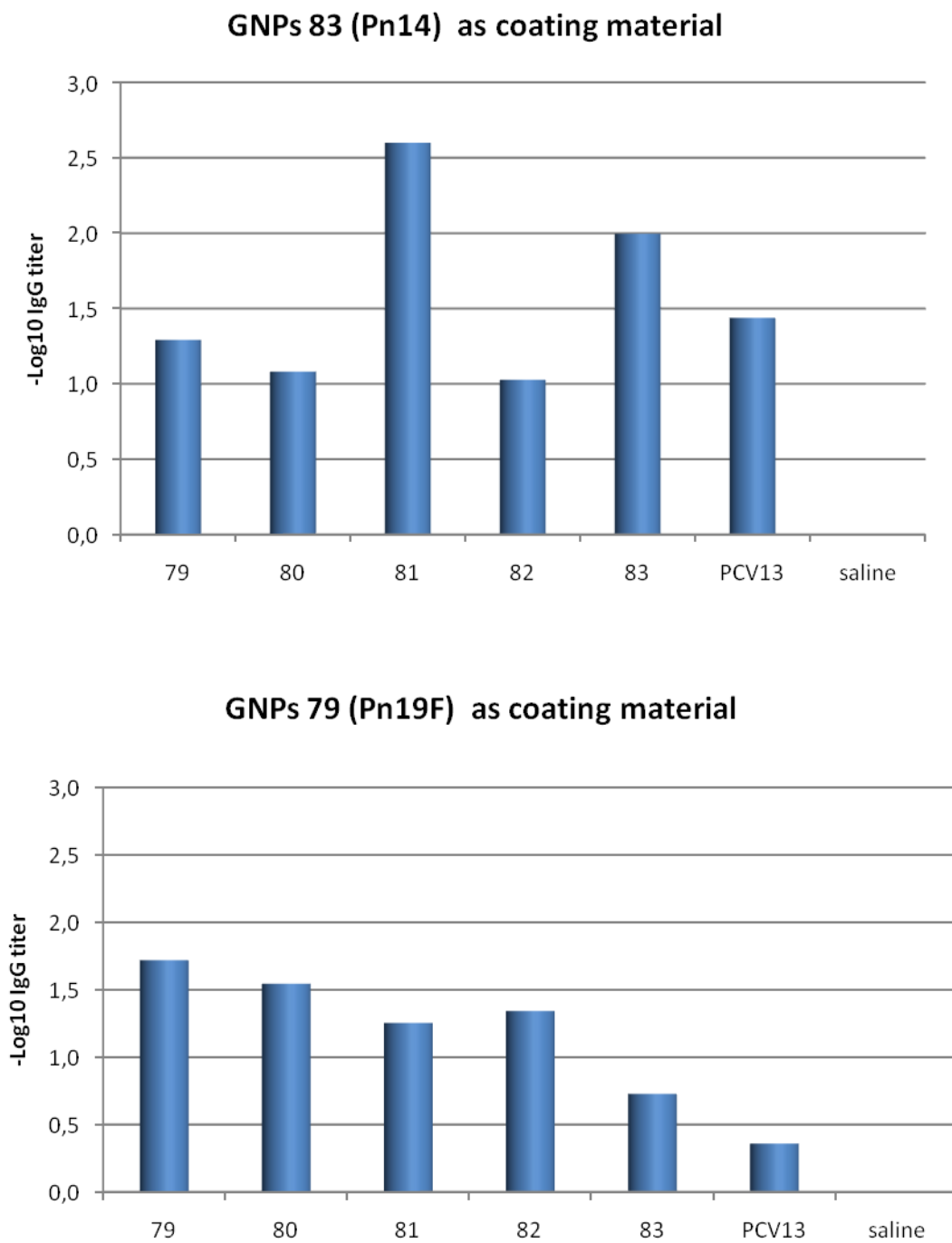


**Figure 4.16:** IgG antibodies against GNP **83** and **79** detected in sera of mice immunized. ELISA was performed using these GNPs as coating materials. The level of antibodies is expressed as the  $\log_{10}$  of the IgG titer.

## 4.5 Conclusions

In this chapter, the preparation and immunological evaluation of gold nanoparticles bearing saccharide antigens related to serotypes Pn19F and Pn14 of *Streptococcus pneumoniae* have been reported. Different percentages of thiol-ending antigens as *active component*, glucose as *inner component*, and OVA<sub>323-339</sub> peptide as T-helper, were used to obtain the glyconanoparticles through a direct method. The GNPs were purified by dialysis and characterized by different techniques, such as Ultraviolet-visible (UV/Vis), Circular Dichroism (CD), Transmission Electron Microscopy (TEM) and Nuclear Magnetic Resonance (<sup>1</sup>H NMR and qNMR). GNPs resulted well-soluble and stable in water and, as solid they can be stored at 4°C in the dark.

All the GNPs prepared has been evaluated for their immunological activity. The most promising result has been achieved with the multiantigenic system **81**, in which the presence of the trisaccharide antigen related to serotype 19F enhances the immunological activity *in vivo* of the GNP carrying the tetrasaccharide serotype 14.

Encouraging results have been also obtained using GNP as coating materials in ELISA assay. In this case, IgG were found in sera of mice immunized with all the gold glyconanoparticles under examination, thus demonstrating the antigenicity of the system.

## 4.6 Experimental section

### 4.6.1 General methods

**Chemical:** All chemicals were purchased as reagent grade from Sigma–Aldrich, except chloroauric acid (Strem Chemicals), and were used without further purification. Dichloromethane ( $\text{CH}_2\text{Cl}_2$ ) and triethylamine (TEA) used in the synthesis of **74** were distilled from calcium hydride. Methanol ( $\text{CH}_3\text{OH}$ ) was degassed with Argon before to use to avoid oxidation of compound **55**. Air- and moisture sensitive liquids and solutions were transferred *via* oven-dried syringe or stainless steel cannula through septa. Reactions were monitored by thin-layer chromatography (TLC) on silica gel 60  $\text{F}_{254}$  aluminium-backed sheets (Merck) with visualization under UV (254 nm) and/or by staining with *p*-anisaldehyde solution [anisaldehyde (25 mL),  $\text{H}_2\text{SO}_4$  (25 mL), EtOH (450 mL), and  $\text{CH}_3\text{COOH}$  (1 mL)], followed by heating at over 200 °C. Size-exclusion column chromatography was performed on Sephadex LH-20 (GE Healthcare). Flash column chromatography (FCC) was performed on silica gel high-purity grade, pore size 60Å, 230-400 mesh particle size. Preparative TLC was performed on TLC plate 20×20 cm Silica gel 60  $\text{F}_{254}$  glass-backed sheets (Merck). Organic solvents were removed by rotary evaporation under reduced pressure at approximately 40°C (water bath). Purified water was obtained from a Simplicity Ultrapure Water System (Millipore). Nanopure water (18.2 MΩ-cm) was obtained by a Thermo Scientific Barnstead NANOpure Diamond Water System.

All the GNPs prepared were purified by centrifugal filtering with AMICON (10.000 MWCO) and dialyses carried out using Slide–A–Lyzer dialysis cassette (3500 MWCO).

UV/Vis spectra were measured with Beckman Coulter DU 800 UV/Vis Spectrophotometer. To perform the measurement a solution of GNPs 0,10mg/ml in HPLC gradient grade water has been prepared and plastic cuvettes with an internal width of 45mm were used. All UV/Vis spectra were subtracted from blank.

Circular Dichroism spectra were performed on a Jasco 720 Spectrophotometer. A solution of GNPs 0,25mg/ml in HPLC gradient grade water and quartz cuvette with a 1 mm path length was used to carry out the measurement. All CD spectra were subtracted from blank.

TEM analysis was performed with a Philips JEOL JEM-2100F microscope, working at 200 kV. A single drop (~2  $\mu$ L) of an aqueous solution 0.05 mg/mL in HPLC gradient grade water of GNPs was placed on a copper grid coated with a carbon film (Electron Microscopy Sciences) that was left to dry in air for several hours at room temperature in order to carry out the experiment. Statistical determination of gold dimension was performed using Image J programme and the average diameter of gold core can be correlated to the number of ligands present on GNP.<sup>142</sup>

<sup>1</sup>H and <sup>13</sup>C NMR spectra were recorded on Bruker 500 MHz (high resolution) spectrometer. Chemical shifts ( $\delta$ ) are given in ppm relative to the residual signal of the solvent used. Specifically 7.26 ppm for CDCl<sub>3</sub>, 3.31 ppm for CD<sub>3</sub>OH and 4.79 ppm for D<sub>2</sub>O in <sup>1</sup>H NMR spectra and 77.0 ppm (central line) for CDCl<sub>3</sub> and 49.0 ppm (central line) for CD<sub>3</sub>OD in <sup>13</sup>C NMR spectra. Coupling constants (J) are reported in Hz. Splitting patterns are described by using the following abbreviations: *br*, broad; *s*, singlet; *d*, doublet; *t*, triplet; *m*, multiplet; *dd*, doublet of doublet; *dt*, doublet of triplet.

Mass spectra were measured with an Esquire 6000 ESI-Ion Trap spectrometer from Bruker Daltonics. High-resolution mass spectra (HRMS) were obtained using the MALDI technique with a 4700 Proteomics Analyzer (Applied Biosystems) operated in MALDI-TOF-TOF configuration.

**Biochemical:** For the immunization assays inbred 6-week-old female BALB/c mice were employed. *Quil-A*<sup>®</sup> saponin used as adjuvant and co-administered with GNPs was a gift from Dr. Erik B. Lindblad and Brenntag Biosector, Denmark.

ELISA plates were coated with purified Pn14PS or Pn19F PS purchased from Statens Serum Institut, Denmark, while Nunc MaxiSorp plates were employed for the GNP-ELISA.

Goat anti-mouse IgG and IgG horseradish peroxidase were purchased from Silenus, Amrad Operations PTY LTD, Australia.

Bovine Serum Albumin, BSA, was purchased from Sigma-Aldrich.

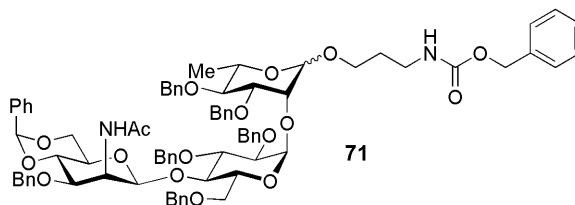
TMB substrate (3,3',5,5'-Tetramethylbenzidine) was achieved by Life technologies

Optical density (OD) values were obtained with a micro-titer plate spectrophotometer at 450 nm (Tecan Infinite F200).

## 4.6.2 Synthesis of thiol-ending trisaccharide related to serotype Pn19F.

**Synthesis of *N*-(benzyloxycarbonyl)-3-amminopropyl (2-acetamido-3-*O*-benzyl-4,6-*O*-benzylidene -2-deoxy- $\beta$ -D-mannopyranosyl-(1 $\rightarrow$ 4)-(2,3,6-tri-*O*-benzyl- $\alpha$ -D-glucopyranosyl)-(1 $\rightarrow$ 2)-3,4-di-*O*-benzyl- $\alpha,\beta$ -L-rhamnopyranoside **71****

The starting material 3-*O*-benzyl-4,6-*O*-benzylidene-2-acetamido-2-deoxy- $\beta$ -D-mannopyranosyl-(1 $\rightarrow$ 4)-2,3,6-tri-*O*-benzyl- $\alpha$ -D-glucopyranosyl-(1 $\rightarrow$ 2)-3,4-di-*O*-benzyl-1-trichloroacetamido- $\alpha,\beta$ -L-



rhamnopyranoside **69** (90 mg, 0.07 mmol, 1 eq.) and *N*-(benzyloxycarbonyl)-3-amminopropyl **70** (58 mg, 0.28 mmol, 4 eq.) were dissolved in dry CH<sub>2</sub>Cl<sub>2</sub> (1.5 ml, 0.05M) containing molecular sieves 4 Å (50 mg). The suspension was left stirring under Ar atmosphere at room temperature for 15 minutes, then it was cooled at 0°C and TMSOTf 0.1 M in CH<sub>2</sub>Cl<sub>2</sub> (140  $\mu$ l, 0.014 mmol, 0.2 eq.) was added. After 15 minutes, the reaction mixture was neutralized with TEA, filtrated over a Celite pad and the solvent evaporated under reduced pressure. Purification through flash chromatography (Hexane/Ethyl Acetate 6:4) of the crude afforded compound **71** (85 mg, 0.063 mmol, 90% yield), in mixture  $\alpha/\beta$  as white foam.

In order to prepare GNPs coated only with the natural alpha anomer, 40 mg of mixture of the product was submitted to a preparative TLC (Hexane/Ethyl Acetate 1:1), and the alpha anomer was also separately characterized.

Alpha/beta mixture:

<sup>1</sup>H-NMR (CDCl<sub>3</sub>):  $\delta$ =1.38 (d, 1.2H,  $J_{6r,5r}$ =6.2 Hz, CH<sub>3</sub> $\alpha$ ), 1.42 (d, 1.8H,  $J_{6r,5r}$ =6.2 Hz, CH<sub>3</sub> $\beta$ ), 1.62-1.69 (m, 2H, CH<sub>2</sub>), 1.76 (*br s*, 1.2H, CH<sub>3</sub>CO $\alpha$ ), 1.77 (*br s*, 1.8H, CH<sub>3</sub>CO $\beta$ ), 3.03-3.09 (m, 0.4H, H-5m $\alpha$ ), 3.12-3.19 (m, 0.6H, H-5m $\beta$ ), 3.21-5.15 (m, 35.4H, OCH<sub>2</sub>CH<sub>2</sub>CH<sub>2</sub>N, OCH<sub>2</sub>CH<sub>2</sub>CH<sub>2</sub>N, 0.4H-1g $\alpha$ , H-2g, H-3g, H-4g, H-5g, 2H-6g, H-1r, H-2r, H-3r, H-4r, H-5r, H-1m, H-2m, H-3m, H-4m, 2H-6m, 7CH<sub>2</sub>Ph), 5.48 (s, 1H, CHPh), 5.53 (*br d*, 1H,  $J$ =10.9 Hz, NH), 5.61 (d, 0.6H,  $J$ =3.6 Hz, H-1g $\beta$ ), 7.19-7.52 (m, 40H, 8Ph);

<sup>13</sup>C-NMR (CD<sub>3</sub>Cl):  $\delta$ =17.9 (CH<sub>3</sub> $\beta$ ), 18.0 (CH<sub>3</sub> $\alpha$ ), 23.1 (CH<sub>3</sub>CO $\beta$ ), 23.3 (CH<sub>3</sub>CO $\alpha$ ), 29.6 (CH<sub>2</sub> $\alpha$ ), 29.8 (CH<sub>2</sub> $\beta$ ), 38.0 (CH<sub>2</sub>N $\beta$ ), 38.8 (CH<sub>2</sub>N $\alpha$ ), 50.5 (C2m), 65.4 (OCH<sub>2</sub>), 66.5 (CH<sub>2</sub>Ph-cbz $\beta$ ), 66.7 (CH<sub>2</sub>Ph-cbz $\alpha$ ), 67.1 (C5m $\alpha$ ), 67.4 (C5m $\beta$ ), 67.9 (C6g $\alpha$ ), 68.2 (C6g $\beta$ ), 68.4 (C5r $\alpha$ ), 68.6 (C5r $\beta$ ), 69.2 (C5g $\beta$ ), 69.8 (C5g $\alpha$ ), 70.9 (CH<sub>2</sub>Ph), 71.2 (CH<sub>2</sub>Ph), 71.9 (CH<sub>2</sub>Ph), 72.1 (CH<sub>2</sub>Ph), 72.7 (CH<sub>2</sub>Ph), 73.4 (CH<sub>2</sub>Ph), 74.2 (CH<sub>2</sub>Ph), 74.7 (CH<sub>2</sub>Ph), 75.0 (C2r), 75.3 (CH<sub>2</sub>Ph), 75.5 (C4g $\alpha$ ), 75.7 (C4g $\beta$ ), 75.9 (C3m), 78.5 (C4m), 79.0 (C3r $\alpha$ ), 79.2 (C3r $\beta$ ), 79.7 (C2g $\alpha$ ), 79.8 (C2g $\beta$ ), 80.0 (C4r $\beta$ ), 80.1 (C4r $\alpha$ ), 80.3 (C3g $\beta$ ), 80.4 (C3g $\alpha$ ), 96.8 (C1g $\beta$ ), 96.9 (C1g $\alpha$ ), 97.5 (C1r), 99.6 (C1m), 101.6 (CHPh benzilidene), 126.1, 126.3, 126.4, 126.5, 126.6, 127.2-127.9 (16C), 128.0-128.6 (18C), 128.9, 129.0, 129.7, 134.4, 136.6 (2C Cbz  $\alpha$  and  $\beta$ ), 134.3, 137.4, 137.6 (3C), 137.7 (2C), 137.8, 138.1 (3C), 138.2,

138.3 (2C), 138.4 (3C), 138.5 (3C), 138.7 (2C), 139.5, 139.6 (2C), 139.7, 156.3 (OCONH linker), 170.4 (CONHAc).

ESI-MS (CH<sub>3</sub>OH, positive-ion mode): *m/z* 1371.5 (100%) [M+Na]<sup>+</sup>, 1372.5 (90%) [M+Na+1]<sup>+</sup>, Calcd for C<sub>80</sub>H<sub>88</sub>N<sub>2</sub>O<sub>17</sub>, *m/z* 1348.61 [M].

Alpha anomer:

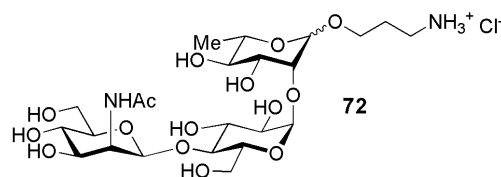
<sup>1</sup>H-NMR (CDCl<sub>3</sub>): δ=1.38 (d, 3H, J<sub>6r,5r</sub>=6.2 Hz, CH<sub>3</sub>), 1.60-1.69 (m, 2H, CH<sub>2</sub>), 1.74 (s, 3H, CH<sub>3</sub>CO), 3.07 (dt, 1H, J<sub>5,6</sub>=4.9 Hz, J<sub>5,6'</sub>=10.0 Hz, H-5m), 3.18 (d, 1H, J<sub>5,6'</sub>=10.0 Hz, H-6'g), 3.22-3.34 (m, 4H, CH<sub>2</sub>N, H-6g, H-3m), 3.35-3.41 (m, 1H, CH<sub>2</sub>'O), 3.47-3.64 (m, 5H, H-2g, H-4r, H-5r, H-4m, H-6m), 3.65-3.75 (m, 1H, -OCH<sub>2</sub>), 3.82-3.90 (m, 2H, H-3g, H-3r), 4.01-4.13 (m, 4H, H-4g, H-5g, H-2r, H-6'm), 4.24 (d, 1H, J=12.0, CHPh), 4.45 (*br s*, 1H, H-1m), 4.48 (d, 1H, J=12.0, CHPh), 4.54-4.75 (m, 9H, H-1r, H-2m, 7 CHPh), 4.80 (d, 1H, J=12.0, CHPh), 4.91 (d, 1H, J<sub>1,2</sub>=3.4 Hz, H-1g), 4.95-4.98 (m, 3H, 2 CHPh, NH), 5.08 (dd, 2H, J=14.2, CH<sub>2</sub>Ph), 5.50 (m, 2H, CHPh benzylidene, NHAc), 7.19-7.52 (m, 40H, 8 Ph);

<sup>13</sup>C-NMR (CD<sub>3</sub>Cl): δ=18.0 (CH<sub>3</sub>), 23.3 (CH<sub>3</sub>CO), 29.6 (CH<sub>2</sub>), 38.8 (CH<sub>2</sub>N), 50.5 (C2m), 65.5 (OCH<sub>2</sub>), 66.7 (CH<sub>2</sub>Ph-cbz), 67.1 (C5m), 67.9 (C6g), 68.4 (C5r), 68.7 (C6m), 69.8 (C5g), 71.2 (CH<sub>2</sub>Ph), 72.1 (CH<sub>2</sub>Ph), 72.7 (CH<sub>2</sub>Ph), 73.4 (CH<sub>2</sub>Ph), 74.7 (CH<sub>2</sub>Ph), 75.0 (C2r), 75.3 (CH<sub>2</sub>Ph), 75.5 (C4g), 75.9 (C3m), 78.5 (C4m), 79.0 (C3r), 79.7 (C2g), 80.1 (C4r), 80.4 (C3g), 96.9 (C1g), 97.5 (C1r), 99.6 (C1m), 101.6 (CHPh benzylidene), 126.1, 126.4, 127.3, 127.4 (2C), 127.6 (2C), 127.7 (2C), 127.9, 128.0, 128.1 (2C), 128.2 (2C), 128.3 (2C), 128.4 (2C), 128.5 (2C), 128.6 (2C), 129.0, 136.6 (C Cbz), 137.4, 137.7, 138.2, 138.4, 138.6, 139.6, 156.3 (OCONH linker), 170.4 (CONHAc);

ESI-MS (CH<sub>3</sub>OH, positive-ion mode): *m/z* 1371.8 (100%) [M+Na]<sup>+</sup>, Calcd for C<sub>80</sub>H<sub>88</sub>N<sub>2</sub>O<sub>17</sub>, *m/z* 1348.61 [M].

**Synthesis of amino-hydroxypropyl 2-acetamido-2-deoxy β-D-mannopyranosyl-(1→4)-α-D-glucopyranosyl-(1→2)- α,β-L-rhamnopyranoside 72**

The protected trisaccharide **71** (39 mg, 0.029 mmol, 1 eq.) was dissolved in a mixture of AcOEt/CH<sub>3</sub>OH/HCl 0.1M in H<sub>2</sub>O 1:1:1 (1 ml, 0.03M) and hydrogenolyzed at atmospheric pressure with palladium hydroxide on activated charcoal (39 mg) for 48 hours. The mixture was filtrated to remove the catalized. The filtrate was concentrated under reduced pressure and then freeze dried to give the product **72** isolated as the chloride salt (17 mg, quant.) as a white solid.



The same procedure above described was used to obtain also the alpha anomer.

Alpha/beta mixture:

<sup>1</sup>H-NMR (D<sub>2</sub>O): δ=1.32 (d, 1.2H, J<sub>6r,5r</sub>=6.2 Hz, CH<sub>3</sub>α), 1.34 (d, 1.8H, J<sub>6r,5r</sub>=5.8 Hz, CH<sub>3</sub>β), 1.97-2.03 (m, 2H, CH<sub>2</sub>), 2.09 (s, 3H, CH<sub>3</sub>CO), 3.15 (t, 2H, J=7.2 Hz, CH<sub>2</sub>N), 3.40-4.05 (m,



15.4H, H-2g, H-3g, H-4g, 2H-6g, 0.4H-2r $\alpha$ , H-3r, H-4r, H-5r, H-3m, H-4m, H-5m, 2H-6m, OCH<sub>2</sub>), 4.06-4.08 (m, 0.4H, H-5g $\alpha$ ), 4.10 (d, 0.6H, J<sub>2,3</sub>=3.1 Hz, H-2r $\beta$ ), 4.18 (dt, 0.6H, J<sub>5,6</sub>=2.7 Hz, J<sub>5,6'</sub>=10.2 Hz, H-5g $\beta$ ), 4.57 (*br* d, 1H, J<sub>2,3</sub>=4.4 Hz, H-2m), 4.74 (s, 0.6H, H-1r $\beta$ ), 4.91 (*br* s, H-1m), 4.93 (d, 0.4H, J<sub>1,2</sub>=1.2 Hz, H-1r $\alpha$ ), 5.01 (d, 0.4H, J<sub>1,2</sub>=3.8 Hz, H-1g $\alpha$ ); 5.15 (d, 0.6H, J=3.8 Hz, H-1g $\beta$ );

<sup>13</sup>C-NMR (D<sub>2</sub>O):  $\delta$ =16.5 (CH<sub>3</sub> $\alpha$ ), 16.6 (CH<sub>3</sub> $\beta$ ), 22.0 (CH<sub>3</sub>CO), 26.6 (CH<sub>2</sub> $\alpha$ ), 26.8 (CH<sub>2</sub> $\beta$ ), 37.5 (CH<sub>2</sub>N $\alpha$ ), 37.6 (CH<sub>2</sub>N $\beta$ ), 53.3 (C2m), 59.6 (C6g $\alpha$ ), 59.8 (C6g $\beta$ ), 60.4 (C3m), 65.1 (OCH<sub>2</sub> $\alpha$ ), 66.6 (C4m), 67.3 (OCH<sub>2</sub> $\beta$ ), 68.9, 69.6, 70.2 (C5g $\beta$ ), 70.3 (C5g $\alpha$ ), 71.1, 71.2, 71.5 (C2g $\beta$ ), 71.8 (C2g $\alpha$ ), 71.9 (C5r $\alpha$  and C5r $\beta$ ), 72.0 (C3r $\alpha$  and C3r $\beta$ ), 72.5 (C4r $\alpha$ ), 76.3 (C5m), 76.5 (C6m), 77.9 (C2r $\beta$ ), 78.6 (C4g $\alpha$  and C4g $\beta$ ), 97.2 (C1r $\alpha$ ), 97.5 (C1g $\alpha$ ), 99.3 (C1m $\alpha$ ), 99.4 (C1m $\beta$ ), 99.8 (C1g $\beta$ ), 100.4 (C1r $\beta$ ), 175.4 (CONHAc);

ESI-MS (CH<sub>3</sub>OH, positive-ion mode): m/z 587.1 (95%) [M+1]<sup>+</sup>, 609.5 (50%) [M+23]<sup>+</sup>, Calcd for C<sub>23</sub>H<sub>42</sub>N<sub>2</sub>O<sub>15</sub>, m/z 586.58 [M].

#### Alpha anomer:

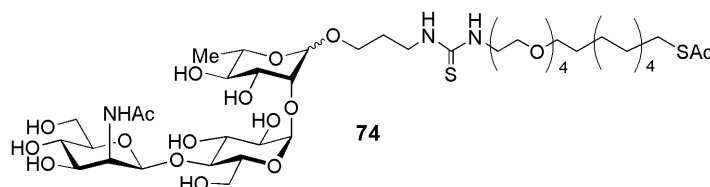
<sup>1</sup>H-NMR (D<sub>2</sub>O):  $\delta$ =1.32 (d, 3H, J<sub>6r,5r</sub>=6.2 Hz, CH<sub>3</sub>), 1.97-2.03 (m, 2H, CH<sub>2</sub>), 2.08 (s, 3H, CH<sub>3</sub>CO), 3.08-3.19 (m, 2H, CH<sub>2</sub>N), 3.44-3.49 (m, 1H, H-5m), 3.49-3.64 (m, 4H, H-4m, H-4r, H-2g, OCH<sub>2</sub>), 3.67-3.72 (m, 2H, H-5r, H-4g), 3.75-3.79 (m, 2H, 2H-6g), 3.80-3.99 (7H, H-3m, 2H-6m, H-2r, H-3r, H-3g, OCH<sub>2</sub>'), 4.06-4.10 (m, 1H, H-5g), 4.56 (dd, 1H, J<sub>1,2</sub>=1.3 Hz, J<sub>2,3</sub>=4.3 Hz, H-2m), 4.90 (d, 1H, J<sub>1,2</sub>=1.3 Hz, H-1m), 4.93 (d, 1H, J<sub>1,2</sub>=1.2 Hz, H-1r), 5.01 (d, 1H, J<sub>1,2</sub>=3.8 Hz, H-1g);

<sup>13</sup>C-NMR (D<sub>2</sub>O):  $\delta$ =16.5 (CH<sub>3</sub>), 22.0 (CH<sub>3</sub>CO), 26.6 (CH<sub>2</sub>), 37.5 (CH<sub>2</sub>N), 53.3 (C2m), 59.6 (C6g), 60.4 (C3m), 65.1 (OCH<sub>2</sub>), 66.6 (C4m), 68.9, 69.6, 70.3 (C5g), 71.1, 71.2 (C2g), 71.8 (C5r), 72.0 (C3r), 76.3 (C5m), 76.5 (C6m), 78.7 (C4g), 97.2 (C1r), 97.5 (C1g), 99.3 (C1m), 175.4 (CONHAc);

ESI-MS (CH<sub>3</sub>OH, positive-ion mode): m/z 609.27 (100%) [M+Na]<sup>+</sup>, 587.29 (95%) [M+1]<sup>+</sup>, Calcd for C<sub>23</sub>H<sub>42</sub>N<sub>2</sub>O<sub>15</sub>, m/z 586.58 [M].

#### Synthesis of 3-[2-acetamido-2-deoxy $\beta$ -D-mannopyranosyl-(1 $\rightarrow$ 4)- $\alpha$ -D-glucopyranosyl-(1 $\rightarrow$ 2)- $\alpha,\beta$ -L-rhamnopyranosyloxy]-1-propyl 3-(23-S-Acetyl-mercapto-3,6,9,12-tetraoxatricosyl) thiourea **74**

To a solution of 3-aminopropyl trisaccharide **72** (3.91 mg, 6.27  $\mu$ mol, 1.0 equiv.) in H<sub>2</sub>O:iPrOH:CH<sub>3</sub>CN (1:1:1, v/v/v, 0.6 mL) a solution of 23-mercapto-



3,6,9,12-tetraoxatricosyl isothiocyanate linker **73** (5.82 mg, 12.55  $\mu$ mol, 2.0 equiv.) in H<sub>2</sub>O:iPrOH:CH<sub>3</sub>CN (1:1:1, v/v/v, 0.6 mL) was added and the pH was set to basic by addition of triethylamine 0.05 M in H<sub>2</sub>O:iPrOH:CH<sub>3</sub>CN (188  $\mu$ L, 9.41  $\mu$ mol, 1.5 equiv.). The mixture was stirred at room temperature for 24 h and then the solvent was

evaporated. The crude material was kept in high vacuum to remove the residual triethylamine and then triturated with Et<sub>2</sub>O (3 × 2ml) in order to get rid of the excess of the linker. Then, the crude was further purified by Sephadex LH-20 chromatography using as eluent CH<sub>3</sub>OH/H<sub>2</sub>O 9:1 to afford the trisaccharide conjugate 74 as a white solid (4.95 mg, 4.71 μmol, 75%).

Alpha/beta mixture:

<sup>1</sup>H-NMR (CD<sub>3</sub>OD): δ=1.27-1.38 (m, 17H, CH<sub>3</sub>, 7CH<sub>2</sub>), 1.53-1.60 (m, 4H, CH<sub>2</sub>CH<sub>2</sub>SAc, OCH<sub>2</sub>CH<sub>2</sub>(CH<sub>2</sub>)<sub>9</sub>SAc), 1.81-1.91 (m, 2H, OCH<sub>2</sub>CH<sub>2</sub>CH<sub>2</sub>N), 2.02 (s, 3H, NHAc), 2.30 (s, 3H, SAc), 2.86 (t, 2H, J=7.3 Hz, CH<sub>2</sub>SAc), 3.27-3.93 (m, 35.4H, H-2g, H-3g, H-4g, 2H-6g, 0.4H-2rα, H-3r, H-4r, H-5r, H-3m, H-4m, H-5m, 2H-6m, 9CH<sub>2</sub>O, 2CH<sub>2</sub>N), 4.00 (d, 0.6H, J<sub>1,2</sub>=3.8 Hz, H-2rβ), 4.04-4.07 (m, 0.4H, H-5gα), 4.13-4.17 (m, 0.6H, H-5gβ), 4.50 (*br d*, 1H, J=4.1 Hz, H-2m), 4.61 (s, 0.6H, H-1rβ), 4.78 (s, 1H, H-1m), 4.83 (d, 0.4H, J<sub>1,2</sub>=0.9 Hz, H-1rα), 4.92 (d, 0.4H, J<sub>1,2</sub>=3.8 Hz, H-1gα), 5.11 (d, 0.6H, J<sub>1,2</sub>=3.8 Hz, H-1gβ);

<sup>13</sup>C-NMR (CD<sub>3</sub>OD): δ=18.0 (2CH<sub>3</sub>), 22.7 (2CH<sub>3</sub>CO), 27.1 (CH<sub>2</sub>), 29.8, 29.9 (CH<sub>3</sub>CO), 30.2 (SAc), 30.5 (2CH<sub>2</sub>), 30.6 (2CH<sub>2</sub>), 30.7 (2CH<sub>2</sub>), 37.5 (CH<sub>2</sub>N), 47.8, 54.9 (C2mα and C2mβ), 61.3, 61.4, 61.9, 66.3, 68.2 (2C), 70.2, 70.7, 70.8, 71.1, 71.3, 71.5, 71.6, 71.7, 71.8, 71.9, 72.4, 73.2, 73.5, 73.7, 73.8, 74.0 (2C), 74.1, 74.2, 74.5 (2C), 78.6, 78.7, 79.9, 80.1, 80.3, 99.2 (C1rα), 99.6 (C1gα), 100.9 (C1m), 101.8 (C1gβ), 102.1 (C1rβ), 174.7 (NCOCH<sub>3</sub>), 190.9 (S=C), 197.6 (SCOCH<sub>3</sub>);

TOF MS ESI (CH<sub>3</sub>OH, positive-ion mode): m/z 1072.7 (100%) [M+Na]<sup>+</sup>, Calcd for C<sub>45</sub>H<sub>83</sub>N<sub>3</sub>O<sub>20</sub>S<sub>2</sub>, m/z 1049.50 [M].

Alpha anomer:

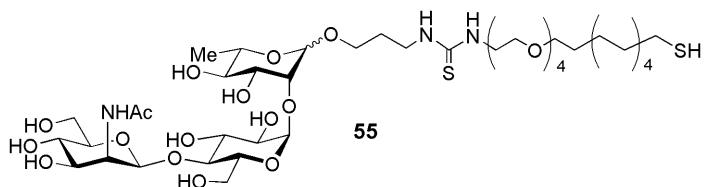
<sup>1</sup>H-NMR (CD<sub>3</sub>OD): δ=1.27-1.39 (m, 17H, CH<sub>3</sub>, 7CH<sub>2</sub>), 1.53-1.59 (m, 3.7H, 1.7 CH<sub>2</sub>CH<sub>2</sub>SAc, OCH<sub>2</sub>CH<sub>2</sub>(CH<sub>2</sub>)<sub>9</sub>SAc), 1.63-1.71 (m, 0.3H, CH<sub>2</sub>CH<sub>2</sub>SS), 1.72-1.79 (m, 1H, OCH<sub>2</sub>CH<sub>2</sub>CH<sub>2</sub>N), 1.83-1.90 (m, 1H, OCH<sub>2</sub>CH<sub>2</sub>'CH<sub>2</sub>N), 2.02 (s, 3H, NHAc), 2.30 (s, 3H, SAc), 2.69 (t, 0.3H, J=7.8 Hz, CH<sub>2</sub>SS), 2.86 (t, 1.7 H, J=7.3 Hz, CH<sub>2</sub>SAc), 3.15-3.92 (m, 36H, H-2g, H-3g, H-4g, 2H-6g, H-2r, H-3r, H-4r, H-5r, H-3m, H-4m, H-5m, 2H-6m, 9CH<sub>2</sub>O, 2CH<sub>2</sub>N), 4.05 (*br d*, 1H, J=8.7 Hz, H-5g), 4.50 (d, 1H, J<sub>1,2</sub>=3.0 Hz, H-2m), 4.78 (s, 1H, H-1m), 4.81 (s, 1H, H-1r), 4.92 (1H, H-1g);

<sup>13</sup>C-NMR (CD<sub>3</sub>OD) Characteristic signals: δ=17.7 (CH<sub>3</sub>), 22.4 (CH<sub>3</sub>CON), 26.0 (CH<sub>2</sub>SS), 29.3 (CH<sub>2</sub>SAc), 30.2 (CH<sub>3</sub>COS), 37.6 (CH<sub>2</sub>N), 54.2 (C2m), 71.8 (C5g), 98.9 (C1r), 99.4 (C1g), 100.6 (C1m), 175.42 (CONHAc);

TOF MS ESI (CH<sub>3</sub>OH, positive-ion mode): m/z= 1072.49 (100%) [M+Na]<sup>+</sup>, Calcd for C<sub>45</sub>H<sub>83</sub>N<sub>3</sub>O<sub>20</sub>S<sub>2</sub>, m/z 1049.50 [M].

**Synthesis of 3-[2-acetamido-2-deoxy  $\beta$ -D-mannopyranosyl-(1 $\rightarrow$ 4)- $\alpha$ -D-glucopyranosyl-(1 $\rightarrow$ 2)-  $\alpha,\beta$ -L-rhamnopyranosyloxy]-propyl 1-(23-mercapto-3,6,9,12-tetraoxatricosyl) thiourea **55****

To a solution of S-protected trisaccharide **74** (4.95 mg, 4.71  $\mu$ mol, 1.0 equiv.) in CH<sub>3</sub>OH (500  $\mu$ L, 0.01M) solid CH<sub>3</sub>ONa (0.500 mg, 9.42  $\mu$ mol, 2.0 eq.) was added.



The mixture was stirred at room temperature for 4 hours under Ar atmosphere until <sup>1</sup>H NMR check analysis attested the complete disappearance of starting material. The solvent was evaporated and the crude material was purified by Sephadex LH-20 chromatography using as eluent CH<sub>3</sub>OH/H<sub>2</sub>O 9:1 to afford the trisaccharide conjugate product **55** as a white solid after lyophilization (4.32 mg, 4.28  $\mu$ mol, 90%).

Alpha/beta mixture:

<sup>1</sup>H-NMR (CD<sub>3</sub>OD):  $\delta$ =1.26-1.44 (m, 17H, CH<sub>3</sub>, 7CH<sub>2</sub>), 1.53-1.62 (m, 3.10H, 1.10 CH<sub>2</sub>CH<sub>2</sub>SH, 2 OCH<sub>2</sub>CH<sub>2</sub>), 1.65-1.71 (m, 0.90H, CH<sub>2</sub>CH<sub>2</sub>SS), 1.72-1.82 (m, 2H, OCH<sub>2</sub>CH<sub>2</sub>CH<sub>2</sub>N), 2.03 (s, 3H, NHAc), 2.49 (t, 0.6H, J=7.3 Hz, CH<sub>2</sub>SH) 2.69 (t, 1.4H, J=7.3 Hz, CH<sub>2</sub>SS), 3.25-4.17 (m, 37H, H-2g, H-3g, H-4g, H-5g, 2H-6g, H-2r, H-3r, H-4r, H-5r, H-3m, H-4m, H-5m, 2H-6m, 9CH<sub>2</sub>O, 2CH<sub>2</sub>N), 4.50 (d, 1H, J = 3.7 Hz, H-2m), 4.78 (s, 1H, H-1m), 4.81 (s, 1H, H-1r), 4.91 (H-1g), 5.11 (d, 0.6H, J=3.8 Hz, H-1g $\beta$ );

<sup>13</sup>C-NMR (CD<sub>3</sub>OD):  $\delta$ =18.0 (CH<sub>3</sub>) 22.7 (CH<sub>3</sub>CON), 27.2 (CH<sub>2</sub>), 29.4, 30.3, 30.6, 30.7, 31.3, 39.8, 40.9, 54.9 (C2m), 61.4, 61.9, 66.3, 68.2, 71.1, 71.2, 71.6, 71.9, 72.0, 72.4, 74.1, 74.5, 78.6, 79.8, 80.1, 80.2, 99.2 (C1r $\alpha$ ), 99.5 (C1g $\alpha$ ), 100.6 (C1m), 101.4 (C1g $\beta$ ), 101.9 (C1r $\beta$ ), 174.7 (NCOCH<sub>3</sub>);

TOF MS ESI (CH<sub>3</sub>OH, positive-ion mode): m/z=1030.48 (100%) [M+Na<sup>+</sup>], Calcd for C<sub>43</sub>H<sub>81</sub>N<sub>3</sub>O<sub>19</sub>S<sub>2</sub>, m/z=1007.49 [M].

Alpha anomer:

<sup>1</sup>H-NMR (CD<sub>3</sub>OD):  $\delta$ =1.24-1.39 (m, 17H, CH<sub>3</sub>, 7CH<sub>2</sub>), 1.51-1.61 (m, 2.9H, 0.9 CH<sub>2</sub>CH<sub>2</sub>SH, 2 OCH<sub>2</sub>CH<sub>2</sub>), 1.64-1.70 (m, 1.1H, CH<sub>2</sub>CH<sub>2</sub>SS), 1.72-1.79 (m, 2H, OCH<sub>2</sub>CH<sub>2</sub>CH<sub>2</sub>N), 2.03 (s, 3H, NHAc), 2.46 (t, 0.9H, J=7.3 Hz, CH<sub>2</sub>SH) 2.69 (t, 1.1H, J=7.3 Hz, CH<sub>2</sub>SS), 3.19-3.92 (m, 36H, H-2g, H-3g, H-4g, 2H-6g, H-2r, H-3r, H-4r, H-5r, H-3m, H-4m, H-5m, 2H-6m, 9CH<sub>2</sub>O, 2CH<sub>2</sub>N), 4.02-4.08 (m, 1H, H-5g), 4.51 (d, 1H, J=4.5 Hz, H-2m), 4.78 (d, 1H, J=1.2 Hz, H-1m), 4.81 (s, 1H, H-1r), 4.91 (H-1g);

<sup>13</sup>C-NMR (CD<sub>3</sub>OD): characteristic signals  $\delta$ =18.0 (CH<sub>3</sub>) 22.7 (CH<sub>3</sub>CON), 54.9 (C2m), 99.2 (C1r), 99.5 (C1g), 100.6 (C1m), 174.7 (NCOCH<sub>3</sub>);

TOF MS ESI (CH<sub>3</sub>OH, positive-ion mode): m/z=1030.48 (100%) [M+Na<sup>+</sup>], Calcd for C<sub>43</sub>H<sub>81</sub>N<sub>3</sub>O<sub>19</sub>S<sub>2</sub>, m/z=1007.49 [M].

### 4.6.3 Synthesis and characterization of the glyconanoparticles

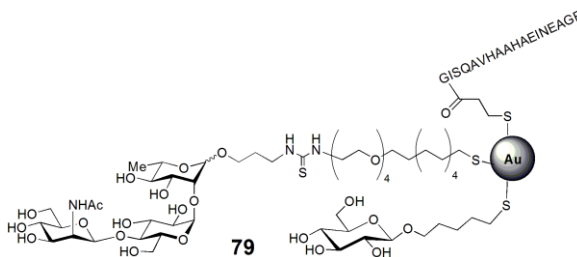
#### General protocol for the preparation of the GNPs

To a 0.012M solution in CH<sub>3</sub>OH of the mixture of the thiol-ending ligands, *e.g.* the trisaccharide related to Pn19F **55**, the tetrasaccharide related to Pn14 **56**, the β-D-glucose **57** and OVA peptide **58** (5 eq.), were added tetrachloroauric acid HAuCl<sub>4</sub> (0.025M in H<sub>2</sub>O, 1 eq.) and sodium borohydride NaBH<sub>4</sub> (1M in H<sub>2</sub>O, 27 eq.) in four portions under vigorous shaking. The black suspension formed was shaken for 2 hours at room temperature. After that, the reaction mixture was diluted with a mixture of HPLC gradient grade H<sub>2</sub>O and CH<sub>3</sub>OH 75/25 v/v and subjected to centrifugal filtering with AMICON 10.000 MWCO (5 min, 10.000 rpm, 10 times). The filtrate phase, which is the volume that pass through the filter containing unreacted ligands, were collected and analyzed by <sup>1</sup>H NMR to verify the conservation of the molar ratio of ligands attached on the gold surface, and eventually use them again to prepare another batch of the same GNP after their purification with Sephadex LH-20 using as eluent CH<sub>3</sub>OH/H<sub>2</sub>O 9:1. On the other hand, the dark concentrated solute, the fraction that does not pass through the membrane containing the GNPs, was purified by dialysis with Slide-A-Lyzer 3.500 MWCO Dialysis Cassette placed in a 2 L beaker full of NANOPURE water under gentle stirring. After changing the water for nine times in three days, the dark solution was freeze-dried to give the GNPs as a dark solid, which can be stored at 4°C for months and redissolved in water prior to use.

For the ligands analysis, proton nuclear magnetic resonance (<sup>1</sup>H NMR) spectra of the initial mixture and of the filtrate phase after GNP formation were recorded and their comparison confirms the expected molar ratio of the components attached on the gold surface of the GNPs prepared. The ratio of the ligands in the GNP was evaluated by integrating the signals of the anomeric protons of the glucopyranosyl unit or the H-2 proton of the mannopyranosyl unit of the trisaccharide **55**, the 4 anomeric protons of tetrasaccharide **56** which collapse in an unique signal, the anomeric proton of glucoside **57** and the methyl groups of isoleucine and valine of OVA<sub>323-339</sub> peptide conjugate **58**.

**Pn19F/Glc/OVA (45:50:5) GNP 79**

A mixture of thiol-ending trisaccharide 19F **55** (0.960 mg, 0.952  $\mu\text{mol}$ , 9 eq.),  $\beta$ -D-glucose conjugate **57** (0.299 mg, 1.050  $\mu\text{mol}$ , 10 eq.), and OVA peptide **58** (0.203 mg, 0.105  $\mu\text{mol}$ , 1 eq.) in MeOH (175  $\mu\text{L}$ , 0.012M) was prepared.  $\text{HAuCl}_4$  (16.80  $\mu\text{L}$ , 0.421  $\mu\text{mol}$ , 0.025M in  $\text{H}_2\text{O}$ , 1eq.) and sodium borohydride  $\text{NaBH}_4$  (11.40  $\mu\text{L}$ , 11.378  $\mu\text{mol}$ , 1M in  $\text{H}_2\text{O}$ , 27 eq.) were added to afford 378  $\mu\text{g}$  of GNP **79**.



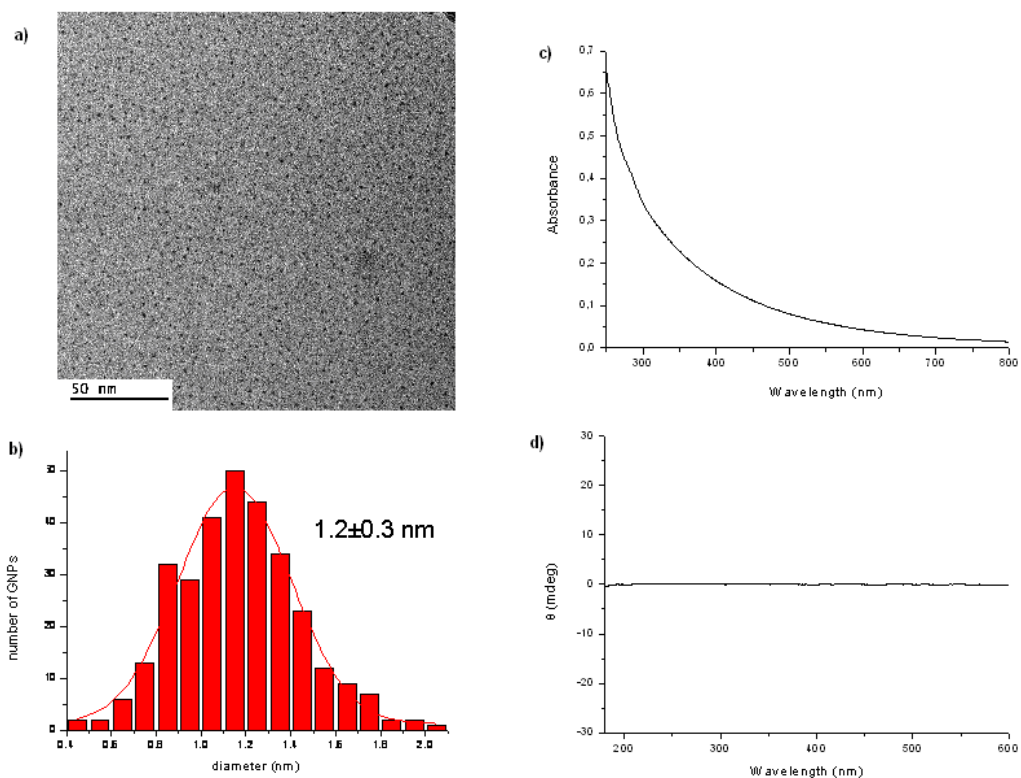
TEM (average diameter):  $1.2 \pm 0.3$  nm;

Average molecular formula estimated based on the size of the cluster obtained from TEM micrographs:  $\text{Au}_{79}(\text{C}_{43}\text{H}_{80}\text{N}_3\text{O}_{19}\text{S}_2)_{17}(\text{C}_{11}\text{H}_{21}\text{O}_6\text{S})_{19}(\text{C}_{79}\text{H}_{126}\text{N}_{27}\text{O}_{27}\text{S})_2 \sim 41.8$  kDa;

UV/Vis ( $\text{H}_2\text{O}$ ,  $c=0.10$  mg/mL): surface plasmon band not observed;

CD ( $\text{H}_2\text{O}$ ,  $c=0.25$  mg/mL): circular dichroism not observed;

$^1\text{H}$  qNMR (500MHz,  $\text{D}_2\text{O}$ ): 160  $\mu\text{g}$  of GNP were dissolved in 180  $\mu\text{L}$  of  $\text{D}_2\text{O}$  and 20  $\mu\text{L}$  of  $\text{D}_2\text{O}$  containing 0.05 wt.% TPS were added. 13.65 nmol of trisaccharide conjugate were found.



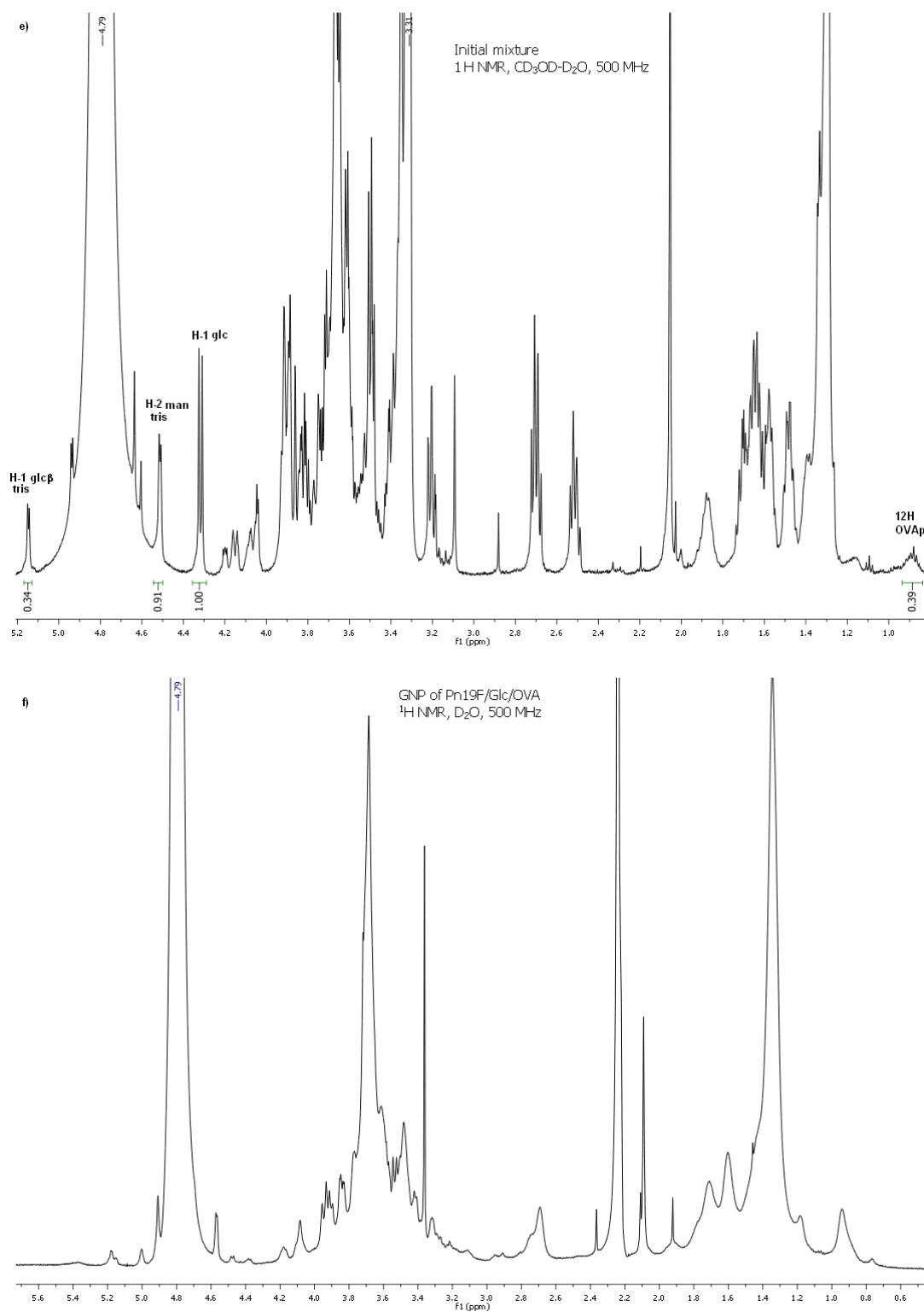
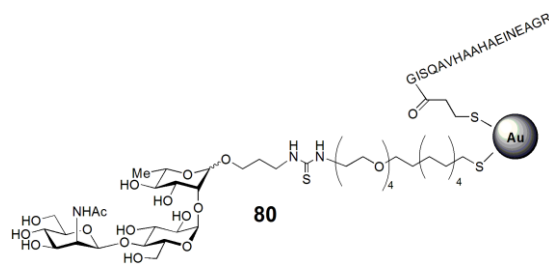


**Figure 4.17:** (a) TEM micrographs and (b) histograms of size distribution, (c) UV/Vis adsorption and (d) circular dichroism spectra of gold GNPs **79**. (e)  $^1\text{H}$  NMR spectrum (500MHz,  $\text{CD}_3\text{OD}:\text{D}_2\text{O}$  5:1) of the mixture used to prepare GNP and (f)  $^1\text{H}$  NMR spectrum (500MHz,  $\text{D}_2\text{O}$ ) of GNP **79** obtained. Integration of selected signals shows that the ratio between trisaccharide **55**, glucose conjugate **57** and OVAp **58** is about 45:50:5.

**Pn19F/OVA (95:5) GNP 80**

A mixture of thiol-ending trisaccharide 19F **55** (1.400 mg, 1.390  $\mu\text{mol}$ , 19 eq.) and OVA peptide **58** (0.140 mg, 0.073  $\mu\text{mol}$ , 1 eq.) in MeOH (122  $\mu\text{L}$ , 0.012M) was prepared.  $\text{HAuCl}_4$  (11.70  $\mu\text{L}$ , 0292  $\mu\text{mol}$ , 0.025M in  $\text{H}_2\text{O}$ , 1eq.) and sodium borohydride  $\text{NaBH}_4$  (7.90  $\mu\text{L}$ , 7.90  $\mu\text{mol}$ , 1M in  $\text{H}_2\text{O}$ , 27 eq.) were added to afford 336  $\mu\text{g}$  of GNP **80**.



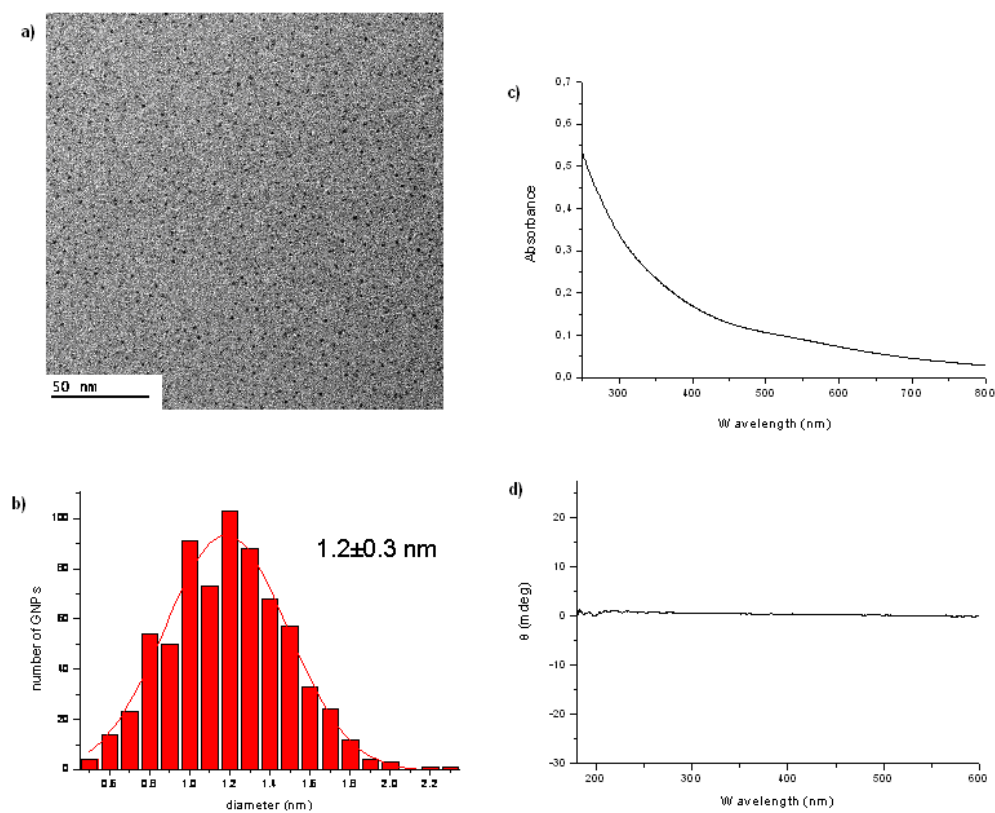
TEM (average diameter):  $1.2 \pm 0.3$  nm;

Average molecular formula estimated based on the size of the cluster obtained from TEM micrographs:  $\text{Au}_{79}(\text{C}_{43}\text{H}_{80}\text{N}_3\text{O}_{19}\text{S}_2)_{36}(\text{C}_{79}\text{H}_{126}\text{N}_{27}\text{O}_{27}\text{S})_2 \sim 55.6$  KDa;

UV/Vis ( $\text{H}_2\text{O}$ ,  $c=0.10$  mg/mL): surface plasmon band not observed;

CD ( $\text{H}_2\text{O}$ ,  $c=0.25$  mg/mL): circular dichroism not observed;

$^1\text{H}$  qNMR (500MHz,  $\text{D}_2\text{O}$ ): 160  $\mu\text{g}$  of GNP were dissolved in 180  $\mu\text{L}$  of  $\text{D}_2\text{O}$  and 20  $\mu\text{L}$  of  $\text{D}_2\text{O}$  containing 0.05 wt.% TPS were added. 10.40 nmol of trisaccharide conjugate were found.



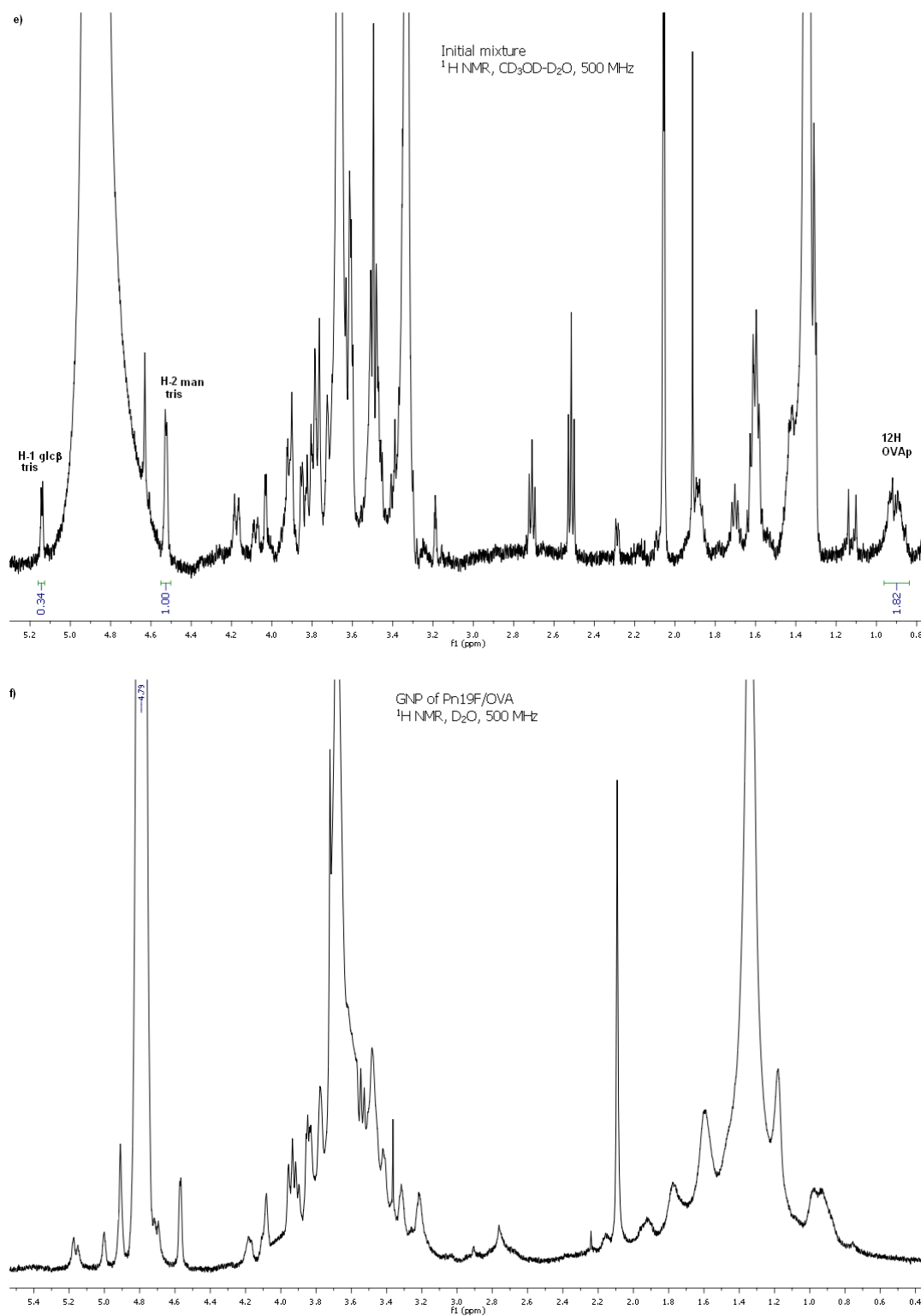
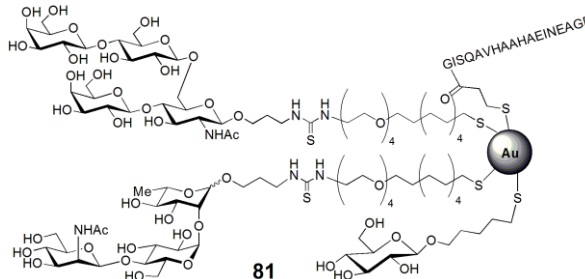


**Figure 4.18:** (a) TEM micrographs and (b) histograms of size distribution, (c) UV/Vis adsorption and (d) circular dichroism spectra of gold GNPs **80**. (e)  $^1\text{H}$  NMR spectrum (500MHz,  $\text{CD}_3\text{OD}:\text{D}_2\text{O}$  5:1) of the mixture used to prepare GNP and (f)  $^1\text{H}$  NMR spectrum (500MHz,  $\text{D}_2\text{O}$ ) of GNP **80** obtained. Integration of selected signals shows that the ratio between trisaccharide **55** and OVAp **58** is about 95:5.



**Pn19F/Pn14/Glc/OVA (40:40:15:5) GNP 81**

A mixture of thiol-ending trisaccharide 19F **55** (1.300 mg, 1.290  $\mu\text{mol}$ , 8 eq.), tetrasaccharide thiol-ending tetrasaccharide 14 **56\*** (1.530 mg, 1.290  $\mu\text{mol}$ , 8 eq.),  $\beta$ -D-glucose conjugate **57** (0.147 mg, 0.520  $\mu\text{mol}$ , 3 eq.), and OVA peptide **58** (0.334 mg, 0.174  $\mu\text{mol}$ , 1 eq.) in MeOH (273  $\mu\text{l}$ ,



0.012M) was prepared.  $\text{HAuCl}_4$  (26.20  $\mu\text{l}$ , 0.655  $\mu\text{mol}$ , 0.025M in  $\text{H}_2\text{O}$ , 1 eq.) and sodium borohydride  $\text{NaBH}_4$  (17.7  $\mu\text{l}$ , 17.7  $\mu\text{mol}$ , 1M in  $\text{H}_2\text{O}$ , 27 eq.) were added to afford 770  $\mu\text{g}$  of GNP **81**.

\*Tetrasaccharide amino-hydroxypropyl  $\beta$ -D-galactopyranosyl-(1 $\rightarrow$ 4)- $\beta$ -D-glucopyranosyl-(1 $\rightarrow$ 6)-[ $\beta$ -D-glucopyranosyl-(1 $\rightarrow$ 4)]-2-acetamido-2-deoxy-D-glucopyranoside was provided by Dr. Martina Lahmann, School of Chemistry, Bangor University, Bangor, UK. The thiol-ending derivative was synthesized following synthetic procedure reported.<sup>133</sup>

TEM (average diameter): 1.2 $\pm$ 0.3 nm;

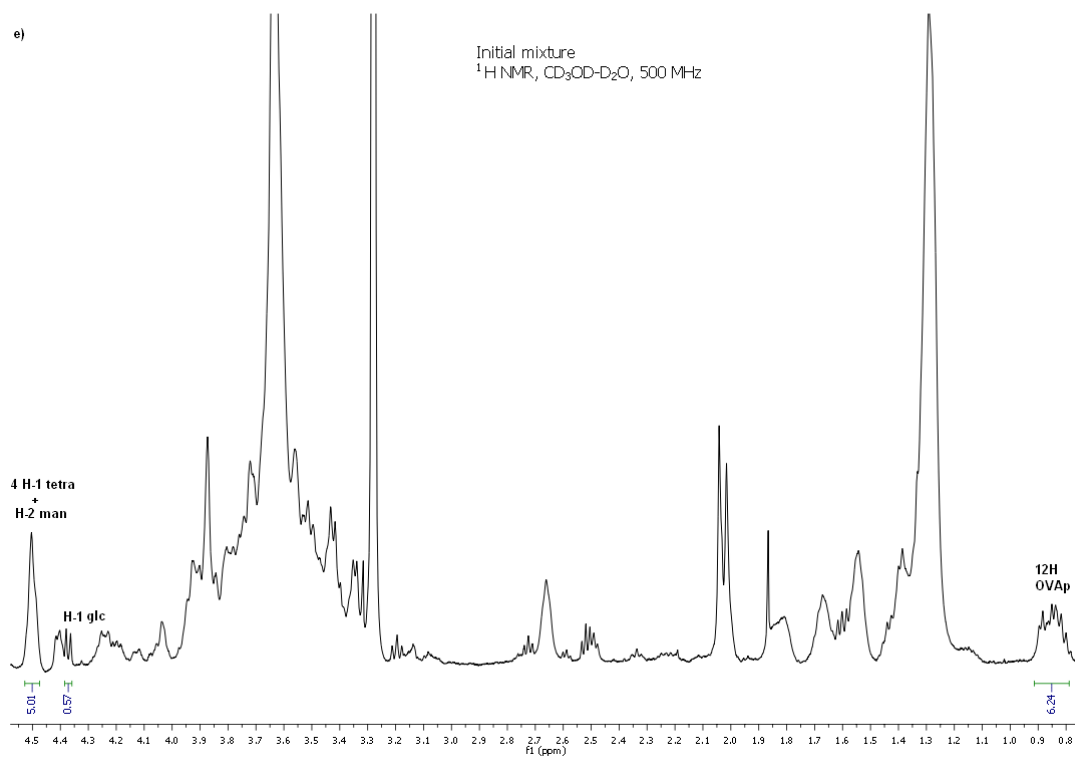
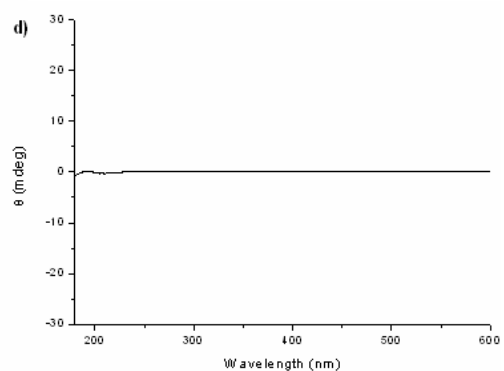
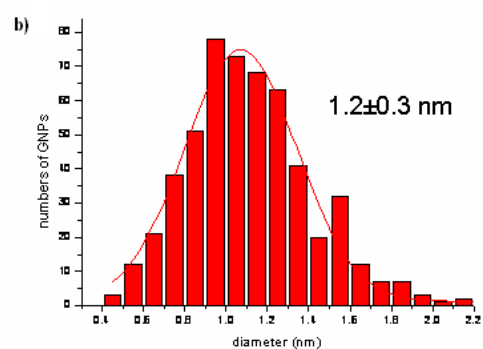
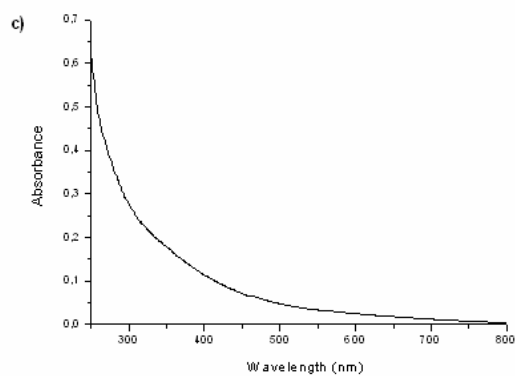
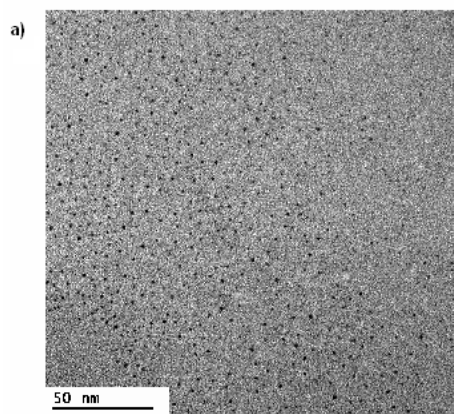
Average molecular formula estimated based on the size of the cluster obtained from TEM micrographs:

$\text{Au}_{79} (\text{C}_{43}\text{H}_{80}\text{N}_3\text{O}_{19}\text{S}_2)_{15} (\text{C}_{49}\text{H}_{90}\text{N}_3\text{O}_{25}\text{S}_2)_{15} (\text{C}_{11}\text{H}_{21}\text{O}_6\text{S})_6 (\text{C}_{79}\text{H}_{126}\text{N}_{27}\text{O}_{27}\text{S})_2 \sim 53.9 \text{ Kda}$ ;

UV/Vis ( $\text{H}_2\text{O}$ ,  $c=0.10 \text{ mg/mL}$ ): surface plasmon band not observed;

CD ( $\text{H}_2\text{O}$ ,  $c=0.25 \text{ mg/mL}$ ): circular dichroism not observed;

$^1\text{H}$  qNMR (500MHz,  $\text{D}_2\text{O}$ ): 372  $\mu\text{g}$  of GNP were dissolved in 180  $\mu\text{L}$  of  $\text{D}_2\text{O}$  and 20  $\mu\text{L}$  of  $\text{D}_2\text{O}$  containing 0.05 wt.% TPS were added. 37.70 nmol of trisaccharide conjugate and 38.35 nmol of tetrasaccharide conjugate were found.



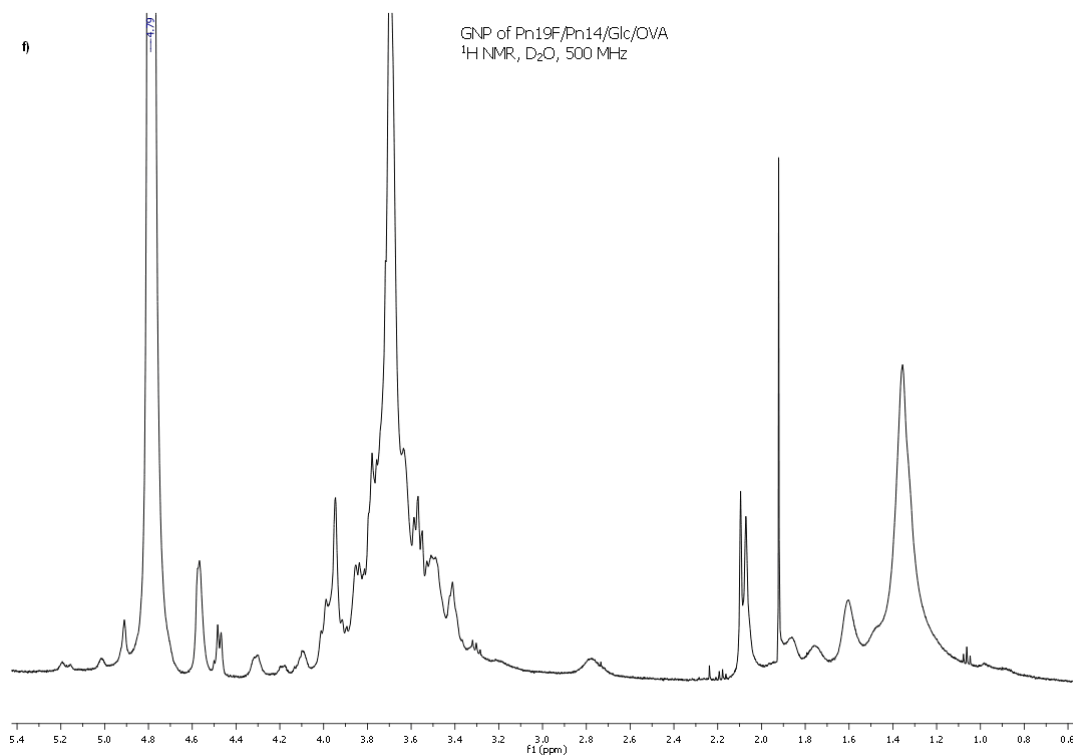
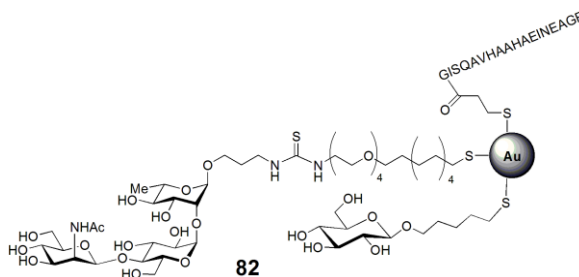


**Figure 4.19:** (a) TEM micrographs and (b) histograms of size distribution, (c) UV/Vis adsorption and (d) circular dichroism spectra of gold GNPs **81**. (e)  $^1\text{H}$  NMR spectrum (500MHz,  $\text{CD}_3\text{OD}:\text{D}_2\text{O}$  5:1) of the mixture used to prepare GNP and (f)  $^1\text{H}$  NMR spectrum (500MHz,  $\text{D}_2\text{O}$ ) of GNP **81** obtained. Integration of selected signals shows that the ratio between trisaccharide **55**, tetrasaccharide **56**, glucose conjugate **57** and OVAp **58** is 40:40:15:5.

**Pn19F $\alpha$ /Glc/OVA (45:50:5) GNP 82**

A mixture of thiol-ending trisaccharide 19F **55a** (0.732 mg, 0.726  $\mu$ mol, 9 eq.),  $\beta$ -D-glucose conjugate **57** (0.228 mg, 0.807  $\mu$ mol, 10 eq.) and OVA peptide **58** (0.155 mg, 0.0807  $\mu$ mol, 1 eq.) in MeOH (135  $\mu$ l, 0.012M) was prepared. HAuCl<sub>4</sub> (12.90  $\mu$ l, 0.323  $\mu$ mol, 0.025M in H<sub>2</sub>O, 1 eq.) and sodium borohydride NaBH<sub>4</sub> (8.80  $\mu$ l, 8.713  $\mu$ mol, 1M in H<sub>2</sub>O, 27 eq.) were added to afford 504  $\mu$ g of GNP **82**.

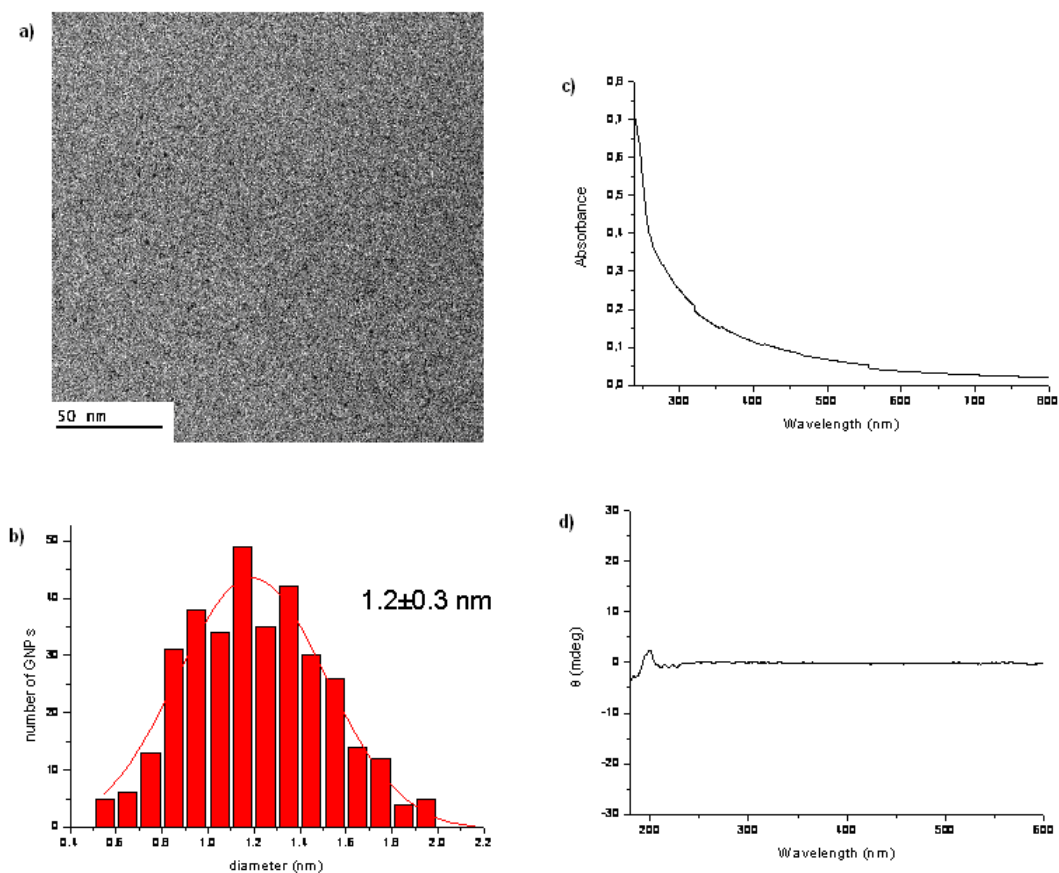


TEM (average diameter): 1.2 $\pm$ 0.3 nm;

Average molecular formula estimated based on the size of the cluster obtained from TEM micrographs: Au<sub>79</sub>(C<sub>43</sub>H<sub>80</sub>N<sub>3</sub>O<sub>19</sub>S<sub>2</sub>)<sub>17</sub>(C<sub>11</sub>H<sub>21</sub>O<sub>6</sub>S)<sub>19</sub>(C<sub>79</sub>H<sub>126</sub>N<sub>27</sub>O<sub>27</sub>S)<sub>2</sub> ~41.8 KDa;

UV/Vis (H<sub>2</sub>O, c=0.10 mg/mL): surface plasmon band not observed;

CD (H<sub>2</sub>O, c=0.25 mg/mL): only a small signal is evident;



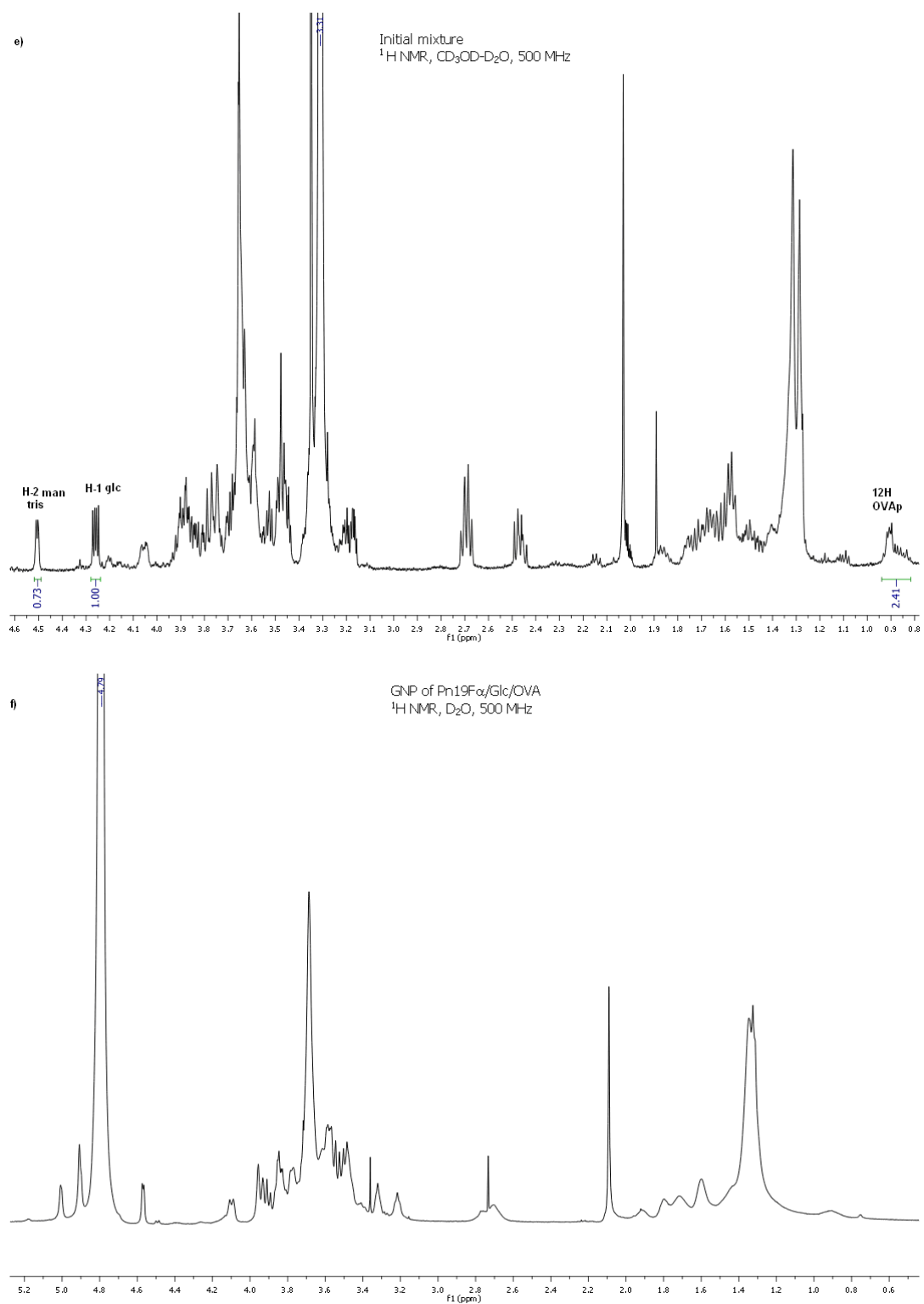


**Figure 4.20:** (a) TEM micrographs and (b) histograms of size distribution, (c) UV/Vis adsorption and (d) circular dichroism spectra of gold GNPs **82**. (e)  $^1\text{H}$  NMR spectrum (500 MHz,  $\text{CD}_3\text{OD}:\text{D}_2\text{O}$  5:1) of the mixture used to prepare GNP and (f)  $^1\text{H}$  NMR spectrum (500 MHz,  $\text{D}_2\text{O}$ ) of GNP **82** obtained. Integration of selected signals shows that the ratio between trisaccharide **55**, glucose conjugate **57** and OVAp **58** is 45:50:5.

#### 4.6.4 Immunization studies

The mouse immunization study was approved by the Animal Care and Use Committee of PT. Bimana Indomedical, Bogor, Indonesia. Inbred 6-week-old female BALB/c mice were maintained at the Animal Laboratory of PT. Bimana Indomedical, Bogor, Indonesia.

Five mice per group were immunized intradermal with 6.0 µg of GNPs containing approximately 2.4 µg of antigen per dose in mixture with 20 µg of *Quil-A*<sup>®</sup> saponin adjuvant (A gift from Dr. Erik B. Lindblad and Brenntag Biosector, Denmark).<sup>133,95</sup>

PCV13 vaccines (13-valent pneumococcal conjugate vaccine, Pfizer, Inc.) were commercially acquired and were diluted in saline 1:10 (100 µl per mouse)<sup>150</sup> and saline (0.9% [wt/vol] NaCl in water) were used as positive and negative control respectively. A booster of 6 µg of GNPs antigen was given on day 35 without adjuvant. Blood samples were taken one week after the booster immunization.

#### 4.6.5 Enzyme-linked immunosorbent assay

The enzyme-linked immunosorbent assay (ELISA) was performed to measure the antibodies to native Pn14 PS and to Pn19F PS at the Eijkman Institute for Molecular Biology, Jakarta, Indonesia as described previously.<sup>133</sup>

Briefly, serially diluted sera were incubated for 1 h at 37 °C in flat-bottom plates, coated with 100 µl of purified Pn14 PS or Pn19F PS (5 µg/mL).

After coating the plates were blocked with 3% gelatin, then washed and horseradish peroxidase-conjugated goat anti-mouse IgG was added and incubated for 1 h at 37°C. A ready-to-use TMB substrate was added to visualize the amount of bound peroxidase. The reaction was stopped by the addition of 0.5 M H<sub>2</sub>SO<sub>4</sub>. Optical density (OD) values were obtained with a micro-titer plate spectrophotometer at 450 nm. Antibody titers were expressed as the log<sub>10</sub> of the dilution giving twice the OD obtained for control mice.

#### 4.6.6 GNP-ELISA

GNP-ELISA was performed to measure the antibodies towards gold nanoparticles in sera of mice immunized at the Eijkman Institute for Molecular Biology, Jakarta, Indonesia following a reported procedure.<sup>149</sup>

50 µL of a 25µg/mL in sodium buffer solution (50 mM, pH 9.7) of GNPs **83** or **78**, were used to coat the Nunc MaxiSorp plate. After discarding the GNPs solutions and

washing 2 times with 200  $\mu$ L of PBS (Phosphate buffered saline) solution (10mM, pH=7.4), the wells were blocked with 200 $\mu$ L of 1% BSA in PBS at room temperature for 30 min. The blocking solution was discarded and 100 $\mu$ L of mice pool serum at different dilution in assay buffer (0.5% BSA) were added to the plate. After shaking for 1 h at 500rpm, the wells were washed with PBS (3x200 $\mu$ L) and then 100  $\mu$ L of anti-mouse IgG horseradish peroxidase was added for mice serum IgG detection. After 30 min of shaking at 500 rpm, the wells were washed with PBS (3x200 $\mu$ L) and, finally, a ready-to-use TMB substrate was added to visualize the amount of bound peroxidase. The reaction was stopped by the addition of 0.5 M  $H_2SO_4$ . The optical density was measured at 450 nm in an ELISA reader. Antibody titers were expressed as the log<sub>10</sub> of IgG titer.

## Bibliography

1. Manning, G., Whyte, D.B., Martinez, R., Hunter, T., Sudarsanam, S., The Protein Kinase Complement of the Human Genome. *Science* **2002**, *298*, 1912-1934.
2. Cohen, P., Protein kinases—the major drug targets of the twenty-first century? *Nat. Rev. Drug Discov.* **2002**, *1*, 309–315.
3. Lapenna, S., Giordano, A., Cell cycle kinases as therapeutic targets for cancer. *Nat. Rev. Drug Discov.* **2009**, *8*, 547-566.
4. Brazil, D.P., Hemmings, B.A., Ten years of protein kinase B signalling: a hard Akt to follow. *Trends Biochem. Sci.* **2001**, *26*, 657-664.
5. Nicholson, K.M., Anderson, N.G., The protein kinase B/Akt signalling pathway in human malignancy. *Cellular Signalling* **2002**, *14*, 381–395.
6. Stambolic, V., Woodgett, J.R., Functional distinctions of protein kinase B/Akt isoforms defined by their influence on cell migration. *Trends Cell Biol.* **2006**, *16*, 461-466.
7. Sale, E.M., Sale, G.J., Protein kinase B: signalling roles and therapeutic targeting. *Cell. Mol. Life Sci.* **2008**, *65*, 113-127.
8. Calleja, V., Laguerre, M., Parker, P. J., Larijani, B., Role of a Novel PH-Kinase Domain Interface in PKB/Akt Regulation: Structural Mechanism for Allosteric Inhibition. *PLoS Biology* **2009**, *7*, 189-200.
9. Manning, B.D., Cantley, L.C., Akt/PKB signalling: navigating downstream. *Cell* **2007**, *129*, 1261-1274.
10. Hanada, M., Feng, J., Hemmings, B.A., Structure, regulation and function of PKB/Akt—a major therapeutic target. *Biochim. Biophys. Acta* **2004**, *11*, 3-16.
11. Leslie, N.R., Batty, I.H., Maccario, H., Davidson, L., Downes, C.P., Understanding PTEN regulation: PIP2, polarity and protein stability. *Oncogene* **2008**, *27*, 5464–5476.
12. Pestell, R.G., Albanese, C., Reutens, A.T., Segall, J.E., Lee, R.J., Arnold, A., The cyclin and cyclin-dependent kinase inhibitors in hormonal regulation of proliferation and differentiation. *Endocr. Rev.* **1999**, *20*, 501-534.
13. Zhou, B.P., Liao, Y., Xia, W., Spohn, B., Lee, M.H., Hung, M.C., Cytoplasmic localization of p21Cip1/WAF1 by Akt-induced phosphorylation in HER-2/neu-overexpressing cells. *Nat. Cell. Biol.* **2001**, *3*, 245-252.
14. Maddika, S., Sande, S.R., Wiechec, E., Hansen, L.L., Wesselborg, S., Los, M., Akt-mediated phosphorylation. *J. Biol. Chem.* **2004**, *279*, 35510-35517.
15. Kandel, E.S., Skeen, J., Majewski, N., Di Cristofano, A., Pandolfi, P.P., Feliciano, C.S., Gartel A., Hay, N., Activation of Akt/Protein Kinase B overcomes a G2/M cell cycle checkpoint induced by DNA damage. *Mol. Cell. Biol.* **2002**, *22*, 7831-7841.
16. Baldin, V., Theis-Febvre, N., Benne, C., Froment, C., Cazales, M., Burlet-Schiltz, O., Ducommun, B., PKB/Akt phosphorylates the CDC25B phosphatase and regulates its intracellular localisation. *Biol. Cell.* **2003**, *95*.
17. Datta, S.R., Brunet, A., Greenberg, M.E., Cellular survival: a play in three Akts. *Genes Dev.* **1999**, *13*, 2905-2927.
18. Basu, S., Totty, N.F., Irwin, M.S., Sudol, M., Downward, J., Akt phosphorylates the Yes-associated protein, YAP, to induce interaction with 14-3-3 and attenuation of p73-mediated apoptosis. *Mol. Cell* **2003**, *11*, 11-23.
19. Altomare, D.A., Testa, J.R., Perturbations of the AKT signaling pathway in human cancer. *Oncogene* **2005**, *24*, 7455-7464.



20. Lo Piccolo, J., Blumenthal, G.M., Bernstein, W.B., Dennis, P.A., Targeting the PI3K/Akt/mTOR pathway: effective combinations and clinical considerations. *Drug Resist. Updat.* **2008**, *11*, 32-50.
21. Wang, Y., Hou, P., Yu, H., Wang, W., Ji, M., Zhao, S., Yan, S., Sun, X., Liu, D., Shi, B., Zhu, G., Condouris, S., Xing, M., High prevalence and mutual exclusivity of genetic alterations in the phosphatidylinositol-3-kinase/Akt pathway in thyroid tumors. *J. Clin. Endocrinol. Metab.* **2007**, *92*, 2387-2390.
22. Hou, P., Liu, D., Shan, Y., Hu, S., Studeman, K., Condouris, S., Wang, Y., Trink, A., El-Naggar, A.K., Tallini, G., Vasko, V., Xing, M., Genetic alteration and their relationship in the phosphatidylinositol 3-kinase/Akt pathway in thyroid cancer. *Clin. Cancer Res.* **2007**, *13*, 1161-1170.
23. Larue, L., Bellacosta, A., Epithelial-mesenchymal transition in development and cancer: role of phosphatidylinositol 3 kinase/AKT pathways. *Oncogene* **2005**, *24*, 7443-7454.
24. Samuels, Y., Ericson, K., Oncogenic PI3K and its role in cancer. *Curr. Opin. Oncol.* **2006**, *18*, 77-82.
25. Karar, J., Maity, A., PI3K/AKT/mTOR pathway in angiogenesis. *Front. Mol. Neurosci.* **2011**, *4*, 51.
26. Emerling, B.M., Weinberg, F., Liu, J.L., Mak, T.W., Chandel, N.S., PTEN regulates p300-dependent hypoxia-inducible factor 1 transcriptional activity through Fork-head transcription factor 3a (FOXO 3a). *Proc. Natl. Acad. Sci.* **2008**, *105*, 2622-2627.
27. Benedetti, V., Perego, P., Beretta, G., Corna, E., Tinelli, S., Righetti, S., Leone, R., Apostoli, P., Lanzi, C., Zunino, F., Modulation of survival pathways in ovarian carcinoma cell lines resistant to platinum compounds. *Mol. Cancer Ther.* **2008**, *7* (3), 679-687.
28. Collins, I., Caldwell, J., Fonseca, T., Donald, A., Bavetsias, V., Hunter, L.J.K., Garrett, M.D. *et al.*, Structure-based design of isoquinoline-5-sulfonamide inhibitors of protein kinase B. *Bioorg. Med. Chem.* **2006**, *14*, 1255-1273.
29. Luo, Y., Shoemaker, A.R., Liu, X., Woods, K.W., Thomas, S.A., de Jong, R., Han, E.K., Li, T., Stoll, V.S., Powlas, J.A., Oleksijew, A., Mitten, M.J., Shi, Y., Guan, R., McGonigal, T.P., Klinghofer, V., Johnson, E.F., Levenson, J.D., *et al.*, Potent and selective inhibitors of Akt kinases slow the progress of tumors *in vivo*. *Mol. Cancer Ther.* **2005**, *4*, 977-986.
30. Heerding, D.A., Rodhes, N., Leber, J.D., Clark, T.J., Keenan, R.M., LaFrance, L.V., Li, M. *et al.*, Identification of 4-(2-(4-amino-1,2,5-oxadiazol-3-yl)-1-ethyl-7-[(3S)-3-piperidinylmethyl]oxy)-1H-imidazo[4,5-c]pyridin-4-yl)-2-methyl-3-butyn-2-ol (GSK690693), a novel inhibitor of AKT kinase. *J. Med. Chem.* **2008**, *51*, 5663-5679.
31. Saxty, G., Woodhead, S.J., Berdini, V., Davies, T.G., Verdonk, M.L., Wyatt, P.G., Boyle, R.G., Barford, D., Downham, R., Garrett, M.D., Carr, R.A, Identification of inhibitors of protein kinase B using fragment-based lead discovery. *J. Med. Chem.* **2007**, *50*, 2293-2296.
32. Altomare, D., Zhang, L., Deng, J., Di Cristofano, A., Klein-Szanto, A.J., Kumar, R., Testa, J.R., GSK690693 Delays Tumor Onset and Progression in Genetically Defined Mouse Models Expressing Activated Akt, *Clin. Cancer Res.* **2010**, *16*, 486-496.
33. Luo Y., Shoemaker, A.R., Liu, X.S., Woods, K.W., Thomas, S.A., de Jong, R., Han, E.K. *et al.*, Potent and selective inhibitors of AKT kinases slow the progress of tumors *in vivo*. *Mol. Cancer Ther.* **2005**, *4*, 977-986.
34. Arcaro, A., Wymann, M.P., Wortmannin is a potent phosphatidylinositol 3-kinase inhibitor: the role of phosphatidylinositol 3,4,5-trisphosphate in neutrophil responses. *Biochem. J.* **1993**, *296*, 297-301.
35. Bedogni, B., O'Neill, M., Welford, S., Bouley, D., Giaccia, A., Denko, N., Powell, M., Topical treatment with inhibitors of the phosphatidylinositol 3'-kinase/akt and raf/mitogen-activated protein kinase kinase/extracellular signal-regulated kinase pathways reduces

melanoma development in severe combined immunodeficient mice. *Cancer Research* **2004**, *64* (7), 2552-2560.

36. Lindsley, C.W., Zhao, Z., Leister, W.H., Robinson, R.G., Barnett, S.F., Defeo-Jones, D., Jones, R.E., Hartman, G.D., Huff, J.R., Huber, H.E., Duggan, M.E., Allosteric Akt (PKB) inhibitors: discovery and SAR of isozyme selective inhibitors. *Bioorg. Med. Chem. Lett.* **2005**, *15*, 761-764.

37. Zhao, Z., Leister, W.H., Robinson, R.G., Barnett, S.F., Defeo-Jones, D., Jones, R.E., Hartman, G.D., Huff, J.R., Huber, H.E., Duggan, M.E., Lindsley, C.W., Discovery of 2,3,5-trisubstituted pyridine derivatives as potent Akt1 and Akt2 dual inhibitors. *Bioorg. Med. Chem. Lett.* **2005**, *15*, 905-909.

38. Zhao, Z., Robinson, R.G., Barnett, S.F., Defeo-Jones, D., Jones, R.G., Hartman, G.D., Huber, H.E., Duggan, M.E., Lindsley, C.W., Development of potent, allosteric dual Akt1 and Akt2 inhibitors with improved physical properties and cell activity. *Bioorg. Med. Chem. Lett.* **2008**, 49-53.

39. Hirai, K., Sootome, H., Nakatsuru, Y., Miyama, K., Taguchi, S., Tsujioka, K., Ueno, Y., Hatch, H., Majumder, P.K., Pan, B.-S., Kotani, H., MK-2206, an Allosteric Akt Inhibitor, Enhances Antitumor Efficacy by Standard Chemotherapeutic Agents or Molecular Targeted Drugs *In vitro* and *In vivo*. *Mol. Cancer Ther.* **2010**, *9*, 1956-1967.

40. Rong, S.-B., Hu, Y., Enyedy, I., Powis, G., Meuillet, E.J., Wu, X., Wang, R., Wang, S., Kozikowski, A.P., Molecular Modelling studies of the Akt PH Domain and Its Interaction with Phosphoinositides. *J. Med. Chem.* **2001**, *44*, 898-908.

41. Meuillet, E. J., Novel inhibitors of AKT: assessment of a different approach targeting the pleckstrin homology domain. *Curr. Med. Chem.* **2011**, *18*, 2727-2742.

42. Kozikowski, A. P., Qiao, L., Tiickmantel, W., Powis, G., Synthesis of 1D-3-Deoxy- and -2,3-Dideoxyphosphatidylinositol *Tetrahedron* **1997**, *53*, 14903-14914.

43. Kozikowski, A.P., Tückmantel, W., Powis, G., Synthesis and Biological Activity of D-3-Deoxy-3-Fluorophosphatidylinositol—A New Direction in the Design of non-DNA Targeted Anticancer Agents. *Angewandte Chemie International Ed. English* **1992**, *31*, **1379-1381**.

44. Hu, Y., Meuillet, E.J., Berggren, M., Powis, G., Kozikowski, A.P., 3-Deoxy-3-substituted-D-myo-inositol Imidazolyl Ether Lipid Phosphates and Carbonate as Inhibitors of the Phosphatidylinositol 3-Kinase Pathway and Cancer Cell Growth. *Bioorg. Med. Chem. Lett.* **2001**, *11*, 173-176.

45. Meuillet, E.J., Mahadevan, D., Vankayalapati, H., Berggren, M., Williams, R., Coon, A., Kozikowski, A.P., Powis, G., Specific Inhibition of the Akt1 Pleckstrin Homology Domain by D-3-Deoxy-Phosphatidyl- myo-Inositol Analogues. *Mol. Cancer Ther.* **2003**, *2*, 389-399.

46. Piccolo, E., Vignati, S., Maffucci, T., Innominato, P.F., Riley, A.M., Potter, B.V.L., Pandolfi, P.P., Broggin, M., Iacobelli, S., Innocenti, P., Falasca, M., Inositol pentakisphosphate promotes apoptosis through the PI3K/Akt pathway. *Oncogene* **2004**, *23*, 1754-1765.

47. Maffucci, T., Piccolo, E., Cumashi, A., Iezzi, M., Riley, A.M., Saiardi, A., Godage, H.Y., Rossi, C., Broggin, M., Iacobelli, S., Potter, B.V.L., Innocenti, P., Falasca, M., Inhibition of the phosphatidylinositol 3-kinase/Akt Pathway by Inositol Pentakisphosphate Results in Antiangiogenic and antitumor Effects. *Cancer Research* **2005**, *65*, 8339.

48. Cipolla, L., Redaelli, C., Granucci, F., Zampella, G., Zaza, A., Chisci, R., Nicotra, F., Straightforward synthesis of novel Akt inhibitors based on a glucose scaffold. *Carbohydrate Research* **2010**, *345*, 1291-1298.

49. Benning, C., Biosynthesis and function of the sulfolipid sulfoquinovosyl diacylglycerol. *Annu. Rev. Plant Physiol. Plant Mol Biol* **1998**, *49*, 53-75.

50. Dangate, M., Franchini, L., Ronchetti, F., Arai, T., Iida, A., Tokuda, H., Colombo, D., 2-O-beta-D-Glucopyranosyl-sn-glycerol based analogues of sulfoquinovosyl diacylglycerol

(SQDG) and their role in inhibiting Epstein-Barr virus early antigen activation. *Bioorg. Med. Chem.* **2009**, *17*, 5968-5973.

51. Holzl, G., Dormann, P., Structure and function of glycolipids in plants and bacteria. *Progress in Lipid Research* **2007**, *46*, 225–243.

52. Fontaine, T., Lamarre, C., Simenel, C., Lambou, K., Coddeville, B., Delepierre, M., Latgé, J.P., Characterization of glucuronic acid containing glycolipid in *Aspergillus fumigatus* mycelium. *Carbohydr. Res.* **2009**, *344*, 1960–1967.

53. Eichenberger, W., Gribi, C., Lipids of a Pavlova lutheri: cellular site and metabolic role of DGCC. *Phytochemistry* **1997**, *45*, 1561-1567.

54. Okazaki, Y., Otsuki, H., Narisawa, T., Kobayashi, M., Sawai, S., Kamide, Y., Kusano, M., Aoki, T., Hirai, M.Y., Saito, K., A new class of plant lipid is essential for protection against phosphorus depletion. *Nat. Commun* **2013**, *4*, 1510.

55. Semeniuk, A., Sohlenkamp, C., Duda, K., Hölzl, G., A Bifunctional Glycosyltransferase from *Agrobacterium tumefaciens* Synthesizes Monoglucosyl and Glucuronosyl Diacylglycerol under Phosphate Deprivation. *J. Biol. Chem.* **2014**, *289*, 10104-10114.

56. Zhang, Z., Liao, H., Lucas, W.J., Molecular mechanisms underlying phosphate sensing, signaling, and adaptation in plants. *J. Integr. Plant Biol.* **2014**, *53*, 192–220.

57. Shaikh, N., Colombo, D., Ronchetti, F., Dangate, M., SQAGs: A stepping stone in the biotic world. *Comptes Rendus Chimie* **2013**, *16*, 850-862.

58. Colombo, D., Ronchetti, F., Scala, A., Taino, I.M., Albin F.M., Toma, L., Regiodiastereoselective and Diastereoselective Lipase-catalyzed preparation of acetylated 2-O-glucosylglycerols. *Tetrahedron-Asymmetr.* **1994**, *5*, 1377-1384.

59. Manzo, E., Ciavatta, M.L., D. Pagano, D., Fontana, A., An efficient and versatile chemical synthesis of bioactive glyco-glycerolipids. *Tetrahedron Lett* **2012**, *53*, 879–881.

60. Colombo, D., Ronchetti, F., Scala, A., Taino, I., Toma, L., A facile lipase catalyzed access to fatty acid monoesters of 2-O-beta-D-glucosylglycerol. *Tetrahedron-Asymmetry* **1996**, *7* (3), 771-777.

61. Adasch, V., Hoffmann, B., Milius, W., Platz, G., Voss, G., Preparation of alkyl alpha- and beta-D-glucopyranosides, thermotropic properties and X-ray analysis. *Carbohydr. Res* **1998**, *314*, 177–187.

62. Barbier, M., Breton, T., Servat, K., Grand, E., Kokoh, B., Kovensky, J., Selective TEMPO-catalyzed chemical vs. electrochemical oxidation of carbohydrate derivatives. *Journal of Carbohydrate Chemistry*, **2006**, *25*, 253-266.

63. van Blitterswijk, W., Verheij, M., Anticancer mechanisms and clinical application of alkylphospholipids. *Biochimica Et Biophysica Acta-Molecular and Cell Biology of Lipids* **2013**, *1831* (3), 663-674.

64. Gabrielli, L., Calloni, I., Donvito, G., Costa, B., Arrighetti, N., Perego, P. Colombo, D., Ronchetti, F. Nicotra, F. Cipolla, L., Phosphatidylinositol 3-Phosphate Mimics Based on Sulfoquinovose Scaffold: Synthesis and evaluation as Protein Kinase B Inhibitors. *EurJOC* **2014**, *27*, 5962-5967.

65. Albin, F.M., Murelli, C., Patriiti, G., Rovati, M., A simple synthesis of glucosyl glycerols. *Synthetic Commun.* **1994**, *24*, 1651-1661.

66. Colombo, D., Compostella, F., Ronchetti, F., Scala, A., Toma, L., Tokuda, H., Nishino, H., Chemoenzymatic synthesis and antitumor promoting activity of 6'- and 3'-esters of 2-O-beta-D-glucosylglycerol. *Bioorganic & Medicinal Chemistry* **1999**, *7* (9), 1867-1871.

67. Adasch, V., Hoffmann, B., Milius, W., Platz, G., Voss, G., Preparation of alkyl alpha- and beta-D-glucopyranosides, thermotropic properties and X-ray analysis. *Carbohydrate Research* **1998**, *314* (3-4), 177-187.

68. Perego, P., Romanelli, S., Carenini, N., Magnani, I., Leone, R., Bonetti, A., Paolicchi, A., Zunino, F., Ovarian cancer cisplatin-resistant cell lines: Multiple changes including collateral sensitivity to Taxol. *Annals of Oncology* **1998**, *9* (4), 423-430.
69. Herschel, J.F.W., On a case of superficial colour presented by a homogeneous liquid internally colourless. *Phil. Trans. R. Soc. London* **1845**, *135*, 143-145.
70. Stokes, G.G., On the change of refrangibility of light. *Phil. Trans. R. Soc. London* **1852**, *142*, 463-562.
71. Hemmilä, I.A., Applications of Fluorescence in Immunoassays. Wiley: New York, 1991.
72. Bright, F.V., Munson, C.A., Time-resolved fluorescence spectroscopy for illuminating complex systems. *Analytica Chimica Acta* **2003**, *500* (1-2), 71-104.
73. Owicki, J.C., Fluorescence polarization and anisotropy in high throughput screening: Perspectives and primer. *Journal of Biomolecular Screening* **2000**, *5* (5), 297-306.
74. Lavis, L.D., Raines, R.T., Bright ideas for chemical biology. *Acs Chemical Biology* **2008**, *3* (3), 142-155.
75. Teale, F.W., Weber, G., Ultraviolet fluorescence of the aromatic amino acids. *Biochem. J.* **1957**, *65*, 476-482.
76. Beechem, J., Brand, L., Time-resolved fluorescence of proteins. *Annual Review of Biochemistry* **1985**, *54*, 43-71.
77. Sahoo, D., Narayanaswami, V., Kay, C., Ryan, R., Pyrene excimer fluorescence: A spatially sensitive probe to monitor lipid-induced helical rearrangement of apolipoprotein III. *Biochemistry* **2000**, *39* (22), 6594-6601.
78. Ghosh, P.B., Whitehouse, M.W., 7-Chloro-4-nitrobenzo-2-oxa-1,3-diazole: A new fluorogenic reagent for amino acids and other amines. *Biochem. J.* **1968**, *108*, 155-156.
79. Levi, J., Cheng, Z., Gheysens, O., Patel, M., Chan, C., Wang, Y., Namavari, M., Gambhir, S., Fluorescent fructose derivatives for imaging breast cancer cells. *Bioconjugate Chemistry* **2007**, *18* (3), 628-634.
80. Chattopadhyay, A., Chemistry and biology of N-(7-nitrobenz-2-oxa-1,3-diazol-4-yl)-labeled lipids-fluorescent-probes of biological and model membranes. *Chemistry and Physics of Lipids* **1990**, *53* (1), 1-15.
81. Dai, Z., Dulyaninova, N., Kumar, S., Bresnick, A., Lawrence, D., Visual snapshots of intracellular kinase activity at the onset of mitosis. *Chemistry & Biology* **2007**, *14* (11), 1254-1260.
82. Ohta, K., Hanashima, S., Mizushima, Y., Yamazaki, T., Saneyoshi, M., Sugawara, F., Sakaguchi, K., Studies on a novel DNA polymerase inhibitor group, synthetic sulfoquinovosylacylglycerols: inhibitory action on cell proliferation. *Mutation Research-Genetic Toxicology and Environmental Mutagenesis* **2000**, *467* (2), 139-152.
83. Mond, J. J., Lees, A., Snapper, C.M., T Cell-Independent Antigens Type 2. *Annu. Rev. Immunol.* **1995**, *13*, 655-692.
84. Avery, O.T., Goebel, W.F., Chemo-immunological studies on conjugated carbohydrate-protein: The immunological specificity of an antigen prepared by combining the capsular polysaccharide of type III pneumococcus with foreign protein. *J. Exp. Med.* **1931**, *54*, 437-447.
85. Berti, F., Adamo, R., Recent Mechanistic Insights on Glycoconjugate Vaccines and Future Perspectives. *ACS Chem. Biol.* **2013**, *8*, 1653-1663.
86. Astronomo, R.D., Burton, D.R., Carbohydrate vaccines: developing sweet solutions to sticky situations? *Nature Reviews Drug Discovery* **2010**, *9*, 308-324.
87. Rappuoli, R., Black, S., Lambert, P.H., Vaccine discovery and translation of new vaccine technology. *Lancet* **2011**, *378*, 360-368.

88. Anish, C., Schumann, B., Pereira, C.L., Seeberger, P.H., Chemical Biology Approaches to Designing Defined Carbohydrate Vaccines. *Chemistry & Biology* **2014**, *16*, 38-50.
89. Verez-Bencomo, V., Fernandez-Santana, V., Hardy, E. *et al.*, A Synthetic Conjugate Polysaccharide Vaccine Against Haemophilus influenzae Type b. *Science* **2004**, *305*, 522-525.
90. Kamena, F., Tamborrini, M., Liu, X., Know, Y.U., Thompson, F., Pluschke, G., Seeberger, P.H., Synthetic GPI array to study antitoxin malaria response. *Nature Chemical Biology* **2008**, *4*.
91. Bélot, F., Costachel, C., Wright, K., Phalipon, A., Mulard, L.A., Synthesis of the methyl glycoside of a branched octasaccharide fragment specific for the Shigella flexneri serotype 2a O-antigen. *Tetrahedron letters* **2002**, *43*, 8215-8218.
92. Berkin, A., Coxon, B., Pozsgay, V., Towards a Synthetic Glycoconjugate Vaccine Against Neisseria meningitidis A. *Chem. Eur. J.* **2002**, *8*, 4424-4433.
93. Slattegard, R., Teodorovic, P., Kinfe, H., Ravenscroft, N., Gammonb, D.W., Oscarson, S., Synthesis of structures corresponding to the capsular polysaccharide of Neisseria meningitidis group A. *Org. Biomol. Chem.* **2005**, *3*, 3782-3787.
94. Parameswar, A.R., Park, I.H., Saksena, R., Kovàc, P., Nahm, M.H., Demchenko, A.V., Synthesis, Conjugation, and Immunological Evaluation of the Serogroup 6 Pneumococcal Oligosaccharides. *ChemBioChem* **2009**, *10*, 2893-2899.
95. Safari, D., Dekker, H. A. T., Joosten, J. A. F., Michalik, D., Carvalho de Souza, A., Adamo, R., Lahmann, M., Sundgren, A., Oscarson, S., Kamerling, J.P., Snippe, H, Identification of the smallest structure capable of evoking opsonophagocytic antibodies against *Streptococcus pneumoniae* type 14. *Infect. Immun.* **2008**, *76*, 4615-4623.
96. Legnani, L., Ronchi, S., Fallarini, S., Lombardi, G., Campo, F., Panza, L., Lay, L., Poletti, L., Toma, L., Ronchetti, F., Compostella, F., Synthesis, molecular dynamics simulations, and biology of a carba-analogue of the trisaccharide repeating unit of Streptococcus pneumoniae 19F capsular polysaccharide. *Organic & Biomolecular Chemistry* **2009**, *7* (21), 4428-4436.
97. Teodorovic, P., Slattegard, R., Oscarson, S., Synthesis of stable C-phosphonate analogues of Neisseria meningitidis group A capsular polysaccharide structures using modified Mitsunobu reaction conditions. *Org. Biomol. Chem.* **2006**, *4*, 4485-4490.
98. Torres-Sanchez, M.I., Zaccaria, C., Buzzi, B., Miglio, G., Lombardi, G., Polito, L., Russo, G., Lay, L., Synthesis and Biological Evaluation of Phosphono Analogues of Capsular Polysaccharide Fragments from *Neisseria meningitidis* A. *Chem. Eur. J* **2007**, *13*, 6623-6635.
99. Fahmy, T.M., Demento, S.L., Caplan, M.J., Mellman, I., Saltzman, W.M., Design opportunities for actively targeted nanoparticle vaccines. *Nanomedicine* **2008**, *3*.
100. Smith, D.M., Simon, J.K., Baker Jr, J.R., Applications of nanotechnology for immunology. *Nature Reviews Immunology* **2013**, *13*, 592-605.
101. Bernardi, A., Jiménez-Barbero, J., Casnati, A., Imberty, A., *et al.* Multivalent Glycoconjugates as anti-pathogenic agents *Chem. Soc. Rev.* [Online], 2013, p. 4709-4727.
102. Rojo, J., Morales, J.C., Penadés, S., Carbohydrate-carbohydrate interactions in biological and model systems. *Top. Curr. Chem.* **2002**, *218*, 45-92.
103. Lee, Y.C., Lee, R.T., Carbohydrate-protein interactions: basis of glycobiology. *Acc. Chem. Res.* **1995**, *28*, 321.
104. Bertozzi, C.R., Kiessling, L.L., Chemical glycobiology. *Science* **2001**, *291*, 2357-2364.
105. Pieters, R.J., Maximising multivalency effects in protein-carbohydrate interactions. *Org. Biomol. Chem.* **2009**, *7*, 2013-2025.
106. Marradi, M., Chiodo, F., Garcia, I., Penadés, S., Glycoliposomes and Metallic Glyconanoparticles in Glycoscience. In *Synthesis and Biological Applications of*

*Glycoconjugates*, Renaudet, O., Spinelli, N, Ed. Bentham Science Publishers Ltd.: 2011; Vol. 10, pp 164-202.

107. Kiessling, L.L., Gestwichi, E.J., Strong, L.E, Synthetic multivalent ligand as probes of signal transduction. *Angew. Chem. Int. ed.* **2006**, *45*, 2348.

108. Davis, B.G., Synthesis of glycoprotein. *Chem. Rev.* **2002**, *102*, 579-602.

109. Dondoni, A., Marra, A., Calixarene and calixresorcarene glycosides: their synthesis and biological applications. *Chem. Rev.* **2010**, *110*, 4949-4977.

110. Heidecke, C.D., Lindhorst, T.K, Iterative Synthesis of Spaced Glycodendrons as Oligomannoside Mimetics and Evaluation of Their Antiadhesive Properties. *Chem. Eur. J* **2007**, *13*, 9056-9067.

111. Gomez-García, M., Benito, J.M., Butera, A.P., Ortiz Mellet, C., García-Fernandez, J. M., Jimenez Blanco, J.L., Probing Carbohydrate-Lectin Recognition in Heterogeneous Environments with Monodisperse Cyclodextrin-Based Glycoclusters. *J. Org. Chem.* **2012**, *77*, 1273-1288.

112. Cecioni, S., Oerthel, V., Iehl, J. Holler, M., Goyard, D., Praly, J. P., Imberty, A., Nierengarten, J. F., Vidal, S., Synthesis of Dodecavalent Fullerene-Based Glycoclusters and Evaluation of their Binding Properties towards a Bacterial Lectin. *Chem. Eur. J.* **2011**, *17*, 3252-3261.

113. Marradi, M., Martin-Lomas, M., Penadés, S., Glyconanoparticles: polyvalent tools to study carbohydrate-based interactions. *Adv. Carbohydr. Chem. Biochem.* **2010**, *64*, 211-290.

114. Adamo, R., Nilo, A., Castagner, B., Boutureira, O., Berti, F., Bernardes, G.J.L., Synthetically defined glycoprotein vaccines: current status and future directions. *Chem. Sci.* **2013**, *4*, 2995-3008.

115. Hassane, F.S., Phalipon, A., Tanguy, M., Guerreiroc, C., Bélot, F., Frischa, B., Mulard, L.A., Schuber, F., Rational design and immunogenicity of liposome-based diepitope constructs: Application to synthetic oligosaccharides mimicking the *Shigella flexneri* 2a O-antigen. *Vaccine* **2009**, *27*.

116. Deng, S., Bai, L., Reboulet, R., Matthew, R., Engler, D.A., Teyton, A., Bendelac, A., Savage, P.B., A peptide-free, liposome-based oligosaccharide vaccine, adjuvanted with a natural killer T cell antigen, generates robust antibody responses *in vivo*. *Chem. Sci* **2014**, *5*, 1437-1441.

117. Ingale. S., Wolfert, M.A., Gaekwad, J., Buskas, T., Boons, G.J., Robust immune responses elicited by a fully synthetic three-component vaccine. *Nat. Chem. Biol.* **2007**, *3*, 663-667.

118. Yin, Z., Comellas-Aragones, M., Chowdhury, S., Bentley, P., Kaczanowska, K., Mohamed, L.B., Gildersleeve, J.C., Finn, M.G., Huang, X., Boosting Immunity to Small Tumor-Associated Carbohydrates with Bacteriophage Q $\beta$  Capsids. *ACS Chem. Biol.* **2013**, *8*, 1253-1262.

119. Li, H., Wang, L.-X., Design and synthesis of a template-assembled oligomannose cluster as an epitope mimic for human HIV neutralizing antibody 2G12. *Org. Biomol. Chem.* **2004**, *2*, 483-488.

120. Wang, L.X., Ni, J., Singh, S., Li, H., Binding of high-mannose-type oligosaccharide and synthetic oligomannose cluster to human antibody 2G12:implication for HIV-1 vaccine design. *Chem. Biol.* **2004**, *11*, 127-134.

121. Krauss, I.J., Joyce, J.G., Finnefrock, A.C., Song, H.C., Dudkin, V.Y., Geng, X., Warren, D.J., Chastain, M., Shiver, J.W., Danishefsky, S.J., Fully Synthetic Carbohydrate HIV Antigens Designed on the Logic of the 2G12 Antibody. *JACS* **2007**, *129*, 11042-11044.

122. Wang, S.K., Liang, P.H., Astronomo, R.D., Hsu, T.L., Hsieh, S.L., Burton, D.R., Wong, C.H., Targeting the carbohydrates on HIV-1: Interaction of oligomannose dendrons with human monoclonal antibody 2G12 and DC-SIGN. *PNAS* **2008**, *105*, 3690-3695.

123. Astronomo, R.D., Kaltgrad, E., Udit, A.K., Wang, S.K., Doores, K.J., Huang, C.Y., *et al.*, Defining criteria for oligomannose immunogens for HIV using icosahedral virus capsid scaffolds. *Chem. Biol.* **2010**, *17*, 357-370.
124. de la Fuente, J.M., Barrientos, A.G., Rojas, T.C., Rojo, J., Canada, J., Fernández, A., Penadés, S., Gold glyconanoparticles as water-soluble polyvalent models to study carbohydrate interaction. *Angew. Chem. Int. Ed. Engl* **2001**, *40*, 2258-2261.
125. Barrientos, A.G., de la Fuente, J.M., Rojas, T.C., Fernández, A., Penadés, S., Gold glyconanoparticles: synthesis polivalente ligands mimicking glycolyxlike surfaces as tools for glycobiological studies. *Chem.-Eur. J* **2003**, *9*, 1909.
126. Ojeda, R., de Paz, J. L., Barrientos, A.G., Martín-Lomas, M., Penadés, S., Preparation of multifunctional glyconanoparticles as a platform for potential carbohydrate-based anticancer vaccines. *Carbohydrate Research* **2007**, *342*, 448-459.
127. Martínez-Ávila, O., Hijazi, K., Marradi, M., Clevel, C., Campion, C., Kelly, C., Penadés, S., Gold Manno-Glyconanoparticles: Multivalent systems to block HIV-1 gp120 binding to the Lectin DC-SIGN<sup>+</sup>. *Chem. Eur. J* **2009**, *15*, 9874-9888.
128. Marradi, M., Chiodo, F., García, I., Penadés, S., Glyconanoparticles as multifunctional and multimodal carbohydrate systems. *Chem. Soc. Rev.* **2013**, *42*, 4728-4745.
129. Brinãs, R.P., Sundgren, A., Sahoo, P., Morey, S., Rittenhouse-Olson, K., Wilding, G. E., Deng, W., Barchi, T.J., Design and Synthesis of Multifunctional Gold Nanoparticles Bearing Tumor-Associated Glycopeptide Antigens as Potential Cancer Vaccines. *Bioconjugates Chem.* **2012**, *23*, 1513-1523.
130. Svarovsky, S.A., Szekely, Z., Barchi, J.J., Synthesis of gold nanoparticles bearing theThomsen–Friedenreich disaccharide: a new multivalent presentation of an important tumor antigen. *Tetrahedron: Asymmetry* **2005**, *16*, 587-598.
131. Manea, F., Bindoli, C., Fallarini, S., Lombardi, G., Polito, L., Lay, L., Bonomi, R., Mancin, F., Scrimin, P., Multivalent, Saccharide-Functionalized Gold Nanoparticles as Fully Synthetic Analogs of Type A *Neisseriameningitidis* Antigens. *Adv. Mater.* **2008**, *20*, 4348-4352.
132. Fallarini, S., Paoletti, T., Orsi Battaglini, C., Ronchi, P., Lay, L., Bonomi, R., Jha, S., Mancin, F., Scrimin, P., Lombardi, G., Factors affecting T cell responses induced by fully synthetic glyco-gold-nanoparticles. *Nanoscale* **2013**, *5*, 390-400.
133. Safari, D., Marradi, M., Chiodo, F., Dekker, H. A. T., Shan, Y., Adamo, R., Oscarson, S., Rijkers, G. T., Lahmann, M., Kamerling, J. P., Penadés, S., Snippe, H., Gold nanoparticles as carriers for a synthetic *Streptococcus pneumoniae* type 14 conjugate vaccine. *Nanomedicine* **2012**, 651-662.
134. World Health Organization. Pneumococcal conjugate vaccine for childhood immunization. *Epidemiol.Rec.* **2007**, *82*, 93-104.
135. Bryce, J., Boschi-Pinto, C., Shibuya K., Black, R.E., WHO estimates of the causes of death in children. *Lancet* **2005**, *365*, 1147-1152.
136. Park, I.H., Moore, M.R., Treanor, J.J., Pelton, S.I., Pilishvili, T., Beall, B., Shelly, M.A., Mahon, B.E., Nahm, M.H, Differential effects of pneumococcal vaccines against serotypes 6A and 6C. *J. Infect. Dis.* **2008**, *198*, 1818-1822.
137. Tyo, K.R., *et al.*, Cost-effectiveness of conjugate pneumococcal vaccination in Singapore: comparing estimates for 7-valent, 10-valent, and 13-valent vaccines. *Vaccine* **2011**, *29*, 6686–6694.
138. Brandau, D.T., Jones, L.S., Wiethoff, C.M., Rexroad, J., Middaugh, C.R., Thermal stability of vaccines. *J. Pharm. Sci.* **2003**, *92*, 218–231.

139. Love, J.C., Estroff, L.A., Kriebel, J.K., Nuzzo, R.G., Whitesides, G.M., Self-Assembled Monolayers of Thiolates on Metals as a Form of Nanotechnology. *Chem. Rev.* **2005**, 1103-1169.
140. Panza, L., Ronchetti, F., Russo, G., Toma, L, *J. Chem. Soc., Perkin Trans. 1*, **1987**, 2745; Bousquet, E., Khitri, M., Lay, L., Nicotra, F., Panza, L., Russo, G., *Carbohydr. Res* **1998**, 172, 195.
141. Brust, M., Walker, M., Bethell, D., Schiffrin, D.J., Whyman, R. *J. Chem. Soc. Chem. Commun.* **1994**, 7, 801-802.
142. Hostetler, M.J., Wingate, J.E., Zhong, C.J., Harris, J E., Vachet, R.W., Clarck, M.R., Lonodon, J.D., Green, S.J., Stokes, J.J., Wignall, G.D., Glish, G.L., Porter, M.D., Evans, N.D., Murray, R.W., Alkanethiolate gold cluster molecules with core diameters from 1.5 to 5.2 nm: core and monolayer properties as a function of core size. *Langmuir* **1998**, 14, 17-30.
143. Mie, G., *Ann. Phys* **1908**, 25, 377-445.
144. Slocik, J.M., Govorov, A.O., Naik, R.R., Plasmonic Circular Dichroism of Peptide-Functionalized Gold Nanoparticles. *Nano Letters* **2011**, 11 (2), 701-705.
145. Polito, L., Colombo, M., Monti, D., Melato, S., Caneva, E., Prosperi, D., Resolving the structure of ligands bound to the surface of Superparamagnetic Iron Oxide Nanoparticles by High-Resolution Magic-Angle Spinning NMR Spectroscopy. *J. Am. Chem. Soc.* **2008**, 130, 12712-12724.
146. Grant, L.R., O'Brien, S.E., Burbidge, P., Haston, M., Zancolli, M., Cowell, L., Johnson, M., Weatherholtz, R.C., Reid, R., Santosham, M., O'Brien, K.L., Goldblatt, D., Comparative Immunogenicity of 7 and 13-Valent Pneumococcal Conjugate Vaccines and the Development of Functional Antibodies to Cross-Reactive Serotypes. *PlosOne* **2013**, 8.
147. Cooper, P.D., Vaccine Design: The Subunit and Adjuvant Approach. Plenum Press, Ed. Powell, M.F., Newman, M.J.: New York, 1995, 559-580.
148. De Becker, G., Moulin, V., Pajak, B., Bruck, C., Francotte, M., Thiriart, C., Urbain, J., Moser, M., The adjuvant monophosphoryl lipid A increases the function of antigen-presenting cells. *International Immunology* **2000**, 12 (6), 807-815.
149. Chiodo, F., Marradi, M., Tefsen, B., Snippe, H., van Die, I., Penadés, S., High Sensitive Detection of Carbohydrate Binding Proteins in an ELISA-Solid Phase Assay Based on Multivalent Glyconanoparticles. *PLoS ONE* **2013**, 8, 1-11.
150. Rosch, J.W., Iverson, A.R., Humann, J., Mann, B., Gao, G., Vogel, P., Mina, M., Murrah, K.A., Perez, A.C., Swords, E.W., Tuomanen, E.I., McCullers, J.A., A live-attenuated pneumococcal vaccine elicits CD4+ T-cell dependent class switching and provides serotype independent protection against acute otitis media. *EMBO Mol Med* **2014**, 6 (1), 141-54.



Part of this thesis has been the object of publications and communications at meeting.

#### **PUBLICATIONS**

Vetro M., Costa B., Donvito, G., Arrighetti N., Cipolla, L., Perego P., Compostella F., Ronchetti F., Colombo D., Novel Anionic glycolipids related to glucuronosyldiacylglycerol inhibit protein kinase Akt. *OBC*, **2014**, DOI: 10.1039/C4OB01602E.

Costa, B., Dangate, M., Vetro, M., Donvito, G., Gabrielli, L., Amigoni, L., Cassinelli, G., Lanzi, C., Michela Ceriani, De Gioia, L., Filippi G., Cipolla, L., Zaffaroni, N., Perego, P., and Colombo, D., Synthetic sulfoglycolipids targeting the serine-threonine protein kinase Akt. *Chem.Med.Chem.*, **2014**, *Submitted*

#### **CONFERENCE PRESENTATIONS AND SEMINARS**

**Vetro M.**, Marradi M., Compostella F., Lay L., Ronchetti F., Penadés S., Gold nanoparticles as carriers of *Streptococcus pneumoniae* carbohydrate antigens for fully synthetic vaccines. XIV *Convegno-Scuola sulla Chimica dei Carboidrati* and *COST meeting*, Certosa di Pontignano, Siena, 22-28 June 2014, OC-3 and PC-29

Colombo D., Compostella F., Legnani L., Ronchetti F., Perego P., Arrighetti N., Cipolla L., Costa B., **Vetro M.**, Synthesis of anionic glycolipid fluorescent probes targeting protein kinase B (Akt). XIV *Convegno-Scuola sulla Chimica dei Carboidrati*, Certosa di Pontignano, Siena, 22-25 June 2014, PC-28

**Vetro M.**, Marradi M., Compostella F., Lay L., Ronchetti F., Penadés S., Gold nanoparticles as carriers of *Streptococcus pneumoniae* carbohydrate antigens for fully synthetic vaccines. XXVI *Riunione Nazionale "A. Castellani" dei Dottorandi di Ricerca in Discipline Biochimiche*, Brallo di Pregola (PV), 9-13 June 2014, OC-5

**Vetro, M.**; Colombo, D.; Costa, B.; Comelli, F.; Cassinelli, G.; Lanzi, C., Evaluation of the biochemical and biological activity of sulfoglycolipids targeting protein kinase B (Akt). XXV *Riunione Nazionale "A. Castellani" dei Dottorandi di Ricerca in Discipline Biochimiche*, Brallo di Pregola (PV), 10-14 June 2013, PB-6

**Vetro M.**, Colombo D., Compostella F., Ronchetti F., New anionic glycolipids targeting protein kinase B (Akt). 10<sup>th</sup> *Carbohydrate Bioengineering Meeting (CBM10)*, Prague, Czech Republic, 21-24 April 2013, PC-168

**Vetro M.**, Costa B., Comelli F., Gabrielli L., Cipolla L., Colombo D., Sulfoglycolipids as potential protein kinase B (AKT) inhibitors. *XIII Convegno-Scuola sulla Chimica dei Carboidrati*, Certosa di Pontignano, Siena, 24-27 June 2012, PC-4

#### **CONFERENCE PRESENTATIONS AS CO-AUTHOR**

**Cipolla L.**, Gabrielli L., Vetro M., Colombo D., Legnani L., Costa B., Perego P., Calloni I., 6-Sulphonate glucose derivatives as potential kinase inhibitors. *XIV Convegno-Scuola sulla Chimica dei Carboidrati*, Certosa di Pontignano, Siena, 22-25 June 2014, PC-16

**Colombo, D.**; Ronchetti, F.; Compostella, F.; Legnani L., Arrighetti, N.; Larcher, V.; Vetro, M.; Synthesis and evaluation of new anionic glyco glycerolipids targeting protein kinase B (Akt). *17<sup>th</sup> European Carbohydrate Symposium*, Tel-Aviv, Israel, July 7-11, 2013, P-61

**Gabrielli, L.**; Calloni, I.; Vetro, M.; Colombo, D.; Bini, D.; Costa, B.; Cipolla, L.; New sulfoglycophosphoramidates as phosphoinositide mimetics. *17<sup>th</sup> European Carbohydrate Symposium*, Tel-Aviv, Israel, July 7-11, 2013, P-64

Costa, B.; Vetro, M.; Comelli, F.; Gabrielli, L.; Cipolla, L.; Cassinelli, G.; Lanzi, C.; **Colombo, D.** Evaluation of the biochemical and biological activity of sulfoglycolipids targeting protein kinase B (Akt). *26<sup>th</sup> International Carbohydrate Symposium, ICS*, Madrid, 22-27 July 2012, P197

## Ringraziamenti/Aknowledgements

La mia massima gratitudine va alla Prof.ssa Ronchetti per questa entusiasmante avventura da cui ho imparato molto e per tutte le volte che mi ha incoraggiato ad affrontare le sfide di questo lavoro spingendomi sempre a credere di più in me stessa. Grazie al mio tutor, Prof. Diego Colombo, che con molta pazienza ha seguito il mio lavoro in questi anni. Un grazie speciale, pieno d'affetto, va alla Dr. Federica Compostella. Grazie per tutto l'entusiasmo che mi hai regalato e per essere stata una certezza fondamentale in tutti questi anni!

Many thanks to Prof. Soledad Penadés for giving me the opportunity to carry out part of my PhD work in her Laboratory allowing me to learn about glyconanotechnology. E grazie mille a te, Dr. Marco Marradi, per il tuo aiuto prima, durante e dopo i sei mesi a San Sebastián. Grazie per avermi sempre incoraggiato "a vedere il bicchiere mezzo pieno" e per aver accettato la mia testardaggine...anche quando prendeva il sopravvento!

Grazie a tutti quelli che hanno collaborato a questo lavoro contribuendo all'aspetto biologico del progetto: Dr. Barbara Costa, Dr. Paola Perego e Dr. Dodi Safari.

Grazie a tutti i tesisti che hanno contornato le mie giornate trascorse nei laboratori di via Saldini, in particolar modo ai "più recenti" che mi hanno accompagnato a questo traguardo. È anche grazie a voi che ricorderò sempre con un sorriso questi anni!

Grazie a Cecilia, per la nostra amicizia nata "sotto cappa" e per essere stata sempre presente anche da lontano in ogni momento importante di questa esperienza.

Grazie a Camilla senza la quale San Sebastián non sarebbe stata così bella...Grazie amica!

Mucha gracias a mis compañeros de piso porque han sido como un familia para mí...nunca ve olvidarè!

Grazie a tutta la mia famiglia che mi è stata vicina in questo percorso. Grazie per avermi insegnato che i sogni vanno inseguiti e gli ostacoli superati. Un grazie particolare va a mia sorella che più di tutti mi ha sostenuto ascoltando pazientemente tutti i racconti delle mie vicissitudini giornaliere...non so come farei senza di te!